ABSTRACT

Title of Document: IDENTIFICATION AND CHARACTERIZATION OF PRESUMPTIVE BOVINE MAMMARY STEM CELLS

Ratan Kumar Choudhary, Ph.D., 2011

Directed By: Adjunct Professor, Anthony V. Capuco, Bovine Functional Genomics Laboratory, USDA, Beltsville, Maryland, USA

An understanding of the characteristics and regulation of mammary stem cells (MaSCs) is needed to gain insight into normal gland development and carcinogenesis. Previous profiling of MaSCs relied upon immunophenotypic selection of enzymatically dispersed cells by flow cytometry. However, these approaches involved the selection of cells that are removed from their tissue location and cellular microenvironment. In this study, I have utilized an alternative approach called laser microdissection, to excise putative MaSCs, based upon their ability to retain bromodeoxyuridine labeled DNA for an extended period, and control cells from their in situ locations in prepubertal bovine mammary cryosections. First, I established a protocol to immunostain putative MaSCs in tissue cryosections and isolate RNA of high quality. Next, I excised putative MaSCs and control cells from immunostained cryosections using laser microdissection. Global gene

expression analysis by microarray provided evidence that MaSCs were located in the basal epithelium and progenitor cells located in suprabasal layers. A number of genes that were up-regulated in MaSCs and progenitor cells were identified and these are potential biomarkers. Analysis of the expression pattern of four genes (NR5A2, NUP153, HNF4A and FNDC3B) by immunohistochemistry showed that the protein expression profile was consistent with microarray data. Detailed immunohistochemical analyses of NR5A2, NUP153, HNF4A and FNDC3B in calf and cows (at various stages of lactation) revealed that their frequency and distribution were consistent with stem/progenitor cell characteristics. Finally, I attempted to manipulate stem/progenitor cells number using cultures of primary mammary epithelial cells. Expansion of stem/progenitor cell is a prerequisite for stem cell therapeutics and facilitates stem cell research. The effect of xanthosine on bovine mammary epithelial cells (MEC) was evaluated. The result of this study showed that xanthosine treatment increased cell proliferation, promoted symmetric cell division and increased expression of telomerase and a novel stem cell marker (FNDC3B). Together, these studies identified novel, potential markers for MaSCs and progenitor cells, and supported the ability of xanthosine to increase stem/progenitor cell number.

IDENTIFICATION AND CHARACTERIZATION OF PRESUMPTIVE BOVINE MAMMARY STEM CELLS

By

Ratan Kumar Choudhary

Dissertation submitted to the Faculty of the Graduate School of the
University of Maryland, College Park, in partial fulfillment
of the requirements for the degree of
Doctor of Philosophy
2011

Advisory Committee:
Professor Ian H. Mather, Chair
Adjunct Professor Anthony V. Capuco (Advisor)
Associate Professor Carol L. Keefer
Assistant Professor Lisa A. Taneyhill
Associate Professor Jason D. Kahn (Dean's Rep.)

Dedication

I dedicate this research to my mother, Meera Choudhary, who left her physical entity before completion of this dissertation. The expressions of deep and spiritual feelings help my research as I struggle to make sense of this life.

And to my daughter, Anika Choudhary, who harbingers fortune in my life.

Acknowledgements

First, I would like to thank my mentor, Dr. Anthony V. Capuco, for the opportunity to work in his lab. His experience, knowledge, and mentorship have provided me with a strong foundation that I am grateful for and will carry with me in my future career. Thank you for the opportunity to study such a wonderful and dream topic. I would also like to thank the members of my advisory committee, Drs. Ian H. Mather, Carol L. Keefer, Jason D. Kahn, and Lisa A. Taneyhill, for their invaluable guidance and support.

I would like to thank our support scientist, Ms. Chris Clover, for timely help and advice. I thank post-doctoral friend, Dr. Kristy M. Daniels (now a faculty member at the Ohio State University) for the lessons taught and encouragement given during early difficult years. I will never forget the time we spent together developing a protocol for BrdU immunostaining.

I owe my sincere thanks to research scientists at USDA building 200 for their friendly behavior, encouraging words, timely helpful discussion - especially, Drs. Wesley Garrett, Neil Talbot, Robert Li, Congjun Li, George Liu, Theodore Elsasser, Ransom Baldwin and Lakshmi Mutukumalli.

I would like to thank the Department of Animal and Avian Sciences, University of Maryland for providing me with the opportunity to pursue the Ph.D. degree and the USDA, Agricultural Research Service and the USDA, National Institute of Food and Agriculture, National Research Initiative Competitive Grants Program, for providing funds.

Finally, I thank my wife, Shanti, for her patience, sacrifice, and for allowing me to work in the lab at odd hours throughout the years. I would not have gotten this far without her unconditional love and support.

Table of Contents

List of Abbreviations

°C	Degree centigrade
µg	Microgram
µL	Microliter
µm	Micrometer
µM	Micromolar
ACEPEG	Combination of acetone and polyethylene glycol 300 (9:1; volume/volume)
ALDH1	Aldehyde dehydrogenase 1
bp	Base pair
BrdU	5-bromo-2'-deoxyuridine
CD24	Cluster of differentiation 24 (also called heat stable antigen)
CD29	Cluster of differentiation 29 (also called β1-integrin)
CD31	Cluster of differentiation 31
CD44	Cluster of differentiation 44
CD45	Cluster of differentiation 45
CD49f	Cluster of differentiation 49 (also called α6- integrin)
CSF1	Colony stimulating factor 1
d	day
DAB	3'-3'-diaminobenzidine
DAVID	Database for annotation, visualization and integrated discovery
DNA	Deoxyribonucleic acid
ECb	Basal epithelial cells (control LRECb)

ECe	Embedded epithelial cells (control LRECe)
ERα	Estrogen receptor alpha
ESR1	Estrogen receptor alpha, official gene abbreviation (this abbreviation was used in genomics manuscript rather than ERα)
FBS	Fetal bovine serum
FGF	Fibroblast growth factor
FNDC3B	Fibronectin type III domain containing 3B
g	Gravity
G1-phase	Gap 1 phase of the cell cycle
G2 –phase	Gap 2 phase of the cell cycle
GSK-3b	Glycogen synthase kinase 3b
h	Hour
H_2O_2	Hydrogen peroxide
HCl	Hydrochloric acid
Hh	Hedgehog
HNF4A	Hepatocyte nuclear factor 4 alpha
IGF	Insulin-like growth factor
IMPDH	Inosine-5’-monophosphate dehydrogenase
IPA	Ingenuity pathway analysis
iPSC	Induced pluripotent stem cell
kb	Kilobase
KEGG	Kyoto encyclopedia of genes and genomes
LEF/TCF	Lymphoid enhancer factor/T-cell specific transcription factor

Lin^-	Lineage negative
LMD	Laser microdissection
LREC	Label retaining epithelial cells
LRECb	Basal label retaining epithelial cells
LRECe	Embedded label retaining epithelial cells
M	Molar (concentration)
MaSC	Mammary stem cells
MEC	Mammary epithelial cells
min	Minute
mL	Milliliter
mM	Millimolar
mo	Month
M-phase	Mitotic phase of the cell cycle
MSI1	Musashi 1
N	Normal (concentration)
NaOH	Sodium hydroxide
nfPBS	Nuclease free phosphate buffer saline
NR5A2	Nuclear receptor subfamily 5 group A member 2
NUP153	Nucleoporin 153
OCT	Optimum cutting temperature
PBS	Phosphate buffer saline
PBST	Phosphate buffer saline containing 0.05% triton-X100
PEN	Polyethylenenapthalate

pg	Picogram
PI	Propidium iodide
pmol	Picomole
PTCH	Patched
RIN	RNA integrity number
RNA	Ribonucleic acid
rpm	Revolutions per minute
RT	Room temperature
s	Second
SE	Standard error
SMAD	Mothers against decapentaplegic homolog
SMO	Smoothened
SP	Side population
S-phase	Synthetic phase of the cell cycle
TDLU	Terminal ductal lobular units
TDU	Terminal ductal units
TEB	Terminal end bud
TER119	Also called lymphocyte antigen 76 (Ly76)
TFG	Transforming like growth factor
UMFIX	Universal molecular fixative
W	Watt
wk	Week
XIST	X- inactive specific transcript

List of Tables

List of Figures

Chapter 1: Introduction

Stem cells are nonspecialized cells that generate more differentiated cells within an organism and are capable of self-renewal throughout the lifespan of that organism. There are two broad categories of stem cells, namely embryonic stem cells and adult stem cells (also referred to as somatic stem cells). Embryonic stem cells are pluripotent, derived from the inner cell mass of the embryonic blastocyst, and differentiate to form all the tissues present in an organism. Adult stem cells can be multipotent, bipotent, or unipotent and are named based on the tissue or organ in which they reside and populate. Mammary stem cells (MaSCs) are the adult stem cells present within the mammary gland.

An essential property of adult stem cells is their ability to undergo asymmetric and symmetric cell division. Asymmetric stem cell division permits renewal of mammalian tissues while maintaining a constant tissue mass, through the production of one daughter stem cell and one more differentiated progenitor cell. Symmetric cell division facilitates exponential growth kinetics by yielding two daughter cells with equivalent stem cell capacity. Clonal expansion of mammalian adult stem cells is hindered by the predominance of asymmetric cell division in vivo. Xanthosine, a purine nucleoside, has been found to suppress asymmetric cell division kinetics and to promote exponential growth of adult stem cells in culture (Lee et al., 2003).

The main goal of this dissertation research was to expand our knowledge of bovine mammary stem cells. *Specific aims were to: (1) characterize the global gene expression profiles of putative bovine MaSCs and progenitor cells in vivo (2) identify*

potential protein biomarkers of MaSCs and progenitor cells and (3) confirm the utility of xanthosine for increasing expansion of MaSCs using an in vitro model system.

Characterization of MaSCs and progenitor cells are important steps towards understanding their regulation, expansion and proliferation. In dairy animals, appropriate regulation of the expansion and proliferation of MaSCs and progenitor cells can likely lead to increased milk production and lactation persistency, improved dry period management, and enhanced repair of damaged tissue in the event of injury or infection. Additionally, knowledge of MaSCs will enhance understanding of tissue homeostasis and facilitate investigations of mammary tumorigenesis. Most research attempts to provide molecular profiles of MaSCs in mice, human and bovine species have utilized fluorescence-activated cell sorting or in vitro cultivation of cells from enzymatically dissociated tissues. However, the microenvironments encountered by MaSCs and progenitor cells are lost prior to analysis using these approaches. Data suggest that bromodeoxyuridine label retaining epithelial cells (LREC) represent mammary stem and progenitor cells. In this thesis research, these putative MaSCs and progenitor cells (LREC) were excised from their in situ locations in tissue cryosections using laser microdissection, and their transcriptome profiles were evaluated using microarray analysis. The overall hypotheses of this research was that LREC are MaSCs and that comparison of the molecular profile of these cells with that of control cells can provide potential MaSCs biomarkers, which can then be evaluated by immunohistochemistry. In liver hepatocyte culture, xanthosine appears to be a regulator of stem cell karyokinesis (Lee et al., 2003). Similarly, intramammary infusion of xanthosine appears to lead to expansion of the population of bovine MaSCs (Capuco et al. 2009). An additional

objective of my thesis research was to confirm that xanthosine enhances expansion of the MaSC population. To this end, the ability of xanthosine to enhance cell proliferation by promoting symmetric division of MaSCs was investigated using cultures of primary mammary epithelial cells.

Chapter 2: Literature review

2.1 Bovine mammary gland structure and development

The mammary gland is composed of two major tissue compartments, epithelium and stroma, which are separated by a basement membrane. The epithelium is a single tissue that is the primary component of the mammary ducts and alveoli. The stroma is the connective tissue matrix in which the ducts and alveoli develop, and includes many cell types such as fibroblasts, adipocytes, endothelial cells, mast cells, leukocytes and neural cells.

In cattle, mammary ducts develop as highly arborescent structures called terminal ductal units (TDU), which resemble the terminal ductal lobular units (TDLU) of the human breast. TDU are the predominant histological feature of the mammary glands of prepubertal heifers. Ductal elongation occurs by the coordinated growth, branching and extension of the TDU (Capuco et al. 2002). The TDU of the prepubertal gland typically consists of 2-3 layers of epithelial cells and contains 5-10 ductular outgrowths arranged around a central epithelial cord (Figure 1). Layers of epithelial cells within the TDU may be designated as basal, embedded and lumenal (Figure 2). The basal layer of cells is adjacent to the basement membrane. The lumenal layer of epithelium is located most apically from the basement membrane and cells of this layer are in contact with the ductal lumen. The embedded layer(s) of cells are sandwiched between the basal and lumenal layers. There is a large amount of loose fibrous stroma surrounding the TDU.

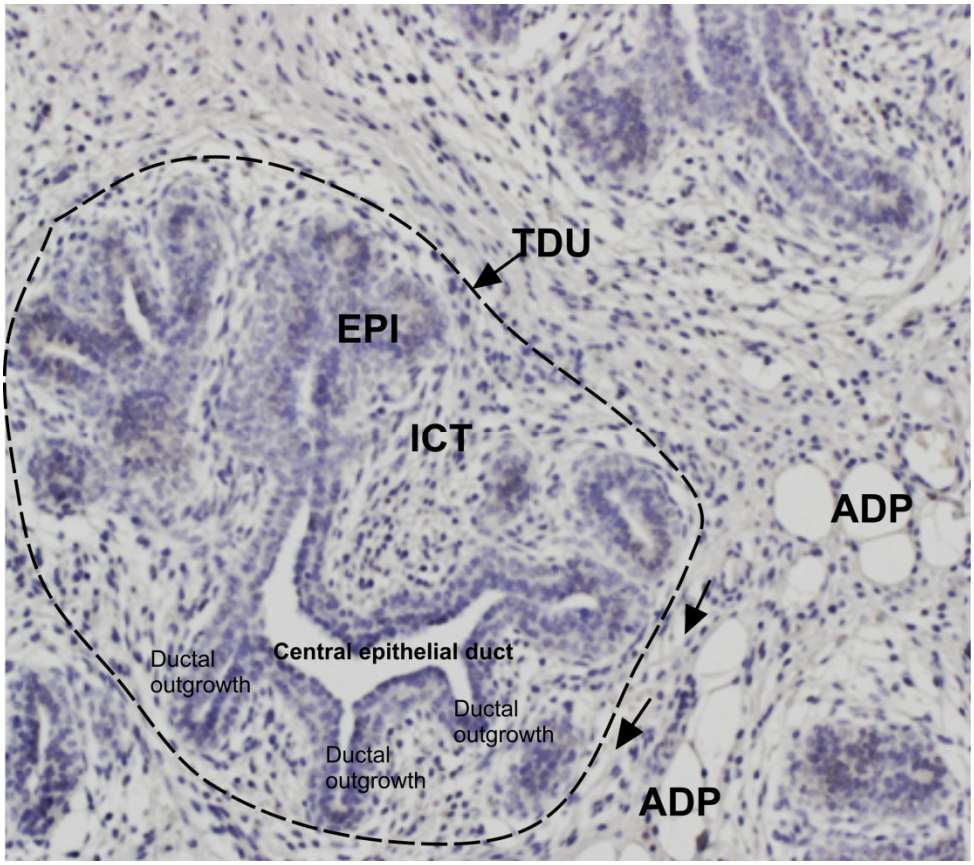

Figure 1. Histological structure of the prepubertal bovine mammary gland.

Mammary ducts develop as a highly arborescent structure called a terminal ductal unit (TDU) in which there are 5-10 separate ductal outgrowths, with 2-3 layers of epithelial cells in each ductal growth. Epithelial cells (EPI) of the elongating ducts are surrounded by intralobular loose connective tissue (ICT) and adipocytes (ADP). Adipocytes are not in direct contact with the epithelium but separated by loose connective tissue (arrows).

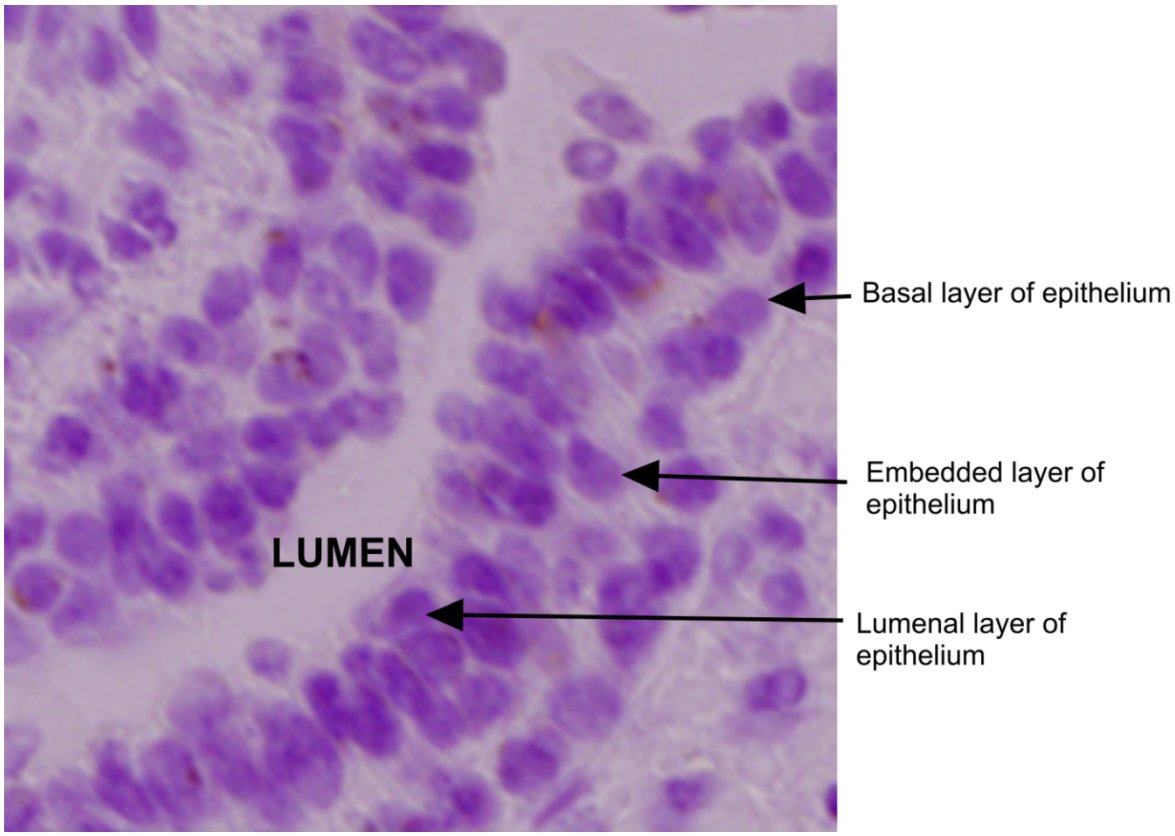

Figure 2. Epithelial cell arrangement in the prepubertal bovine mammary gland.

Epithelial cells (EPI) are arranged in 2-3 distinct layers (basal and lumenal or basal, embedded and lumenal) around a clearly defined central lumen. However, immature ducts may not contain a clear lumen. Cells in the basal layer are hypothesized to contain mammary stem cells.

The microanatomy of the peripubertal bovine mammary gland differs from that of the murine mammary gland. Adipose tissue is generally more abundant in the peripubertal murine mammary gland than it is in the bovine gland, in which the amount of adipose tissue varies between animals and by location (periphery vs. internal structures) of the TDU within the gland. In contrast to the bovine mammary gland, ducts of the murine gland grow with minimal branching. At the distal end of each murine mammary duct is a mass of proliferating cells within a bulbous structure called the terminal end- bud (TEB). At the distal end of the TEB, a layer of proliferating cells called cap cells contact the surrounding stroma mainly composed of adipocytes (Williams and Daniel, 1983). There is little to no basement membrane present between the cap cells and the stroma. With the exception of the TEB, murine mammary ducts are typically composed of two layers of epithelium, a single basal layer of myoepithelium and an inner layer of lumenal epithelium. Thus, a developing ruminant mammary gland is different from a murine mammary gland in terms of number of epithelial cell layers, absence of a definitive layer of myoepithelium, composition of the stroma, and the nature of ductal elongation.

During early postnatal life, the mammary gland grows at an impressive rate that is faster than that of the rest of the body (allometric growth); this rate declines after puberty when its rate of growth equals that of the rest of the body (isometric) (Sinha and Tucker, 1969). During pregnancy, there is extensive proliferation of the mammary epithelium, additional lateral side branching of ducts, and the appearance of alveoli that differentiate

under the influence of hormones of pregnancy and serve as the basic epithelial structure responsible for milk secretion.

2.2 Existence of mammary stem cells and their identification

In the mouse mammary gland, the first evidence for the existence of MaSCs came from the work of DeOme and coworkers (DeOme et al, 1959), who demonstrated that small pieces of mammary tissue could expand and differentiate into a fully functional and reconstituted mammary gland when transplanted into the cleared fat pad (devoid of endogenous epithelium) of recipient mice. Other experiments have provided evidence for the existence of MaSCs. In the human breast, clonal expansion of cells from stem cells has been suggested to explain the presence of entire lobules and ducts with the same X-chromosome inactivation patterns (Tsai et al., 1996). In murine mammary gland, Kordon and Smith (1998) employed retroviral tagging to demonstrate the existence of multipotent MaSCs capable of regenerating a functional mammary gland.

Based on biological and morphological features, investigators have identified putative MaSCs/progenitor cells in human, murine and bovine mammary glands. In mice, mammary epithelium stained with Blue-Azure II dye identified a distinct population of pale-staining mammary epithelial cells and hypothesized to represent MaSCs. These pale cells were characterized by light staining of cytoplasm, presence of a large round nucleus, sparse cytoplasmic organelles and presence of tight junctions (Smith and Medina, 1988). The more darkly staining cells were considered more differentiated cells. These pale staining cells were refractory to differentiation signals, evidenced by their lack of casein immunostaining in mammary explants that were cultured in the presence of lactogenic hormones. Based on quantitative and morphological properties (cell frequency, size,

shape, staining characteristics, organelle distribution, and nuclear morphology), Chepko and Smith developed a model for epithelial cell lineage in mouse and rat mammary glands (Chepko and Smith, 1997). Pale staining cells were subdivided into small light cells (SLC) and large light cells (LLC). The abundance of SLC was unaltered across physiological developmental stages and these were concluded to be stem cells. These SLC (putative MaSCs) were characterized by morphological features including, small cell size, high nucleus to cytoplasm ratio, condensed chromosomes and unspecialized cytoplasmic organelles. In human breast, a study of proliferating cells provided evidence for the existence of cells that are morphologically similar to the pale staining cells in mouse and rat mammary gland (Ferguson, 1985). In mammary glands of calves, Ellis and Capuco found similar morphologically distinct populations of epithelial cells and categorized them as light, intermediate and dark cells based upon intensity of their cytoplasmic staining (Ellis and Capuco, 2002). The difference in nomenclature from that used to describe analogous cells in rodents reflected differences in parenchymal architecture, cellular morphology and location of cells within the multiple epithelial layers (basal, embedded and lumenal) of bovine mammary tissue. In prepubertal bovine mammary gland, the frequency of light staining cells were reported to be approximately 10% of total mammary epithelial cells (Ellis and Capuco, 2002).

Using a different approach, investigators have identified potential MaSCs based on increased expression of membrane transporter proteins like breast cancer resistance protein (BCRP) (Zhou et al., 2001). Increased expression of these ATP binding cassette transporters in cells effectively excludes dyes like rhodamine from their cytoplasm, allowing for the identification and separation of a population of cells, known as the side

population (SP), by flow cytometry. In various studies, the SP fraction was demonstrated to possess an enriched capacity to regenerate a murine mammary gland upon transplantation (Welm et al., 2002; Alvi et al., 2003). The SP fraction averaged 0.2% to 1% in human (Dontu et al., 2003), 0.5% to 3% in murine (Welm et al., 2002) and 0.5% in bovine (Motyl et al., 2011) mammary glands. A recent review discusses the importance of cell-cell interactions in dictating stem cell behavior and the value of in vivo transplantation studies in elucidating this aspect (Smith and Medina, 2008).

A population of mammary epithelial cells enriched with MaSCs, based on expression of a combination of cell surface protein markers, was identified by use of a multiparameter cell sorting in mouse mammary gland (Shackleton et al., 2006; Stingl et al., 2006). The Shackleton and Stingl groups carried out independent research in which they enriched the MaSCs population by selecting cells for CD29 (β1-integrin) and/or CD49f (α6-integrin), and CD24 (heat stable antigen). This enrichment followed the exclusion of cells that were of endothelial and hematopoietic lineage, so-called Lin+ cells (CD31+, CD45+ and TER119+). CD31, a platelet cell adhesion molecule, is expressed by endothelial cells. CD45, a transmembrane tyrosine phosphatase, is expressed in hematopoietic cells with the exception of erythrocytes. TER119 is exclusively expressed on cells in the erythrocyte lineage. Hence, CD31 was used as a marker to exclude endothelial cells and CD45 and TER119 were used as markers to exclude hematopoietic cells. In contrast, CD29 (β1-integrin) and CD49f (α6-integrin) are integrin adhesion proteins that are expressed by mammary epithelial cells and mediate interactions with stroma (Streuli, 2009). Expression of β1-integrin along with α2-integrin has been used to isolate skin stem cells (Jones and Watt, 1995). CD24 is also not very specific to MaSCs

as it has been used as a neuronal stem cell marker (Rietze et al., 2001) and as a marker of aggressive breast cancer (Kristiansen et al., 2003). Using the aforementioned surface markers, Lin^{-} $CD24^{+}CD29^{high}$ cells (Shackleton et al., 2006) and Lin^{-} $CD24^{+}CD49^{high}$ cells (Stingl et al., 2006) were shown to be enriched for MaSCs. These marker-sorted cells displayed increased capacity, compared to unsorted cells, to generate a functional mammary gland when transplanted into genetically identical mice.

Another approach to characterize MaSCs has employed use of anchorage independent culture systems. Under these conditions, human, mouse and bovine mammary epithelial cells produce spherical colonies called "mammospheres" (Dontu et al., 2003; Morrison and Cutler, 2009; Riley et al., 2010). Mammospheres are solid spheres of cells that are hypothesized to originate from a single MaSCs and appear to be enriched in stem cell/progenitor cell populations. This approach was based upon the use of neurospheres to study neural stem cells (Reynolds et al., 1992). Typically, mammospheres are 200-250 µm in diameter and contain approximately 150-300 cells (Dontu et al., 2003) in human cell suspension culture. In Matrigel, a single cell isolated from mammospheres was demonstrated to develop a complex functional structure, with ductal and alveolar cells (Dontu et al., 2003). Because the efficiency of human mammosphere formation was 0.4%, it was inferred that each mammosphere contains approximately one sphere-initiating cell (1/250 cells per mammosphere = 0.4%). In a recent study, mammosphere initiating cells were reported to be $CD44^{high}CD24^{low}$ and their ability to form next generation mammospheres was exhausted after five generations (Dey et al., 2009). Thus mammosphere culture conditions will need further improvement for their long-term maintenance. Limited use of mammospheres culture in research

community may be due to the inability to maintain mammosphere for a long time and the difficulty in separating cell aggregates and quantifying different types of cells within the mammosphere.

Another approach to identify putative stem cells is based on the observation that many somatic stem cells retain label in their DNA for a prolonged period after initial labeling with tritiated thymidine or bromodeoxyuridine (BrdU) (Bickenbach, 1981; Potten et al., 1978). In mice, intestinal crypt cells (Potten et al. 2002), muscle satellite cells (Conboy, et al., 2007) and putative mammary stem cells (Smith, 2005) retained the label. In bovine mammary gland, Capuco and coworkers (Capuco, 2007; Capuco et al., 2009) proposed that these label-retaining epithelial cells (LREC) are putative stem cells. However, the phenomenon of label retention by adult stem cells does not appear to be a universal marker for these cells. In hematopoietic tissue, label retaining cells are not stem cells (Kiel et al., 2007). There are two schools of thought as to why stem cells may retain label; one school of thought says that MaSCs (not progenitor cells) are quiescent cells and the other school of thought says that MaSCs retain label due to asymmetric segregation of DNA strands (immortal strand hypothesis). In mammary gland, label retaining epithelial cells were suggested to be the result of asymmetric segregation of DNA stands (Smith, 2005; Capuco, 2007). A schematic representation of the immortal strand hypothesis to explain the retention of labeled DNA is depicted in Figure 3.

2.3 Important signals in the mammary microenvironment

Mammary epithelial cells are regulated by a complex network of communication between basement membrane, basal cells, embedded cells, lumenal cells, stromal cells, and extracellular matrix. In addition to the ovarian hormones (estrogen and progesterone)

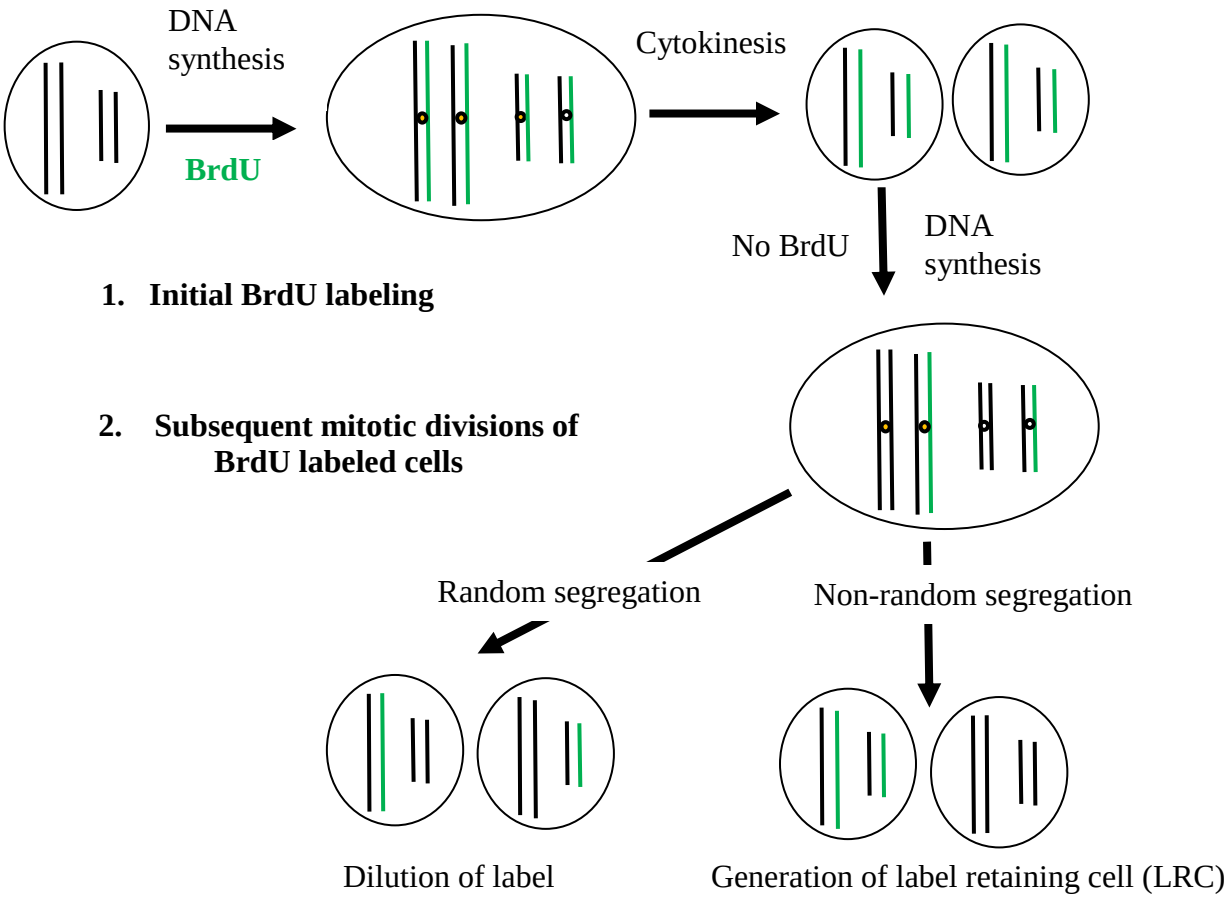

Figure 3. Concept of retention of labeled DNA strands in stem cells by asymmetric division. Retention of label (e.g. BrdU) by putative adult stem cells may be due to selective segregation of labeled DNA strands during asymmetric division giving rise to cells that retain label (LRC) despite multiple cell divisions. Random segregation of DNA after initial labeling would cause dilution of label by ~50% in each division and the label is "lost" after a few mitotic divisions.

which are necessary for mammary gland development, a variety of other hormones and factors These structures, along with cell-cell communication and soluble factors, direct cellular activity through direct contact or paracrine signaling. The role of endocrine hormones as master coordinating regulators of mammary gland development is well established (Brisken and O'Malley, 2010). including physical factors such as cell-cell contact, cell-stoma interactions (Muschler and Streuli, 2010; Wiseman and Werb, 2002) and diffusible factors such as growth factors, growth suppressors and cytokines provide for regulation and development of the mammary gland. The number of regulators and interactions is enormous. Only those deemed most relevant to this investigation of bovine mammary stem cells will be discussed.

Local signals generated from the epithelial and stromal compartments of the gland have important roles in controlling development of the mammary gland. These signals are growth factors, hormones and soluble factors that direct gland development (Silberstein, 2001). In a recent study, loss of adipocytes resulted in loss of TEB formation and fewer ductal branching in mouse mammary gland, suggesting an important role of adipocyte secreted factors in maintaining lobular architecture (Landskroner-Eiger et al., 2010). Adiponectin, a protein secreted by adipocytes has been demonstrated to influence proliferation and differentiation of mammary epithelial cells via estrogen receptor dependent and independent mechanisms (Rahal and Simmen, 2011). An additional stromal factor that is secreted by mammary macrophages, is colony stimulating factor -1 (CSF1), which promotes mammary gland development during pregnancy (Pollard and Hennighausen, 1994) and plays a role in mammary stem cell function in mice (Gyorki et al., 2009).

Numerous growth factors of the epidermal growth factor (EGF), insulin-like growth factor (IGF) and fibroblast growth factor (FGF) families regulate the proliferation of MaSCs in coordination with activated endocrine pathways (Hynes and Watson, 2010). The EGF family of growth factors, amphiregulin, and transforming growth factor-α (TGFα) are expressed during all phases of mammary gland development and a collaborative role of EGF and TGFα has been suggested in mammopoiesis and lactogenesis (Luetteke et al., 1999). Amphiregulin serves as a mediator of estrogen signaling and is necessary for ductal development and the formation of TEB in murine mammary gland (Booth et al., 2010). FGF-mediated signaling is initiated by dimerization of the receptor tyrosine kinase upon ligand binding, which ultimately promotes cell growth, differentiation and functions that are important for normal development and tissue maintenance (Katoh and Katoh, 2006). Expression of FGF1 protein and mRNA has been demonstrated during mammogenesis, lactation and involution stages suggesting the possible role of FGF1 in changing morphological and functional properties of the bovine mammary gland (Sinowatz et al., 2006).

Considerable evidence suggests that IGF1 has an important role in mediating ductal growth. IGF1-null mice have diminished ductal growth and TEB formation (Ruan and Kleinberg, 1999) and locally implanted IGF1 induced development of TEB and formation of alveolar structures (Ruan, et al., 1992). Similarly, IGF1 and IGF-binding proteins are produced locally and regulate growth and development of the bovine mammary gland peripubertally (Akers et al., 2000).

The nuclear receptors for ovarian steroids, estrogen receptor-alpha (ERα) and progesterone receptor are essential for normal development of the mammary gland.

Proliferation of mammary epithelial cells is mediated in paracrine fashion, and these paracrine factors are derived from estrogen receptor (ER)-positive and progesterone receptor (PR)-positive cells of the epithelial or stromal compartments of the mammary gland (Capuco et al., 2002; Hovey and Aimo, 2010; Li and Capuco, 2008; Mallepell et al., 2006). Without these essential ER-positive and PR-positive cells in the microenvironment, the MaSCs and progenitor cells do not function properly. A recent report on ovariectomized mice reported a decreased number and diminished self-renewal capacity of MaSCs (Asselin-Labat et al., 2010). Loss of ERα in the mammary epithelium resulted in impaired ductal branching and elongation in estrogen receptor null pubertal mice (Feng, et al., 2007; Mallepell et al., 2006). Current evidence indicates that MaSCs are ERα-negative and PR-negative in mouse (Asselin-Labat et al., 2006), human (Anderson and Clarke, 2004) and cow (Capuco et al., 2002).

The Wnt signaling pathway is one of the most complex pathways in multicellular organisms. This complexity is due to the large number of Wnt protein ligands (Wnt 1-16) and proteins that regulate the production of Wnt, the interactions with receptors on target cells and the resulting signaling cascade and physiological responses (Katoh and Katoh, 2006). The canonical Wnt/β-catenin pathway is the best-characterized Wnt pathway. The signaling pathway includes Wnt ligands, cell surface fizzled receptor and β-catenin. Upon ligand binding, cytoplasmic protein disheveled is activated and destroys the second complex of proteins that includes glycogen synthase kinase-b (GSK-3b), axin, and adenomatous polyposis coli (APC). Destruction of GSK3b/axin/APC spares destruction of β-catenin in the cytoplasm and promotes β-catenin translocation into the nucleus. In the nucleus, β-catenin interacts with the nuclear lymphoid enhancer factor/ T-cell specific

transcription factor (LEF/TCF) family of transcription factors and activates Wnt target genes. Non-canonical Wnt pathways are independent of β1-catenin. Among various non-canonical pathways, planar cell polarity (PCP) and Wnt/calcium are well known. In the mammary gland, various Wnt proteins (Wnt-2, Wnt-4, Wnt-5a, Wnt-5b, Wnt-6 and Wnt-7b) appear to be synthesized in the epithelium and stroma based upon localization by in situ hybridization, and an essential role of Wnt proteins in breast development has been suggested (Weber-Hall, et al., 1994). Wnt-5a ligand binds with Frizzed receptor and has been shown to regulate intercellular calcium level through a non-canonical Wnt/calcium pathway. In mouse, transcriptome analysis of mammary epithelial subpopulations revealed that expression of Wnt-4, Wnt-5a, and Wnt-7b was enriched in lumenal ERα positive cells (Kendrick et al., 2008). A role for Wnt-4 in progesterone-induced ductal side-branching (Brisken et al., 2000) and Wnt-1 and Wnt-10b in alveolar development (Robinson, et al., 2000) have been suggested. Musashi-1 (MSI1), a neuroglial stem cell marker and proposed MaSCs marker, has been demonstrated to promote proliferation of progenitor cells ($CD24^{high}CD29^{+}$) by activating the Wnt pathway in a mouse mammary epithelial cell line (Rezza et al., 2010; Wang et al., 2008). In a recent study, Wnt responsive cells were shown to be enriched for MaSCs and exogenous exposure of Wnt protein promoted clonal expansion of stem cells and the ability to generate a functional mammary gland for many generations in transplantation studies (Zeng and Nusse, 2010).

The TFG-β pathway has a variety of roles that are pertinent to mammary development, including regulation of cell differentiation, cell growth and epithelial-mesenchymal transition. The signaling pathway consists of ligands (TFG super family members) and receptors (type 1 and type 2). The TGF-β family of ligands binds with

type 2 receptor dimer, which recruits and phosphorylates type 1 receptor dimer, forming a heterotetramer complex with ligand. This results in phosphorylation of SMAD proteins (SMAD 1-9) in the cytoplasm, and dimers of SMAD proteins translocate into the nucleus and mediate transcription of target genes. In the mammary gland, TFG-β1 has been recognized as a negative regulator of mammary proliferation, regulator of mammary stem cells, promotor of apoptosis and inducer of epithelial-mesenchymal transition. In vivo studies using slow releasing implants of TGF-β1 in mouse mammary gland have demonstrated that growth of the mammary ductal network is reduced by TGF-β1 (Daniel, et al., 1989; Silberstein and Daniel, 1987). Other studies in mice have established a role for TGF-β1 in regulation of stem cells (Kordon et al., 1995) and induction of apoptosis during post-lactation involution of the mammary gland (Nguyen and Pollard, 2000). Recent studies demonstrated a role for TGF-β1 in epithelial-mesenchymal transition and maintenance of stem cell states in breast tissue (Fuxe et al., 2010; Scheel et al., 2011).

The Notch signaling pathway is a highly conserved pathway in multicellular organisms. It regulates cell fate during development and determines differentiation of MaSCs and progenitor cells. The Notch pathway is mediated by juxtacrine signaling among adjacent cells, wherein ligand (Notch 1 to 4) presenting cells send the signal to receptor (Jagged family-JAG1,2 and Delta-like family-DLL1, 2 and 4) presenting cells. Ligand binding to the extracellular domain of the receptor induces proteolytic cleavage and release of the intracellular domain, which then translocates into the nucleus and binds with its partner of the CSL family (CBF1, Su, Lag-1) of transcription factors and mediates transcription of target genes like *Myc* and *p21*. In mammary gland, the Notch pathway has been shown to be associated with MaSCs self-renewal, cell fate

specification and progenitor cell expansion. In vitro, increased expression of Notch activating DSL peptides promoted stem cell self-renewal, which was evidenced by a 10-fold increase in the number of mammospheres and increased ductal branching in 3D Matrigel upon differentiation; whereas blocking the Notch 4 signal blocked mammosphere formation in human mammary epithelial cells (Dontu et al., 2004). In vivo, knock-down of the canonical Notch effector gene CBF1 led to an increase in the stem cell ($CD29^{hi}CD24^{+}$) population and aberrant ductal morphogenesis, suggesting a role for Notch in restricting stem cell expansion (Bouras et al., 2008). Conversely, constitutive activation of the pathway led to an expansion of lumenal progenitor cells ($CD29^{lo}CD24^{+}CD61^{+}$) (Bouras et al., 2008).

The Hedgehog (Hh) signaling pathway is a well-studied and conserved pathway in multicellular organisms. The Hh pathway is mediated in autocrine and paracrine fashion. The signaling pathway includes secreted glycoprotein ligands (Sonic Hh, Desert Hh, and Indian Hh), receptors (Patched 1 and 2, PTCH), an effector (Smoothened, SMO), and transcription factors (Gli 1 to 3). Paracrine mode of action requires another protein called 'dispatched'. In absence of ligand, PTCH and SMO form a receptor complex and SMO activity remains inhibited. Upon ligand binding, the receptor complex dissociates and relieves SMO inhibition causing activation of transcription factors Gli 1, 2 (activator) and Gli 3 (repressor). The transcription factors translocate into the nucleus and regulate transcription of target genes (e.g. *myc*, *cyclin D*, *cyclin E,* components of the EGF pathway). Hh signaling components (Sonic Hh, PTCH1, Gli 1, 2) are highly expressed in human mammospheres and their expression is associated with an increase in mammosphere-initiating cells as well as mammosphere size (Lee et al., 2003). An

important role of Hh signaling in mediating epithelial-stromal interaction has been demonstrated in mouse mammary gland by genetic analysis (Lewis et al., 2001). Likewise, activation of the Hh signaling pathway in vivo increases the number of mammary progenitor cells by increasing the mitotic activity of MaSCs (Li et al., 2008). This pathway regulates multiple phases of mammary gland development, including ductal development and lactation (Lewis and Veltmaat, 2004). These results suggest that Hh signaling plays a role in the regulation and self-renewal of mammary progenitor cells.

2.4 ***Manipulations of stem cells and uses***

Techniques to induce stem cell de-, re-, or transdifferentiation into tissue-specific cell lineages and to promote proliferation require an understanding of tissue microenvironment wherein cell-to-cell and cell to environment interactions occur (Figure 4). Recent efforts have focused on the manipulation of adult stem cell differentiation using soluble factors, chemicals and hormones to produce a suitable physiological environment that mimics tissue microenvironment for the stem cells to renew, divide or differentiate depending upon the need. A role of progesterone in expansion of MaSCs has been demonstrated (Joshi et al., 2010). In a model experiment with mammary cancer stem cells, cytotoxicity targeted towards differentiated cells enhanced proliferation of stem cells (Agur et al., 2010). Earlier I discussed various signaling pathways that regulate expansion and differentiation of MaSCs and progenitor cells. Manipulation of these signaling pathways could alter cell division kinetics to achieve expansion, propagation and finally differentiation of MaSC. Indeed, a role of the β-catenin pathway in regulation of MaSC and progenitor cells has been suggested (Korkaya et al., 2009). In an in vitro

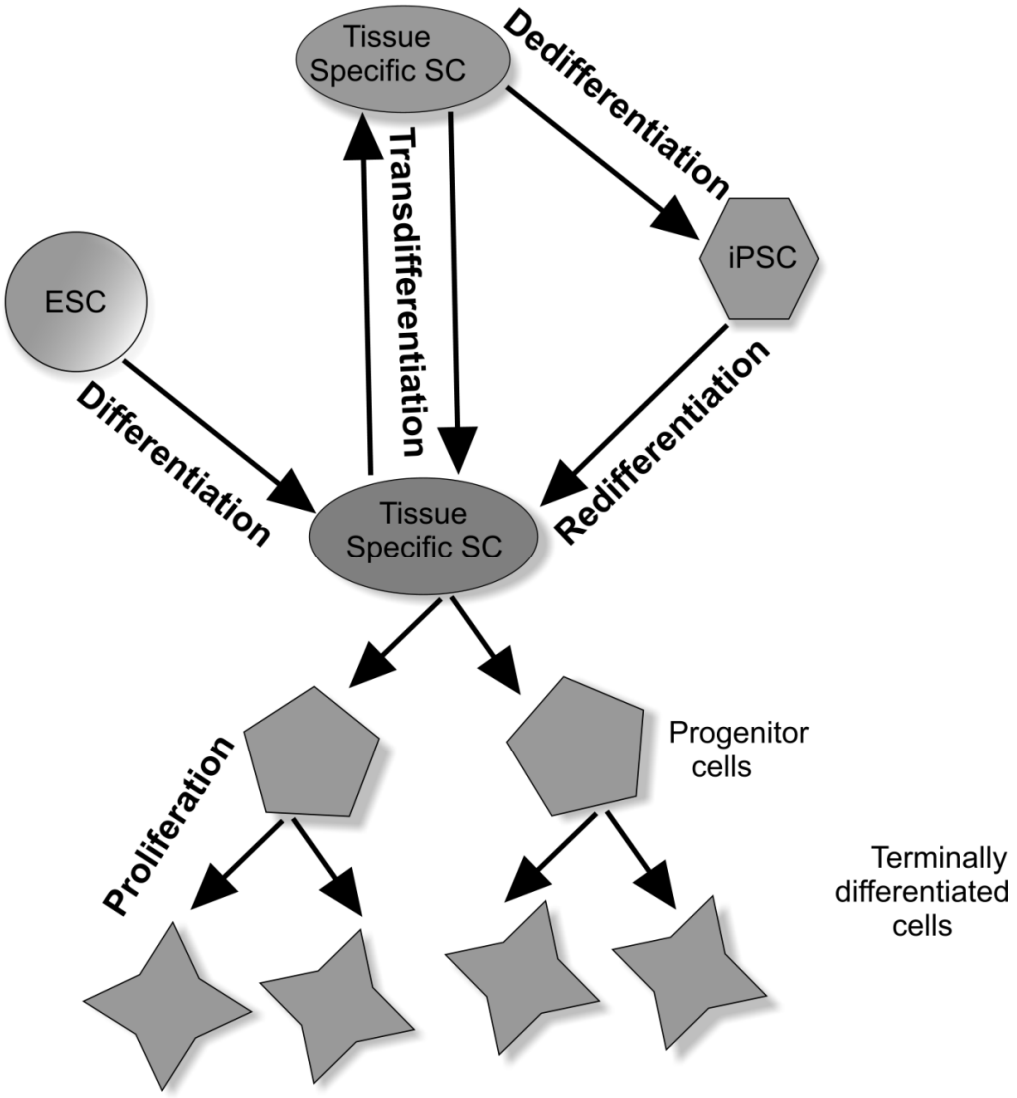

Figure 4. Possible sources of tissue specific stem cells (e.g. MaSCs) and their proliferation. The dairy industry, MaSCs and their proliferative population of cells are likely to help in mammary gland development, increasing the persistency of lactation, and management of dry period. Knowledge of bovine embryonic stem cells (ESC) and induced pluripotent stem cells (iPSC) is still rudimentary.

study, protein p53 mediated the down-regulation of inosine-5'-monophosphate dehydrogenase (IMPDH) and promoted symmetric proliferation of hepatic stem cells (Sherley and Johnson, 1995). Exogenous treatment with xanthosine overcame this down regulation of IMPDH, increased guanine ribonucleoside concentration in the cell and promoted symmetric division of stem cells and expansion of the stem cell population (Lee et al., 2003) (Figure 5). Analogously, intra-mammary infusion of xanthosine in prepubertal heifers increased the abundance of BrdU label-retaining epithelial cells i.e. MaSCs (Capuco et al., 2009). Conversely, natural compounds such as curcumin and piperine, which have been used as cancer preventative agents, have been shown to abolish mammosphere formation and Wnt signaling (Kakarala et al., 2010). Taken together, manipulation of MaSCs and progenitor cells may be a feasible means of promoting mammary growth, cell turnover and tissue regeneration, with the ultimate goals being improving milk production and udder health of dairy cattle.

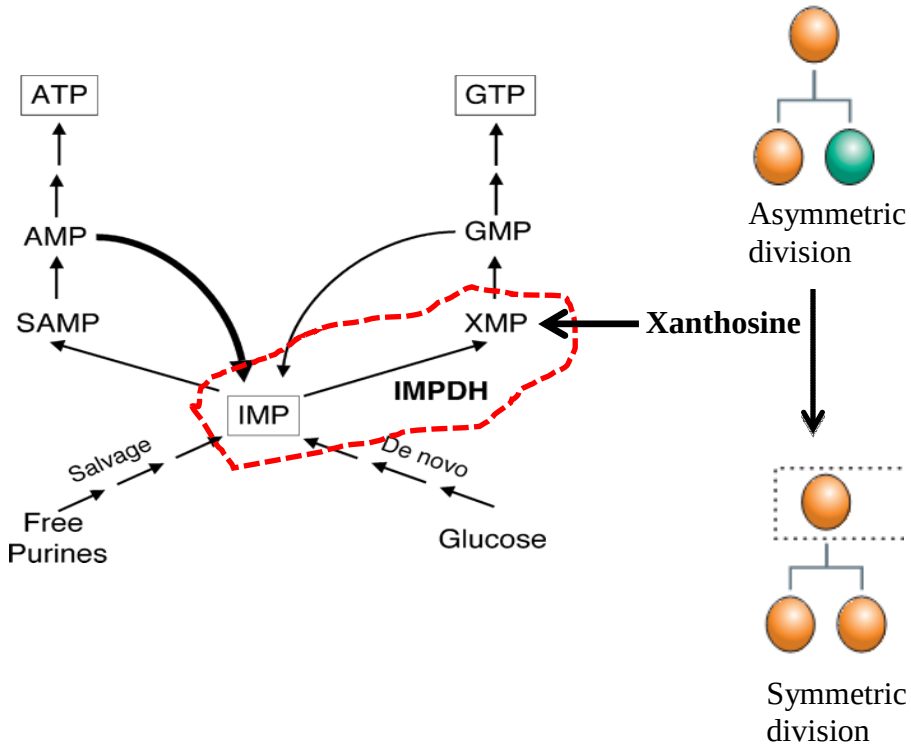

Figure 5. Exogenous administration of xanthosine promotes symmetric cell division. Xanthosine enters the ribonucleoside biosynthesis pathway and forms xanthosine monophosphate (XMP), which promotes synthesis of guanosine monophosphate (GMP). Xanthosine circumvents the inosine monophosphate dehydrogenase (IMPDH) -mediated conversion of IMP to XMP, a rate limiting enzymatic step in XMP synthesis. This increases the GMP concentration in the cell, which favors symmetric cell division.

Chapter 3: Development of a protocol for rapid 5-bromo-2′-deoxyuridine (BrdU) immunostaining

Abstract

A rapid method of immunostaining was developed for 5-bromo-2′-deoxyuridine (BrdU) -labeled cryosections of bovine mammary tissue while preserving RNA quality of the stained section. BrdU is a thymidine analog that is incorporated into the DNA of proliferating cells, and serves as a proliferation marker. Immunostaining of BrdU-labeled cells within a histological section requires heat, enzymatic or chemical-mediated antigen retrieval to open double stranded DNA, and exposure of the BrdU antigen. Although these established treatments permit staining, they preclude use of cells within the tissue section for further gene expression experiments. Additionally, long antibody incubations and washing steps lead to extensive RNA degradation and elution. A protocol was developed for immunolocalization of BrdU-labeled cells in cryosections of bovine mammary tissue. The protocol does not require harsh DNA denaturation and it preserves RNA integrity and quantity. This protocol comprised an initial acetone:polyethylene glycol 300 [9:1 (vol/vol)] fixation (2 min) followed by staining with methyl green (0.5% aqueous; 2 min) to stabilize macromolecules, antigen retrieval with deionized formamide (70% in nuclease-free phosphate buffered saline; 4 min incubation), antibody incubation in the presence of RNase inhibitors (5 min), and minimal washing to facilitate recovery of RNA from cells from the stained sections. Applicability of this protocol to other nuclear antigens was evaluated by testing its suitability for staining estrogen receptor-alpha and Ki-67 antigen. In both cases, use of the protocol provided good

immunostaining and tissue morphology. The RNA quality of estrogen receptor α- and Ki-67- stained sections was not evaluated. Quality of the isolated RNA from BrdU-stained sections was evaluated by micro-fluidic electrophoresis and its utility was confirmed using quantitative reverse transcription-PCR. Staining intensity obtained with this labeling protocol was similar to that obtained using conventional immunohistochemistry protocols. When coupled with laser microdissection and RNA or cDNA amplification, this immunostaining protocol will provide a means for future transcriptome analysis of BrdU-labeled cells within a complex tissue.

Key words: **5-bromo-2′-deoxyuridine, cryosection, gene expression, laser microdissection**

3.1 Background

5-Bromo-2′-deoxyuridine (BrdU) has been used extensively to identify proliferating cells, study cell lineages, and identify putative stem cells (Capuco, 2007; Conboy et al., 2007; Plickert and Kroiher, 1988). A thymidine analog, BrdU is incorporated into DNA during the S-phase of the cell cycle and can be detected by standard immunohistochemical procedures. These procedures have limitations for subsequent transcriptome analysis of BrdU-labeled cells. Antibodies against BrdU can access only the antigen in single-stranded DNA (Gratzner, 1982), so staining procedures require DNA denaturation before antibody incubation. These procedures typically involve high heat (~100°C) in sodium citrate buffer or treatment with harsh chemicals (e.g., HCl; (Tang et al., 2007)). Such treatments affect RNA integrity and can affect cell morphology. Establishing a procedure that could identify BrdU-labeled cells without damaging cellular RNA would facilitate subsequent in situ hybridization or isolation of cells by laser microdissection for subsequent analysis of gene expression in these cells. In this study, a novel strategy was developed whereby good-quality RNA was extracted from BrdU-immunostained cryosections of bovine mammary gland. Our future application will be to use this protocol to identify putative bovine mammary stem cells for laser excision and subsequent downstream analyses. Putative bovine mammary stem cells can be identified on the basis of their ability to retain BrdU for extended periods of time after initial labeling (Capuco, 2007), because of selective segregation of parental DNA strands during asymmetric cell division (Smith, 2005).

3.2 Materials and Methods

Tissues were obtained from an experiment that was performed in compliance with the Beltsville Agricultural Research Center's Animal Care and Use Committee. Five Holstein heifers (3 mo of age) were injected with BrdU (Sigma-Aldrich Co., St. Louis, MO) intravenously once daily for 5 d as described previously (Capuco, 2007). Forty-five d after the last BrdU injection, heifers were humanely killed at the Beltsville Agricultural Research Center abattoir. Animals were stunned with a captive bolt pistol and exsanguinated, udders were removed and mammary tissue was collected from parenchymal regions within rear mammary glands (i.e., quarters) of the udder. Individual tissue samples ($5 \times 5 \times 5$ mm^3) were immediately embedded in optimal cutting temperature (OCT) compound (Sakura, Torrance, CA), frozen in liquid nitrogen vapor, transported on dry ice, and stored at −80°C. Serial sections (8 μm thick) were thaw-mounted on glass slides, UV-irradiated previously to destroy potential nuclease activity, and stored at −80°C until the time of microdissection (~2 wk maximum storage). These glass slides were covered with a membrane (2 μm thick) of polyethylene naphthalate (PEN slides, Leica AS, Wetzlar, Germany). Testing and evaluation of various protocols was performed as a linear process. Different parameters were tested and chained together to evolve the final and effective protocol. If a parameter was found to be ineffective, it was not repeated. However, successful tests were repeated and used as the basis for chaining additional steps in the protocol. The final protocol was tested repeatedly and found to be effective ($n > 24$).

Tissue cryosections were fixed with a variety of noncrosslinking fixatives including alcohols and acetone. Crosslinking fixatives, such as formalin, severely impair the ability to extract quality RNA from tissue (Lewis et al., 2001) and were not used. A list of fixatives evaluated is provided in Table 1**.** Sections were treated with these fixatives to optimize morphology and BrdU staining while maintaining good RNA quality. Sections fixed in acetone: polyethylene glycol (ACEPEG) 300 [9:1 (vol/vol); Sigma-Aldrich], our newly developed fixative, at -20°C for 2 min possessed good morphology and consistent immunostaining and yielded RNA of highest quality. This fixative was prepared on the day of use. Preliminary experiments with acetone alone as a fixative yielded acceptable tissue morphology. These results were much improved with the addition of polyethylene glycol (PEG) 300 to acetone. This fixative was derived from the composition of universal molecular fixative (UMFIX) (Vincek et al., 2003), which is a combination of methanol and PEG [9:1 (vol/vol)]. Further, PEG is a component of OCT compound, so it was thought that adding it to the fixative would aid in the preservation of morphology by providing a more gradual transition from OCT compound to acetone fixative.

Different methods were evaluated for their ability to retain the quality of RNA extracted from the tissue sections. These methods included 1) the use of methyl green to precipitate RNA in aqueous solution without affecting immunostaining and RNA isolation procedures; 2) use of RNase inhibitors in antibody incubation buffer (RNasin Plus RNase inhibitor, Promega, Madison, WI); and 3) the use of small volumes of wash solutions (200 μL instead of submersion in wash jar) and abbreviated wash time.

Table 1. Fixatives and antigen retrieval agents, their modes of action, and effects on morphology, BrdU staining, and RNA quality in bovine mammary cryosections**.**

Item	Mode of action	Morphology[2]	Staining	RNA quality[1]
Fixatives				
Methacorn[3]	Nonprecipitating + precipitating	+ + +	+	-
75% ethanol	Precipitating	+ +	+	+
Acetone	Precipitating	+ +	+ +	+ +
UMFIX[4]	Precipitating	+ + +	+ +	+ +
ACEPEG[5]	Precipitating	+ + +	+ + +	+ + +
Antigen retrieval agents				
2 *N* HCl	Denatures DNA	+ +	+ + +	-
DNase1	Cleaves DNA	+ + +	-	-
0.01 *N* NaOH	Denaturing and hydrolysis	Destroyed	-	-
U.V. irradiation	Crosslinks double stranded DNA	Destroyed	-	-
Formamide 100%	Lowers DNA melting temperature	+	+ +	-
Formamide 10%	Lowers DNA melting temperature	Destroyed	-	-
Formamide 70%	Lowers DNA melting temperature	+ +	+ +	+ +

[1] Companion slides were processed and used to quality of BrdU staining and the quality of RNA obtained from the stained slides. RNA quality is expressed as the RNA integrity number (RIN), The RIN is automatically generated from the electrophoretic data obtained by the microfluidic analysis of RNA with the Agilent Bioanalyzer (Agilent Technologies, Wilmington, DE). The algorithm used for calculating the RIN uses several features commonly used for assessing RNA quality, e.g. area under rRNA bands, ratio of 18S and 28S rRNA peaks, height of the lower marker peak (Schroeder et al., 2006). RIN is expressed on a scale of 1-10. Lower RIN corresponds to degraded RNA and high RIN corresponds to high quality RNA.
[2] Quality graded as bad (–), poor (+), moderate (+ +), or good (+ + +). RNA integrity numbers corresponded as follows: – = RIN 1 to 3; + = RIN 3 to 4; + + = RIN 4 to 6; + + + = RIN 6 to 8.
[3] Methanol + chloroform + glacial acetic acid [6:3:1 (vol/vol)].
[4] Universal molecular fixative: a mixture of methanol and polyethylene glycol 300 [9:1 (vol/vol)].
[5] A mixture of acetone and polyethylene glycol 300 [9:1 (vol/vol)].

The effects of different antigen retrieval agents on immunostaining, tissue morphology, and RNA quality were evaluated. Most treatments were time consuming and yielded unsuitable morphology and unacceptable RNA quality (Table 1). Denaturation of DNA with 70% deionized formamide (Amresco, Solon, OH) in nuclease free PBS (nfPBS) for 4 min at 60°C maintained tissue morphology and facilitated immunostaining. This approach was an application of results obtained by Mayer et al. (2006), who successfully used deionized formamide for BrdU antigen retrieval in an in situ hybridization experiment. Formamide lowers the melting temperature of DNA by destabilizing its helical structure (Blake and Delcourt, 1996).

The final protocol developed to rapidly detect BrdU-labeled cells and retain RNA quality is described below. In all cases, slides were processed singly in RNase-free LockMailer microscope slide jars (Ted Pella Inc., Redding, CA). The optimized short method for immunostaining started with ACEPEG fixation at -20°C for 2 min followed by air drying for 1 min. Air drying was essential for best fixation and adherence of the tissue to the slide during subsequent steps. Drying of the slide was followed by incubation of the section with 200 μL of 0.5% aqueous methyl green (Vector Laboratories Inc., Burlingame, CA) for 2 min at RT. After a brief (10 s) wash with nfPBS, the slide was incubated with 400 μL of prewarmed 70% deionized formamide at 60°C for 4 min, on a metal block placed in a dry bath. Immediately after formamide treatment (antigen retrieval), the section was washed twice with ice-chilled antibody dilution buffer at 4°C using 200 μL of buffer for 30 s/wash.. Antibody dilution buffer consisted of nfPBS with 1% normal goat serum and 0.1% Triton X-100 (Sigma-Aldrich) and was formulated to reduce background staining and to enhance antibody penetration in

the tissue. Washing the section with ice chilled buffer immediately after formamide treatment was essential to prevent re-annealing of denatured DNA. One-step immunostaining was performed using mouse monoclonal anti-BrdU antibody conjugated to Alexa 488 fluorophore (Clone PRB-1, Invitrogen, Carlsbad, CA) at 1:10 dilution in antibody dilution buffer for 5 min at RT in the dark. The section was then briefly washed with 200 μL of nfPBS (twice for 10 s each), counterstained with 100 μL of propidium iodide (2.5 μg/μL in nfPBS) for 20 s, and rinsed in 200 μL of nuclease-free water twice for 10 s each (counter staining with propidium iodide permitted visualization of all nuclei in the tissue section). The slide was dehydrated in freshly prepared ascending concentrations of ethanol: 70% for 10 s, 95% for 10 s, 100% for 10 s and 100% for 1 min. The slide was air dried at RT in the dark for 5 min before sample acquisition and total RNA isolation.

To assess RNA quality, whole immunostained tissue sections were lysed with the manufacturer's lysis buffer and total RNA was isolated using an RNeasy micro kit according to the protocol for the purification of total RNA from microdissected cryosections (Qiagen, Valencia, CA). The optional on-column DNase digestion was performed as described by manufacturer (Qiagen). Quality and quantity of RNA were evaluated using a Bioanalyzer (Agilent Technologies, Wilmington, DE), and a comparison was made between the RNA isolated from immunostained versus unstained cryosections. The RNA integrity number (RIN) generated by analysis (Agilent Bioanalyzer) of the RNA electropherogram provided an objective measure of RNA quality (Fleige and Pfaffl, 2006; Schroeder et al., 2006).

Applicability of the protocol to other nuclear antigens (not specifically DNA) was tested using indirect immunolabeling and bright field microscopy in the presence and absence of 70% formamide, our antigen retrieval agent. Test antibodies were estrogen receptor α (ERα) and Ki-67. Because of the preliminary nature of this test, an indirect (2-step) immunostaining protocol was used and RNA quality was not evaluated after staining. For ERα labeling, slides were incubated with mouse ERα antibody (Clone c-311, Santa Cruz Biotechnology, Santa Cruz, CA) used at a concentration of 0.01 μg/μL in antibody dilution buffer for 10 min at RT. Similarly, for Ki-67 labeling, slides were incubated with prediluted mouse Ki-67 antibody (Clone MIB-1,Invitrogen) for 10 min at RT. Slides were then incubated with horseradish peroxidase conjugated broad spectrum secondary antibody (SuperPicture HRP Polymer Conjugate Broad Spectrum, Invitrogen) after brief washings with PBS. Positively labeled cells were visualized with the 3,3'-diaminobenzidine (DAB) reaction (2-3 min incubation) and then rinsed in water. Slides were counterstained with hematoxylin for 30 s and washed briefly with water and then PBS (Counter staining with hematoxylin permitted the visualization of all cells in the tissue section; immunostained nuclei appear brown and non-labeled nuclei appear blue). Finally, slides were dehydrated in ascending grades of ethanol and viewed by bright field microscopy.

3.3 Results and Discussion

Identification and isolation of immunophenotypically different cells from morphologically indistinguishable cell populations and subsequent characterization of their transcriptome profiles requires successful immunostaining and isolation of good quality RNA from the same cryosection. All steps of the immunostaining method were

optimized to ensure acceptable tissue morphology, consistent BrdU staining, and good RNA quality. Because the immediate application of this protocol was for isolation of BrdU-labeled cells using laser microdissection and subsequent transcriptome analysis, the slides were viewed without coverslips and digital micrographs were captured using a Leica AS-LMD laser microdissection system (Leica Microsystems, Bannockburn, IL). The initial fixatives tested resulted in tissue morphology of variable quality and low RNA quality and quantity (Figure 6A and B; only representative micrographs are presented among all fixatives tried). Similarly, several antigen retrieval agents were evaluated and resulted in morphology and RNA quality that varied according to the retrieval agent tested (Figure 6C; only 1 micrograph from all antigen retrieval agents initially tested is depicted). The newly developed ACEPEG fixative and 70% formamide in nfPBS as antigen retrieval agent yielded good morphology and immunostaining (Figure 6D). Use of a fluorescently conjugated primary antibody simplified immunostaining, and minimized protocol time and RNA degradation. The BrdU-labeled cells were identified using an Alexa 488-conjugated mouse monoclonal anti-BrdU antibody and counterstained with propidium iodide (Figure 6E). The 4',6-Diamidino- 2-phenylindole (DAPI) or Hoechst stains were not used as nuclear stains because the polyethylene naphthalate membrane fluoresced with excitation–emission characteristics that were similar to those for these stains.

Retention of RNA quality (assessed by increase in RIN value) was achieved by addition of RNase inhibitors to the antibody incubation buffer (Figures 7A, B, C, and D) and exposure to aqueous buffers was limited to a total of 15 min. Antibody incubation time was limited to 5 min to minimize RNA degradation, but less than a 5 min incubation

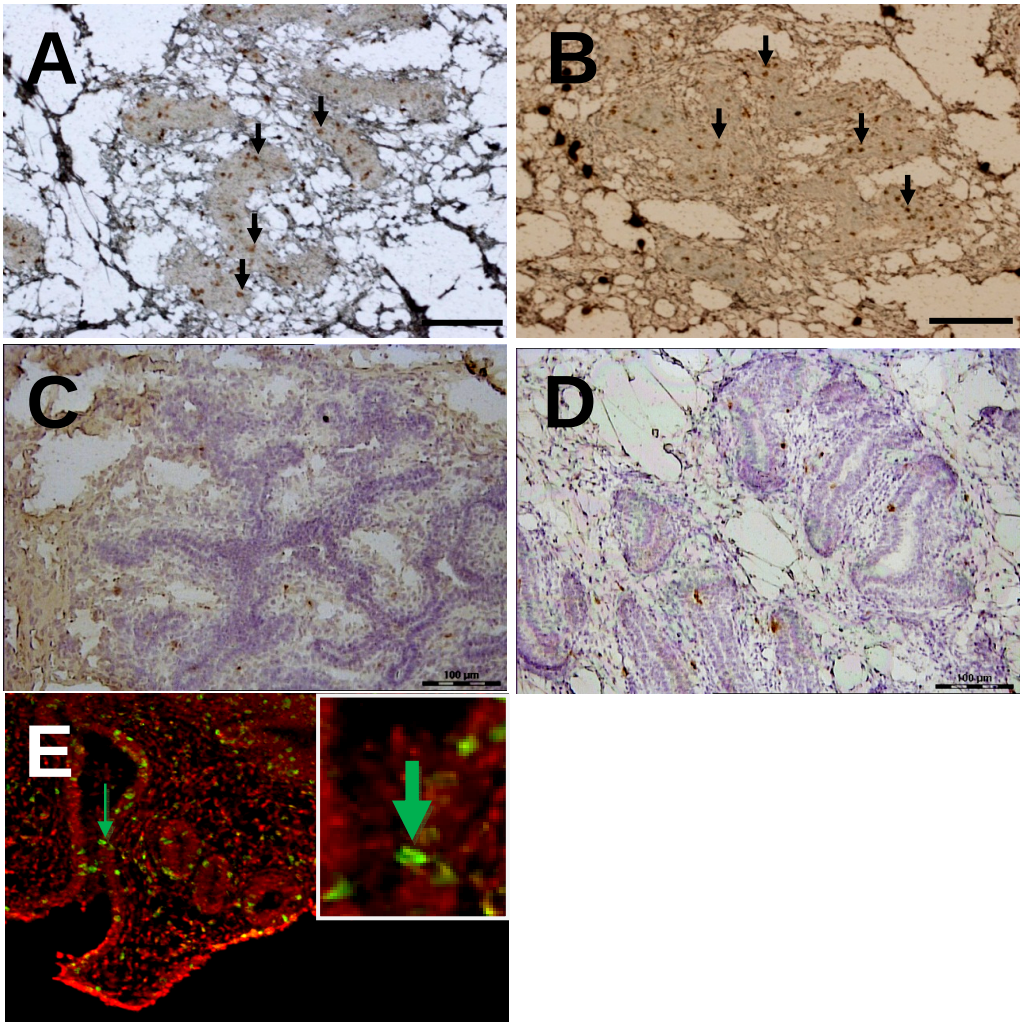

Figure 6. Effects of selected fixatives and antigen-retrieval agents on tissue morphology and bromodeoxyuridine (BrdU) staining.

A) Acetone-fixed cryosection permitted good BrdU staining (arrows) when coupled with 70% deionized formamide as antigen retrieval agent. B) Methanol-polyethylene glycol (UMFIX)-fixed section resulted in good BrdU staining when coupled with 70% deionized formamide as antigen retrieval agent; UMFIX provided better preservation of stromal tissue compared with acetone-fixed sections. C) Deoxyribonuclease 1 failed to expose BrdU in the current protocol, contrary to expectation. D) Acetone-polyethylene glycol (ACEPEG) fixation and formamide antigen retrieval provided an effective fixative and antigen retrieval agent, yielding good morphology. Section was counterstained with hematoxylin to stain all nuclei blue. E) Cryosection, fixed with ACEPEG and treated with 70% formamide, was labeled with Alexa 488-conjugated anti-BrdU (green; arrow indicates labeled nucleus of epithelial cell) and counterstained with propidium iodide (red nuclei). This was the optimal protocol, providing good morphology, immunostaining and best RNA quality (see Figure 7F for RNA quality). Inset shows the highlighted BrdU-positive epithelial cell at greater magnification. Scale bar = 100 μm.

resulted in inconsistent immunostaining. The adverse effect of longer incubation times on RNA quality was consistent with the findings of Fend and coworkers (Fend et al., 1999). To successfully utilize a short incubation time, a high concentration of antibody was employed as suggested for staining tissues for laser microdissection (Murakami, et al., 2000). The dilution used for BrdU antibody (1:10) was titrated for our system. Finally, the quality of RNA from tissue sections that were immunostained using the optimized protocol (outlined in Materials and Methods) was analyzed and compared with the RNA from fixed but unstained tissue sections (Figure 7E and F; Figure 7F corresponds to micrograph in Figure 6E). RNA quality was high for both the stained and unstained sections. Furthermore, the utility of the isolated RNA for gene expression analysis was tested using quantitative reverse transcription-PCR. Successful amplification of genes with reverse transcriptase quantitative PCR (RT-qPCR) using gene specific primers confirmed good quality of RNA (data not shown). To obtain a preliminary evaluation of the efficacy of the antigen retrieval with 70% formamide for detection of other cellular antigens, tissue cryosections were stained for ERα or Ki-67, with or without formamide treatment.

The ERα staining was restricted to mammary epithelium, consistent with previous results (Capuco et al., 2002), and Ki-67-labeled cells were primarily seen in mammary epithelium (Figure 8). Convincingly, more ERα-labeled cells were seen in formamide-treated slides (Figure 8A) than in PBS-treated slides (Figure 8B). In addition, formamide enhanced overall tissue morphology of cryosections with clear nuclear staining. Similar findings were observed with Ki-67 staining; with formamide increasing detection of Ki-67-stained cells (Figure 8C) in comparison with a control slide having no formamide

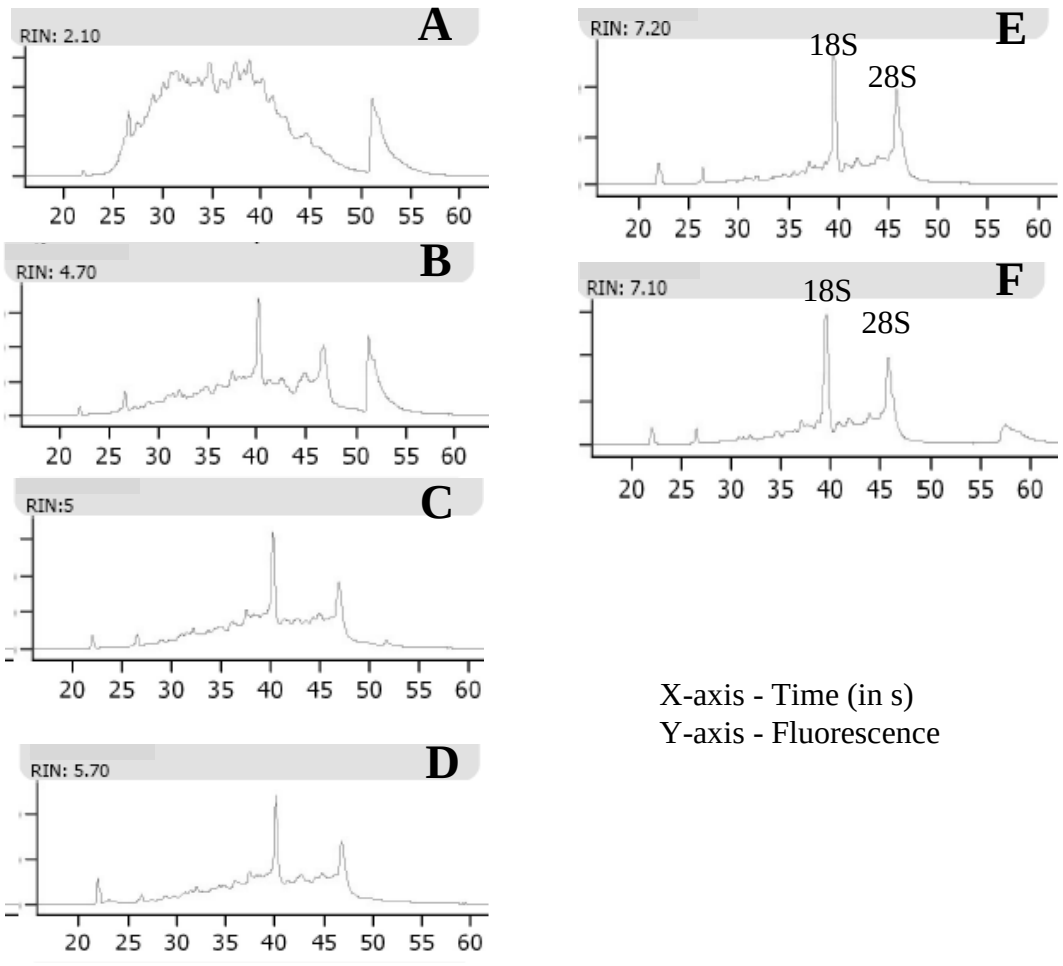

Figure 7. Electropherograms of total RNA obtained from stained serial tissue sections.

Effect of incorporating RNase inhibitor in incubation buffer on RNA quality was tested and is depicted in comparison with fixed, unstained sections and sections stained with the final optimized protocol.

A) No RNase inhibitor; RNA integrity number (RIN) = 2.1.

B) One unit of inhibitor (RNasin plus)/µL; RIN = 4.7.

C) Two units of inhibitor/µL; RIN = 5.0.

D) Three units of inhibitor/µL; RIN = 5.7.

E) RNA isolated from acetone-polyethylene glycol (ACEPEG)-fixed, unstained slide from different serial sections yielded a maximum RIN = 7.2.

F) Optimized protocol with ACEPEG-fixed, stained sections yielded RIN = 7.1 (micrograph provided in Figure 1D).

Both panels E and F had similar RIN, indicative of good-quality RNA.

Migration of 18S and 28S ribosomal RNA is depicted.

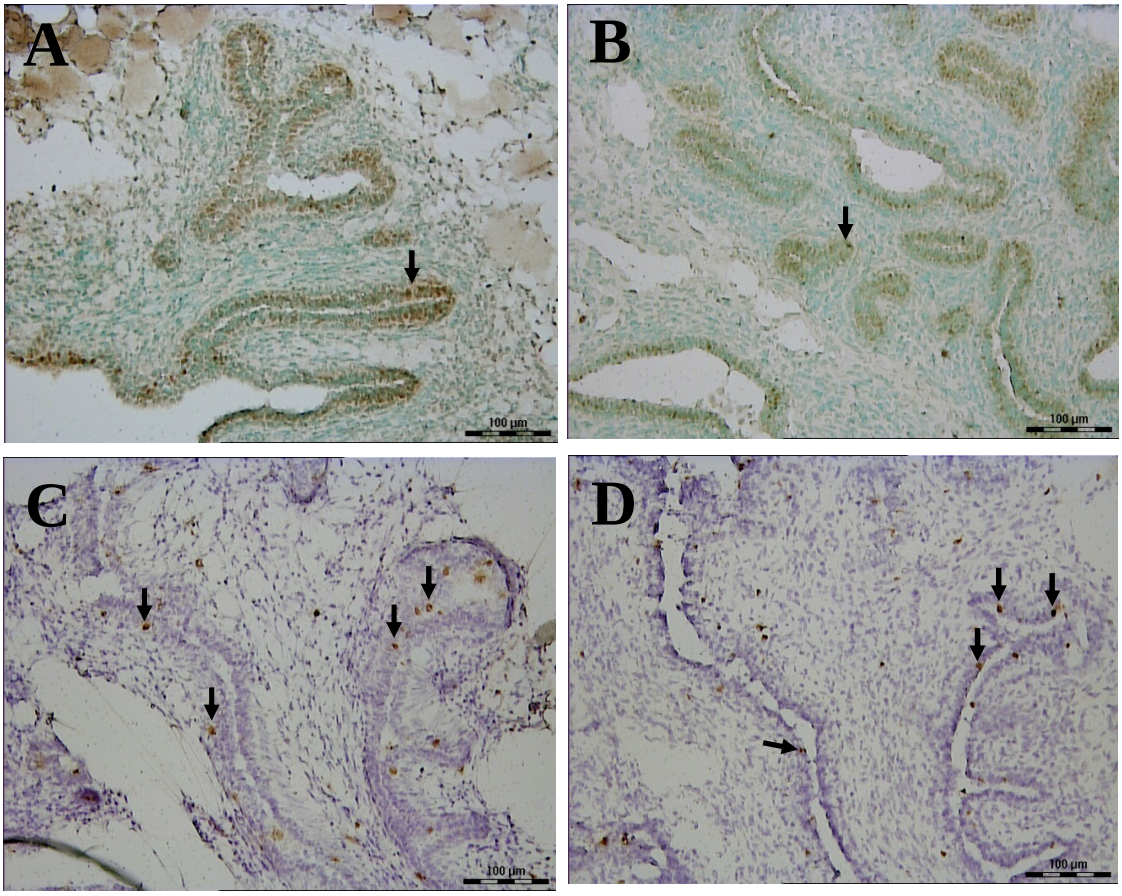

Figure 8. Serial cryosections of bovine mammary gland stained with estrogen receptor α (ERα) and Ki-67 antibody.

A) Immunostaining with ERα antibody in formamide-treated cryosection. Good tissue morphology and improved ERα labeling (more intensely labeled nuclei in terminal ductal units) were evident in formamide-treated sections.
B) Immunostaining with ERα antibody in PBS treated cryosection.
C) Immunostaining with Ki-67 antibody in formamide-treated cryosections. Good tissue morphology and more Ki-67-labeled cells were noted in formamide-treated sections.
D) Immunostaining with Ki-67 antibody in untreated cryosections.
Scale bar = 100 µm. Arrows indicate examples of labeled nuclei in each panel.

treatment (Figure 8D). This provided suggestive evidence for the applicability of our protocol to other non-DNA-specific nuclear antigens. The RNA integrity within these stained sections was not evaluated.

In conclusion, a rapid nuclear immunostaining method was developed with BrdU as the main antigen of study for bovine mammary cryosections. The method resulted in clear localization of BrdU-labeled cells and retention of good-quality RNA in the stained sections. This was achieved by fixation in ACEPEG, antigen retrieval with 70% formamide, and brief antibody incubation in the presence of RNase inhibitors. This protocol also resulted in clear localization of two other nuclear antigens, ERα and Ki-67, in cryosections.

This chapter is a modified version of the manuscript that was published in a peer-reviewed journal:

J. Dairy Sci. 93:2574–2579
doi:10.3168/jds.2009-2837

***Technical note*: A rapid method for 5-bromo-2′-deoxyuridine (BrdU) immunostaining in bovine mammary cryosections that retains RNA quality[1]**

R. K. Choudhary,* K. M. Daniels,†[2] C. M. Evock-Clover,† W. Garrett,‡ and A. V. Capuco†[3]
*Department of Animal and Avian Sciences, University of Maryland, College Park 20742
†Bovine Functional Genomics Laboratory, and
‡Animal Biosciences and Biotechnology Laboratory, USDA-ARS, Beltsville, MD 20705

Chapter 4: Mammary stem cells: Molecular profiling to identify novel biomarkers and the stem cell niche

Abstract

Mammary stem cells (MaSCs) account for the cell lineage of mammary epithelia and provide for mammary growth, development and tissue homeostasis. Previous molecular characterizations of MaSCs have utilized fluorescence-activated cell sorting or the in vitro cultivation of cells from enzymatically dissociated tissue to enrich for MaSCs. However, utilization of these approaches necessitates the loss of histological information encoding the in vivo locale of MaSCs and their more committed progenitor cell progeny. Here we report use of an alternative approach, laser microdissection, to excise putative MaSCs and control cells from their in situ locations in cryosections and to characterize the molecular properties of these cells. We identified MaSCs based upon their ability to retain bromodeoxyuridine for an extended period. Using laser microdissection, we isolated four categories of cells from mammary epithelium of female calves: bromodeoxyuridine label retaining epithelial cells (LREC) from basal (LRECb) and embedded layers (LRECe), and epithelial control cells from basal (ECb) and embedded layers (ECe). Enriched expression of genes in LRECb was associated with stem cell attributes and with Wnt, Notch and MAPK pathways of self-renewal and proliferation. Genes expressed in LRECe revealed retention of some stem-like properties along with up-regulation of differentiation factors and the Notch pathway involved in lineage commitment. The basal epithelium provided for the stem cell niche, characterized as a microenvironment whose cells expressed numerous survival and proliferation factors,

growth suppressors and chromatin modifiers. Our data suggest that LREC in the basal epithelial layer are MaSCs, as these cells showed enriched expression of genes that impart stem cell attributes; whereas LREC in suprabasal epithelial layers are more committed progenitor cells, expressing some genes that are associated with stem cell attributes along with those indicative of cell differentiation. Our results provide a molecular profile and novel candidate markers, evaluated by immunohistochemistry, for bovine MaSCs. Insights into the biology of stem cells will be gained by further confirmation of candidate MaSCs markers identified in this study. Genes encoding cell surface markers may prove useful for future isolation and investigation of MaSCs properties and their regulation.

Key words: mammary stem cell, laser microdissection, microarray

4.1 Background

In female mammals, growth and development of mammary glands occur primarily postnatally, with mammary function in the mature animal being tightly coupled to reproductive strategy. This dictates cycles of mammary growth, differentiation, lactation and regression, during which MaSCs provide for the lineages of lumenal and basal (myoepithelial) epithelial cells in the ducts and alveoli. Although mice have provided the primary model for study of mammary growth and development, a single model species cannot provide comprehensive knowledge. Because mammary glands of prepubertal calves have a tissue architecture resembling that of the prepubertal human breast more closely than does mouse (Capuco et al., 2002), cows provide an alternative experimental model for human breast development and a viable model for other species. Increased knowledge of MaSCs is directly applicable to agriculture and the development of management schemes to enhance the lifetime productivity of dairy cows.

A method that has been used to identify MaSCs is based upon the capacity of these cells to retain bromodeoxyuridine (BrdU) labeled DNA for an extended period (Capuco, 2007; Smith, 2005). We previously reported that label retaining epithelial cells (LREC) in the mammary epithelium of calves were localized in the basal layer (LRECb) or in the embedded (LRECe) layers between the basal and lumenal cells of a multilayered epithelium (Capuco, 2007; Capuco et al., 2009). LRECb were estrogen receptor-α (ESR1) negative and hypothesized to be MaSCs, whereas ESR1-positive LRECe were hypothesized to be progenitor cells. The estrogen receptor status of MaSCs is of considerable interest because of the importance of estrogens for MaSC function,

mammary ductal growth, and tumorigenesis. MaSCs of mouse and human are ESR1-negative (Anderson and Clarke, 2004; Sleeman et al., 2007).

Morphological evidence suggests that MaSCs are basally localized within the mammary epithelium, typically underlain by cytoplasmic extensions of epithelial cells and in close proximity to ESR1-positive epithelial cells (Brisken and Duss, 2007; Smith and Chepko, 2001). However, MaSCs have not been fully characterized due to technical limitations inherent in stem cell identification and in isolation of cells from known locations within the mammary epithelium. Based on fluorescence-activated cell sorting with multiple biomarkers and use of mammary transplantation methods to evaluate multi-lineage potency, Shackleton, Stingl and colleagues obtained and characterized a population of cells, from enzymatically dispersed mammary tissue, that was enriched for MaSCs (Shackleton et al., 2006; Stingl et al., 2006). Critical to success of this approach was use of markers to deplete the population of hematopoietic (CD45 and TER119) and endothelial cells (CD31), as well as markers to select epithelial cells (CD29, CD24), likely from a basal location. Another approach involved characterization of mammary epithelial cells that possess multipotency potential (MaSCs) in vitro (Dontu et al., 2003). These previous studies evaluated MaSCs after removing them from their stem cell niche, i.e. the microenvironment of surrounding signaling molecules and other noncellular components that support stem cell function and survival. We have taken an approach that retains histological information by characterizing gene expression in putative MaSCs directly after their in situ excision.

In the present study, putative stem and progenitor cells (LREC) were identified and excised from cryosections using laser microdissection. LREC and neighboring

epithelial control (non-LREC) cells were excised from two different locations: basal and embedded layers of the mammary epithelium. We hypothesized that LRECb are MaSCs and LRECe are more committed progenitor cells, and that by comparing the transcriptomes of these cells with neighboring control cells we would obtain molecular profiles and biomarkers for MaSCs and progenitor cells. Results support these hypotheses and provide novel candidate markers for MaSCs.

4.2 Materials and Methods

Experimental animals and mammary tissue

Use of animals for this study was approved by the Beltsville Agricultural Research Center's Animal Care and Use Committee. A flow chart of methodology for identification, isolation and characterization of LREC is provided in Appendix Figure 1. Tissues were obtained from five Holstein heifers, 3 months of age. Heifers were injected intravenously with BrdU (Sigma-Aldrich Co., St. Louis, MO) for 5 consecutive d. BrdU was administered in a saline solution containing 20 mg BrdU/mL (0.9% sodium chloride; pH 8.2) at a dosage of 5 mg/kg body weight, as described previously (Capuco, 2007). Heifers were sacrificed humanely (stunning with captive bolt and exsanguination) at the Beltsville Agricultural Research Center abattoir forty-five d after the last BrdU injection. Mammary tissue (~5x5x5 mm^3) was collected from the outer parenchymal region (region in close proximity to the border with mammary fat pad) of a rear mammary gland. Individual samples were immediately embedded in OCT compound (Sakura, Torrance, CA, USA), frozen in liquid nitrogen vapor and stored at -80°C until use. Cryosections of 8 μm thickness were thaw-mounted on ultraviolet-irradiated PEN slides (Leica AS, Wetzlar, Germany) and stored at -80°C until BrdU immunostaining and laser

microdissection within 8 d. Mammary tissues harvested for histological validation of microarray data were fixed overnight in 10% neutral buffered formalin at 4°C and then stored in 70% ethanol until further processing. Tissues were then dehydrated and embedded in paraffin according to standard techniques, sectioned at 5 μm thickness and placed onto Superfrost–plus™ slides (Erie Scientific Co., Portsmouth, NH, USA).

BrdU immunostaining to identify putative MaSCs

Putative MaSCs were identified as those cells in cryosections that retained BrdU label, visualized using an optimized method for BrdU immunostaining that retains RNA quality in tissue cryosections (Choudhary et al., 2010a). Sections were individually processed immediately before laser microdissection. The cryosections were fixed in acetone/polyethylene glycol 300 (9:1 v/v) at -20°C for 2 min and air dried for 1 min and then incubated with 0.5% methyl green for 2 min at RT. After a brief wash (10 s) with nuclease-free phosphate buffered saline (nfPBS), 400 μL of a pre-warmed solution of 70%, deionized formamide in nfPBS was pipetted onto the tissue and the section incubated at 60°C for 4 min. The section was washed with antibody dilution buffer (nfPBS with 1% normal goat serum and 0.1% triton-X 100) at 4°C on a metal plate kept on ice to prevent re-annealing of DNA strands and then incubated with mouse monoclonal anti-BrdU antibody conjugated to Alexa 488 (Clone PRB-1, 1:10 dilution, Molecular Probes, Carlsbad, CA, USA) for 5 min at RT in the dark. The section was washed briefly before counterstaining with propidium iodide (2.5 μg/μL in nfPBS). Finally, the slide was washed with nuclease-free water (10 s), dehydrated in ascending concentrations of ethanol and air dried before laser microdissection.

Laser microdissection and cDNA amplification

Immediately after staining, sections were examined and cells excised with a laser microdissection system equipped for epifluorescence microscopy (Leica AS-LMD, Mannheim, Germany). The laser setting was determined empirically and dissection performed using the 40X objective. We dissected 6 to 13 cells (equivalent to 3 to 7 cells by volume) per category per heifer. For each animal, cells in a given category were collected into the cap of a 0.2 mL thin walled PCR tube (Biozyme Scientific GmbH, Hess Oldendorf, Germany). Total processing time for immunostaining and microdissection was less than one hour, and only one slide was processed at a time. Four categories of cells were dissected: LREC from basal (LRECb) and embedded layers (LRECe), and epithelial control cells from basal (ECb) and embedded layers (ECe). Cells within the cap were dissolved in 2 µL of lysis buffer (WT-Ovation™ One-Direct RNA Amplification System; NuGEN Technologies, Inc. San Carlos, CA, USA). The tube was capped and centrifuged for one min at 13000 rpm, after which the tube and contents were vortexed gently for 30 s and centrifuged briefly before placing on ice. First strand cDNA synthesis and amplification reaction was carried out using Ribo-SPIA-based methodology according to the manufacturer's recommendations (NuGEN). Concentrations of amplified cDNA were determined spectrophotometrically (ND-1000, NanoDrop Technologies, Rockland, DE, USA). A known amount of high quality RNA (250 pg) was used as positive control for cDNA amplification. Nuclease-free water was used as a no-template control for cDNA amplification. The amplified cDNA was evaluated using RNA Nano-chips to estimate the median fragment size (Agilent Technologies, Palo Alto, CA, USA). Median fragment size for amplified samples was similar to the positive

control and fell within the expected range of 100-300 bp, whereas products for the no-template control were <50 bp.

Microarray analysis

Oligonucleotide microarray analysis was performed using a custom bovine microarray (Nimblegen, Inc., Madison, WI, USA) as described previously (Li et al., 2006). The bovine microarray consisted of 86,191 unique 60-mer oligonucleotides, representing 45,383 bovine sequences. After hybridization, scanning, and image acquisition, the data were extracted from the raw images using NimbleScan software (NimbleGen). A total of 21 microarrays (5 animals × 4 categories of cells, and no-template amplification control) were used. Relative signal intensities (log2) for each feature were generated using the robust multi-array average algorithm (Irizarry et al., 2003) and data were processed based on the quantile normalization method (Bolstad et al., 2003). Fold-change ≥ 2 and $P \leq 0.05$ were used to identify transcript abundance that differed among cell categories. Use of fold change and less stringent P-value cutoff has been reported to provide for consistent results and relevant biological pathway analysis (Guo et al., 2006). Genes that were differentially expressed were subjected to Ingenuity pathway analysis (IPA, Ingenuity Systems, www.ingenuity.com). IPA is biological data analysis software in which expression data differentially expressed genes, after preliminary background corrections and statistical analysis, are fed into the Ingenuity knowledge-based systems. IPA uses its knowledge base to build a network of genes with their interactions and identifies significant molecular and biological relationships. Known gene interactions are derived from curated literature. Significance of a biologically relevant network of genes is expressed in IPA score, which is derived from P-value and

indicates likelihood of the focused genes in a network being found together due to random chance. The IPA score is expressed as the negative log of the P-value. The data discussed have been deposited in NCBI's Gene Expression Omnibus (Edgar et al., 2002) and are accessible through GEO Series accession number GSE31541 (http://www.ncbi.nlm.nih.gov/geo/query/acc.cgi?acc=GSE31541).

Brightfield immunohistochemistry

Paraffin sections were dewaxed in xylene and hydrated in a graded series of ethanol to phosphate buffered saline (PBS, pH 7.4). Tissue sections were quenched with 3% H_2O_2 in PBS for 10 min and then washed in PBS. Antigen retrieval was performed by incubation with 70% formamide in PBS at 60°C for 5 min, or microwave heating in 10 mM Tris containing 1 mM EDTA, pH 9.0 (5 min heat, 5 min rest, 5 min heat, 25 min cooling). Sections were blocked with casein (CAS-block^{TM}, Invitrogen, Carlsbad, CA, USA). Primary antibodies NR5A2, NUP13 and HNF4A (Abcam Inc. Cambridge, MA, USA) were used at 1:200 dilution and FNDC3B (Santa Cruz, Santa Cruz, CA, USA) at 1:50. Sections were incubated with primary antibody for 2 h at RT or overnight at 4°C. After washing in PBS, sections were incubated with horseradish peroxidase-conjugated broad spectrum secondary antibody (ImmPRESS anti-mouse/anti-rabbit, Vector Labs, Burlingame, CA, USA). Positively labeled cells were visualized brown or purple using 3,3'-diaminobenzidine or ImmPACT VIP (Vector Labs), respectively. Slides were washed and then counterstained with hematoxylin or methyl green.

To determine if cells expressing FNDC3B were LREC, dual antigen labeling was performed. Tissue sections were processed as described earlier and incubated with mouse monoclonal BrdU antibody (Clone BMC 9318, 2 μg/mL; Roche Diagnostics Corp.,

Indianapolis, IN, USA) for 2 h at RT. Sections were then incubated with vector ImmPRESS anti-mouse polymer detection reagent (Vector Labs) for 20 min, followed by washing in PBS. BrdU was detected by incubation for 10 min with the chromagen 3,3'-diaminobenzidine. Sections were then washed in deionized water. Peroxidase activity was quenched for a second time with 3% H_2O_2 in PBS, followed by washings with water. Sections were blocked with casein and then incubated overnight at 4°C with FNDC3B rabbit polyclonal antibody (1:50 dilution), washed and then incubated with ImmPRESS anti-rabbit polymer detection reagent (Vector Labs) for 20 min. Sections were washed with PBS and FNDC3B staining was visualized after incubation with a contrast purple chromogen, ImmPACT VIP peroxidase substrate (Vector Labs). Sections were washed in deionized water, counterstained with 0.5% aqueous methyl green (Vector Labs), differentiated in 0.05% acetic acid/acetone, washed and dehydrated in ethanol, cleared in xylene and mounted in DPX (Sigma). Sections in which primary antibodies were omitted served as negative controls.

4.3 Results and Discussion

Transcriptomes of LRECb versus ECb

To evaluate the hypothetical stem cell nature of LRECb, we compared the transcript profiles of LRECb vs. neighboring control cells (ECb). Out of 611 genes, 592 identified and mapped to corresponding genes of IPA database (Appendix Table 1). Enriched expression of 387 genes in LRECb were involved in pathways linked to cancer, cell growth and proliferation, organism survival, cell cycle, and post-translational modifications (Appendix Table 5). A number of genes with documented relevance to MaSCs were identified in this analysis. Low expression of ESR1 and high expression of

aldehyde dehydrogenase 3B1 (ALDH3B1) in LRECb were consistent with MaSC character. Similar to the situation in mouse and human, bovine MaSCs appear to be ESR1-negative (Capuco et al., 2009), and aldehyde dehydrogenase activity has been used as a stem and progenitor cell marker in several tissues, including mammary gland (Douville et al., 2009). Increased abundance of HNF4A, NR5A2, NUP153 and FNDC3B mRNA and decreased abundance of X-chromosome inactivation factor (XIST) in LRECb are noteworthy (Appendix Table 1). Hepatocyte nuclear factor (HNF4A) is a liver stem cell transcription factor (Battle et al., 2006; Delaforest et al., 2011), and NR5A2 is a pluripotency transcription factor analogous to OCT4 (Heng et al., 2010). Lack of XIST in LRECb is consistent with MaSCs identity, as absence of XIST expression and low XIST expression have been associated with hematopoietic stem and progenitor cells, respectively (Savarese et al., 2006). Transcripts of several genes that are involved in epigenetic modification of chromatin were also enriched in LRECb. Relative to ECb, LRECb expressed a greater number of transcription regulators, zinc fingers and nuclear transporters (e.g., NUP153, IPO13). Overall, the transcriptome profile of LRECb is consistent with expectations for MaSCs. Further evidence in support of the stem cell nature of LRECb comes from biological pathway analysis of differentially expressed genes. Ingenuity Pathway Analysis of genes that were differentially expressed in LRECb and ECb revealed biological processes and networks that were highly significant. The most significant networks associated with LRECb related to cellular growth and proliferation (Figure 9A, IPA score = 58), and cell cycle and posttranslational modification (Figure 9B, IPA score = 34). The network of cellular growth and

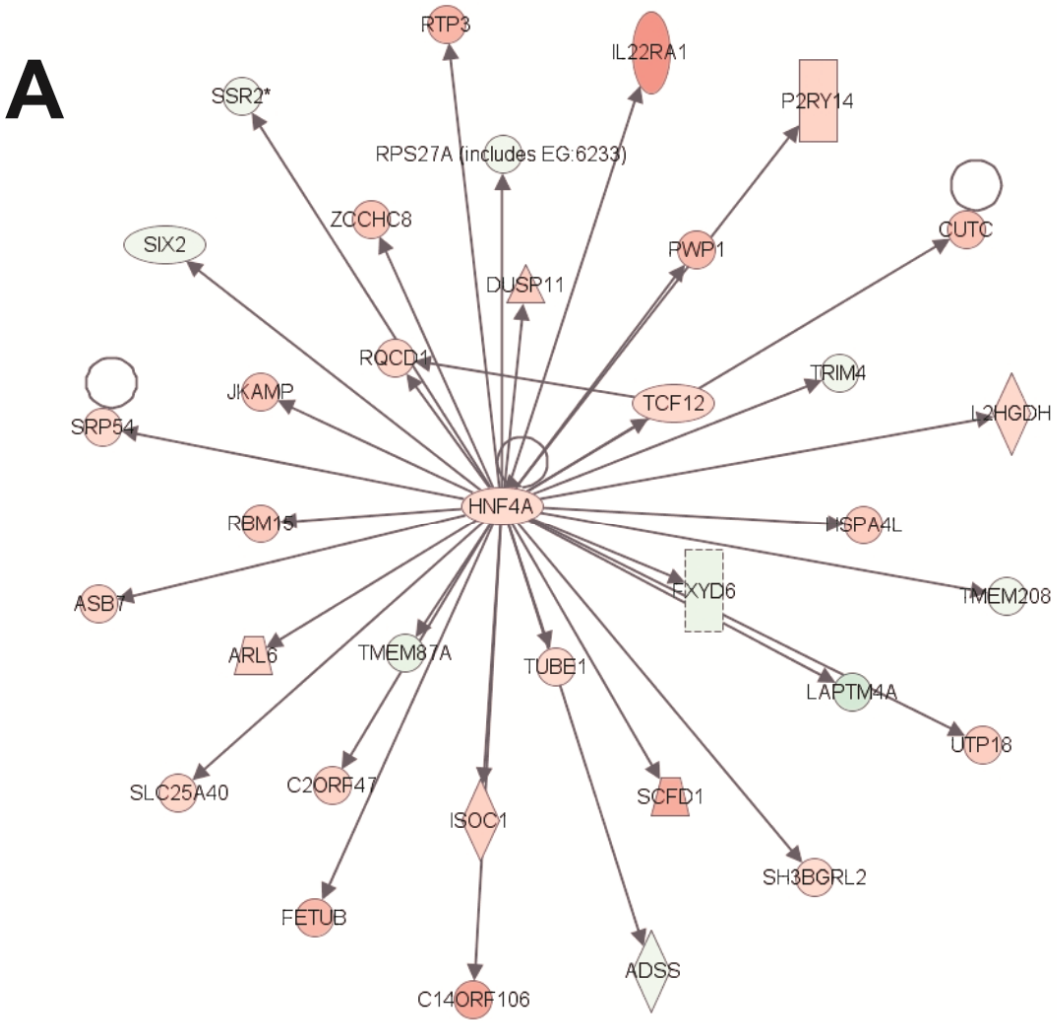

Figure 9A. Network of cellular growth and proliferation: Ingenuity Pathway Analysis (IPA) on genes differentially expressed in LRECb vs. ECb.Genes that were differentially expressed in LRECb vs. ECb were imported into IPA software, which revealed the involvement of several networks pertinent to LRECb. Network (A) pertains to cellular growth and proliferation and shows a single module with HNF4A at its hub. Red color denotes up-regulation in LRECb and green color denotes down-regulation in LRECb relative to control cells. The IPA legend is shown in Appendix Figure 2.

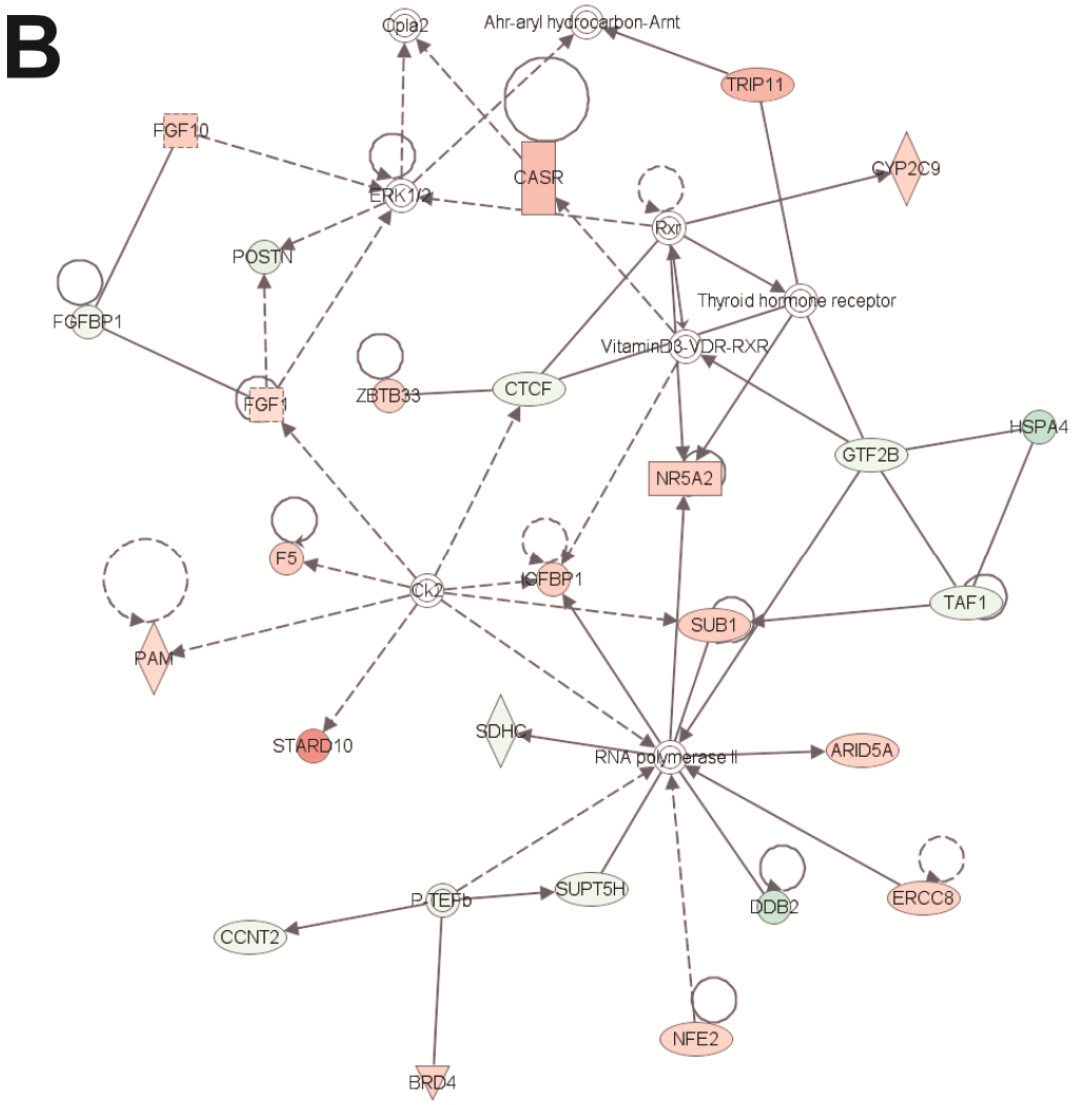

Figure 9B. Network of cell cycle and post-translational modification: Ingenuity Pathway Analysis (IPA) on genes differentially expressed in LRECb vs. ECb.Genes that were differentially expressed in LRECb vs. ECb were imported into IPA software, which revealed the involvement of several networks pertinent to LRECb. Network (B) relates to cell cycle and post translational modification. Red color denotes up-regulation in LRECb and green color denotes down-regulation in LRECb relative to control cells. The IPA legend is shown in Appendix Figure 2.

proliferation (Figure 9A) contains a single module with HNF4A, up-regulated in LRECb, as the hub. Down-regulation of developmental genes like SIX2 and XIST suggests that LRECb are undifferentiated cells. KEGG pathway analysis using DAVID (Huang et al., 2009) revealed that genes which were differentially expressed in LRECb vs. ECb (FGF, BRAF, ATF4, CREB3, GLK, HSPA8,TAOK3, CDC25B) were components of the MAPK pathway, a pathway involved in cellular growth and proliferation, and components of the Wnt (Dvl, PPP2R5E, SMAD4) and TGF-β (FST and SMAD4) pathways, which are associated with stem cell renewal (Esmailpour and Huang, 2008; Mazumdar et al., 2010).

Transcriptomes of LRECe versus ECe

Comparison of transcriptome profiles of LRECe and neighboring ECe identified 101 functionally identifiable genes that were differentially expressed (Appendix Table 2) and supported classification of LRECe as progenitor cells. The most significant network associated with these genes was related to cancer (Figure 10A, IPA score = 51), followed by a network associated with DNA replication, recombination and repair (Figure 10B, IPA score = 36) that contained an HNF4A module. Conservation of the HNF4A module in LRECe and LRECb suggests a hierarchical similarity between LRECe and LRECb; although HNF4A transcripts were not significantly up regulated in LRECe and genes involved in this module differed between the two categories of LREC. Enriched expression of NR5A2, NUP153 and FNDC3B in both LRECe and LRECb (vs. ECe and ECb, respectively) provides another line of evidence for the similarity of LREC in basal and embedded epithelial layers. NR5A2 is a pluripotency factor, and NUP153 and

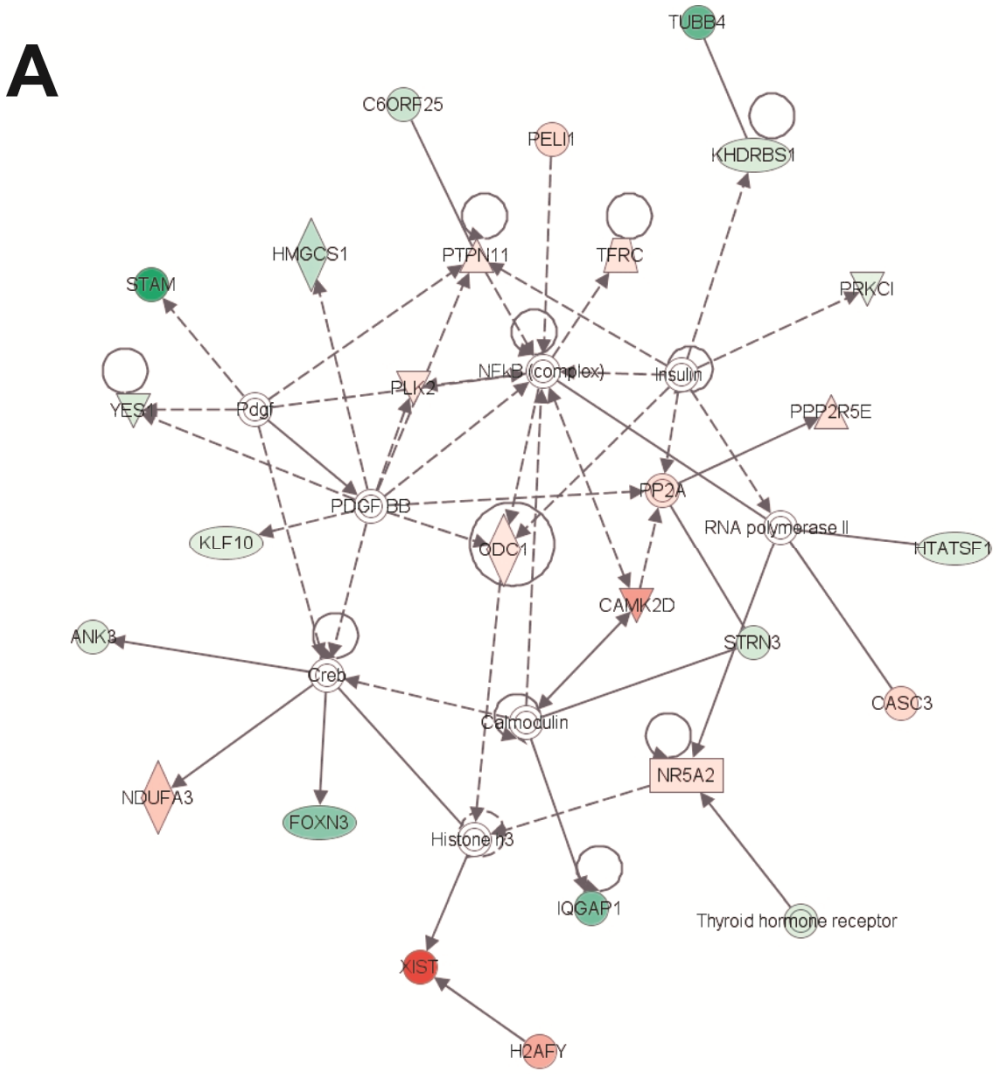

Figure 10A. Network of cancer: Ingenuity Pathway Analysis (IPA) on genes differentially expressed in LRECe vs. ECe. Genes that were differentially expressed in LRECe vs. ECe were imported into IPA software, which revealed the involvement of several networks pertinent to LRECb. Network (A) relates to cancer. Red color denotes up-regulation in LRECe and green color denotes down regulation in LRECe relative to control cells. The IPA legend is shown in Appendix Figure 2.

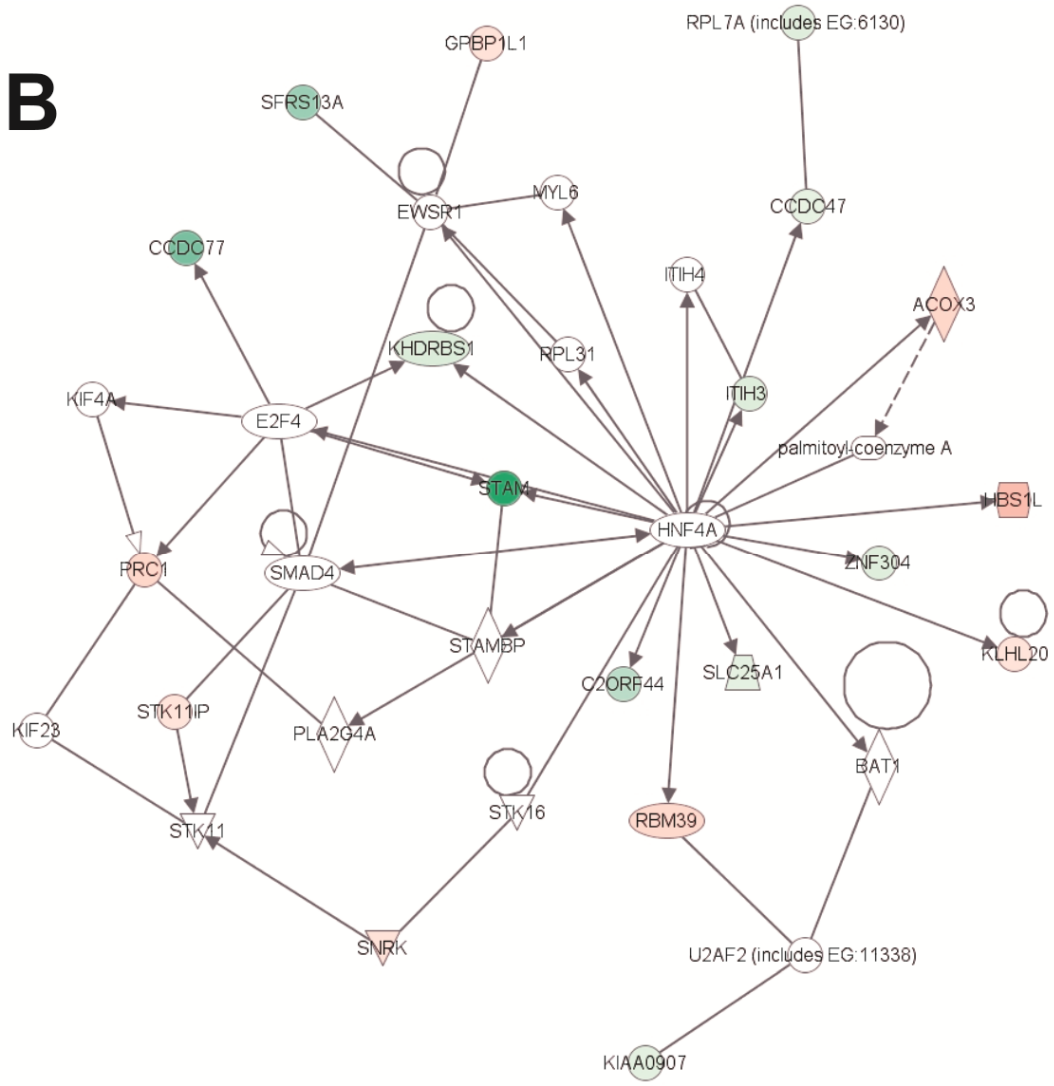

Figure 10B. Network of DNA replication, recombination and repair: Ingenuity Pathway Analysis (IPA) on genes differentially expressed in LRECe vs. ECe.Genes that were differentially expressed in LRECe vs. ECe were imported into IPA software, which revealed the involvement of several networks pertinent to LRECb. Network (B) pertains to DNA replication, recombination and repair and contains a HNF4A module. Red color denotes up-regulation in LRECe and green color denotes down regulation in LRECe relative to control cells. The IPA legend is shown in Appendix Figure 2.

FNDC3B have been characterized as markers of proliferation and cell migration. KEGG pathway analysis of transcripts that were up-regulated in LRECe vs. ECe using DAVID (data not shown) identified upregulation of Wnt pathway (Dvl, PP2A, CaMKII) and actin cytoskeleton pathway (GPCR, CALMKII).

Transcriptomes of LRECb versus LRECe

To evaluate the relative characteristics of LRECb and LRECe, transcript profiles for these cells were compared. We identified 274 genes that were differentially expressed in LRECb vs. LRECe (Appendix Table 3). The molecular profile of LRECb included increased abundance of transcripts for stem cell markers (NR5A2, NES), cell survival and proliferation factors (IGF2, FGF2, FGF10, HSPB6, LAMC1) and DNA repair enzymes (EXO1, MSH60, MDC1). Relatively high expression of stem cell markers, growth and survival factors, DNA repair enzymes and low expression of apoptotic genes and differentiation markers supported greater "stemness" of LRECb vs. LRECe. In addition, enriched expression of cell adhesion molecules (CADM3, NCAM, AOC3), growth factors (CSF3, FGF2, FGF10, FST, IGF2, IL33, MESDC2, AGT), and a number of cell surface markers (ANX46, CPRC5, CXCR4, DRD2, GNB4, GRB14, SDPR, THY1/CD90, TRIB2) were noted in LRECb. The LRECe were characterized (Table 2) by increased expression of XIST, splicing factor arginine/serine-rich 5 (SFRS5), THAP domain containing apoptosis associated protein 3 (THAP3), and calcium/calmodulin-dependent protein kinase II delta (CAMK2D). Increased expression of glucose metabolic enzymes, glucose phosphate isomerase (GPI) and UDP-glucose pyrophosphorylase 2 (UGP2) were also characteristics of LRECe. Additionally, KEGG pathway analysis revealed upregulaton of the Notch pathway (Dvl, CAMK2D) in LRECe. The most

Table 2. Top 10 up-regulated and down-regulated genes in LRECb vs. LRECe

Gene Symbol	Chromosome	Gene summary
Up-regulated in LRECb		
FBXO34	14	Members of F-box proteins, act as protein-ubiquitin ligase
USP15	12	Ubiquitin, a highly conserved protein involved in the regulation of intracellular protein breakdown, cell cycle regulation, and stress response, is released from degraded proteins by disassembly of the polyubiquitin chains.
RPS7	2	This gene encodes a ribosomal protein that is a component of the 40S subunit. The protein belongs to the S7E family of ribosomal proteins.
CFL1	11	Cofilin is a widely distributed intracellular actin-modulating protein that binds and depolymerizes filamentous F-actin
COLIA2		This gene encodes the pro-alpha2 chain of type I collagen whose triple helix comprises two alpha1 chains and one alpha2 chain.
RRN3	16	Biogenesis, proliferation, apoptosis, survival
HSPB6		HSPB6 is associated with actin, response to heat
TRIB2	2	An oncogene that inactivates the transcription factor C/EBPalpha (CCAAT/enhancer-binding protein alpha) and causes acute myelogenous leukemia.
NUP153	6	Epigenetic role in modifying chromatin structures
LAMC1	1	Laminins, has a wide variety of biological processes including cell adhesion, differentiation, migration, signaling, neurite outgrowth and metastasis.
UP-regulated in LRECe		
XIST	X	The XIST gene is expressed exclusively from the XIC of the inactive X chromosome.
C17ORF49	19	Unknown
SFRS5	14	Nuclear mRNA splicing, via spliceosome; mRNA splice site selection; RNA splicing; regulation of cell cycle
THAP3		An apoptosis associated protein 3, Function unknown
STK11IP	2	Serine/threonine kinase 11 interacting protein, Function unknown
UGP2	2	The enzyme transfers a glucose moiety from glucose-1-phosphate to MgUTP and forms UDP-glucose and MgPPi. In liver and muscle tissue, UDP-glucose is a direct precursor of glycogen; in lactating mammary gland it is converted to UDP-galactose which is then converted to lactose.
SLC3A2	11	This gene is a member of the solute carrier family and encodes a cell surface, transmembrane protein
EIF4E3	3	EIF4E3 belongs to the EIF4E family of translational initiation factors that interact with the 5-prime cap structure of mRNA and recruit mRNA to the ribosome
CAMK2D	4	The product of this gene belongs to the serine/threonine protein kinase family and to the Ca(2+)/calmodulin-dependent protein kinase subfamily.
CPEB1	15	Members of this protein family regulate translation of cyclin B1 during embryonic cell divisions.

significant network associated with genes that were differentially expressed in LRECb vs. LRECe was related to tissue development, cell growth and proliferation (Figure 11A, IPA score = 43). This network showed up-regulation inLRECb of HIP1, which may be required for differentiation or survival of somatic progenitors, and TRIB2, which modulates signal transduction pathways and may promote growth of mouse myeloid progenitors. This was followed by a network associated with tissue injury (Figure 11B, IPA score = 34), featuring up regulation of a heat shock protein module in LRECb. The top three canonical pathways associated with LRECb vs. LRECe pertained to the mitotic roles of polo-like kinases, cleavage and polyadenylation of pre-mRNA, and chemokine signaling. Polo-like kinases are key centrosome regulators. Asymmetric localization of polo-kinase promotes asymmetric division of adult stem cells (Rusan and Peifer, 2007).

Transcriptomes of ECb versus ECe

Epithelial cells isolated from basal and embedded layers exhibited transcriptome profiles that were consistent with their location. Analysis identified 318 genes that were differentially expressed (Appendix Table 4), 267 of which were functionally identifiable. Among these, ECb expressed increased transcript levels for cell structural and motility genes, including actin (ACTA2), myosin (MYL12A, MYO6), tropomyosin (TPM4), catenin, tubulin, titin (myosin head adaptor protein), spectrin (actin cross linking scaffold protein) and tetraspanin 31. Transcripts for JAG-1 (a ligand of Notch pathway) fibroblast growth factors (FGF1, FGF2, FGF10), insulin like factor-2 (IGF2), follistatin (FST), and IGF2 were enriched in basal epithelial cells. The enriched expression of integrin-β1 within ECb was consistent with its use as a marker to isolate MaSCs (Shackleton et al., 2006), most likely to enrich the sorted populations of basal epithelial cells. Additionally,

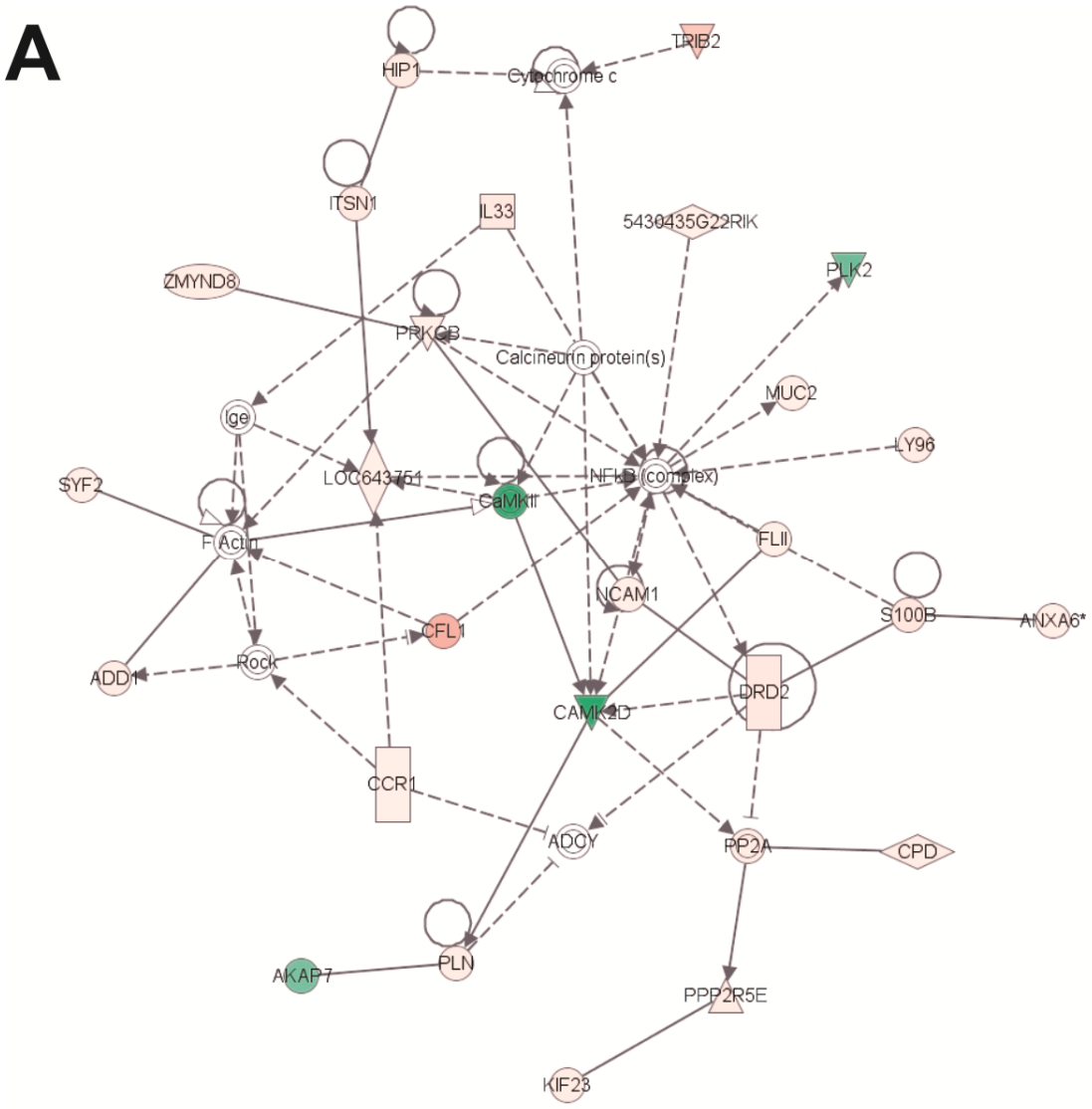

Figure 11A. Network of tissue development, cell growth and proliferation: Ingenuity Pathway Analysis (IPA) on genes differentially expressed in LRECb vs. LRECe.

Genes that were differentially expressed in LRECb vs. LRECe were imported into IPA software, which revealed the involvement of several networks pertinent to LRECb. Network (A) pertains to tissue development, cell growth and proliferation. Red color denotes up-regulation in LRECb and green color denotes down-regulation in LRECb relative to control cells. The IPA legend is shown in Appendix Figure 2.

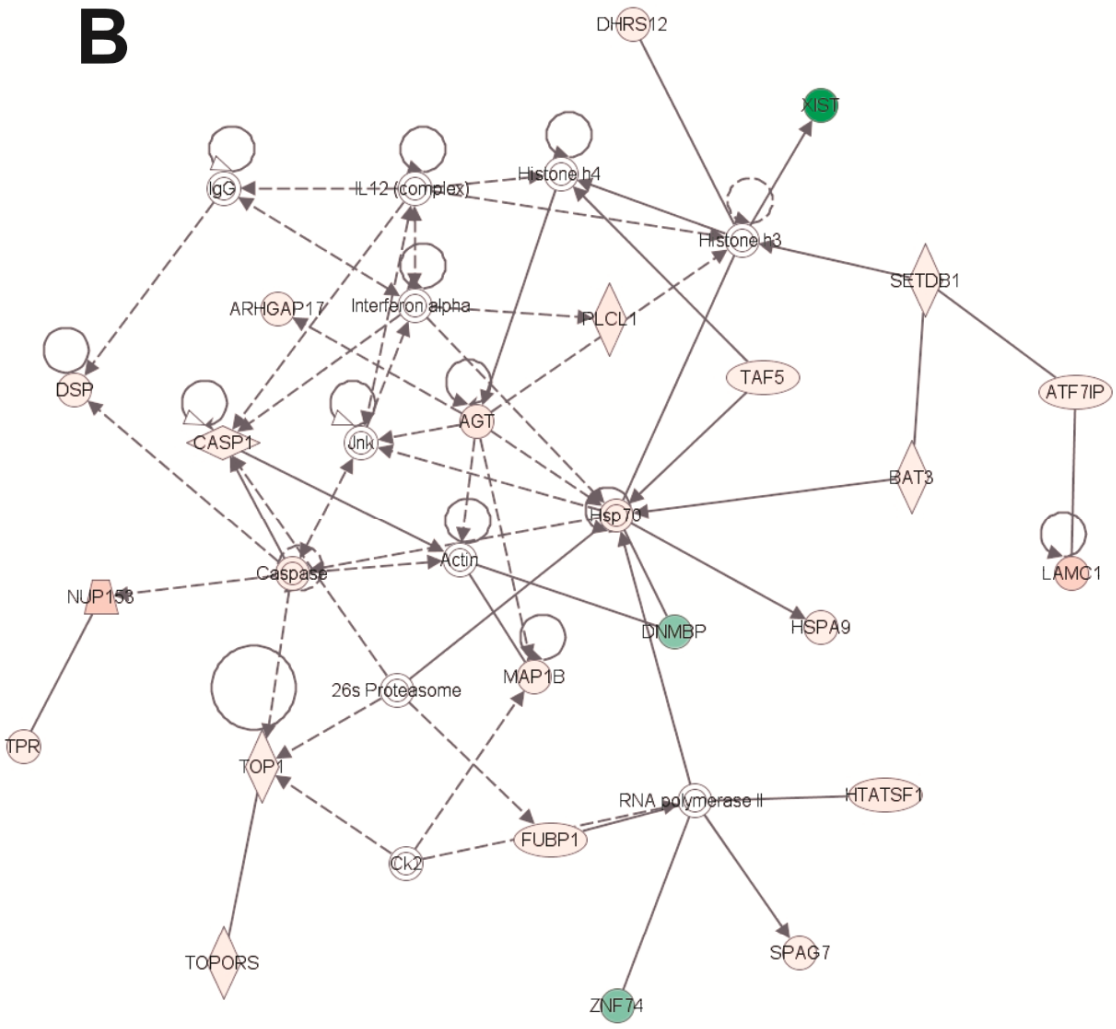

Figure 11B. Network of tssue injury featuring heat shock proteins (HSPs): Ingenuity Pathway Analysis (IPA) on genes differentially expressed in LRECb vs. LRECe.

Genes that were differentially expressed in LRECb vs. LRECe were imported into IPA software, which revealed the involvement of several networks pertinent to LRECb. Network (B) is associated with tissue injury and contains a heat shock protein module that was up-regulated in LRECb. Red color denotes up-regulation in LRECb and green color denotes down-regulation in LRECb relative to control cells. The IPA legend is shown in Appendix Figure 2.

a number of heat shock proteins (HSAA8, HSPA4, HSP90AB1, HSP90A1), peptidases (USP4, USP16, USP54, PRSS3, TTN, PSMD14, MME, PDIA3), ribosomal proteins, translational regulators, components of the ECM and its regulators (collagens, MFAP5, FBN, FSTL1, CHAD, ERBB2IP, SPARC), and tumor suppressors (MTSS1, Myc binding proteins) were also up-regulated in ECb. However, transcripts of membrane transporters (AP1M1, APOE, AQP7, SLC13A3, SLC38A3, TMED3, CLCN3) were more highly expressed in ECe than ECb. Thus, control cells harvested from basal and embedded layers within the mammary epithelium possess different character and represent two distinct cell populations. To understand key biological processes occurring in basal and embedded epithelium, we utilized Ingenuity pathway analysis (IPA) to generate gene networks and canonical pathways for genes that are differentially expressed between ECb and ECe. All identified networks (Networks of endocrine system development and function, cancer, cell cycle, tissue development) were highly significant as measured by IPA score (ranges from 35 to 42). The identified network for endocrine development and function, lipid metabolism (Figure 12A) features an estrogen signaling module, peptidase, ubiquitination and ubiquitin modules. The identified network for cancer (Figure 12B) contains two heat shock protein modules. The canonical pathways identified by IPA analysis were protein ubiquitination, hypoxia signaling and clathrin mediated endocytosis. Consistent with expression in the basal epithelium, specific cell adhesion molecules, extrinsic growth factors and regulators, and hypoxia-inducing factor have been identified as molecules prevalent in the stem cell niche of the basal epithelium (Figure 13).

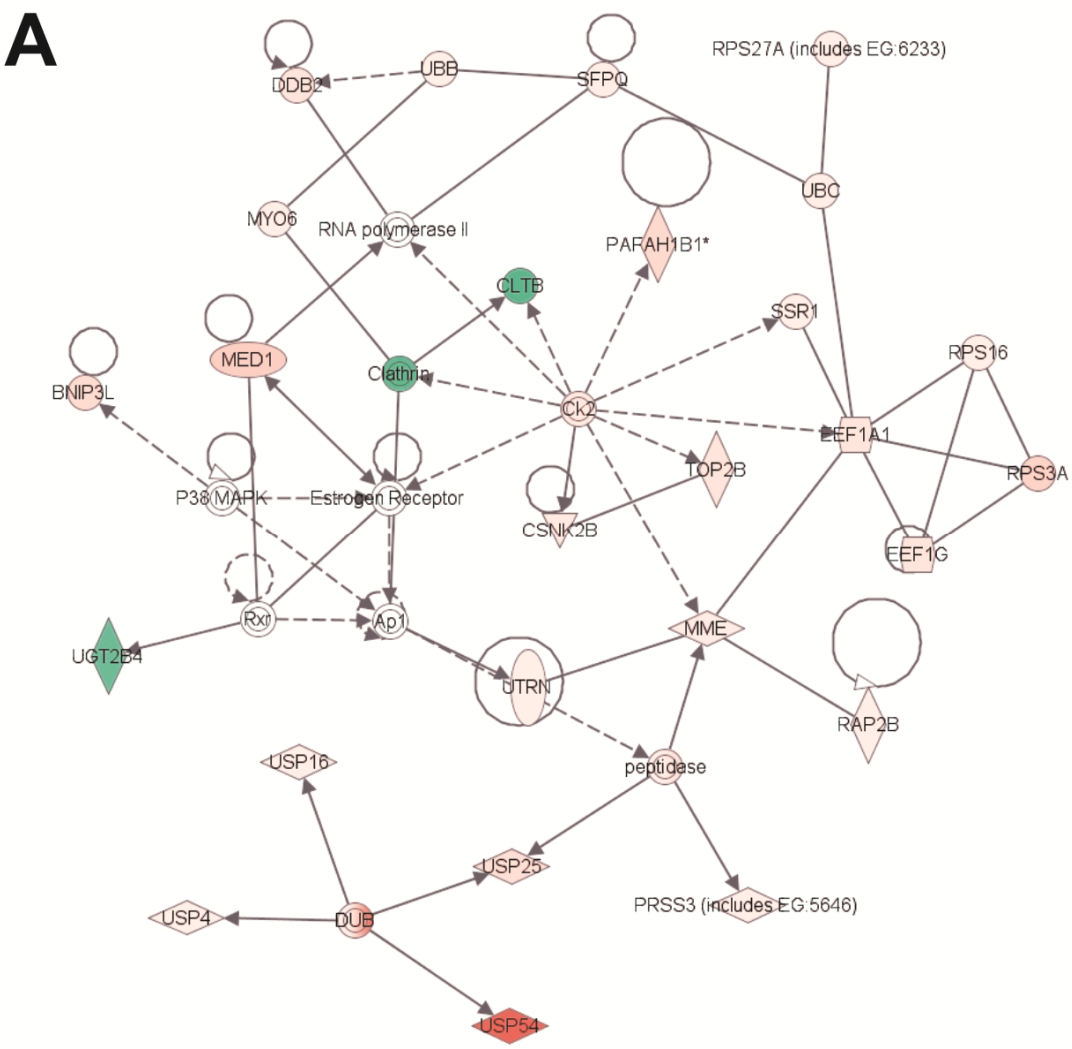

Figure 12A. Network for endocrine development and fuction: Ingenuity Pathway Analysis (IPA) on genes differentially expressed in ECb vs. ECe.

Genes that were differentially expressed in ECb vs. ECe were imported into IPA software, which revealed the involvement of several networks pertinent to ECb. Network (A) pertains to endocrine development and function, lipid metabolism.. Red color denotes up-regulation in LRECb and green color denotes down-regulation in LRECb relative to control cells. The IPA legend is shown in Appendix Figure 2.

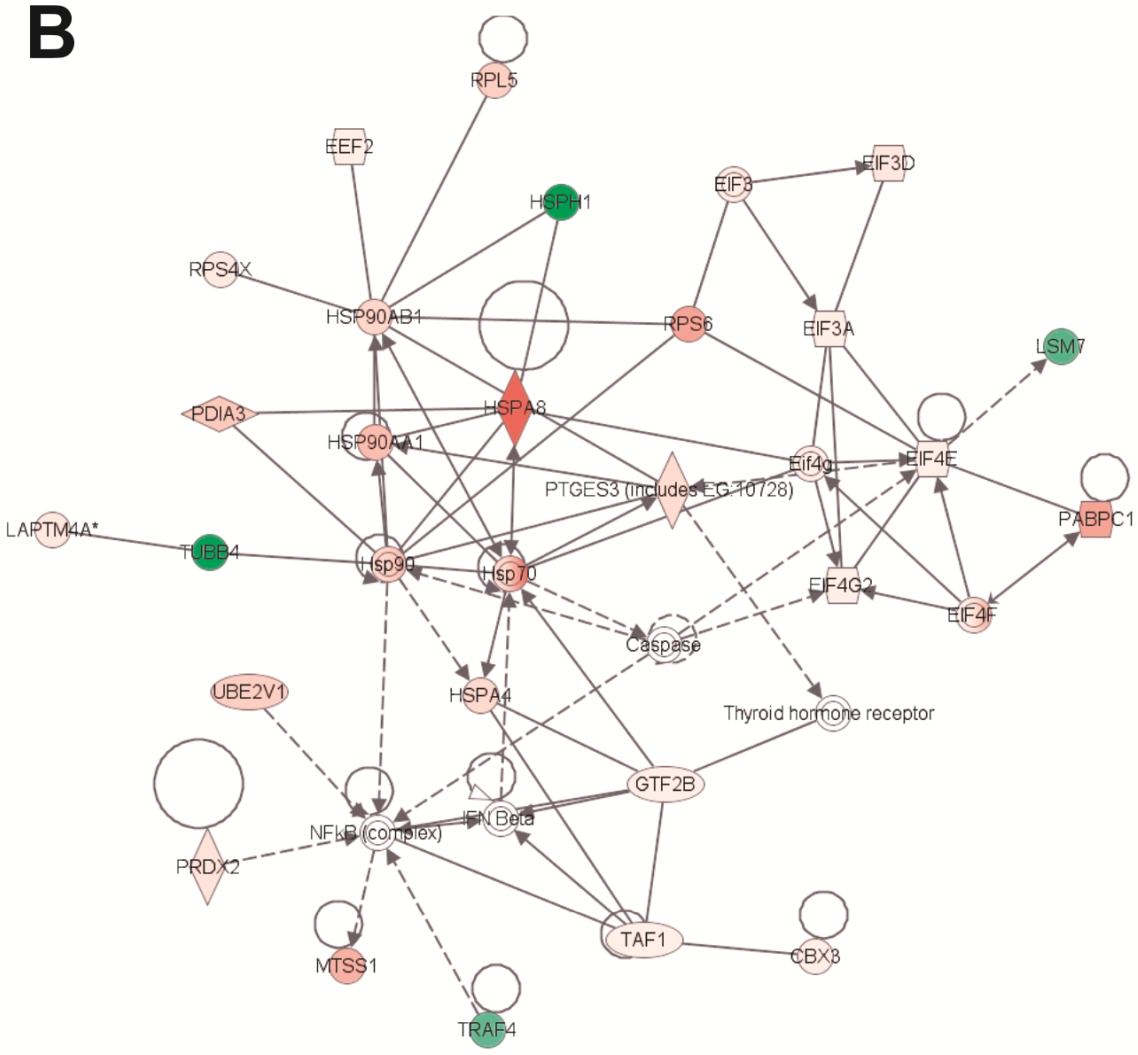

Figure 12B. Network for cancer: Ingenuity Pathway Analysis (IPA) on genes differentially expressed in ECb vs. EC. Genes that were differentially expressed in ECb vs. ECe were imported into IPA software, which revealed the involvement of several networks pertinent to ECb. Network (B) is associated with cancer and contains two heat shock protein modules. Red color denotes up-regulation in LRECb and green color denotes down-regulation in LRECb relative to control cells. The IPA legend is shown in Appendix Figure 2.

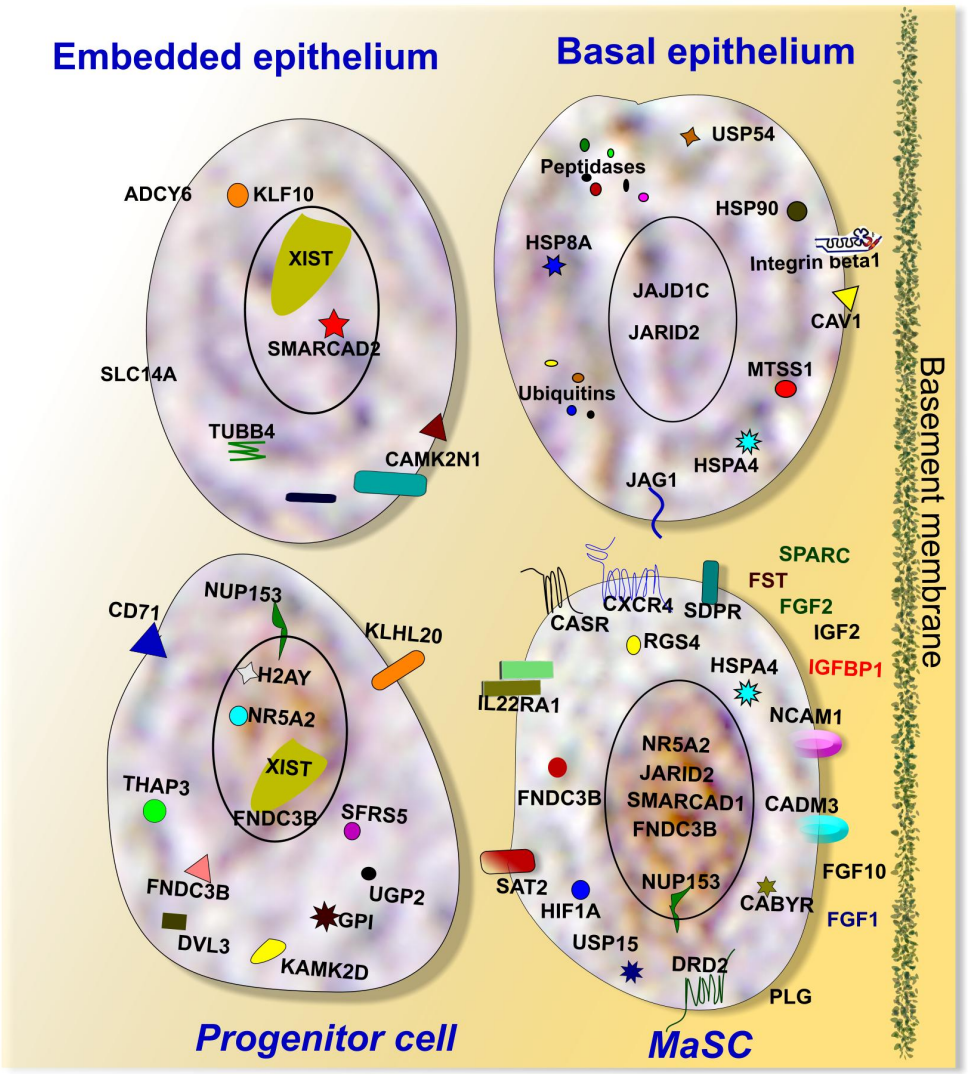

Figure 13. Schematic representation of characteristics of bovine putative MaSCs (LRECb) and progenitor cells (LRECe). Putative MaSCs (LRECb) are localized in the basal epithelium in a stem cell niche characterized as an environment enriched for extracellular growth factors, tumor suppressors for regulating MaSCs function. LRECb exhibit enriched expressions of adhesion molecules and a variety of potential MaSCs biomarkers including HNF4A and the pluripotency marker, NR5A2. Putative progenitor cells (LRECe) also express NR5A2 but at a reduced level along with increased expression of differentiation factors including XIST.

Immunohistochemical evaluation of LRECb and LRECe markers

Genes that are highly expressed in LRECb and LRECe may provide novel markers for MaSCs and progenitor cells. Those that were evaluated by immunohistochemistry were: *NR5A2, NUP153, FNDC3B* and *HNF4A*. *NR5A2* is a pluripotency gene that aids in inducing somatic cells into pluripotency (iPSC) (Heng et al., 2010). *NUP153* is a nuclear basket protein that can cause chromatin modification (Vaquerizas et al., 2010), and *FNDC3B* is a regulator of adipogenesis and cell proliferation, adhesion, spreading and migration (Nishizuka et al., 2009). *HNF4A* may serve as a stem cell regulator (Koh et al., 2010; Douville et al., 2009; Battle et al., 2006) and was identified as a key pathway component by IPA analysis of expression data for LRECb and LRECe. Transcripts for *NR5A2, NUP153, FNDC3B* and *HNF4A* were more abundant (> log2 fold change) in LRECb than in control cells, with the greatest expression in LRECb (LRECb>LRECe>EC).

Immunohistochemical analysis showed that a small number (1-6%) of epithelial cells expressed these potential markers. In agreement with transcript abundance, positive cells in the basal epithelium appeared intensely stained than those in suprabasal locations. The abundance and localization of NR5A2, NUP153 FNDC3B and HNF4A-positive cells (Figure 14A-D) were similar to that of LRECs. Co-localization studies showed that LREC expressed these markers. Surprisingly, expression of FNDC3B was not limited to the cytoplasmic compartment of the cell. Expression of FNDC3B was found to be cytoplasmic (arrows) and nuclear (arrowheads) and co-expressed with BrdU in approximately half of the LRECb (Figure 14E). Because of their potential utility for cell

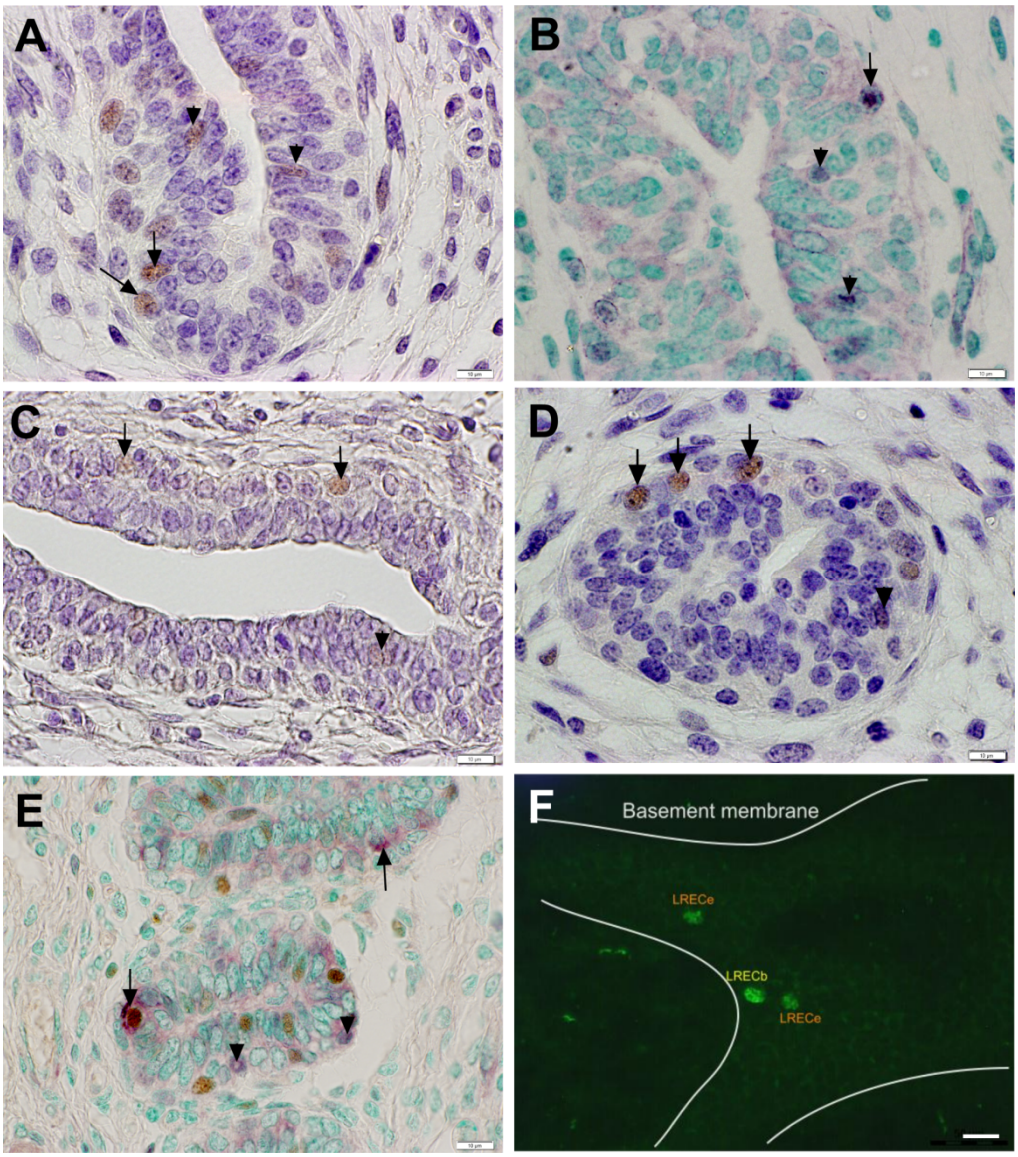

Figure 14. Immunohistochemical localization of potential mammary stem/ progenitor cell markers.

A-D- Consistent with transcriptome data, cells that were positive for these novel markers were more strongly labeled (brown nuclei) in the basal layer of mammary epithelium than in the embedded layers. Solid arrows designate labeled nuclei of basal cells and arrowheads designate labeled nuclei of embedded epithelial cells. NR5A2.(A), NUP153 (B), FNDC3B (C), HNF4A (D), FNDC3B (E) expression by LREC. Localization of FNDC3B (purple) to the nucleus (arrow) and cytoplasm (arrowhead) of LRECb (brown) is depicted (E). F- Identification of LREC in cryosections used for laser microdissection. Basal and embedded cells retaining BrdU label are designated, along with the location of the basal membrane. Scale bar = 10 μm.

sorting, we also identified transcripts that encoded surface proteins and were up-regulated in LRECb. These included *SAT2,CXCR4, SDPR, RTP3, CASR, GNB* and *DRD2.* However, we have not evaluated the suitability of these membrane markers for identifying and enriching stem cell populations by flow cytometry.

Discussion

To address our hypothesis that LRECb represent MaSCs and that LRECe more committed progenitors, we performed transcriptome analyses on four populations of bovine mammary epithelial cells obtained by laser microdissection of LREC and EC from different epithelial layers (basal and embedded layers). Microarray analysis revealed distinct gene signatures for the four categories of mammary epithelial cells: LRECb, LRECe, ECb and ECe. Comparison of LRECb vs. ECb and LRECe vs. ECe suggested that LRECb are enriched for MaSCs and LRECe for progenitor cells. Furthermore, factors that are important for maintenance of the stem cell niche were evident in the basal epithelium.

The ECb and ECe were distinguishable by the increased abundance of transcripts in the basal cells for genes encoding structural and motility proteins, extracellular growth factors, extracellular matrix (ECM) proteins and ECM regulators. Additionally, increased expression of transcripts for heat shock proteins, peptidases, ribosomal proteins, ubiquitins, proteins that provide interaction between the cell and the ECM (caveolin-1, β1-integrin), tumor suppressors, and epigenetic modifiers (JARID2, JMJD1C) are also characteristic of ECb. Myoepithelial cells, present in the basal layer of mature mammary epithelium, may be a part of the stem cell niche and their paracrine factors may regulate the proliferation, polarity and motility of mammary epithelial cells (Polyak and Hu,

2005). However, the precise nature of the ECb in a calf is uncertain. Expression of markers for myoepithelial cells in mammary tissue from prepubertal heifers is absent or expressed in a limited fashion (Ballagh et al., 2008; Capuco et al., 2002).

Transcriptome analysis of LRECb vs. ECb showed that LRECb possess characteristics of MaSCs. Our mRNA data were consistent with the lack of expression of ESR1 and increased expression of ALDHB1 in LRECb. As in mouse (Sleeman et al., 2007) and human (Anderson and Clarke, 2004) bovine MaSCs appear to be ESR1-negative (Capuco et al., 2009). Further, ALDH1 activity has been used as an effective stem and progenitor cell marker in several tissues including blood, lung, prostate, pancreas and breast (Douville et al., 2009). However, 17 isoforms of ALDH have been identified (Sladek, 2003) with different cellular and species expression patterns (Hess et al., 2004). ALDHB1 is expressed by bovine MaSCs. Increased abundance of HNF4A, NR5A2, NUP153 and FNDC3B mRNA and decreased abundance of XIST transcripts (noncoding) in LRECb are noteworthy. HNF4A is a hepatic stem cell transcription factor whose associated network was highly up-regulated in LRECb, suggesting a key role in these cells. It is noteworthy that HNF4A has recently been implicated as a regulator of mesenchymal stem cells (Koh et al., 2010). Lack of expression or low expression of XIST has been associated with stem and progenitor cells, respectively, in hematopoietic tissue (Savarese et al., 2006). Subsequently, we evaluated four potentially novel markers for stem/progenitor cells (NR5A2, NUP153, FNDC3B, HNF4A) immunohistochemically and found protein expression profiles that were consistent with the observed transcript abundance in LRECb and LRECe.

Because of their potential utility for cell sorting, we identified transcripts that encoded surface proteins and were up-regulated in LRECb. Among the cell surface markers, THY1/CD90 is a proposed marker for mesenchymal, liver, keratinocyte, endometrial and haematopoietic stem cells. TRIB2 is an oncogene shown to prolong growth of mouse myeloid progenitors (Keeshan et al., 2010). CXCR4 is a receptor for stromal derived factor 1 (SDF-1) and its activation was associated with breast cancer invasiveness (Kang et al., 2005). SAT2 is the target of DNA methyltransferse 1 (DNMT1) and an epigenetic modifier, whose methylation status may serve as a marker for cancer prognosis (Jackson et al., 2004). CXCR4 is a proposed marker of non-hematopoietic stem cells and regulator of neural stem cell trafficking and tumor metastasis (Ratajczak et al., 2006). SDF-1 is positively regulated by HIF1α and negatively regulated by CXCR4 receptor, which in turn is regulated by G-protein signaling (RGS) proteins. RGS4, which was up regulated in LRECb, is likely to be an RGS protein regulating SDF-1 responsiveness to CXCR4 in the mammary gland.

Up-regulation of growth factors such as fibroblast growth factors (FGF1, FGF2, FGF10), insulin-like factor-2 (IGF2) and plasminogen (PLG) in the basal epithelial layer suggest a function of these molecules as regulators of MaSCs. Role of FGFs in mammary gland development and growth has been demonstrated (Mailleux et al., 2002; Sinowatz et al., 2006).

Further evidence in support of LRECb being mammary stem cells comes from biological pathway analysis of differentially expressed genes. A number of differentially expressed genes (LRECb vs. ECb) were involved in MAPK, Wnt and TGF-β pathways. The MAPK pathway regulates cellular growth and proliferation. Wnt and TGF-β

pathways are both involved in mechanism of mammary stem cell renewal. A theme emerging from a variety of data is that stem cells exhibit characteristics of cells under stress (Covello et al., 2006; Mazumdar et al., 2010). An up-regulation of chaperones, ubiquitin/proteosome, DNA repair and chromatin remodeling in LRECb are consistent with this characteristic and support identification of these cells as MaSCs.

Comparison of the transcript profiles of LRECe with those of ECe and LRECb supports classification of LRECe as progenitor cells. As with LRECb, presence of an HNF4A network and BrdU label retaining ability suggest that LRECe possess some stem cell attributes. However, up-regulation of metabolic enzymes and differentiation factors suggest that LRECe are more differentiated than LRECb. XIST is a non-coding RNA that inactivates one of the X-chromosomes in the early embryo, initiates gene repression, and defines epigenetic transitions during development. Pluripotency genes (NANOG, OCT4 and SOX2) cooperate to repress XIST (Navarro et al., 2008). Our mRNA data revealed no expression of XIST in LRECb, moderate expression in LRECe and greatest expression in control cells, consistent with classification of LRECb as MaSCs and LRECe as progenitor cells (Savarese et al., 2006). Finally, comparison of transcript abundance in LRECb vs. LRECe revealed upregulation of the Notch signaling pathway in LRECe. The Notch pathway plays a critical role in cell fate determination in human mammary stem and progenitor cells (Dontu et al., 2004). We hypothesize that the Notch pathway regulates the generation of progenitor cells from MaSCs.

Our study provides evidence that the stem cell niche lies in the basal layer of mammary epithelium. In this study, LREC and control cells were isolated from known locations within the mammary epithelium without previously destroying cellular

microenvironments. LREC and control cells were adjacent or in close proximity to allow evaluations of potential cross talk between stem cells and neighboring cells. Microarray analyses of LRECb and LRECe identified features of LRECb that are reflective of mammary stem cells residing in a stem cell niche. Distinct features of a stem cell niche, as discussed by Li and Xie (Li and Xie, 2005), are the presence of (1) cell adhesion molecules that provide anchorage for stem cells within the niche, (2) extrinsic factors within the niche that regulate stem cell behavior and (3) factors that cause asymmetric cell division of stem cells, that is upon cell division, one daughter cell is maintained in the niche as a stem cell (self-renewal) and the other daughter cell leaves the niche to proliferate and differentiate. A very recent study also suggested that a stem cell niche is hypoxic, resulting in the induction of proteins of the family of hypoxia inducible transcription factor (HIF), such as HIFA1 and targets Wnt, OCT4, IGF2 and Notch signaling molecules (Kaufman, 2010; Mazumdar et al., 2010). In our study, we identified specific cell adhesion molecules, extrinsic growth factors and regulators, factors that promote asymmetric cell division, and hypoxia inducing factor as molecules that are prevalent in the stem cell niche of the basal epithelium (Figure 13).

In summary, transcriptome analysis of mammary epithelial cell subpopulations has provided a framework for future studies of normal mammary epithelial cell development and homeostasis, and for the pathobiology of breast cancer. First, we provided the evidence that LRECs represent MaSCs and progenitor cells, with LRECb being MaSCs and LRECe more committed progenitor cells. Second, we showed the evidence the basal layer of epithelium as the location of the MaSCs niche. Lastly, we

provide the first transcriptome profile of MaSCs and progenitor cells excised from their in situ locations and identified potential novel biomarkers for these cells.

Insights into the biology of stem cells will be gained by further confirmation of candidate MaSCs markers identified and evaluated in this study. Appropriate biomarkers will provide means to identify MaSCs and facilitate our understanding of their functions in mammary development and homeostasis and cancer. Specific cell surface markers will be useful for future isolation of MaSCs and investigations of their biology.

This manuscript has been submitted for publication.

Chapter 5: Expression of NR5A2, NUP153, HNF4A and FNDC3B is consistent with their use as novel biomarkers for mammary stem/progenitor cells

Abstract

Mammary stem cells (MaSCs) are essential for growth and maintenance of mammary epithelium. Previous studies have utilized morphological characteristics or retention of bromodeoxyuridine (BrdU) label to identify MaSCs, but these approaches may not be feasible or may not identify all resident stem cells. Alternatively, MaSCs may be identified by expression of appropriate protein markers. The focus of this study was to evaluate staining patterns of four novel candidate markers for bovine MaSCs, in mammary tissue from prepubertal and lactating Holsteins. These proteins were identified as candidate MaSCs markers because their transcripts were highly expressed in laser-microdissected cells, identified as putative MaSCs by their retention of BrdU label and their basal location within the mammary epithelium. The four candidate markers for MaSCs were: nuclear receptor subfamily 5 group A member 2 (NR5A2), nucleoporin 153 (NUP153), hepatocyte nuclear factor 4-alpha (HNF4A) and fibronectin type III domain containing 3B (FNDC3B). We also evaluated presumptive MaSCs markers [aldehyde dehydrogenase 1 (ALDH1) and Musashi 1 (MSI1)] and notch 3 receptor (Notch3), which have been used in other species. We found that NR5A2, NUP153 and HNF4A -labeled cells represented 2.5-6% of epithelial cells prepubertally and were distributed in a fashion consistent with the location and abundance of MaSCs/progenitor cells. A transient increase in expression of these markers was observed at peak lactation.

FNDC3B was localized mainly in the nucleus prepubertally and in the cytoplasm of myoepithelial cells and nuclei of a limited number of alveolar cells during lactation. Abundant expression of ALDH1 precludes its use as a marker for bovine MaSCs, whereas MSI1 staining was consistent with MaSCs localization. Onset of lumen formation in mammary ducts of prepubertal gland was associated with Notch 3 expression in the apical surface of lumenal cells. Nuclear expression of NR5A2, NUP153, HNF4A and FNDC3B are likely markers for bovine MaSCs and progenitor cells.

Key words: mammary stem cell, progenitor cell, biomarker

5.1 Background

Mammary stem cells (MaSCs) provide for mammary growth and cell replacement. Accordingly, they provide a biological target for increasing milk production, persistency of lactation and tissue repair. Several approaches have been used to identity, isolate and enrich MaSCs in order to characterize their molecular properties. Among these, the long-term retention of bromodeoxyuridine (BrdU) to identify putative MaSCs has been of considerable interest. The long-term retention of labeled DNA by somatic stem cells is based on the following hypotheses: (1) stem cells are relatively quiescent and (2) stem cells retain the original DNA strands and transfer newly synthesized stands to daughter cells. Although the precise mechanism for label retention remains obscure, studies have demonstrated that asymmetric DNA segregation is a common property of somatic stem cells (Shinin et al., 2006). Using this technique, we have identified label-retaining epithelial cells (LREC) that are present in low abundance in mammary glands of prepubertal heifers (Capuco, 2007; Capuco et al., 2009). We suggested that LREC in the basal epithelium (estrogen receptor-negative) are MaSCs and those in suprabasal layers (estrogen receptor-positive) are progenitor cells (Capuco, 2007; Capuco et al., 2009). However, application of label retention as a means for identifying MaSCs is limited by of the minimal labeling of relatively quiescent cells and its use in large animals is constrained by cost and logistical concerns. As a result, there is a need for other types of markers for MaSCs identification. An alternative approach to identify resident MaSCs is based on detection of appropriate protein markers by immunohistochemistry. Although a single reliable marker for MaSCs has been difficult to obtain, MaSCs express a number of potential markers that have been used alone or in

combination to study MaSCs/progenitor cells in other species. Among those used for investigations in mouse and human are aldehyde dehydrogenase 1 (ALDH1), Musashi 1 (MSI1) and Notch 3 receptor. Based upon microarray analysis of LREC, which were excised from mammary tissue of prepubertal bovine mammary glands using laser microdissection, we recently identified novel, potential MaSCs markers (NR5A2, NUP153, FNDC3B and HNF4A).

Notch signaling components are conserved proteins that have been associated in lineage commitment, cell proliferation, differentiation and apoptosis (Bray, 2006). Over-expression of the Notch pathway has been associated with breast cancer development (Shi and Harris, 2006). Notch signaling has also been found to direct bipotent mammary progenitors to lumenal lineages (Raouf et al., 2008). In agreement with previous morphological data, we have molecular profiling data demonstrating that mammary stem cells are localized in the basal layer of the mammary epithelium whereas progenitor cells are more apically localized (Choudhary et al, 2010b). We anticipate that evaluating the expression pattern of the Notch 3 protein will facilitate our understanding of lineage specification in the epithelium of the bovine mammary gland.

Our objective was to evaluate the expression patterns of novel MaSCs markers and additional putative MaSCs/differentiation cell markers in bovine mammary epithelium. We conclude that epithelial cells expressing NR5A2, NUP153, FNDC3B, HNF4A and MSI1 in the nucleus are potential MaSCs/progenitor cells. In contrast, ALDH1 is not a good marker for bovine MaSCs due to its expression by many epithelial cells and its lumenal localization. Interestingly, Notch3 may be associated with lumen formation of the mammary duct.

5.2 Materials and Methods

Tissue Samples

In this study, we used tissues from prepubertal and from lactating Holstein cows. The tissues were archived samples of two previous studies. Paraffin-embedded tissues from prepubertal heifers were from a study (Capuco et al., 2009) designed to identify putative MaSCs based upon the ability of these cells to retain BrdU. Paraffin-embedded tissues from nonpregnant lactating cows were from a study designed to evaluate the kinetics of epithelial turnover (Capuco et al., 2001). Animal use and protocols for the original experiments were approved by the Beltsville Agricultural Research Center Animal Care and Use Committee.

Immunohistochemistry

Mammary tissues were sectioned at 5 µm thickness and placed on Superfrost™ plus slides (Erie Scientific Co, Portsmouth, NH, USA) for immunohistochemical analysis, and all incubations were carried out at RT unless stated. Slides were dewaxed in xylene and rehydrated in ascending concentrations of ethanol to water. Tissue sections were quenched with a solution containing a specific inhibitor of endogenous peroxidase (Peroxo-block; Invitrogen Co. Frederick, MD) for 2 min. After washing sections in deionized water (3 x 2 min), antigen retrieval was performed by heating in 10 mM Tris-HCl, 1 mM EDTA, pH 9. Slides were heated in a microwave oven at high power (650 W) in 400 mL of buffer in a covered glass staining dish for 5 min, left undisturbed for 5 min, then were microwaved for additional 5 min. Slides remained in buffer for a 25 min cooling period before washing with phosphate-buffered saline containing 0.05% Triton X-100 (PBST; 3 x 3 min). Although antigen retrieval using 70% deionized formamide in

PBS at 60 ºC for 5 min (Choudhary et al., 2010a) followed by treatment with trypsin (Trypsin Histo-kit; Invitrogen Co., Camarillo, CA) for 30 min at 37 ºC produced similar results, the former method was used for convenience. Antigen retrieval using microwave heating in 10 mM citrate buffer (pH 6.0) produced nonspecific staining with these markers.

After antigen retrieval, slides were blocked with casein (CAS-Block™, Invitrogen, CA) for 10 min and then incubated with primary antibodies for 1-2 h at RT or overnight at 4°C. Primary antibodies and dilutions were: BrdU mouse monoclonal (Roche Diagnostics; Mannheim, Germany, BMC9318; 1:50 dilution), NR5A2 rabbit polyclonal (Sigma-Aldrich, St. Louis, MO, USA, 1:100 dilution), NUP153 mouse monoclonal (Abcam Inc. Cambridge, MA, USA, 1:200 dilution), HNF4A mouse monoclonal (Abcam, 1:200 dilution), FNDC3B (Santa Cruz Biotech., Santa Cruz, CA, USA, 1:50 dilution), MSI1 (Sigma-Aldrich, rabbit polyclonal, 1:100 dilution), ALDH1 mouse monoclonal (BD Transduction Lab, mouse monoclonal, 1:100 dilution), Notch 3 mouse monoclonal (Santa Cruz, 1:100 dilution).

After incubation with primary antibody, sections were washed with PBST (3 x 3 min), and then incubated with Vector ImmPRESS™ anti-mouse/anti-rabbit Ig peroxidase conjugated secondary antibody (Vector Labs Inc. Burlingame, CA, USA) for 30 min, followed by washing with PBST (3 x 2 min) to remove unbound polymer. Markers were detected using Vector peroxidase substrate kits for brown (ImmPACT™ DAB), purple (ImmPACT™ VIP) or red (ImmPACT™ NovaRED™) staining. Negative controls were performed by omitting primary antibody. Sections were counterstained with 0.5% aqueous methyl green (Vector Labs) for 2 min, washed briefly in water, differentiated in

0.05% acetic acid/acetone for 10 s and dehydrated in ascending concentrations of ethanol. In the case of hematoxylin counterstaining, slides were washed in water and dipped into PBS (30 s) to develop blue color nuclei before dehydration in ethanol. Slides were mounted in DPX (Sigma-Aldrich Co. St. Louis, MO, USA). Photomicrographs were obtained using a light microscope (Olympus BX81; Olympus, Japan) equipped with a DP70 digital camera.

For each marker (NR5A2, NUP153 and HNF4A) quantified, immunopositive cells were quantified from photomicrographs and expressed as as percentage of total epithelial cells counted (labeling index). For each stained slide (3-4 tissue sections per slide), 10-12 areas were photographed at a magnification of 320x. The NR5A2, NUP153 and HNF4A-labeled epithelial cells and total epithelial cells were enumerated from the digital images and labeling indices were calculated.

5.3 Results and Discussion

To evaluate the expression patterns of various markers for MaSCs, we performed immunohistochemistry on formalin-fixed paraffin-embedded tissue sections from prepubertal and lactating bovine mammary glands. Specificity, distribution and quantitation of the stained cells were performed. All data are expressed as mean percentage and standard error (mean $\pm$ SE). Negative controls for staining procedures were the omission of primary antibody and always showed no immunostaining of cells (Figure 15A).

Expression of the novel MaSC/progenitor cell markers, NR5A2, NUP153, HNF4A and FNDC3B were distributed in a fashion similar to LREC. As previously

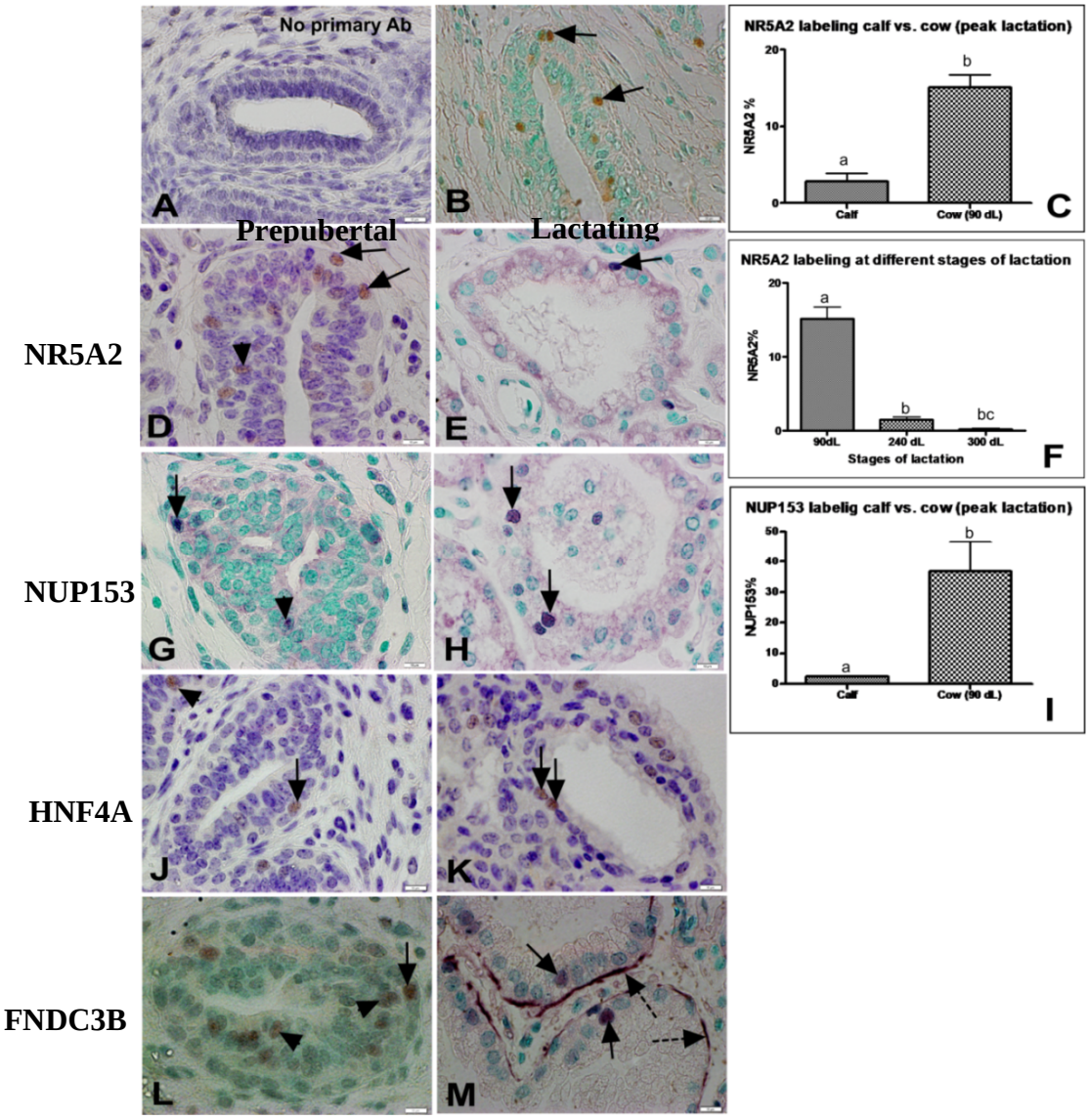

Figure 15. Immunohistochemical localization of potential novel stem/progenitor cell markers in prepubertal and lactating mammary gland.

Shown are the results of indirect immunostaining on paraffin sections using (A) no antibody (negative control), (B) BrdU antibody detecting label retaining epithelial cells. (C) Bar graph depicting percent of NR5A2 labeled mammary epithelium in prepubertal heifer calf and lactating mammary gland. NR5A2 staining in (D) calf and (E) lactating cow. (F) Bar graph depicting percent of NR5A2 labeled mammary epithelium at 90, 120 and 240 d of lactation (dL). NUP153 staining in calf (G) and (H) lactating cow. (I) Bar graph depicting percent of NUP153 labeled mammary epithelium in prepubertal and peak lactating mammary gland. HNF4A staining in (J) calf and (K) lactating cow and FNDC3B staining in (L) calf and (M) lactating cow. Arrows indicate nuclear expression of markers in basal cells, arrowheads in embedded/lumenal cells and broken arrows point to cytoplasmsic expression of markers. Means without a common superscript differ ($P < 0.05$). Scale bar = 10 µm.

reported (Capuco, 2007; Capuco et al., 2009) staining for BrdU revealed LREC, which were located primarily in the basal layer or one or two cells above the basal layer in the mammary epithelium of prepubertal heifers (Figure 15B). LREC were seldom found to be in contact with the ductal lumen.

We evaluated expression of NR5A2 in mammary tissue from prepubertal heifers and lactating cows. In prepubertal heifers, immunostaining of NR5A2 was observed in the nuclei of a small number of basal and embedded epithelial cells, with the basal cells visually appearing more intensely labeled (arrows) than embedded (arrowhead) (Figure 15D). They were observed at a frequency of 2.6 $\pm$ 0.51 % of total epithelial cells. However, the frequency of basally located NRA2-positive epithelial cells was approximately 1% of total epithelial cells. Our previous research (Capuco, 2007; Capuco et al., 2009) and recent transcriptome profiling of LREC (Choudhary et al., 2010a) suggested that the basally located LREC are MaSCs, which is consistent with the abundance of MaSCs in other species (Kordon and Smith, 1998; Shackleton et al., 2006). In lactating mammary gland, we evaluated NR5A2 expression at 90 (near peak), 240 (late) and 300 d of lactation. Abundance of NR5A2-positive cells differed significantly between mammary tissues from prepubertal (Figure 15D) and lactating cows (Figure 15E) and was influenced by stage of lactation (Figure 15F). There was a significant difference in abundance of NR5A2-positive cells from prepubertal vs. near peak lactation ($P < 0.01$; 2.6 $\pm$ 0.51 vs. 14.9 $\pm$ 2.6), near peak vs. 240 d lactation ($P < 0.01$; 14.9 $\pm$ 2.7 vs. 1.5 $\pm$ 0.3) (Figure 15C). As lactation advanced to 300 d there was a further numerical decrease in abundance of NR5A2-positive cells; however, this differences was not significant ($P > 0.05$; 1.5 $\pm$ 0.3 vs. 0.16 $\pm$ 0.09). Interestingly, we observed a notable

difference in the nuclear staining pattern of NR5A2 in prepubertal and lactating mammary epithelium. In prepubertal heifers, NR5A2 staining appeared to be intense and uniform throughout the nucleoplasm. In lactating gland, some cells displayed intense and uniform nuclear staining; whereas others exhibited punctate nuclear staining (data not shown). The intense and uniform nuclear staining pattern was observed at all the stages of lactation. However, the punctate nuclear staining pattern was predominant at peak lactation. We hypothesize that intense, uniform nuclear staining is a characteristic of MaSCs, whereas punctuate nuclear staining is characteristic of more committed progenitor cells. Accordingly, the data suggest that there is a temporary increase in the progenitor cell population during early lactation and a decline as lactation advances. This is consistent with the role of the preparturient dry period in promoting the turnover of epithelial cells (Capuco, et al., 1997) and replacement of senescent cells, including senescent progenitors (Capuco and Akers, 1999).

The frequency and distribution of NUP153 expression in mammary tissue of prepubertal and lactating Holsteins was similar to the expression of NR5A2. NUP153-positive cells were distributed in the basal and embedded epithelial layers of the prepubertal gland. Immunostaining was detected in the nuclei, either in the nuclear envelope or in the nucleoplasm or both, of a limited number of epithelial cells. Nuclear staining in mammary tissue from prepubertal heifers was intense in basal (arrow) and moderate or weak in embedded cells (arrowhead) (Figure 15G). Abundance of NUP153-positive cells was 2.5 $\pm$ 0.4 % of total epithelial cells. Basally located NUP153-positive cells accounted for 0.5% of total epithelial cells and these exhibited strong nuclear staining. Around the time of peak lactation (90 d), most of the NUP153-positive cells

were characterized by staining around the nuclear envelope, with a small population of cells showing stronger staining of the nucleoplasm (Figure 15H). We also observed weak to moderate nucleoplasmic staining in epithelial cells within developing / regressing alveoli. The cells expressing weak to moderate nuclear envelope or nucleoplasmic staining might represent more committed progenitor cells. The frequency of NUP153-positive cells differed between mammary tissues from prepubertal and lactating animals near peak lactation ($P < 0.05$; 2.5 ± 0.45 vs. 36.7 ± 3.3) (Figure 15I).

Immunolocalization of HNF4A was exclusively nuclear during prepubertal and lactation phases of mammary development. In epithelium of prepubertal heifers, HNF4A-positive cells were scattered in basal (arrow), embedded (arrowhead) and lumenal (not shown) layers (Figure I5J) and represented 6.1 ± 0.7% of total epithelial cells. HNF4A-labeled cells located in the basal epithelium accounted for 1.5 ± 0.21 % of total mammary epithelial cells in prepubertal heifers. In lactating cows, mammary tissue obtained at 90 d of lactation contained 10.79 ± 0.97 % HNF4A-positive cells of total alveolar cells (Figure 15K). The proportion of HNF4A-positive cells was significantly different in prepubertal vs. lactating mammary tissues ($P < 0.05$; 6.1 vs. 10.8).

We next examined the expression of Fibronectin type III domain containing 3B (FNDC3B) in the mammary gland of prepubertal and lactating Holsteins. FNDC3B was localized exclusively in the nucleus of epithelial cells in prepubertal heifers, but localized in the nucleus and cytoplasm of lactating cows. In prepubertal heifers, the strongest nuclear staining was found in cells of basal epithelium (arrow), with moderate staining in embedded cells (arrowheads) (Figure 15L). In lactating cows, FNDC3B was localized in

the nucleus of a small number of alveolar cells (arrows), and the cytoplasm of myoepithelial cells (broken arrows) (Figure 15M).

We also evaluated putative MaSCs and differentiation markers that other investigators have used in studies of mouse and human mammary gland. We found intense nuclear staining of the putative MaSCs marker, MSI1, in basal (arrow) and moderate to weak staining (arrowhead) in embedded layers of the ductal epithelium of the calf (Figure 16A). In lactating mammary gland, MSI1 was localized in the nuclei of a small proportion of alveolar cells (Figure 16B).

We found abundant expression of ALDH1 in nuclei and cytoplasm of lumenal mammary epithelial cells of prepubertal calves (Figure 16C). In lactating cows (120 d) we found that many alveolar cells (48 $\pm$ 2.25 %) were ALDH1-positive, expressing ALDH1 in the nucleus (Figure 16D). Because mammary stem cells are present in low abundance and appear to be located within the basal layer of the prepubertal mammary gland, the distribution and abundance of ALDH1-positive cells is inconsistent with the utility of this enzyme as a marker for bovine MaSCs. However, this does not preclude the possibility that another isoform of ALDH may serve as a potential MaSCs marker.

Immunodetection of Notch 3 protein appeared to coincide with the formation of the lumenal space in mammary ducts of prepubertal heifers. In this study, we found strong cytoplasmic staining at the apical border of the lumenal epithelium as the ductal lumen was formed. Developing mammary ducts with no lumen did not express Notch 3 protein (Figure 16E). Notch 3 expression was evident with the onset of lumen formation (Figure 16F, 16G) and was maximal in lumenal cells bordering the lumena of fully patent

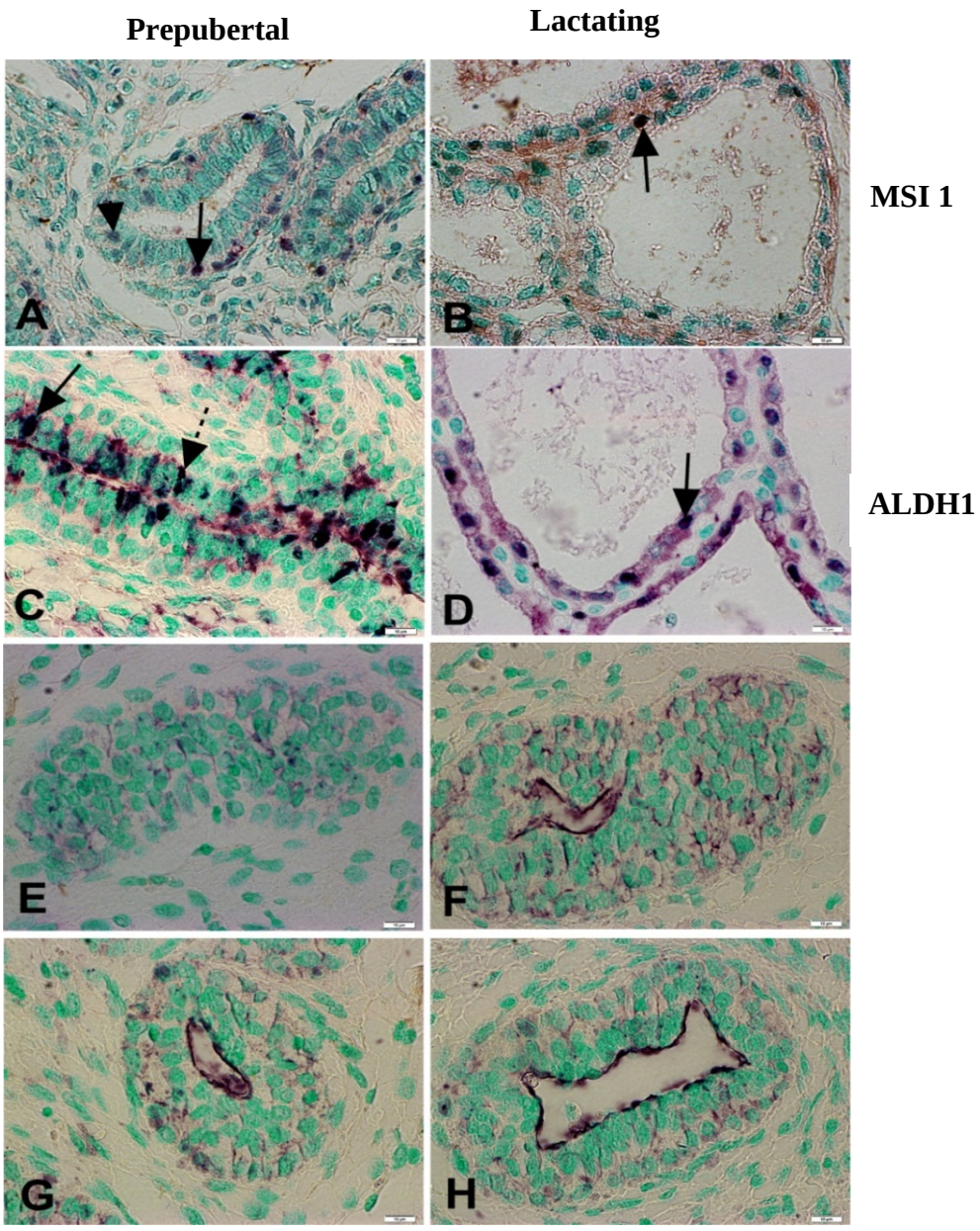

Figure 16. Immunohistochemical localization of putative stem/progenitor cell markers in prepubertal and lactating mammary gland.

MSI1 staining in (A) calf and (B) lactating cow; ALDH1 staining in (C) calf and (D) lactating cow. Arrows indicate nuclear expression of markers in basal cells, arrowheads in embedded cells and broken arrows indicate cytoplasmic expression. (E-H) Notch 3 expression and lumen formation in prepubertal mammary duct. (E) Notch 3 was not expressed in a cluster of unorganized epithelial cells (an underdeveloped duct). (F) Initiation of Notch 3 expression was observed in concomitant with lumen formation. (G) Small developing duct with narrow lumen shows Notch 3 expression in apical side of lumenal cells. (H) Fully developed duct shows increased expression of Notch 3. Cells are counterstained with aqueous methyl green (green nuclei). Scale bar = 10 µm.

ducts (Figure 16H). The immunohistochemical expression pattern of other Notch proteins might suggest their definite involvement in lumen formation of mammary ducts.

Discussion

The limited information available for NR5A2 is consistent with its potential utility as a MaSCs marker. NR5A2 has been used as a component for transforming somatic cells into induced pluripotent stem cells (iPSC). Specifically NR5A2 can replace OCT4, a pluripotency transcription factor, previously thought to be essential for generation iPSC from somatic cells (Heng et al., 2010). Similarly, up-regulation of NR5A2 has been suggested to regulate OCT4 transcription factor in embryonic stem cells via SOX2 (Rizzino, 2009). In mammary gland, NR5A2 has also been shown to exert potential oncogenic effects through the estrogen receptor during breast cancer formation (Annicotte et al., 2005). In conjunction with our finding that LREC express NR5A2 (Choudhary et al., 2010a), our immunohistochemical results suggest that NR5A2 is a pluripotency transcription factor and potential MaSCs marker.

Although nucleoporins (NUP) are structural elements of mammalian nuclear pore complexes (NPCs), other roles are emerging from recent studies. NUP153 has been shown to play a role in organization of the nuclear envelope and indirectly regulates cytoskeleton architecture and mechanical properties of the cells (Zhou and Pante, 2010). Association of NUP153 with large genomic regions (10-500 kb) reduced expression of X-linked genes in NUP153 knockout Drosophila and lack of efficient transcription of heat shock proteins in NUP98 knockdown cells provide evidence for a role of nucleoporins in regulation of transcription (Mendjan et al., 2006; Vaquerizas et al., 2010; Capelson et al., 2011). Therefore, it appears that nucleoporins are mobile structural

proteins, but shuttle between the NPC and nucleoplasm. Another study demonstrated a role for NUP133 in cell differentiation and found that expression of NUP133 is cell type specific and developmental stage-restricted, with prominent expression in dividing progenitors (Lupu, et al., 2009). Our transciptome profiling data (Choudhary et al., 2010a) indicate that NUP153 is differentially expressed by MaSC/progenitor cells. We now show that NUP153 is expressed in the nuclear envelope and/or nucleoplasm. This supports a novel role for NUP153 in the nucleoplasm, possibly in regulating proliferation and differentiation of cells. The transient increase in NUP153-positive cells at peak lactation may reflect an increase in the progenitor cell population. The functional significance of the varied intensity of nucleoplasmic staining requires further investigation. However, we suggest that the strongly positive cells in the basal epithelium of prepubertal heifers are MaSCs, as are strongly positive alveolar cells of lactating gland.

The abundance and distribution pattern of HNF4A in the mammary epithelium suggest that HNF4A is a potential MaSCs/progenitor marker. It is noteworthy that HNF4A was at the hub of the most significant gene network to be highly expressed in putative MaSCs (basal LREC) (Choudhary et al., 2010a). Whether, HNF4A-positive cells co-expressing NR5A2 or NUP153 are more primitive MaSCs remains a topic for future investigation.

Cytoplasmic expression of FNDC3B in myoepithelial cells, which are juxtaposed to the extracellular matrix (ECM), is consistent with the affinity of FNDC3B for fibronectin (a component of ECM) and integrin. FNDC3B binds to extracellular and cell surface molecules like integrin and regulates cell adhesion, migration, spreading, growth

and differentiation (Geiger, et al., 2001) by activating integrin-mediated intracellular signals (Bowditch et al., 1994). FNDC3B null mice exhibit increased postnatal mortality and decreased proliferation, adhesion, spreading and migration of adipocytes and fibroblasts (Nishizuka et al., 2009). Altogether, these observations suggest the importance of interaction between FNDC3B and integrins in cell growth, migration and differentiation. This is the first suggested involvement of FNDC3B in the bovine mammary gland and its possible association with MaSCs.

MSI1 has been hypothesized to be a marker of somatic stem/progenitor cells in a variety of tissues including intestine, endometrium, and mammary gland (Gotte et al., 2008; Gotte et al., 2011; Potten et al., 2003). A role for MSI1 in progenitor cell expansion, acting through Wnt and Notch pathways, has been suggested (Okano et al., 2005; Rezza et al., 2010; Wang et al., 2008). Our results are consistent with MSI1 expression in ewe mammary epithelium (Colitti and Farinacci, 2009) and we conclude that MSI1 is a potential marker of MaSCs/progenitor cells in bovine mammary gland.

In contrast to our findings in bovine mammary gland, ALDH1-positive cells in human breast possess characteristics of MaSCs (Ginestier et al., 2007). Similarly, ALDH1 appears to serve as a stem cell marker in other tissues, including hematopoietic tissue (Hess et al., 2004; Armstrong et al., 2004). Typically, identification of ALDH1-postive cells has been based primarily on enzymatic activity of living cells for the fluorogenic ALDH1 substrate, aldefluor. However, a recent study using ALDH1A1 knockout mice indicated that not only is ALDH1A1 not essential for hematopoietic stem cell function, but that ALDH1A1 deficiency did not affect aldefluor staining (Levi, et al., 2009), which was likely maintained by the presence of other ALDH isoforms.

Furthermore, a recent study indicated that expression of ALDH1 protein alone does not predict outcome of breast cancer prognosis (Neumeister, et al., 2010) In bovine mammary gland, we have found increased expression of ALDH3B1 in putative bovine mammary stem cells (Choudhary et al., 2010a). However, due to the absence of specific antibodies for this ALDH isoform, we have been unable to evaluate the abundance and distribution of ALDH3B1-positive cells within the bovine mammary gland.

The mechanism of lumen formation in bovine mammary gland is unknown, but is not mediated by apoptotic death of epithelial cells in the central region of the ductal cord (Capuco et al., 2002) as occurs during lumen formation of murine ducts (Humphreys, et al., 1997). Therefore, regulation of apoptosis is unlikely to be a function of increased Notch 3 expression during lumen formation in bovine mammary gland. We also observed a rare subset of basal cells and adjacent embedded cells showing Notch 3 expression (not shown). We speculate that MaSCs divides asymmetrically in the basal layer leading to formation of daughter progenitor or transit amplifying cells in the above layer. The Notch pathway may be associated with this phenomenon, as it is associated with differentiation of human mammary stem cells to progenitor cells (Dontu et al., 2004). A role for Notch 3 in development of the ductal lumen of the bovine mammary gland requires additional research.

In summary, the abundance and localization of cells that express NR5A2, NUP153, HNF4A and FNDC3B is consistent with the utility of these proteins as novel markers for bovine mammary stem/progenitor cells. Cells that express the markers most strongly are located in the basal layer of the mammary epithelium of prepubertal calves, the apparent locale of MaSCs. During lactation, these markers are evident in the alveoli.

The pattern of nuclear expression during lactation may provide a means to distinguish stem and progenitor cells and suggests that stem cells are present in the alveoli during lactation, not only in the mammary ducts. Expression of other putative stem cell/differentiation markers were also evaluated and showed that ALDH1 is not an appropriate marker for bovine MaSC/progenitor cells, but MSI appears to be a MaSC/progenitor cell marker. Expression of Notch 3 in the mammary epithelium of calves suggests that it may play a role in lumen formation and in regulation of asymmetric division of MaSCs.

This is the final draft of the manuscript to be submitted for publication.

Chapter 6: In vitro expansion of mammary stem/progenitor cell population by xanthosine treatment

Abstract

Mammary stem cells are critical for growth and maintenance of the mammary gland and therefore of considerable interest for improving productivity and efficiency of dairy animals. Xanthosine treatment has been demonstrated to promote expansion of putative mammary stem cells in vivo and hepatic stem cells in vitro. In the latter case, xanthosine promoted the symmetrical division of hepatic stem cells. The objective of this study was to determine if treating primary cultures of bovine mammary epithelial cells (MEC) with xanthosine increases the stem/progenitor cell population by promoting symmetrical division of mammary stem cells. In vitro treatment with xanthosine increased the population of MEC during the exponential phase of cell growth, reducing the doubling time from 86 h in control cultures to 60 h in xanthosine-treated cultures. The bromodeoxyuridine (BrdU) labeling index and the proportion of MEC in S-phase both were increased by xanthosine treatment, indicating that increased cell accretion was due to increased cell proliferation. Analysis of daughter-pairs indicated that xanthosine promoted a shift from asymmetric to symmetric cell division. Moreover, the 30% increase in symmetric cell division was concomitant with an increase in the proportion of MEC that were positive for a putative stem cell marker (FNDC3B) and a trend toward increased telomerase activity. These results suggest that xanthosine treatment in vitro can increase cell proliferation, promote symmetric cell division and enhance

stem/progenitor cell activity. Xanthosine treatment increased the proliferation rate of bovine MEC in vitro. This was likely to be mediated by an increase in the proportion of stem/progenitor cells in the MEC population due to promotion of symmetrical stem cell division by xanthosine.

Key words: **mammary epithelial cell, stem cell, xanthosine**

6.1 ***Background***

Expansion of stem/progenitor cells is a prerequisite for their therapeutic or research uses. Mammary stem cells (MaSCs) are somatic stem cells that provide for the lineage of mammary epithelial cells. Consequently, they are of considerable interest to developmental biologists, agricultural scientists and cancer researchers. Bovine MaSCs have received little attention despite the inherent economic importance of the species and the potential for impacting animal production by MaSCs manipulation, and despite the similarity in cytoarchitecture of bovine mammary tissue to that of the human breast (Capuco et al., 2002). Bovine mammary epithelial cells and their stem cells are important in agricultural production and bioengineering applications. Additionally, information gained will potentially broaden our knowledge of human mammary epithelial cells and stem cells.

Somatic stem cells can divide symmetrically or asymmetrically. Symmetric division of stem cells produces two identical stem cells and results in expansion of the stem cell population. Asymmetric division produces a stem cell and a differentiated progenitor cell of more committed cell lineage, while maintaining the existing stem cell population. A novel method of expanding the rat hepatic stem cell population has been identified and is based on suppression of asymmetric cell kinetics. Several in vitro experiments indicated that p53 promotes asymmetric proliferation of somatic stem cells through suppression of inosine-5'-monophosphate dehydrogenase (IMPDH) (Rambhatla, et al., 2005; Sherley, 1991; Sherley et al., 1995), a rate-limiting enzyme in guanine ribonucleotide biosynthesis. A decrease in guanine ribonucleotide concentration promotes asymmetric division of stem cells. Compounds like xanthosine (a purine

nucleoside) bypass IMPDH-mediated guanine synthesis and increase guanine concentration in the cell, thereby promoting symmetric division and expanding the stem cell population (Lee et al., 2003).

Earlier, we reported that xanthosine promotes expansion of label-retaining epithelial cells (LREC), putative stem cells, in prepubertal mammary gland in vivo (Capuco et al., 2009). In order to understand the role of xanthosine, in the current study we evaluated growth characteristics of primary mammary epithelial cells from the lactating bovine mammary gland. The objective of this study was to investigate the impact of xanthosine on cell proliferation and the kinetics of stem/progenitor cell expansion. We show that xanthosine enhances cell proliferation, promotes symmetrical cell division and increases the stem/progenitor cell population. Symmetric division was assessed by daughter pair analysis and stem cell number was assessed by expression of a potential novel stem cell marker (FNDC3B) and by telomerase activity.

6.2 Materials and Methods

Cultivation of bovine primary mammary epithelial cells

Frozen stocks of bovine mammary epithelial (MEC) cells from lactating cows were kindly provided by Dr. David Kerr, University of Vermont. Isolation of these cells was described previously (Wellnitz and Kerr, 2004).

Cell culture conditions

Frozen cells were revived in growth medium consisting of DMEM/F12 with 5% FBS, ITS supplement (5 μg/mL insulin, 5 μg/mL transferrin and 0.005 μg/mL sodium selenite), glutamine dipeptide (2 mM; GlutaMAX^{TM}-I), penicillin G (100 μg/mL), and streptomycin (100 μg/mL) and plated in a 75-cm^2 tissue culture flask (T75, Corning Inc.,

Corning, NY, USA). These medium supplements were obtained from Gibco/Invitrogen (Carlsbad, CA, USA). Initially, cells were allowed to attach to the bottom of the T75 tissue culture flask for 5 h and then the medium was replaced with fresh medium. Cells were grown at 37°C in a humidified atmosphere of 5% CO_2 in air. For cell passage, the medium was discarded and the monolayer washed with phosphate buffer saline (PBS). Cells were then incubated in 2 mL of 0.05% trypsin-EDTA (Invitrogen, Carlsbad, CA) for 10-15 min at 37°C, until most cells became detached. Trypsinization was stopped by adding 5 mL of growth medium. After centrifugation (23°C, 6 min, 210 x *g*), the cell pellet was resuspended in 5 mL of growth medium. For routine passage, cells were subcultured at a 1:4 ratio. Cells grew to 70-80% confluency in 5 to 7 d, at which time they were subcultured. Medium was replaced every 2-3 d.

Growth characteristics of bovine mammary epithelial cells

To evaluate the impact of xanthosine on growth characteristicics of MEC, cells were seeded at a density of 3×10^4 cells/well of 24-well flat bottom tissue culture plates (Falcon, Oxnard, CA, USA) containing one mL of growth medium with or without 200 µM xanthosine (Sigma, Saint Louis, MO), prepared from a 10 mM stock solution of xanthosine (prepared in alkaline distilled water and filtered through a sterile membrane, 0.2 µ pore size). Cell number and viability of triplicate wells were determined daily for 8 d. Cell number was assessed by haemocytometer counts of trypsinzed cell suspensions and viability by dye exclusion, using 0.4% trypan blue (Gibco, Carlsbad, CA, USA). Morphology of cells in confluent monolayers was evaluated by microscopy on day 8 after hematoxylin staining. Three independent experiments were conducted using two populations of MEC, each isolated from a different cow.

Bromodeoxyuridine labeling index and FNDC3B staining

MEC were seeded in 5-cm^2 Petri dishes (Corning) containing growth medium with or without 200 µM xanthosine and grown for five d (~80% confluent). BrdU (Sigma, St Louis, MO, USA) was added to culture medium at a concentration of 10 µM during the logarithmic phase of growth. Cells in six replicate plates per treatment were incubated with BrdU for 5 h, after which the monolayers were washed with chilled PBS (2 x 1 min) and fixed in pre-chilled methanol for 15 min at -20°C. Cells were then treated with 0.3% Triton X-100 (Sigma) for 30 min, and endogenous peroxidase was blocked with Peroxo-block (Invitrogen) for 1 min. Cells were treated with 2N HCl for 30 min at RT followed by acid neutralization with 0.1 M borate buffer (2 x 5 min) and 3 washes (3 x 2 min) in PBST (PBS + 0.05% Triton X-100). Cells were blocked with casein (CAS-Block™, Invitrogen) for 10 min, and then incubated with mouse monoclonal anti-BrdU (Roche Diagnostics, Mannheim, Germany) at 1:100 dilution in CAS-Block for 1-2 h at RT. After washing with PBST (3 x 3 min), cell monolayers were incubated with Vector ImmPRESS™ anti-mouse/anti-rabbit Ig peroxidase conjugated polymer detection reagent (Vector Labs Inc., Burlingame, CA, USA) for 30 min, followed by washing with PBST (3 x 2 min) to remove unbound polymer. Immunostained cells were visualized with DAB (Vector). Negative control staining was performed by omitting primary antibody. Sections were counter-stained with hematoxylin for 1 min, washed briefly in water and color developed in PBS (30 s). Cells were dehydrated in ascending concentrations of ethanol. Photomicrographs were obtained using brightfield optics with an Olympus BX81 microscope (Olympus, Japan) equipped

with a DP70 digital camera. The percentage of immuno-positive cells was enumerated from photomicrographs of 10-12 random fields per culture plate.

FNDC3B staining was performed as for BrdU staining, except that neither HCl treatment nor other antigen retrieval step was used prior to incubation with primary antibody. Primary antibody was a rabbit polyclonal (Santa Cruz Biotechnology, Santa Cruz, CA, USA) used at 1:100 dilution. The influence of xanthosine and culture passage on the FNDC3B labeling index was tested by two-way ANOVA with Bonferroni correction using GraphPad Prism (version 3; GraphPad Software Inc., San Diego,CA, USA).

Flow cytometry analysis

To support evaluations of population doubling time and BrdU labeling index, we analyzed the impact of xanthosine on cell cycle distribution, using a flow cytometric assay. BrdU (10 µM) was added to cell culture medium for 45 min during the log phase of cell growth. Cells were then harvested by trypsinization and fixed with 70% ethanol in PBS overnight at 4°C. Cells were pelleted, permeabilized with 0.3% Triton-X100 in PBS for 30 min at RT, and then re-pelleted. Nuclei were suspended and incubated in 2N HCl for 20 min at 37°C and then neutralized with 0.1 M sodium borate buffer. Nuclei were pelleted and re-suspended in PBST before blocking with 200 µL of casein (CAS Block, Invitrogen) for 10 min and incubating with an Alexa 488-conjugated BrdU antibody (4 µg/mL, Molecular Probes, Invitrogen) at RT for 40 min in the dark. Samples were then rinsed twice in PBST and resuspended in 500 µL of propidium iodide/RNase staining buffer (BD Pharmingen, San Diego, CA) for 15 min before flow cytometry. Samples were kept on ice in the dark before analysis. Analyses were performed on a FC500 flow

cytometer (Beckman Coulter Inc., Palatine, IL) and collected data were analyzed using Cytomics RXP (Beckman). This experiment was repeated twice with 3-5 replicates per group, using cells at two different passages.

Label retention assay

Cells were seeded at $3x10^4$ cells/well of 6-well plates (Corning) with added BrdU (10 µM) and grown for one wk. At each weekly passage, two wells were fixed and processed for BrdU immunostaining, while cells in the remaining four wells were enzymatically dissociated and sub-cultured in six wells of another 6-well plate in control medium. Cell monolayers during the 3^{rd} (n=2), 4^{th} (n =2), 5^{th} (n = 2), and 6^{th} (n = 6) wks after BrdU labeling were immunostained and the number of LREC were counted. Wells used for negative control staining were not incubated with anti-BrdU antibody.

Daughter pair analysis

Cells were seeded at 1.5 x 10^5 per T25 flask and grown until approximately 80% confluent. Incorporation of BrdU into nuclear DNA was performed during the log phase of growth to label the maximum number of cycling cells. BrdU (10 µM) was added to the medium for 1 h prior to cell harvest. After trypsinization, cells were plated at a concentration of 200 cells per well (n = 4) of a 24-well plate. This cell density allowed for discrimination of individual cells and subsequent daughter-pairs. The influence of xanthosine on the proportion of cells undergoing symmetric vs. asymmetric division was evaluated by seeding cells in control medium or medium containing 200 µM xanthosine. Cells were cultured for an additional 48 h (doubling time 50-60 h). The cell monolayer was then washed with chilled PBS (2 x 1 min), fixed in methanol at -20ºC and processed for BrdU immunocytochemistry. Cell pairs containing one or two BrdU-labeled cells

were counted to determine the percentage of asymmetrical (one labeled daughter cell) versus symmetrical (two labeled daughter cells) division. Three independent experiments were performed and provided analogous results.

Telomerase assay

To determine cellular telomerase activity, MEC were seeded in 12-well tissue culture plates (Corning) at 6 x 10^4 cells per well in 2 mL of media with or without 200 µM xanthosine. At 80% confluency, 0.2 mL of trypsin-EDTA solution was added to each well and incubated for 15 min at 37°C. Cells were dislodged and a single cell suspension obtained by titurating in the micropipette tip. Then 0.8 mL of growth medium was added to inhibit trypsin activity and the cell suspension collected in a 1.5 mL microcentrifuge tube. A 50 µL aliquot of the cell suspension was removed from each tube to assess cell viability and cell number. The remaining cell suspension (950 µL) was used to determine telomerase activity using a quantitative real-time PCR-based telomerase assay (US Biomax, Rockville, MD, USA). Briefly, the cell suspension was centrifuged at 220 x g for 6 min and the pelleted cells (~ 1.0 - 1.5x10^5 cells) were lysed by vortexing for 1 min in 200 µL of the provided lysis buffer and incubating on ice for 30 min. The cell lysate was then centrifuged for 30 min at 12,000 x g at 4°C. The supernate was removed and collected in a 0.5 mL plastic microfuge tube. A portion of each supernate was heat inactivated (85°C for 10 min) and served as the negative control for that sample. One µL of each of sample supernate and heat-inactivated supernate were assayed along with a serial dilution of the provided standards (in lysis buffer), according to the manufacturer's recommendations.

6.3 Results and Discussion

Growth kinetics and effect of xanthosine

The initial experiment evaluated the impact of Xs on growth of primary bovine MEC. MEC plated on plastic growth surfaces in both xanthosine and control culture conditions displayed a cobblestone-like morpohology typical of epithelia cells in monolayer (Figure 17A-B). This cell morphology is consistent with characteristics of bovine mammary epithelial cells as reported by others (Zhao, et al., 2010). The viability assessed by trypan blue staining of xanthosine-treated cells and control cells did not differ (mean >98%). These observations suggest that neither cell morphology nor cell death rate was influenced by xanthosine treatment. The population growth rate was equivalent for both groups until day 3 of culture but diverged on d 4 – 6 ($P < 0.05$). On d 4 and 5, xanthosine-treated cultures showed an 18% increase in cell number over control cultures. Cell number plateaued by day 7 for both treatments, as the cultures reached confluence (Figure 17C). Doubling time was calculated during the last 3 d of the exponential phase of growth using population doubling time software (http://www.doubling-time.com) (Roth, 2006). At passage 3, doubling times were 50 h vs. 66 h for xanthosine and control cultures, respectively. MEC from a different cow at passage 6 grew more slowly and doubling times were 71 h vs. 106 h for xanthosine and control cultures, respectively. Overall, the doubling time of xanthosine treated cultures was 71% of that for control cultures.

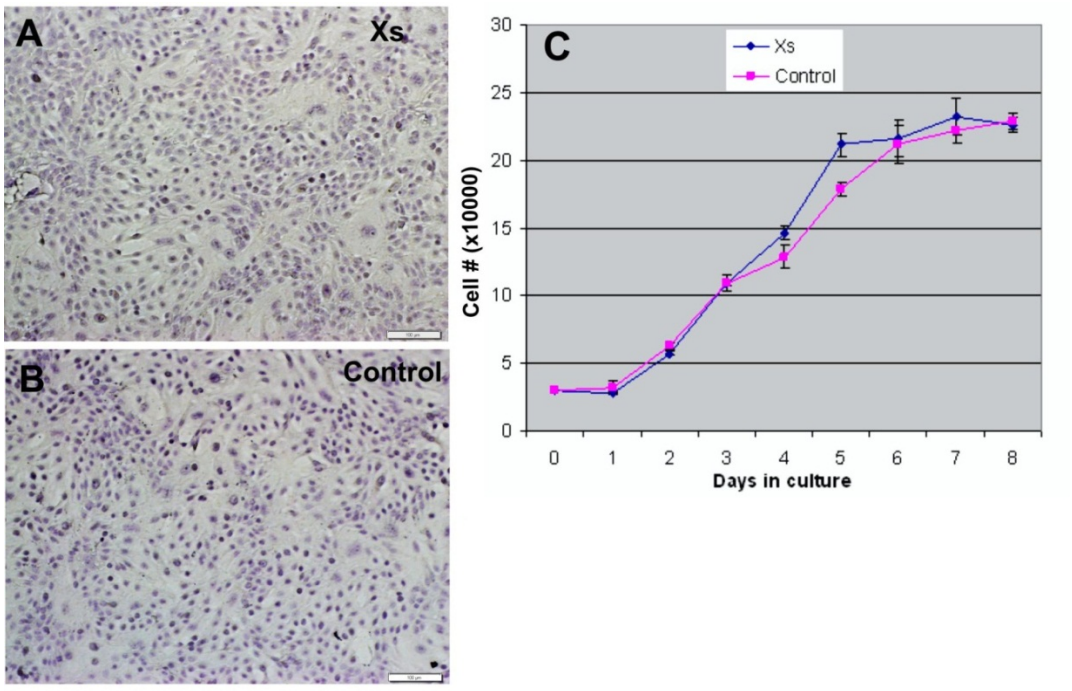

Figure 17. Evaluation of the effects of xanthosine on cell morphology and growth rate of bovine MEC. A-B- Micrographs of hematoxylin stained monolayers of early-passage bovine MEC, demonstrating typical cobblestone morphology of cells cultured in xanthosine (A) and control (B) medium. C- Growth of primary MEC in the presence and absence of 200 µM xanthosine. Data are from a representative experiment using MEC at passage 3 presented as the mean number of cells per well (± standard error) for triplicate cultures. An increase ($P < 0.05$) in cell number of xanthosine-treated cultures was evident on d 4 and 5. Scale bar = 100 µm.

Cell cycle progression

Consistent with the increased population growth rate of xanthosine-treated cells, cultures that were continuously exposed to xanthosine for five d showed an increase ($P < 0.05$) in the proportion of cells in S-phase (16 ± 0.8; n =6) compared with control cultures (10.8 ± 1.2; n =5) (Figure 18A-D). Additionally, cell cycle analysis (~ 5000-10000 cells) of xanthosine-treated and control cultures demonstrated that the percentage of cells in the S-phase plus G2/M-phases was greater in xanthosine-treated than control cultures (7.3 vs. 2.2; Figure 18E-F). Differences in the proliferation indices between these two experiments are likely a function of the duration of BrdU labeling and the proliferation status of cells in the two experiments presented. Together with the lack of effect of xanthosine on cell viability, these data indicate that xanthosine decreases the culture doubling time by promoting proliferation of MEC.

Label retaining epithelial cells

Monolayer cultures of MEC were continuously labeled with BrdU for 7 d and then the persistence of BrdU label retaining epithelial cells (LREC) was evaluated for the following 6 wk, with passage every week. At the end of the first week, most of the cells were proliferating and were labeled with BrdU. On each subsequent weekly passage the number of LREC decreased gradually from 13.1% (3^{rd} wk), 3.5% (4^{th} wk), 0.46% (5^{th} wk) to 0.4% (6^{th} wk) (Figure 19 A-E). These LREC were cycling on every passage as evidenced by karyokinesis (arrows) and dilution of label (arrowheads) (Figure 19 A-D). This low frequency (0.4% by 6^{th} wk) of LREC was consistent with the result of an in vivo study in which the frequency of LREC after 42 d (6 wk) were 0.4% of total epithelial cells counted in prepubertal bovine mammary gland (Capuco et al., 2009).

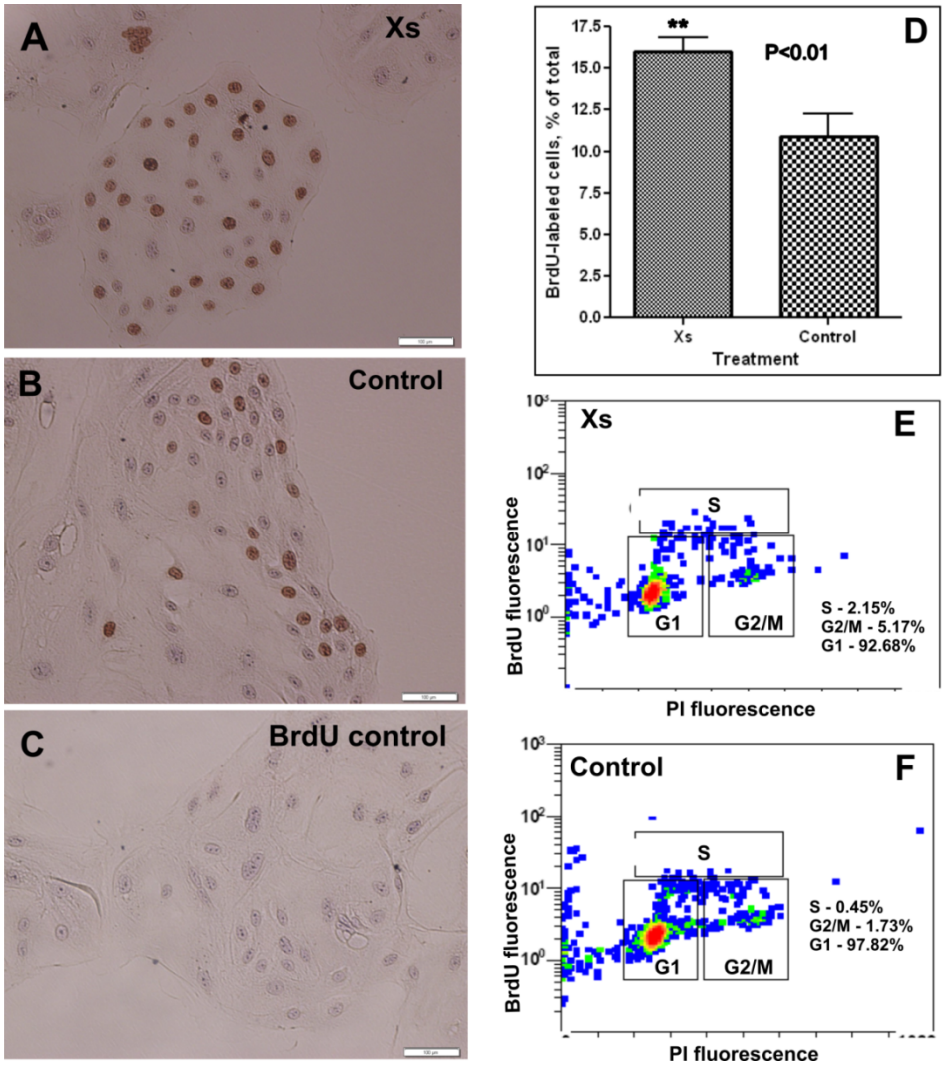

Figure 18. Effect of xanthosine on cell cycle progression.

A-D- BrdU labeling of proliferating cultures. Micrograph depicting BrdU-labeled cells (brown nuclei) in xanthosine-treated (A) and control (B) cultures. Negative control for BrdU immunostaining (C). Quantification of the BrdU labeling index in xanthosine-treated and control cultures (D), expressed as a percentage of total cells. Treatment with xanthosine led to an increase in the percentage (mean $\pm$ SE, n = 6) of BrdU positive cells. Scale bar = 100 µm. E - F- Flow cytometric evaluation (see Methods) of cell cycle distribution for MEC in xanthosine-treated (E) and control cultures (F). Xanthosine treatment led to an increase in the number of cells in S+G2/M phases of the cell cycle.

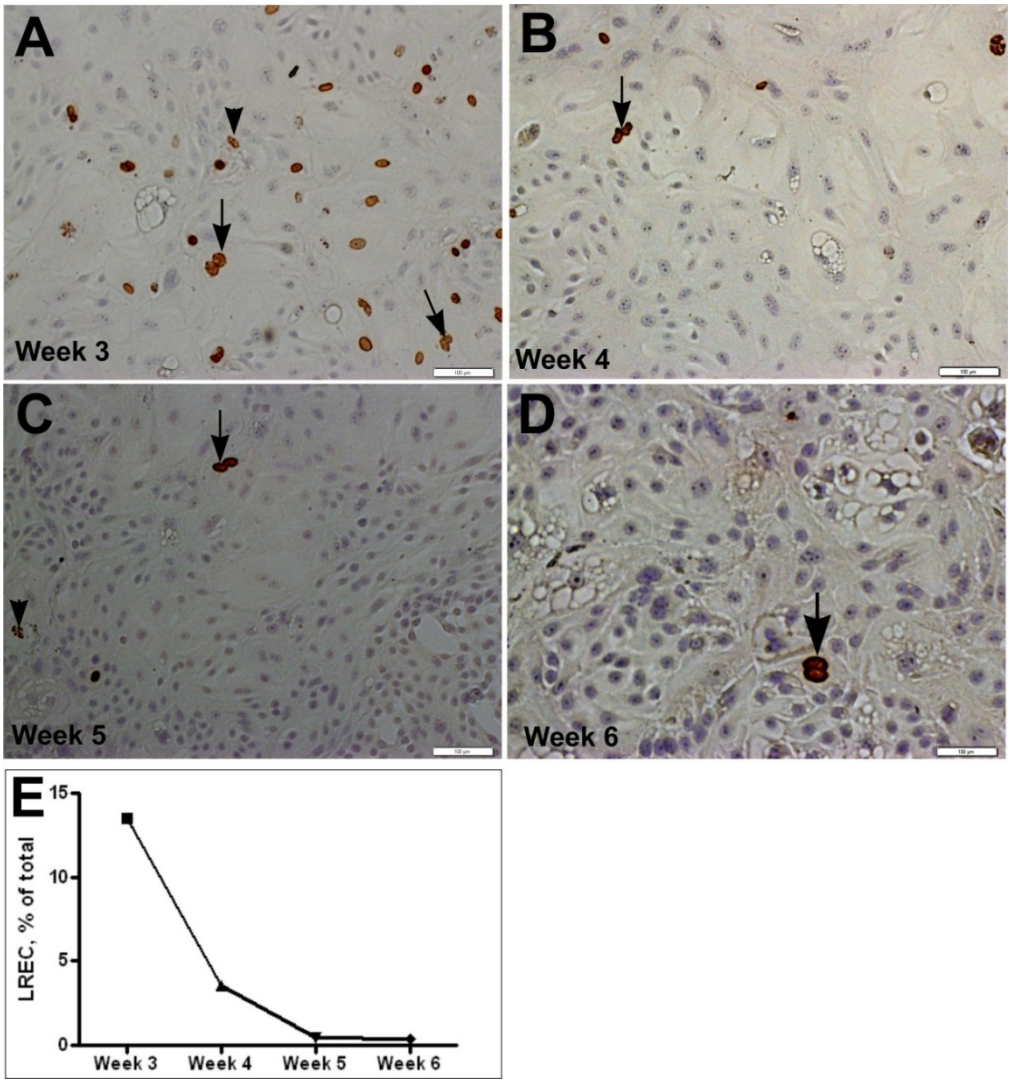

Figure 19. Primary cultures of bovine MEC contain label-retaining epithelial cells (LREC). Growing cultures of MEC were labeled with BrdU for one wk and the percentage of BrdU-positive cells tracked weekly thereafter, with cell passage every wk. There was a progressive decrease in the number of BrdU-positive cells from wk 3 (A; n =2), 4 (B; n =2) and 5 (C; n = 2) to wk 6 (D; n =6), depicted in panel E. By the 6th wk the percentage of LREC plateaued. The LREC were actively dividing, non-quiescent cells, as evidenced by karyokinesis (arrows) and dilution of BrdU label in some LREC (arrowheads). Scale bars: (A-C) =100 µm, (D) =50 µm

Recent studies have suggested that LREC represent mammary stem/progenitor cells in bovine mammary gland in vivo (Capuco et al., 2009; Choudhary et al., 2010a) and in human mammosphere cultures (Dey et al., 2009). Our preliminary data (not shown) indicate the xanthosine increases symmetric division of LREC in bovine MEC cultures. However, further characterization of these LREC is necessary.

Symmetrical cell division and stem/progenitor cells

To evaluate the influence of xanthosine on symmetric/asymmetric division, an in situ immuno-cytochemical assay was used to visualize the distribution of BrdU label between the two daughter cells of a parental cell division. MEC were incubated with BrdU, plated at cloning density, and the distribution of label was then tracked in daughter cells of a parental division. When grown in the absence of xanthosine, 56% of daughter pairs contained two BrdU-positive cells, indicative of symmetrical cell division and the even distribution of BrdU-labeled DNA between the daughter cells (Figure 20A); whereas 44% of daughter pairs contained a single BrdU-positive cell, indicative asymmetrical parental cell division (Figure 20B). In contrast, when cells were incubated with xanthosine the proportion of cells undergoing symmetrical cell division increased from the 56% observed in control cultures to 72% in xanthosine-treated cultures ($P < 0.05$; Figure 20C). We assume that these dividing cells contain a substantial proportion of stem cells (or progenitor cells) and their population is expanded by the symmetrical division induced by xanthosine. This is consistent with in vitro studies by Sherley and colleagues, who demonstrated that treatment of rat hepatocytes with xanthosine increased symmetrical division of hepatocyte stem cells (Lee et al., 2003).

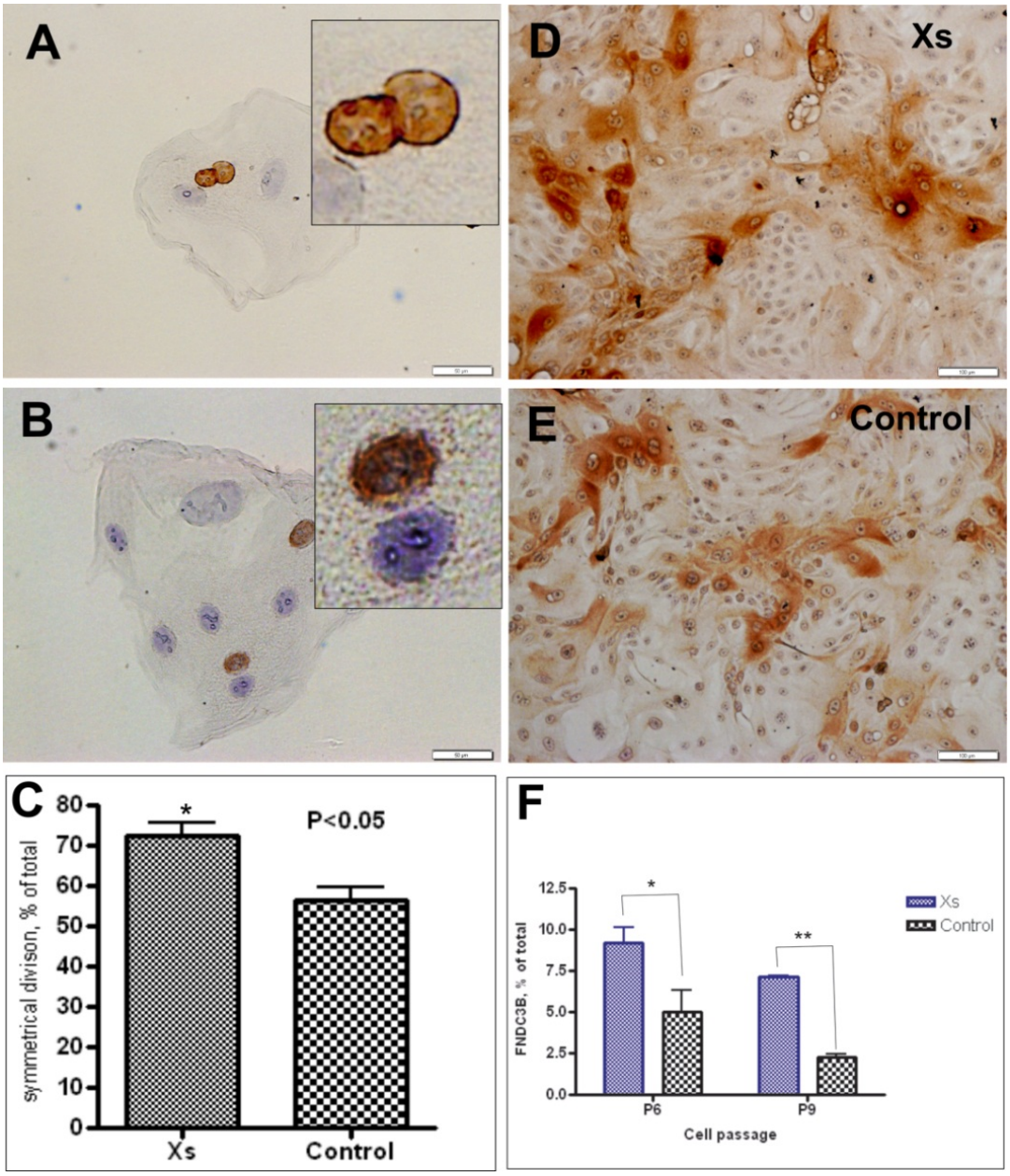

Figure 20. Detection of symmetric and asymmetric cell division by daughter pair analysis**.** Representative micrographs illustrating symmetric division (A) and asymmetric division (B) of MEC (insets are higher magnification images of two daughter cells depicted in the panel). C- Treatment of MEC with xanthosine led to an increase in the proportion of cells undergoing symmetric cell division ($P < 0.05$) (representative data of three independent experiments). Photomicrographs of FNDC3B immunostaining in xanthosine-treated (D) and control (E) cultures. F- Xanthosine led to an increase in the percentage (mean $\pm$ SE, n = 3) of FNDC3B-positive cells across different passage (P). Scale bars: (A-B) =50 µm, (D-E) =100 µm.

Additional support for the conclusion that xanthosine increased the population of stem/progenitor cells is provided by increased telomerase activity and FNDC3B expression by xanthosine-treated cells. We observed that xanthosine-treated cultures tended to have more telomerase activity (pmol/10^6 cells) than control cultures (0.14 vs. 0.075; P = 0.11). This trend toward increased telomerase activity in xanthosine-treated cells was consistently observed in repeated experiments. Because telomerase activity is primarily found in stem cells and progenitor cells (Meeker and Coffey, 1997). These data are consistent with a xanthosine-induced increase in the population of these cells. Furthermore, we showed that xanthosine treatment increased the number of FNDC3B-positive cells in culture (Figure 20D-F). FNDC3B is a potential marker of bovine mammary stem and progenitor cells that we recently identified by microarray analysis of LREC, which were excised by laser microdissection from cryosections of mammary tissue (Choudhary et al., 2010a). We quantified the percentage of FNDC3B-positive cells and found an increased percentage of FNDC3B-positive cells in xanthosine-treated cultures (n =3) compared with control cultures (9.2 $\pm$ 0.9 vs. 5.0 $\pm$ 1.2; P < 0.05; passage 6). In a cell later passage, mean percentage of FNDC3B-positive cells declined but the effect of xanthosine was highly significant (7.1 $\pm$ 1.3 vs. 2.2 $\pm$ 0.4; P <0.01; passage 9). The effect of xanthosine on two passages were significant (P = 0.015). Together these observations strengthen the hypothesis that xanthosine increases the population of bovine mammary stem/progenitor cells in vitro, which is consistent with an earlier in vivo study of prepubertal bovine mammary gland wherein intramammary infusion of xanthosine increased the putative mammary stem cell population (Capuco et al., 2009). We evaluated expression of additional novel markers for bovine mammary stem/progenitor

cells, NR5A2 and NUP153 (Choudhary et al., 2010a). However, unlike the situation in histological sections, where NR5A2 staining was exclusively nuclear, cells in culture showed varied NR5A2 staining that ranged from faint to intense nuclear staining and diffuse cytoplasmic staining. NUP153 stained the majority of epithelial cells with a gradient that ranged from intense to weak (data not shown), making quantitation difficult. Apart from having a role in maintaining nuclear envelope structure, NUP153 has been associated with spreading and migration of breast carcinoma cells (Zhou and Pante, 2010) and may play a role in spreading and migration of epithelial cells in culture, rendering it a poor progenitor cell marker in vitro.

In the present study, we evaluated the impact of xanthosine on proliferation of bovine MEC in culture. We found that xanthosine enhanced proliferation of bovine MEC. Xanthosine increased the number of stem/progenitor cells in culture, as evidenced by an increase in the expression of FNDC3B and telomerase activity and that this was accomplished by enhancing symmetrical division of mammary stem cells. This study provides support for the ability of xanthosine to expand the mammary stem cell population and support for the exciting prospect of regulating mammary stem cell number by treatment with a naturally occurring nucleoside.

This is the final draft of the manuscript to be submitted for publication.

Chapter 7: Conclusions

The overall goal of this dissertation research was to expand our knowledge of bovine mammary stem cells. Specific aims were to: (1) characterize the global gene expression profiles of putative bovine MaSCs and progenitor cells in vivo (2) identify potential protein biomarkers of MaSCs and progenitor cells and (3) confirm the utility of xanthosine to increase expansion of MaSCs using an in vitro model system.

Previous studies have evaluated MaSCs after removing them from their stem cell niche, *i.e.* the microenvironment of surrounding signaling molecules and other noncellular components that support stem cell function and survival. In this thesis research, a novel approach was taken that retains histological information by characterizing gene expression in putative MaSCs directly after their in situ excision from intact tissue. Putative stem and progenitor cells (LREC) were identified and excised from cryosections using laser microdissection. To enable this approach, a method for staining LREC within tissue cryosections while maintaining RNA quality was first developed. Using this method, LREC and neighboring epithelial control (non-LREC) cells were identified and excised from two different locations: basal and embedded layers of the mammary epithelium. The underlying hypotheses were that LREC in the basal epithelial layer are MaSCs, whereas those in embedded layers are more committed progenitor cells, and that by comparing the transcriptomes of these cells with neighboring control cells one can obtain molecular profiles and biomarkers for MaSCs and progenitor cells.

Results support these hypotheses and provide novel candidate markers for MaSCs. Transcriptome analysis uncovered several underlying networks consistent with stem cell function and the stem cell niche. Genes that were highly expressed in LREC

served as potential biomarkers of MaSCs and progenitor cells. Among these, NR5A2, NUP153, HNF4A and FNDC3B genes were of particular note and have been evaluated by immunohistochemistry as novel potential markers of prepubertal and lactating gland. Frequencies and distributions of these markers were consistent with the expectation of their being stem/progenitor cell characteristics. Together, these results suggest that LREC in the basal layer are MaSCs and that the LREC in the suprabasal layers (*e.g.* embedded layer) are progenitor cells.

Additionally, genes that were highly expressed in LREC and encode surface proteins were identified (Appendix Table 6). Some, if not all, of these genes might serve as potential surface markers, either alone or in combination. Whereas biomarkers expressed in nuclei facilitate histological identification of these target cells, biomarkers expressed on the cell surface facilitate the isolation of viable target cells for additional characterization.

In another study, I attempted to manipulate stem cell number by treating primary cultures of bovine mammary epithelium with xanthosine. Previous studies had suggested that xanthosine in increases stem cell number in hepatic tissue in vitro and bovine mammary stem cells (LREC) in vivo. In this study, I found that xanthosine treatment increases cell proliferation, promotes symmetric cell division and increases stem/progenitor cell activity. This study also suggests that primary cultures of mammary epithelium contain LREC and that these are actively dividing cells.

Insights into the biology of stem cells will be gained by further confirmation of candidate MaSCs markers identified and evaluated in this research. Appropriate biomarkers will provide means to identify MaSCs and facilitate our understanding of

their functions in mammary development, homeostasis and cancer. Specific cell surface markers will be useful for future isolation of MaSCs and investigations of their biology. In vitro studies showing that xanthosine promotes symmetric division and increased proliferation of primary bovine mammary epithelial cells confirm previous reports in other systems and suggest that this nucleoside may provide an effective means to promote the expansion of MaSCs.

The research described in this dissertation provides a foundation for a number of important future studies. (1) It is necessary to quantify the relationship between LREC and the candidate biomarkers identified by this thesis research. This would involve an immunohistochemical evaluation of coexpression of the various markers to each other and the relationship to LREC. (2) Because data profiling gene expression in LREC and control cells were derived from evaluation of cells in specific locations, it is possible to identify paracrine factors that regulate cell-cell interactions. This has not yet been fully explored and remains an area for future data analysis and research. (3) The data presented in this thesis support the hypothesis that LRECb are stem cells and that embedded LREC are progenitor cells. However, demonstration of the differentiation potentcy of these cells necessitates their isolation and evaluation using and in vitro system or an in vivo system, such as the cleared fat of an immunodeficient mouse (perhaps made more like the bovine fat pad by prior implantation of bovine fibroblasts). Utilization of the putative membrane MaSC/progenitor cell markers may make such cell isolations possible by single or multiparametric flow cytometry (4) Applicability of these potential biomarkers to other species should be investigated. This would involve quantitative immunohistochemistry or an anaylsis of cell populations in other species

(e.g., mouse) that are known to have increased stem cell functionality. (5) The in vitro study evaluating effects of xanthosine on primary cultures of bovine mammary epithelial cells supports the hypothesis that xanthosine can induce expansion of the stem cell population. Thus, further studies are warrented to evaluate the impact of intramammary infusions of xanthosine on mammary growth, cell turnover, and milk production efficiency.

Appendix

Appendix Figure 1. Flow chart for identification, isolation and characterization of presumptive bovine MaSCs

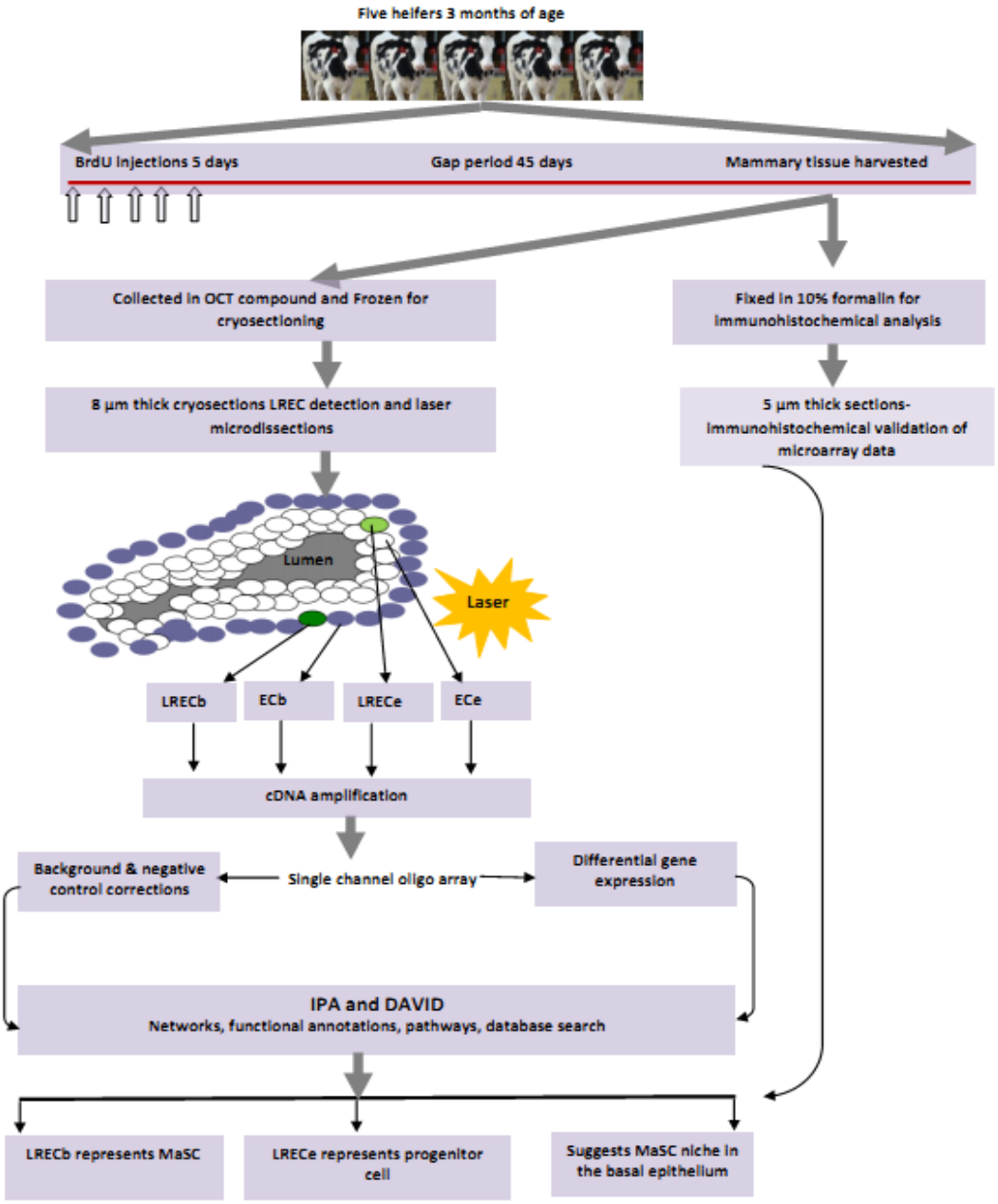

Appendix Table 1: Transcripts that were differentially expressed in LRECb vs. ECb
(*positive values for fold-change indicate that expression is higher in LRECb)

Bovine RefSeq_ID	**Bovine RefSeq_Description**	**P value**	**Fold change***
XM_584232.4	PREDICTED: Bos taurus hypothetical LOC539014, transcript variant 1 (LOC539014), mRNA	0.0000090	4.34
XM_001788604.1	PREDICTED: Bos taurus similar to guanylate binding protein 4 (LOC507055), mRNA	0.0000774	2.38
XM_001790319.1	PREDICTED: Bos taurus sirtuin (silent mating type information regulation 2 homolog) 2 (S. cerevisiae) (SIRT2), mRNA	0.0001415	2.04
XM_614275.4	PREDICTED: Bos taurus similar to one twenty two protein, transcript variant 1 (RBM15), mRNA	0.0003939	2.70
NM_001102150.1	Bos taurus phosphoserine aminotransferase 1 (PSAT1), mRNA	0.0006365	2.08
XM_001251199.1	PREDICTED: Bos taurus similar to SWI/SNF-related, matrix-associated actin-dependent regulator of chromatin, subfamily a, containing DEAD/H box 1, transcript variant 1 (SMARCAD1), mRNA	0.0007888	2.27
NM_001037629.1	Bos taurus translocase of inner mitochondrial membrane 8 homolog B (yeast) (TIMM8B), nuclear gene encoding mitochondrial protein, mRNA	0.0010158	3.44
XR_028625.1	PREDICTED: Bos taurus misc_RNA (LOC521100), miscRNA	0.0010857	2.43
NM_001046166.1	Bos taurus PWP1 homolog (S. cerevisiae) (PWP1), mRNA	0.0010980	3.22
NM_001035424.1	Bos taurus myoneurin (Mynn), mRNA	0.0012259	2.22
NM_001077928.1	Bos taurus plexin domain containing 2 (PLXDC2), mRNA	0.0012746	3.22
XM_001249400.2	PREDICTED: Bos taurus similar to fibronectin type III domain containing 3B, transcript variant 1 (FNDC3B), mRNA	0.0013167	2.85
NM_001100293.1	Bos taurus chemokine (C-C motif) receptor 4 (CCR4), mRNA	0.0014255	2.77
XM_610845.4	PREDICTED: Bos taurus serum deprivation response (phosphatidylserine binding protein) (SDPR), partial mRNA	0.0014426	3.57
NM_001076532.1	Bos taurus cell division cycle and apoptosis	0.0016439	2.00

	regulator 1 (CCAR1), mRNA		
NM_001035405.1	Bos taurus SLAIN motif family, member 2 (SLAIN2), mRNA	0.0017160	2.32
NM_001075966.1	Bos taurus reticulon 1 (RTN1), mRNA	0.0017330	2.22
XM_615384.4	PREDICTED: Bos taurus hypothetical LOC535329, transcript variant 1 (LOC535329), mRNA	0.0017493	2.94
XM_611687.3	PREDICTED: Bos taurus similar to WW and C2 domain containing 2 (WWC2), mRNA	0.0018918	2.17
XM_602501.4	PREDICTED: Bos taurus similar to CG10038 CG10038-PB (LOC524181), mRNA	0.0019341	2.94
NM_001001153.2	Bos taurus monoacylglycerol O-acyltransferase 1 (MOGAT1), mRNA	0.0019923	2.38
XM_588427.3	PREDICTED: Bos taurus similar to cell division cycle 2-like 5, transcript variant 3 (CDC2L5), mRNA	0.0019942	2.32
NM_001035489.1	Bos taurus mitochondrial ribosomal protein L38 (MRPL38), nuclear gene encoding mitochondrial protein, mRNA	0.0020430	2.56
XM_864360.3	PREDICTED: Bos taurus DEAH (Asp-Glu-Ala-His) box polypeptide 29, transcript variant 3 (DHX29), mRNA	0.0020763	2.00
XM_591626.4	PREDICTED: Bos taurus similar to NKG2A (LOC513869), mRNA	0.0022039	2.08
NM_001076853.1	Bos taurus zinc finger, CW type with PWWP domain 1 (ZCWPW1), mRNA	0.0024420	6.25
XM_582828.3	PREDICTED: Bos taurus similar to exonuclease 1 (EXO1), mRNA	0.0025101	3.33
NM_001046051.1	Bos taurus PRP3 pre-mRNA processing factor 3 homolog (S. cerevisiae) (PRPF3), mRNA	0.0025905	4.76
XM_001787646.1	PREDICTED: Bos taurus similar to phospholipase C-like 1 (LOC537873), partial mRNA	0.0026253	2.94
NM_001101278.1	Bos taurus family with sequence similarity 108, member B1 (FAM108B1), mRNA	0.0026324	2.22
XM_867682.3	PREDICTED: Bos taurus hypothetical LOC615784 (LOC615784), mRNA	0.0027999	3.44
NM_001038167.1	Bos taurus ubiquitin-conjugating enzyme E2D 1 (UBC4/5 homolog, yeast) (UBE2D1), mRNA	0.0029172	2.56
NM_001077009.1	Bos taurus purinergic receptor P2Y, G-protein coupled, 14 (P2RY14), mRNA	0.0029755	2.38

NM_001080272.1	Bos taurus oncostatin M receptor (OSMR), mRNA	0.0029895	2.12
NM_001077885.1	Bos taurus transcription factor 12 (TCF12), mRNA	0.0030053	2.17
NM_001080232.1	Bos taurus regulator of G-protein signaling 13 (RGS13), mRNA	0.0030566	2.04
NM_001045944.1	Bos taurus cysteinyl-tRNA synthetase 2, mitochondrial (putative) (CARS2), nuclear gene encoding mitochondrial protein, mRNA	0.0031095	2.00
NM_001102336.1	Bos taurus hypothetical protein LOC785165 (MGC157332), mRNA	0.0032146	2.22
NM_001076549.1	Bos taurus zinc finger protein 181 (ZNF181), mRNA	0.0035618	2.32
NM_001102038.1	Bos taurus hippocampus abundant transcript 1 (HIAT1), mRNA	0.0037120	2.04
XM_584315.4	PREDICTED: Bos taurus similar to chromosome 14 open reading frame 106 (LOC507661), mRNA	0.0038451	3.84
NM_001099378.1	Bos taurus solute carrier family 15 (oligopeptide transporter), member 1 (SLC15A1), mRNA	0.0039187	2.17
XM_001251108.2	PREDICTED: Bos taurus similar to mitogen-activated protein kinase kinase kinase kinase 3, transcript variant 1 (MAP4K3), mRNA	0.0039209	2.50
XM_612879.3	PREDICTED: Bos taurus zinc finger CCCH-type containing 13, transcript variant 1 (ZC3H13), mRNA	0.0040668	2.50
XM_001250449.2	PREDICTED: Bos taurus mitogen-activated protein kinase 8 (MAPK8), mRNA	0.0040971	2.12
XM_592304.4	PREDICTED: Bos taurus similar to Protein flightless-1 homolog, transcript variant 1 (FLII), mRNA	0.0041069	2.12
NM_001014923.1	Bos taurus nuclear factor (erythroid-derived 2), 45kDa (NFE2), mRNA	0.0041825	2.38
NM_203323.2	Bos taurus spermidine/spermine N1-acetyltransferase family member 2 (SAT2), mRNA	0.0041956	4.34
XM_864360.3	PREDICTED: Bos taurus DEAH (Asp-Glu-Ala-His) box polypeptide 29, transcript variant 3 (DHX29), mRNA	0.0043129	2.08
NM_001046430.1	Bos taurus ubiquitin specific peptidase 15 (USP15), mRNA	0.0043334	10.00
XM_868974.2	PREDICTED: Bos taurus THAP domain containing 9 (THAP9), mRNA	0.0043682	5.55

NM_001102190.1	Bos taurus regulating synaptic membrane exocytosis 2 (RIMS2), mRNA	0.0044392	2.12
XM_001789737.1	PREDICTED: Bos taurus hypothetical protein LOC616962 (LOC616962), mRNA	0.0044770	2.50
NM_001098066.1	Bos taurus poly(A) polymerase gamma (PAPOLG), mRNA	0.0045062	3.44
NM_001034419.1	Bos taurus hydroxyprostaglandin dehydrogenase 15-(NAD) (HPGD), mRNA	0.0046655	2.70
NM_001037463.1	Bos taurus WW domain containing E3 ubiquitin protein ligase 1 (WWP1), mRNA	0.0046752	3.03
XM_599499.4	PREDICTED: Bos taurus similar to iroquois homeobox protein-like 1 (MKX), mRNA	0.0048161	2.27
XM_593139.4	PREDICTED: Bos taurus similar to 5033413D22Rik protein (LOC515167), mRNA	0.0048473	2.43
NM_001083500.1	Bos taurus hypothetical LOC541171 (MGC143035), mRNA	0.0050889	2.56
XM_001788244.1	PREDICTED: Bos taurus similar to ceramide kinase-like (LOC617767), mRNA	0.0052627	2.27
NM_001046143.1	Bos taurus CDKN2A interacting protein (CDKN2AIP), mRNA	0.0053890	4.54
NM_001035412.1	Bos taurus mitochondrial fission regulator 1 (MTFR1), nuclear gene encoding mitochondrial protein, mRNA	0.0053943	2.32
XM_596359.4	PREDICTED: Bos taurus crumbs homolog 1 (Drosophila) (CRB1), mRNA	0.0054225	3.22
XM_606001.4	PREDICTED: Bos taurus similar to Elongation factor Tu GTP-binding domain-containing protein 1 (EFTUD1), partial mRNA	0.0054279	2.08
XM_864645.3	PREDICTED: Bos taurus similar to alkylglycerone phosphate synthase, transcript variant 2 (AGPS), mRNA	0.0054312	3.22
XM_584095.4	PREDICTED: Bos taurus similar to ankyrin repeat and SOCS box-containing protein 7 (ASB7), mRNA	0.0055161	2.32
NM_001098106.1	Bos taurus basic transcription factor 3-like 4 (BTF3L4), mRNA	0.0055990	2.00
XM_001249810.2	PREDICTED: Bos taurus similar to LON peptidase N-terminal domain and RING finger protein 3, transcript variant 1 (LONRF3), mRNA	0.0057335	2.38
XM_617670.4	PREDICTED: Bos taurus similar to ankyrin repeat domain 41 (ANKRD41), mRNA	0.0058692	2.63
XM_869350.3	PREDICTED: Bos taurus similar to histone deacetylase 7A, transcript variant 2	0.0058891	2.08

	(LOC509843), mRNA		
XM_581038.3	PREDICTED: Bos taurus similar to myeloid/lymphoid or mixed-lineage leukemia (trithorax homolog, Drosophila); translocated to, 4 (MLLT4), mRNA	0.0059144	2.00
NM_174554.2	Bos taurus insulin-like growth factor binding protein 1 (IGFBP1), mRNA	0.0059435	2.56
XM_581757.3	PREDICTED: Bos taurus similar to cytochrome P450 2C92 (LOC505468), mRNA	0.0059466	2.38
XM_605785.4	PREDICTED: Bos taurus similar to Pygopus homolog 1 (PYGO1), mRNA	0.0059950	2.94
XM_603252.4	PREDICTED: Bos taurus similar to progesterone-induced blocking factor 1 (PIBF1), mRNA	0.0059989	2.17
NM_001076926.1	Bos taurus neuronal guanine nucleotide exchange factor (NGEF), mRNA	0.0060157	2.27
XM_616050.3	PREDICTED: Bos taurus similar to LATS homolog 1, transcript variant 1 (LATS1), mRNA	0.0061121	2.27
XM_001790585.1	PREDICTED: Bos taurus similar to cytoplasmic FMR1 interacting protein 1 (LOC100141021), mRNA	0.0063718	2.27
XM_589504.3	PREDICTED: Bos taurus similar to DIP2 disco-interacting protein 2 homolog B (DIP2B), mRNA	0.0066679	2.63
NM_174056.3	Bos taurus fibroblast growth factor 2 (basic) (FGF2), mRNA	0.0066798	3.03
NM_001038201.1	Bos taurus signal recognition particle 54kDa (SRP54), mRNA	0.0068338	2.08
XM_589621.4	PREDICTED: Bos taurus similar to NFX1-type zinc finger-containing protein 1 (ZNFX1), mRNA	0.0071001	2.63
XM_615492.4	PREDICTED: Bos taurus similar to membrane bound O-acyltransferase domain containing 1 (MBOAT1), mRNA	0.0071345	2.04
XM_615597.4	PREDICTED: Bos taurus similar to nuclear receptor subfamily 5, group A, member 2, transcript variant 1 (NR5A2), mRNA	0.0072373	2.50
NM_001040510.2	Bos taurus Down syndrome critical region protein 3 (DSCR3), mRNA	0.0072837	2.00
XM_614439.4	PREDICTED: Bos taurus similar to early endosome antigen 1, transcript variant 4 (LOC534614), mRNA	0.0072842	2.22
NM_001035461.1	Bos taurus ribonuclease P/MRP 30kDa	0.0073033	2.38

	subunit (RPP30), mRNA		
NM_001099209.1	Bos taurus hypothetical protein LOC788754 (MGC152484), mRNA	0.0074665	3.12
XR_042701.1	PREDICTED: Bos taurus misc_RNA (LOC786759), miscRNA	0.0075318	3.44
NM_001075518.1	Bos taurus aldehyde dehydrogenase 3 family, member B1 (ALDH3B1), mRNA	0.0075521	2.00
NM_001075547.1	Bos taurus secernin 3 (SCRN3), mRNA	0.0077030	3.12
XM_596263.4	PREDICTED: Bos taurus similar to ATP-binding cassette transporter 13 (LOC518080), mRNA	0.0078359	2.77
NM_173879.2	Bos taurus coagulation factor V (proaccelerin, labile factor) (F5), mRNA	0.0078616	2.56
XM_875092.3	PREDICTED: Bos taurus similar to Cytoplasmic polyadenylation element-binding protein 3 (CPE-binding protein 3) (CPE-BP3) (hCPEB-3), transcript variant 3 (CPEB3), mRNA	0.0079752	2.12
NM_001080289.1	Bos taurus hypothetical LOC526913 (MGC148942), mRNA	0.0079944	3.70
XM_864068.3	PREDICTED: Bos taurus similar to v-raf murine sarcoma viral oncogene homolog B1, transcript variant 2 (BRAF), partial mRNA	0.0080007	2.08
NM_001076865.1	Bos taurus telomeric repeat binding factor (NIMA-interacting) 1 (TERF1), mRNA	0.0080705	3.70
NM_001081616.1	Bos taurus VMA21 vacuolar H+-ATPase homolog (S. cerevisiae) (VMA21), mRNA	0.0082859	4.54
NM_001109789.1	Bos taurus PRP39 pre-mRNA processing factor 39 homolog (S. cerevisiae) (PRPF39), mRNA	0.0084216	2.77
NM_001110181.1	Bos taurus excision repair cross-complementing rodent repair deficiency, complementation group 8 (ERCC8), mRNA	0.0084751	2.38
XM_001790639.1	PREDICTED: Bos taurus NOL1/NOP2/Sun domain family, member 4 (NSUN4), mRNA	0.0087732	2.70
XM_001789358.1	PREDICTED: Bos taurus similar to membrane associated guanylate kinase, WW and PDZ domain containing 1, transcript variant 1 (LOC783484), mRNA	0.0088459	2.43
NM_001046029.1	Bos taurus chromosome X open reading frame 41 ortholog (CXHXORF41), mRNA	0.0088953	2.00
XM_603300.3	PREDICTED: Bos taurus similar to nuclear receptor interacting protein 1 (NRIP1), mRNA	0.0089694	5.55
XM_001789545.1	PREDICTED: Bos taurus similar to Obg-like ATPase 1 (GTP-binding protein 9)	0.0090148	2.04

	(LOC541081), mRNA		
XM_586772.4	PREDICTED: Bos taurus alcohol dehydrogenase 1C (class I), gamma polypeptide, transcript variant 1 (ADH1C), mRNA	0.0091125	2.08
NM_001113232.1	Bos taurus dermatan sulfate epimerase (DSE), mRNA	0.0093964	2.70
XM_592213.4	PREDICTED: Bos taurus coiled-coil domain containing 11 (CCDC11), mRNA	0.0095257	4.16
NM_001076354.1	Bos taurus MAP6 domain containing 1 (MAP6D1), mRNA	0.0096048	2.08
NM_001102215.1	Bos taurus zinc finger, ZZ-type containing 3 (ZZZ3), mRNA	0.0096630	2.63
NM_001046113.1	Bos taurus myocyte enhancer factor 2C (MEF2C), mRNA	0.0096783	2.04
NM_001075823.1	Bos taurus sulfotransferase family, cytosolic, 1B, member 1 (SULT1B1), mRNA	0.0097722	2.77
NM_001075118.1	Bos taurus pyrophosphatase (inorganic) 1 (PPA1), mRNA	0.0097963	2.38
NM_001046309.1	Bos taurus BMP and activin membrane-bound inhibitor homolog (Xenopus laevis) (BAMBI), mRNA	0.0098548	2.00
NM_001075749.1	Bos taurus radixin (RDX), mRNA	0.0099143	2.50
NM_001113282.1	Bos taurus processing of precursor 4, ribonuclease P/MRP subunit (S. cerevisiae) (POP4), transcript variant 1, mRNA	0.0100811	2.94
XM_585315.3	PREDICTED: Bos taurus hypothetical LOC508527 (LOC508527), mRNA	0.0101561	2.32
NM_001046060.1	Bos taurus GTPase, IMAP family member 4 (GIMAP4), mRNA	0.0102828	2.77
NM_174011.3	Bos taurus CD3e molecule, epsilon (CD3-TCR complex) (CD3E), mRNA	0.0103942	2.08
NM_001083734.1	Bos taurus ring finger and SPRY domain containing 1 (RSPRY1), mRNA	0.0104790	2.43
NM_001081736.1	Bos taurus IKK interacting protein (IKIP), mRNA	0.0105793	2.32
XM_001253151.2	PREDICTED: Bos taurus similar to von Willebrand factor C and EGF domains (VWCE), mRNA	0.0106237	2.22
NM_001076112.1	Bos taurus GLI pathogenesis-related 2 (GLIPR2), mRNA	0.0107706	2.50
XM_864958.3	PREDICTED: Bos taurus similar to G elongation factor, transcript variant 3 (GFM1), mRNA	0.0108448	2.17

NM_001015557.1	Bos taurus hepatocyte nuclear factor 4, alpha (HNF4A), mRNA	0.0109094	2.00
XM_615064.4	PREDICTED: Bos taurus similar to Dixin (DIX domain-containing protein 1) (Coiled-coil protein DIX1) (Coiled-coil-DIX1) (DIXDC1), mRNA	0.0109587	2.22
XM_590563.4	PREDICTED: Bos taurus similar to Protein SPT2 homolog (SPT2 domain-containing protein 1) (Protein KU002155) (SPTY2D1), mRNA	0.0110319	2.50
NM_174071.2	Bos taurus glycine receptor, beta (GLRB), mRNA	0.0110402	2.56
NM_001076164.1	Bos taurus protein phosphatase 1, regulatory (inhibitor) subunit 3C (PPP1R3C), mRNA	0.0111674	2.04
NM_001076835.1	Bos taurus kelch-like 20 (Drosophila) (KLHL20), mRNA	0.0113016	2.22
XM_592504.4	PREDICTED: Bos taurus similar to START domain containing 10 (STARD10), mRNA	0.0114595	4.54
XM_878406.3	PREDICTED: Bos taurus similar to protein kinase N2, transcript variant 3 (PKN2), mRNA	0.0115115	2.94
NM_174385.2	Bos taurus latent transforming growth factor beta binding protein 2 (LTBP2), mRNA	0.0116489	2.27
NM_001076065.1	Bos taurus esterase D/formylglutathione hydrolase (ESD), mRNA	0.0118133	2.27
NM_001081529.1	Bos taurus family with sequence similarity 55, member C (FAM55C), mRNA	0.0118487	2.63
NM_001012399.1	Bos taurus hemochromatosis (hfe), mRNA	0.0119556	2.00
XM_001253405.2	PREDICTED: Bos taurus similar to dual specificity phosphatase 11 (LOC786531), mRNA	0.0119634	2.56
NM_001083791.1	Bos taurus SH3 domain binding glutamic acid-rich protein like 2 (SH3BGRL2), mRNA	0.0121882	2.00
NM_001076973.1	Bos taurus hypothetical protein FLJ13868 (FLJ13868), mRNA	0.0122437	2.32
XM_587287.4	PREDICTED: Bos taurus proline-rich cyclin A1-interacting protein (PROCA1), mRNA	0.0122585	2.08
NM_001046523.1	Bos taurus hepatitis A virus cellular receptor 1 N-terminal domain containing protein (MGC137099), mRNA	0.0123479	3.12
NM_001076299.3	Bos taurus solute carrier family 25, member 40 (SLC25A40), nuclear gene encoding mitochondrial protein, mRNA	0.0124654	2.22

XM_581753.4	PREDICTED: Bos taurus similar to pseudouridylate synthase 7 homolog (S. cerevisiae)-like (PUS7L), mRNA	0.0125166	3.84
NM_174456.2	Bos taurus N-myristoyltransferase 2 (NMT2), mRNA	0.0126052	2.38
NM_001034599.1	Bos taurus chromosome 10 open reading frame 58 ortholog (C28H10orf58), mRNA	0.0127909	2.27
NM_001075479.1	Bos taurus paraoxonase 3 (PON3), mRNA	0.0127931	2.12
NM_001113277.1	Bos taurus kininogen 1 (KNG1), transcript variant II, mRNA	0.0127964	2.22
XM_592026.4	PREDICTED: Bos taurus caspase 1, apoptosis-related cysteine peptidase (interleukin 1, beta, convertase), transcript variant 1 (CASP1), mRNA	0.0128057	2.32
XM_588044.3	PREDICTED: Bos taurus similar to Uncharacterized protein KIAA0247 (LOC510837), mRNA	0.0128084	2.27
NM_001015642.2	Bos taurus carboxypeptidase X (M14 family), member 1 (CPXM1), mRNA	0.0129254	2.77
NM_001101167.1	Bos taurus RCD1 required for cell differentiation1 homolog (S. pombe) (RQCD1), mRNA	0.0130297	2.22
NM_001099066.1	Bos taurus solute carrier family 25 (mitochondrial carrier; phosphate carrier), member 24 (SLC25A24), nuclear gene encoding mitochondrial protein, mRNA	0.0131019	2.43
NM_001130931.1	Bos taurus nucleoporin 205kDa (NUP205), mRNA	0.0132027	2.12
NM_001038195.1	Bos taurus IQ motif containing G (IQCG), mRNA	0.0133012	2.70
NM_001014933.2	Bos taurus CSE1 chromosome segregation 1-like (yeast) (CSE1L), mRNA	0.0139152	2.43
XM_864293.3	PREDICTED: Bos taurus similar to Transcription cofactor vestigial-like protein 1 (Vgl-1) (Protein TONDU), transcript variant 4 (VGLL1), mRNA	0.0139606	2.94
XR_043028.1	PREDICTED: Bos taurus misc_RNA (LOC100138100), miscRNA	0.0140994	2.17
XM_606667.4	PREDICTED: Bos taurus similar to jumonji, AT rich interactive domain 2 protein, transcript variant 6 (JARID2), mRNA	0.0141447	2.50
NM_174684.2	Bos taurus ATP synthase, H+ transporting, mitochondrial F1 complex, alpha subunit 1, cardiac muscle (ATP5A1), nuclear gene encoding mitochondrial protein, mRNA	0.0143320	2.22

NM_001015639.1	Bos taurus proteasome (prosome, macropain) 26S subunit, ATPase, 2 (PSMC2), mRNA	0.0144093	3.33
XM_001252669.1	PREDICTED: Bos taurus similar to Endopin 1b, transcript variant 1 (LOC784964), mRNA	0.0145056	2.08
NM_001105457.1	Bos taurus cytotoxic and regulatory T cell molecule (CRTAM), mRNA	0.0145094	2.00
NM_001083437.1	Bos taurus chromosome 8 open reading frame 70 ortholog (C14H8ORF70), mRNA	0.0146269	2.12
NM_001083416.1	Bos taurus EF-hand domain family, member A1 (EFHA1), mRNA	0.0147691	2.04
NM_174714.2	Bos taurus elastase 2A (ELA2A), mRNA	0.0149778	3.22
XM_614458.4	PREDICTED: Bos taurus CAP-GLY domain containing linker protein 1, transcript variant 1 (CLIP1), mRNA	0.0150572	4.76
XM_001251704.2	PREDICTED: Bos taurus GTP cyclohydrolase 1 (dopa-responsive dystonia) (GCH1), mRNA	0.0151185	2.04
XM_865801.2	PREDICTED: Bos taurus similar to DNA polymerase zeta catalytic subunit (hREV3), transcript variant 2 (REV3L), mRNA	0.0151627	2.32
NM_001098157.1	Bos taurus hypothetical protein LOC784871 (MGC155143), mRNA	0.0152206	2.38
XM_871203.3	PREDICTED: Bos taurus similar to cDNA sequence BC004004 (LOC618886), mRNA	0.0152369	2.38
XM_868213.3	PREDICTED: Bos taurus similar to Transcobalamin-1 precursor (Transcobalamin I) (TCI) (TC I) (TCN1), mRNA	0.0153443	3.12
XR_042741.1	PREDICTED: Bos taurus misc_RNA (LOC785805), miscRNA	0.0156604	2.56
XM_594174.3	PREDICTED: Bos taurus NOL1/NOP2/Sun domain family, member 2 (NSUN2), mRNA	0.0157375	4.54
NM_174199.2	Bos taurus transition protein 1 (during histone to protamine replacement) (TNP1), mRNA	0.0157765	2.08
XM_868284.3	PREDICTED: Bos taurus similar to MRG-binding protein (LOC616297), mRNA	0.0160638	2.63
NM_001101217.1	Bos taurus far upstream element (FUSE) binding protein 3 (FUBP3), mRNA	0.0163915	2.00
NM_001083757.1	Bos taurus adenylate kinase 5 (AK5), mRNA	0.0165100	2.50
NM_001098085.1	Bos taurus copine VIII (CPNE8), mRNA	0.0166754	2.38
NM_001098032.1	Bos taurus cytoskeleton associated protein 2 (CKAP2), mRNA	0.0168264	2.63

NM_001105436.1	Bos taurus AU RNA binding protein/enoyl-Coenzyme A hydratase (AUH), nuclear gene encoding mitochondrial protein, mRNA	0.0168548	2.70
NM_001015672.2	Bos taurus family with sequence similarity 134, member B (FAM134B), mRNA	0.0169066	2.04
XM_001250879.2	PREDICTED: Bos taurus similar to Rho guanine nucleotide exchange factor 3 (Exchange factor found in platelets and leukemic and neuronal tissues) (XPLN) (ARHGEF3), mRNA	0.0169439	2.00
NM_001079773.1	Bos taurus sperm equatorial segment protein 1 (SPESP1), mRNA	0.0169528	2.56
NM_001109789.1	Bos taurus PRP39 pre-mRNA processing factor 39 homolog (S. cerevisiae) (PRPF39), mRNA	0.0171074	2.50
XM_614941.4	PREDICTED: Bos taurus similar to ATPase, class I, type 8B, member 1, transcript variant 1 (ATP8B1), mRNA	0.0173030	2.56
NM_001075782.1	Bos taurus ADP-ribosylation factor-like 6 (ARL6), mRNA	0.0173410	2.32
NM_001075430.1	Bos taurus retinoic acid receptor responder (tazarotene induced) 1 (RARRES1), mRNA	0.0173763	2.94
NM_001082601.1	Bos taurus ubiquitin protein ligase E3 component n-recognin 7 (putative) (UBR7), mRNA	0.0175333	2.77
NM_001034447.1	Bos taurus fructose-1,6-bisphosphatase 1 (FBP1), mRNA	0.0176705	2.56
NM_001105258.1	Bos taurus kinesin family member 20B (KIF20B), mRNA	0.0176928	2.32
NM_174301.3	Bos taurus chemokine (C-X-C motif) receptor 4 (CXCR4), mRNA	0.0177191	4.00
NM_194465.2	Bos taurus murine retrovirus integration site 1 homolog (MRVI1), transcript variant 2, mRNA	0.0178000	2.85
XM_594801.4	PREDICTED: Bos taurus non-SMC condensin II complex, subunit G2 (NCAPG2), mRNA	0.0178074	2.56
XR_027254.2	PREDICTED: Bos taurus misc_RNA (LOC530341), miscRNA	0.0178521	2.17
XM_592997.4	PREDICTED: Bos taurus similar to deltex 3-like (Drosophila) (DTX3L), mRNA	0.0178923	2.17
NM_001102264.1	Bos taurus cystinosis, nephropathic (CTNS), mRNA	0.0180025	2.00
NM_001083665.1	Bos taurus chromosome X open reading frame 23 ortholog (CXHXORF23), mRNA	0.0181614	2.04

XM_587403.4	PREDICTED: Bos taurus similar to Zinc finger protein 800, transcript variant 1 (ZNF800), mRNA	0.0182360	2.63
NM_001075523.1	Bos taurus keratin 25 (KRT25), mRNA	0.0183781	2.00
NM_001075704.1	Bos taurus chromosome 12 open reading frame 4 ortholog (C5H12ORF4), mRNA	0.0184511	2.12
XR_028361.2	PREDICTED: Bos taurus misc_RNA (LOC535064), miscRNA	0.0188705	2.22
NM_001100314.1	Bos taurus phosphoinositide-3-kinase, regulatory subunit 4 (PIK3R4), mRNA	0.0189040	2.17
XM_588277.3	PREDICTED: Bos taurus similar to zinc finger, CCHC domain containing 8, transcript variant 1 (ZCCHC8), mRNA	0.0190035	2.85
NM_001029846.1	Bos taurus 2',5'-oligoadenylate synthetase 1, 40/46kDa (OAS1), mRNA	0.0190270	2.27
NM_001100384.1	Bos taurus PPPDE peptidase domain containing 1 (PPPDE1), mRNA	0.0190358	2.12
XM_001788655.1	PREDICTED: Bos taurus similar to ATP-dependent Clp protease ATP-binding subunit clpX-like, mitochondrial (LOC100138870), mRNA	0.0192995	2.04
XM_001253451.1	PREDICTED: Bos taurus CD320 molecule (CD320), mRNA	0.0194922	2.22
XM_614763.4	PREDICTED: Bos taurus asp (abnormal spindle) homolog, microcephaly associated (Drosophila) (ASPM), mRNA	0.0196826	2.70
XM_001252887.2	PREDICTED: Bos taurus regulator of G-protein signaling 1, transcript variant 1 (RGS1), mRNA	0.0199903	3.33
XM_001790155.1	PREDICTED: Bos taurus hydroxysteroid (17-beta) dehydrogenase 6 homolog (mouse) (HSD17B6), mRNA	0.0200277	2.22
XM_612914.4	PREDICTED: Bos taurus killer cell lectin-like receptor subfamily B, member 1 (KLRB1), mRNA	0.0204399	2.12
XM_001253131.2	PREDICTED: Bos taurus similar to solute carrier family 10 (sodium/bile acid cotransporter family), member 5 (SLC10A5), mRNA	0.0204546	10.00
NM_174002.2	Bos taurus calcium-sensing receptor (CASR), mRNA	0.0205922	3.12
XM_582594.4	PREDICTED: Bos taurus similar to zinc finger protein 77 (pT1) (LOC506181), partial mRNA	0.0206840	2.56
NM_001034786.1	Bos taurus transmembrane protein 50B (TMEM50B), mRNA	0.0208215	2.27

NM_001034497.1	Bos taurus solute carrier family 25, member 34 (SLC25A34), mRNA	0.0208241	2.70
XM_581232.3	PREDICTED: Bos taurus similar to Rho GTPase activating protein 21 (ARHGAP21), mRNA	0.0208455	6.25
NM_001081519.1	Bos taurus DNA-damage-inducible transcript 4-like (DDIT4L), mRNA	0.0209815	2.27
NM_174327.1	Bos taurus guanine nucleotide binding protein (G protein), gamma transducing activity polypeptide 1 (GNGT1), mRNA	0.0214050	2.94
NM_001101962.1	Bos taurus tubulin, epsilon 1 (TUBE1), mRNA	0.0214546	2.04
XM_597427.4	PREDICTED: Bos taurus similar to phosphatidylinositol glycan class V (PIGV), mRNA	0.0217290	3.84
NM_001098879.1	Bos taurus UTP18, small subunit (SSU) processome component, homolog (yeast) (UTP18), mRNA	0.0219434	2.56
XM_580785.4	PREDICTED: Bos taurus similar to MORC family CW-type zinc finger protein 2 (Zinc finger CW-type coiled-coil domain protein 1), transcript variant 1 (MORC2), mRNA	0.0221592	2.00
NM_001015619.1	Bos taurus coiled-coil domain containing 51 (CCDC51), mRNA	0.0222191	2.04
XM_591264.3	PREDICTED: Bos taurus similar to phospholipase C-like 3 (PLCH1), mRNA	0.0222957	2.32
NM_001076201.2	Bos taurus C1q and tumor necrosis factor related protein 7 (C1QTNF7), mRNA	0.0223325	2.00
NM_001034687.1	Bos taurus S100P binding protein (S100PBP), mRNA	0.0223941	3.44
XR_028739.2	PREDICTED: Bos taurus misc_RNA (LOC789229), miscRNA	0.0227563	2.43
NM_001046265.1	Bos taurus sclerostin domain containing 1 (SOSTDC1), mRNA	0.0227934	2.00
XM_001788685.1	PREDICTED: Bos taurus similar to Kynureninase (L-kynurenine hydrolase) (KYNU), mRNA	0.0228712	2.00
NM_174083.3	Bos taurus histamine receptor H1 (HRH1), mRNA	0.0229477	2.08
NM_001105407.1	Bos taurus SUB1 homolog (S. cerevisiae) (SUB1), mRNA	0.0230015	2.56
XM_598653.4	PREDICTED: Bos taurus similar to Protein FAM23A (Brush border protein AdRab-C) (LOC520412), mRNA	0.0230439	2.27
NM_001101256.1	Bos taurus hypothetical LOC616371 (LOC616371), mRNA	0.0231841	2.08

NM_181029.2	Bos taurus casein alpha s1 (CSN1S1), mRNA	0.0232999	2.12
XM_614126.4	PREDICTED: Bos taurus similar to CSRP2 binding protein, transcript variant 2 (CSRP2BP), mRNA	0.0234880	2.08
XM_001252642.2	PREDICTED: Bos taurus similar to serine/threonine kinase (TAOK3), mRNA	0.0236494	2.27
NM_001083777.1	Bos taurus receptor (G protein-coupled) activity modifying protein 1 (RAMP1), mRNA	0.0236663	2.38
NM_001105390.1	Bos taurus importin 13 (IPO13), mRNA	0.0239759	2.43
XM_001253780.2	PREDICTED: Bos taurus similar to adiponutrin (PNPLA3), mRNA	0.0239887	2.32
NM_001002883.2	Bos taurus ST3 beta-galactoside alpha-2,3-sialyltransferase 6 (ST3GAL6), mRNA	0.0240124	2.43
XM_608505.4	PREDICTED: Bos taurus neuroligin 1 (NLGN1), mRNA	0.0244244	2.38
NM_001081579.1	Bos taurus ankyrin repeat domain 22 (ANKRD22), mRNA	0.0244657	2.32
NM_001038067.1	Bos taurus calcium binding tyrosine-(Y)-phosphorylation regulated (CABYR), mRNA	0.0244798	5.55
NM_174106.2	Bos taurus microtubule-associated protein tau (MAPT), mRNA	0.0245334	2.17
NM_001079646.1	Bos taurus FXYD domain containing ion transport regulator 3 (FXYD3), mRNA	0.0247732	2.70
XM_001787389.1	PREDICTED: Bos taurus similar to methyl-CpG binding domain protein 5 (LOC541084), mRNA	0.0247842	2.63
XM_001790251.1	PREDICTED: Bos taurus similar to vesicle transport-related protein (LOC100140328), mRNA	0.0249290	3.70
NM_001101090.1	Bos taurus L-2-hydroxyglutarate dehydrogenase (L2HGDH), nuclear gene encoding mitochondrial protein, mRNA	0.0249644	2.12
XM_618164.4	PREDICTED: Bos taurus collagen, type IV, alpha 3 (Goodpasture antigen) (COL4A3), mRNA	0.0249944	2.77
XM_872571.3	PREDICTED: Bos taurus isocitrate dehydrogenase 3 (NAD+) beta, transcript variant 6 (IDH3B), mRNA	0.0250154	2.63
XM_001251796.1	PREDICTED: Bos taurus similar to Zinc finger X-linked protein ZXDB (LOC783265), mRNA	0.0251185	2.17
XR_042808.1	PREDICTED: Bos taurus misc_RNA (EMR3), miscRNA	0.0253114	2.32

NM_001101908.1	Bos taurus transmembrane protein 120B (TMEM120B), mRNA	0.0254946	2.17
NM_001110082.1	Bos taurus RNA binding motif protein 34 (RBM34), mRNA	0.0255110	2.22
NM_001034218.1	Bos taurus fetuin B (FETUB), mRNA	0.0256586	3.33
NM_001098066.1	Bos taurus poly(A) polymerase gamma (PAPOLG), mRNA	0.0257392	2.56
XM_001254432.2	PREDICTED: Bos taurus similar to zinc finger protein 568 (ZNF793), mRNA	0.0258698	2.17
NM_001013601.3	Bos taurus histocompatibility complex, class II, DQ alpha, type 1 (BOLA-DQA1), mRNA	0.0261112	2.38
XM_864818.2	PREDICTED: Bos taurus similar to sirtuin 1, transcript variant 2 (SIRT1), mRNA	0.0262694	2.04
XM_590508.4	PREDICTED: Bos taurus similar to carboxypeptidase A3 (LOC512903), mRNA	0.0271513	2.17
XM_870453.2	PREDICTED: Bos taurus similar to desmuslin (DMN), mRNA	0.0275501	2.38
XM_001252642.2	PREDICTED: Bos taurus similar to serine/threonine kinase (TAOK3), mRNA	0.0275658	2.08
XM_588670.3	PREDICTED: Bos taurus similar to coiled-coil and C2 domain containing 1B (CC2D1B), mRNA	0.0275952	2.27
NM_001035491.1	Bos taurus hypothetical protein LOC617088 (LOC617088), mRNA	0.0279244	2.12
XM_001787333.1	PREDICTED: Bos taurus similar to zinc finger protein 665 (LOC785630), mRNA	0.0280773	2.08
XM_614908.4	PREDICTED: Bos taurus similar to TBC1 domain family, member 8B (with GRAM domain) (TBC1D8B), mRNA	0.0281442	2.17
NM_181812.1	Bos taurus tRNA aspartic acid methyltransferase 1 (TRDMT1), mRNA	0.0282625	2.08
XM_865774.3	PREDICTED: Bos taurus similar to Heat shock 70 kDa protein 4L (Osmotic stress protein 94) (Heat shock 70-related protein APG-1), transcript variant 3 (HSPA4L), mRNA	0.0283125	2.63
NM_001101213.1	Bos taurus isochorismatase domain containing 1 (ISOC1), mRNA	0.0283238	2.43
NM_001102238.1	Bos taurus methyltransferase like 3 (METTL3), mRNA	0.0283867	2.27
NM_001105034.1	Bos taurus GTPase, IMAP family member (LOC100125415), mRNA	0.0284496	2.70
XM_591968.4	PREDICTED: Bos taurus similar to aurora borealis, transcript variant 1 (LOC514162), mRNA	0.0285166	2.56

NM_174015.1	Bos taurus CD8a molecule (CD8A), mRNA	0.0286867	2.50
NM_001075447.1	Bos taurus SP140 nuclear body protein-like (SP140L), mRNA	0.0287418	2.12
XM_603502.3	PREDICTED: Bos taurus similar to acyl-CoA thioesterase 12 (ACOT12), mRNA	0.0289836	2.22
NM_174339.3	Bos taurus hypoxia inducible factor 1, alpha subunit (basic helix-loop-helix transcription factor) (HIF1A), mRNA	0.0291543	2.08
XM_618363.4	PREDICTED: Bos taurus similar to Cyclin-Y-like protein 1 (CCNYL1), mRNA	0.0291846	2.50
XM_589151.4	PREDICTED: Bos taurus similar to Cell division protein kinase 6 (Serine/threonine-protein kinase PLSTIRE) (CDK6), mRNA	0.0293028	2.77
NM_174007.1	Bos taurus chemokine (C-C motif) ligand 8 (CCL8), mRNA	0.0293548	2.00
NM_001101872.1	Bos taurus C1q and tumor necrosis factor related protein 6 (C1QTNF6), mRNA	0.0294489	2.00
XM_001251030.1	PREDICTED: Bos taurus cutC copper transporter homolog (E. coli), transcript variant 1 (CUTC), partial mRNA	0.0296485	2.94
XM_599803.3	PREDICTED: Bos taurus similar to Alpha-mannosidase 2 (Alpha-mannosidase II) (Mannosyl-oligosaccharide 1,3-1,6-alpha-mannosidase) (MAN II) (Golgi alpha-mannosidase II) (Mannosidase alpha class 2A member 1) (MAN2A1), mRNA	0.0297501	2.77
XR_027328.1	PREDICTED: Bos taurus misc_RNA (LOC781692), miscRNA	0.0297995	3.22
NM_001102346.1	Bos taurus protein phosphatase 2 (formerly 2A), regulatory subunit B", alpha (PPP2R3A), mRNA	0.0298039	2.38
NM_001046494.1	Bos taurus dynamin 1-like (DNM1L), mRNA	0.0298650	2.04
XM_001790322.1	PREDICTED: Bos taurus coiled-coil domain containing 84 (CCDC84), mRNA	0.0299294	2.12
XR_042678.1	PREDICTED: Bos taurus misc_RNA (LOC510404), miscRNA	0.0301380	2.00
XM_611908.4	PREDICTED: Bos taurus similar to mutS homolog 6, transcript variant 1 (MSH6), mRNA	0.0301904	4.34
NM_001046600.1	Bos taurus regulator of G-protein signaling 4 (RGS4), mRNA	0.0302189	2.56
XM_594786.4	PREDICTED: Bos taurus similar to RIKEN cDNA 1110067D22 (LOC516629), mRNA	0.0302917	2.32
NM_174651.2	Bos taurus S100 calcium binding protein A12 (calgranulin C) (S100A12), mRNA	0.0303703	2.17

XM_614758.4	PREDICTED: Bos taurus similar to Thrombospondin type-1 domain-containing protein 4 (LOC534844), mRNA	0.0304536	2.17
XM_882711.3	PREDICTED: Bos taurus similar to myosin, heavy chain 14, transcript variant 4 (MYH14), mRNA	0.0306605	2.85
XM_581000.4	PREDICTED: Bos taurus similar to Nuclear pore complex protein Nup107 (Nucleoporin Nup107) (107 kDa nucleoporin) (NUP107), mRNA	0.0316379	2.63
NM_001037597.1	Bos taurus 5'-nucleotidase, cytosolic III (NT5C3), mRNA	0.0319203	2.12
XM_867943.3	PREDICTED: Bos taurus similar to round spermatid basic protein 1, transcript variant 2 (RSBN1), mRNA	0.0320925	2.04
NM_174043.2	Bos taurus dopamine receptor D2 (DRD2), mRNA	0.0321101	3.12
XM_586416.3	PREDICTED: Bos taurus similar to COBW domain-containing protein 2, transcript variant 1 (CBWD2), mRNA	0.0321480	2.04
XM_001250216.2	PREDICTED: Bos taurus similar to mutant UDP-N-acetylglucosamine 2-epimerase/N-acetylmannosamine kinase (GNE), mRNA	0.0323392	2.38
NM_001102115.1	Bos taurus bol, boule-like (Drosophila) (BOLL), mRNA	0.0323714	2.38
NM_174274.1	Bos taurus DnaJ (Hsp40) homolog, subfamily C, member 14 (DNAJC14), mRNA	0.0324111	2.04
NM_173948.2	Bos taurus peptidylglycine alpha-amidating monooxygenase (PAM), mRNA	0.0327065	2.17
NM_001075701.2	Bos taurus DnaJ (Hsp40) homolog, subfamily C, member 22 (DNAJC22), mRNA	0.0327685	2.00
XM_001252924.2	PREDICTED: Bos taurus similar to FLJ20489 protein (LOC784685), mRNA	0.0327946	2.22
NM_174225.1	Bos taurus actin, alpha 1, skeletal muscle (ACTA1), mRNA	0.0333505	2.00
NM_174041.2	Bos taurus dihydropyrimidine dehydrogenase (DPYD), mRNA	0.0333591	2.12
NM_173951.2	Bos taurus plasminogen (PLG), mRNA	0.0333752	2.17
NM_174564.2	Bos taurus NADH dehydrogenase (ubiquinone) 1, subcomplex unknown, 1, 6kDa (NDUFC1), mRNA	0.0333782	2.94
NM_001034361.1	Bos taurus amiloride binding protein 1 (amine oxidase (copper-containing)) (ABP1), mRNA	0.0334221	2.56

NM_174450.3	Bos taurus regulator of G-protein signaling 16 (RGS16), mRNA	0.0335175	2.77
NM_001080247.1	Bos taurus JNK1-associated membrane protein (JAMP), mRNA	0.0335346	2.77
NM_001081530.1	Bos taurus thyroid hormone receptor interactor 10 (TRIP10), mRNA	0.0336298	2.00
NM_001083468.1	Bos taurus protein phosphatase 2, regulatory subunit B', epsilon isoform (PPP2R5E), mRNA	0.0338695	2.50
XM_001251924.2	PREDICTED: Bos taurus similar to enhancer of rudimentary homolog (LOC783761), mRNA	0.0340298	3.57
XM_001787807.1	PREDICTED: Bos taurus similar to Leucine-rich PPR motif-containing protein, mitochondrial precursor (130 kDa leucine-rich protein) (LRP 130) (GP130) (LOC509995), mRNA	0.0341662	2.94
NM_001046088.1	Bos taurus glutathione peroxidase 8 (putative) (GPX8), mRNA	0.0343155	3.03
XR_028567.2	PREDICTED: Bos taurus misc_RNA (LOC615842), miscRNA	0.0343346	2.32
NM_180999.1	Bos taurus lysozyme C-2 (LYZ2), mRNA	0.0345633	2.56
XR_027344.2	PREDICTED: Bos taurus misc_RNA (LOC781850), miscRNA	0.0347901	2.08
XM_588297.4	PREDICTED: Bos taurus similar to laminin 5 gamma 2 subunit (LAMC2), mRNA	0.0349305	2.08
NM_001014382.2	Bos taurus myeloid differentiation primary response gene (88) (MYD88), mRNA	0.0349376	2.08
NM_001102191.1	Bos taurus oculocerebrorenal syndrome of Lowe (OCRL), mRNA	0.0355277	2.70
XM_001787544.1	PREDICTED: Bos taurus similar to cytosolic beta-glucosidase (LOC539625), mRNA	0.0356552	4.76
XM_001787931.1	PREDICTED: Bos taurus similar to shugoshin-like 2 (LOC532412), mRNA	0.0357925	2.43
NM_001007805.1	Bos taurus intestinal lysozyme (LYSB), mRNA	0.0360261	2.43
XM_583697.4	PREDICTED: Bos taurus similar to grancalcin (GCA), mRNA	0.0363803	2.08
NM_001011681.3	Bos taurus growth factor receptor-bound protein 14 (GRB14), mRNA	0.0364831	2.63
XM_001789124.1	PREDICTED: Bos taurus hypothetical protein LOC100137763 (LOC100137763), mRNA	0.0373086	3.84
NM_001075641.1	Bos taurus myotubularin related protein 7 (MTMR7), mRNA	0.0378254	2.56

XR_027276.2	PREDICTED: Bos taurus misc_RNA (LOC530104), miscRNA	0.0378476	3.22
NM_001046118.1	Bos taurus lysosomal multispanning membrane protein 5 (LAPTM5), mRNA	0.0380083	2.38
NM_001098032.1	Bos taurus cytoskeleton associated protein 2 (CKAP2), mRNA	0.0380359	3.12
NM_001035065.1	Bos taurus small nuclear ribonucleoprotein D1 polypeptide 16kDa (SNRPD1), mRNA	0.0382284	3.44
NM_001101072.1	Bos taurus hypothetical LOC510651 (LOC510651), mRNA	0.0384583	2.27
XR_028354.2	PREDICTED: Bos taurus misc_RNA (LOC614048), miscRNA	0.0385518	2.43
XM_882441.2	PREDICTED: Bos taurus hypothetical LOC617028 (LOC617028), mRNA	0.0387272	2.22
XM_608629.4	PREDICTED: Bos taurus similar to membrane glycoprotein SP55 (SLC17A5), mRNA	0.0387823	2.08
XR_028786.2	PREDICTED: Bos taurus misc_RNA (LOC789688), miscRNA	0.0388752	2.43
NM_001083406.1	Bos taurus chromosome 2 open reading frame 47 ortholog (C2H2orf47), mRNA	0.0390070	2.38
NM_174055.2	Bos taurus fibroblast growth factor 1 (acidic) (FGF1), mRNA	0.0395901	2.04
XM_869563.3	PREDICTED: Bos taurus similar to karyopherin beta 1, transcript variant 2 (KPNB1), mRNA	0.0396176	2.32
NM_001075503.1	Bos taurus TATA box binding protein (TBP)-associated factor, RNA polymerase I, B, 63kDa (TAF1B), mRNA	0.0397413	2.04
NM_001102529.1	Bos taurus SCY1-like 2 (S. cerevisiae) (SCYL2), mRNA	0.0398505	2.22
XM_590933.4	PREDICTED: Bos taurus similar to nucleoporin 153kDa (NUP153), mRNA	0.0401906	7.14
NM_001024568.1	Bos taurus ribosomal protein S11 (RPS11), mRNA	0.0402654	2.50
XM_592611.4	PREDICTED: Bos taurus fibroblast growth factor 10, transcript variant 2 (FGF10), mRNA	0.0404237	2.63
NM_001075737.1	Bos taurus CUE domain containing 2 (CUEDC2), mRNA	0.0407237	2.50
NM_001035092.1	Bos taurus LMBR1 domain containing 1 (LMBRD1), mRNA	0.0410314	3.12
XM_580765.4	PREDICTED: Bos taurus similar to Serine/threonine-protein phosphatase with EF-hands 1 (PPEF-1) (Protein phosphatase with EF calcium-binding domain) (PPEF)	0.0413887	3.33

	(Serine/threonine-protein phosphatase 7) (PP7) (PPEF1), mRNA		
XM_584216.4	PREDICTED: Bos taurus similar to ELL associated factor 1, transcript variant 1 (EAF1), mRNA	0.0416540	3.12
NM_001099023.1	Bos taurus zinc finger protein 639 (ZNF639), mRNA	0.0418450	2.32
XM_609023.4	PREDICTED: Bos taurus EF-hand domain family, member B (EFHB), mRNA	0.0419448	2.27
NM_001077991.1	Bos taurus RecQ protein-like (DNA helicase Q1-like) (RECQL), mRNA	0.0422332	3.03
XM_001789789.1	PREDICTED: Bos taurus similar to Myeloid cell surface antigen CD33 precursor (Sialic acid-binding Ig-like lectin 3) (Siglec-3) (gp67) (LOC100138951), mRNA	0.0424703	2.27
NM_001035349.1	Bos taurus AT rich interactive domain 5A (MRF1-like) (ARID5A), mRNA	0.0426112	2.38
XM_001790636.1	PREDICTED: Bos taurus SWI/SNF related, matrix associated, actin dependent regulator of chromatin, subfamily c, member 2 (SMARCC2), mRNA	0.0429422	2.12
NM_001099033.1	Bos taurus guanine nucleotide binding protein (G protein), beta polypeptide 4 (GNB4), mRNA	0.0437781	2.27
XR_042741.1	PREDICTED: Bos taurus misc_RNA (LOC785805), miscRNA	0.0437873	2.22
NM_001034311.1	Bos taurus interleukin 22 receptor, alpha 1 (IL22RA1), mRNA	0.0438179	4.34
XM_867922.3	PREDICTED: Bos taurus similar to zinc finger protein 1 homolog (mouse), transcript variant 2 (ZFP1), mRNA	0.0438789	2.94
XM_866635.2	PREDICTED: Bos taurus similar to Echinoderm microtubule-associated protein-like 4 (EMAP-4) (Restrictedly overexpressed proliferation-associated protein) (Ropp 120), transcript variant 3 (EML4), mRNA	0.0439162	3.70
NM_001082606.1	Bos taurus chromosome 9 open reading frame 102 ortholog (LOC508357), mRNA	0.0439431	2.08
NM_001101205.1	Bos taurus WEE1 homolog (S. pombe) (WEE1), mRNA	0.0440466	2.32
NM_175801.2	Bos taurus follistatin (FST), mRNA	0.0440795	4.00
XM_585347.4	PREDICTED: Bos taurus similar to mesoderm induction early response 1, family member 3 (MIER3), mRNA	0.0442043	2.38

XM_582977.4	PREDICTED: Bos taurus WNK lysine deficient protein kinase 2 (WNK2), mRNA	0.0442389	3.44
NM_174587.1	Bos taurus protein kinase C, beta (PRKCB), mRNA	0.0443706	2.32
XM_864033.3	PREDICTED: Bos taurus similar to Host cell factor 2 (HCF-2) (C2 factor), transcript variant 3 (HCFC2), mRNA	0.0446866	2.43
XM_870414.2	PREDICTED: Bos taurus similar to transmembrane protein 7 (RTP3), mRNA	0.0448472	3.44
XM_581568.3	PREDICTED: Bos taurus dual specificity phosphatase 12 (DUSP12), mRNA	0.0452239	2.77
XM_001787706.1	PREDICTED: Bos taurus similar to zinc finger protein 605 (LOC782885), mRNA	0.0452889	2.63
NM_001100386.1	Bos taurus yippee-like 1 (Drosophila) (YPEL1), mRNA	0.0456279	2.12
NM_174146.3	Bos taurus plasminogen activator, tissue (PLAT), mRNA	0.0457835	2.17
NM_001101143.1	Bos taurus S-adenosylhomocysteine hydrolase-like 2 (AHCYL2), mRNA	0.0462430	2.56
NM_001077994.1	Bos taurus Protein FAM149B1 (FAM149B1), mRNA	0.0463730	2.32
NM_001001441.1	Bos taurus troponin T type 3 (skeletal, fast) (TNNT3), mRNA	0.0465125	2.77
NM_001076320.1	Bos taurus ADP-ribosylation factor-like 10 (ARL10), mRNA	0.0468835	3.33
NM_001083469.1	Bos taurus transmembrane protein 156 (TMEM156), mRNA	0.0474462	2.94
XM_585792.4	PREDICTED: Bos taurus similar to Oxysterol-binding protein-related protein 7 (OSBP-related protein 7) (ORP-7), transcript variant 1 (OSBPL7), mRNA	0.0474739	2.38
NM_177510.2	Bos taurus glucosaminyl (N-acetyl) transferase 1, core 2 (beta-1,6-N-acetylglucosaminyltransferase) (GCNT1), mRNA	0.0475539	2.70
XM_582282.4	PREDICTED: Bos taurus similar to zinc finger protein 709 (ZNF627), mRNA	0.0476163	2.85
NM_001105477.1	Bos taurus glutamate receptor, ionotropic, N-methyl D-aspartate-like 1A (GRINL1A), mRNA	0.0480948	2.04
XM_867982.2	PREDICTED: Bos taurus microseminoprotein, beta- (MSMB), mRNA	0.0483755	2.22
XM_867753.3	PREDICTED: Bos taurus similar to Uncharacterized protein C10orf11 homolog (LOC615835), mRNA	0.0484312	2.08

XM_001787912.1	PREDICTED: Bos taurus pleckstrin homology domain containing, family A (phosphoinositide binding specific) member 2 (PLEKHA2), mRNA	0.0488026	2.94
NM_001101091.1	Bos taurus DnaJ (Hsp40) homolog, subfamily C, member 16 (DNAJC16), mRNA	0.0491185	2.04
XM_582124.3	PREDICTED: Bos taurus similar to GC-rich promoter binding protein 1-like 1, transcript variant 1 (GPBP1L1), mRNA	0.0492615	3.22
NM_001114192.1	Bos taurus heat shock 70kDa protein 4 (HSPA4), mRNA	0.0235230	-8.10
NM_001035052.1	Bos taurus chromosome 10 open reading frame 84 ortholog (C26H10orf84), mRNA	0.0075412	-4.86
XM_001787175.1	PREDICTED: Bos taurus hypothetical LOC784541 (LOC784541), mRNA	0.0181949	-4.39
NM_181008.2	Bos taurus casein beta (CSN2), mRNA	0.0380616	-7.51
XR_028130.2	PREDICTED: Bos taurus misc_RNA (LOC617326), miscRNA	0.0217198	-6.85
NR_001464.2	Bos taurus X (inactive)-specific transcript (XIST), non-coding RNA	0.0102795	-17.12
XM_876383.3	PREDICTED: Bos taurus tubulin, alpha 1a, transcript variant 4 (TUBA1A), mRNA	0.0227675	-5.10
NM_001035497.1	Bos taurus ubiquitin-conjugating enzyme E2 variant 1 (UBE2V1), mRNA	0.0253026	-6.16
NM_001101875.1	Bos taurus thioredoxin interacting protein (TXNIP), mRNA	0.0344490	-5.71
NM_001034548.1	Bos taurus splicing factor 3a, subunit 3, 60kDa (SF3A3), mRNA	0.0125753	-2.11
XM_001789101.1	PREDICTED: Bos taurus similar to endonuclease reverse transcriptase (LOC100140868), mRNA	0.0264338	-10.06
NM_174345.3	Bos taurus heat shock 70kDa protein 8 (HSPA8), mRNA	0.0171717	-11.20
XM_867454.3	PREDICTED: Bos taurus similar to transmembrane anterior posterior transformation 1 (TAPT1), mRNA	0.0273066	-6.14
NM_001037468.1	Bos taurus cell division cycle 7 homolog (S. cerevisiae) (CDC7), mRNA	0.0497627	-2.99
NM_001078121.1	Bos taurus hypothetical protein LOC768255 (LOC768255), mRNA	0.0189405	-2.01
NM_174286.2	Bos taurus cAMP responsive element binding protein 3 (CREB3), mRNA	0.0354769	-7.24
XM_614891.3	PREDICTED: Bos taurus similar to huntingtin interacting protein 14 (ZDHHC17), mRNA	0.0414922	-2.53

NM_176639.2	Bos taurus ATP synthase, H+ transporting, mitochondrial F0 complex, subunit e (ATP5I), nuclear gene encoding mitochondrial protein, mRNA	0.0149600	-8.66
XM_605970.4	PREDICTED: Bos taurus similar to tripartite motif protein TRIM4, transcript variant 1 (TRIM4), partial mRNA	0.0365157	-2.41
NM_001097570.1	Bos taurus STT3, subunit of the oligosaccharyltransferase complex, homolog B (S. cerevisiae) (STT3B), mRNA	0.0105277	-2.21
XM_614825.3	PREDICTED: Bos taurus similar to centrosome-associated protein 350, transcript variant 1 (CEP350), mRNA	0.0381474	-3.35
NM_001098070.1	Bos taurus O-linked N-acetylglucosamine (GlcNAc) transferase (UDP-N-acetylglucosamine:polypeptide-N-acetylglucosaminyl transferase) (OGT), mRNA	0.0100134	-4.20
NM_175780.1	Bos taurus myosin, light chain 6, alkali, smooth muscle and non-muscle (MYL6), mRNA	0.0390013	-9.53
NM_001102041.1	Bos taurus Uncharacterized protein C13orf18 homolog (MGC165939), mRNA	0.0038571	-5.09
XM_864671.2	PREDICTED: Bos taurus WD repeat domain 40A, transcript variant 2 (WDR40A), mRNA	0.0206149	-12.45
NM_001105617.1	Bos taurus homeobox A9 (HOXA9), mRNA	0.0099490	-23.15
NM_001075509.1	Bos taurus transcription factor AP-2 gamma (activating enhancer binding protein 2 gamma) (TFAP2C), mRNA	0.0188863	-14.68
XM_876203.3	PREDICTED: Bos taurus similar to UPF0474 protein C5orf41, transcript variant 2 (LOC513587), mRNA	0.0378321	-10.19
NM_001001443.1	Bos taurus estrogen receptor 1 (ESR1), mRNA	0.0218312	-3.56
NM_001046351.1	Bos taurus thyroid hormone receptor interactor 4 (TRIP4), mRNA	0.0484421	-4.17
NM_001076532.1	Bos taurus cell division cycle and apoptosis regulator 1 (CCAR1), mRNA	0.0451928	-4.76
XM_582135.4	PREDICTED: Bos taurus neurofilament, medium polypeptide (NEF3), mRNA	0.0181622	-38.09
XM_593741.4	PREDICTED: Bos taurus similar to CG33196-PB (LOC515676), mRNA	0.0126734	-5.78
NM_001077114.1	Bos taurus HIG1 domain family, member 1D (HIGD1D), mRNA	0.0396119	-2.72

NM_001046357.1	Bos taurus transmembrane protein 173 (TMEM173), mRNA	0.0363261	-2.60
NR_001464.2	Bos taurus X (inactive)-specific transcript (XIST), non-coding RNA	0.0144777	-5.54
NM_001038647.1	Bos taurus transmembrane protein 57 (TMEM57), mRNA	0.0036628	-2.24
XR_028861.2	PREDICTED: Bos taurus misc_RNA (LOC790266), miscRNA	0.0262241	-3.20
XM_600663.4	PREDICTED: Bos taurus nestin (NES), mRNA	0.0064388	-3.57
NM_001083708.1	Bos taurus arsenate resistance protein 2 (ARS2), mRNA	0.0412354	-2.53
XM_001788694.1	PREDICTED: Bos taurus diazepam binding inhibitor (GABA receptor modulator, acyl-Coenzyme A binding protein) (DBI), mRNA	0.0231186	-2.06
NM_001100294.1	Bos taurus calmodulin binding transcription activator 1 (CAMTA1), mRNA	0.0213992	-3.38
NM_001008663.1	Bos taurus keratin 5 (KRT5), mRNA	0.0060916	-4.74
NM_001099133.1	Bos taurus lactamase, beta (LACTB), nuclear gene encoding mitochondrial protein, mRNA	0.0219931	-2.41
NM_174568.2	Bos taurus poly(A) binding protein, cytoplasmic 1 (PABPC1), mRNA	0.0016273	-22.78
XR_042588.1	PREDICTED: Bos taurus misc_RNA (LOC100139984), partial miscRNA	0.0279057	-3.04
XM_590469.4	PREDICTED: Bos taurus similar to RAS protein activator like 1 (GAP1 like) (RASAL1), mRNA	0.0090279	-2.45
XM_609842.3	PREDICTED: Bos taurus similar to BTB and CNC homology 1 (BACH1), mRNA	0.0022440	-4.33
NM_001076814.1	Bos taurus malic enzyme 2, NAD(+)-dependent, mitochondrial (ME2), nuclear gene encoding mitochondrial protein, mRNA	0.0279784	-4.15
XM_864452.2	PREDICTED: Bos taurus similar to LOC616164 protein (LOC613544), mRNA	0.0426139	-3.43
XM_595505.4	PREDICTED: Bos taurus similar to mediator complex subunit 13-like (MED13L), mRNA	0.0329109	-2.43
NM_001113745.1	Bos taurus DnaJ (Hsp40) homolog, subfamily C, member 13 (DNAJC13), mRNA	0.0274418	-2.73
NM_001083792.1	Bos taurus tetratricopeptide repeat domain 9C (TTC9C), mRNA	0.0071432	-3.00
XM_581038.3	PREDICTED: Bos taurus similar to myeloid/lymphoid or mixed-lineage	0.0303070	-3.72

	leukemia (trithorax homolog, Drosophila); translocated to, 4 (MLLT4), mRNA		
NM_001012682.1	Bos taurus ribosomal protein, large, P0 (RPLP0), mRNA	0.0269574	-7.07
NM_001098929.1	Bos taurus splicing factor, arginine/serine-rich 5 (SFRS5), mRNA	0.0046074	-5.62
NM_001040498.1	Bos taurus MHC Class I JSP.1 (JSP.1), mRNA	0.0003902	-5.76
NM_001040487.1	Bos taurus eukaryotic translation elongation factor 1 gamma (EEF1G), mRNA	0.0196198	-8.68
XM_593043.4	PREDICTED: Bos taurus similar to Zinc finger protein 91 (Zinc finger protein HTF10) (HPF7) (ZNF665), mRNA	0.0025301	-3.92
XM_001250793.2	PREDICTED: Bos taurus similar to small nuclear ribonucleoprotein polypeptide G (SNRPG), mRNA	0.0330865	-5.65
NM_001075623.1	Bos taurus ATP synthase mitochondrial F1 complex assembly factor 2 (ATPAF2), nuclear gene encoding mitochondrial protein, mRNA	0.0451120	-2.16
NM_001098022.1	Bos taurus ATPase, H+ transporting, lysosomal accessory protein 2 (ATP6AP2), mRNA	0.0292548	-3.26
XM_001790089.1	PREDICTED: Bos taurus similar to endonuclease reverse transcriptase (LOC100140273), mRNA	0.0033505	-4.26
NM_001075515.1	Bos taurus 5'-nucleotidase, cytosolic III-like (NT5C3L), mRNA	0.0276110	-4.72
NM_001083515.1	Bos taurus transmembrane protein 87A (TMEM87A), mRNA	0.0126441	-4.78
XM_602857.3	PREDICTED: Bos taurus similar to ubiquitin specific protease 25 (USP25), mRNA	0.0058494	-4.93
NM_001012682.1	Bos taurus ribosomal protein, large, P0 (RPLP0), mRNA	0.0456545	-2.54
XM_611700.4	PREDICTED: Bos taurus similar to SET domain containing 5, transcript variant 2 (SETD5), mRNA	0.0405884	-2.20
NM_174062.3	Bos taurus ferritin, heavy polypeptide 1 (FTH1), mRNA	0.0382741	-4.23
XM_865029.3	PREDICTED: Bos taurus similar to splicing factor 3b, subunit 1, transcript variant 2 (SF3B1), mRNA	0.0013511	-2.11
XM_864599.3	PREDICTED: Bos taurus similar to splicing factor, arginine/serine-rich 12, transcript variant 2 (SFRS12), mRNA	0.0089113	-2.29

NM_001109807.1	Bos taurus peptidylprolyl isomerase G (cyclophilin G) (PPIG), mRNA	0.0203114	-2.78
XM_865383.3	PREDICTED: Bos taurus similar to Protein strawberry notch homolog 1 (Monocyte protein 3) (MOP-3), transcript variant 2 (SBNO1), mRNA	0.0167606	-13.50
XM_594174.3	PREDICTED: Bos taurus NOL1/NOP2/Sun domain family, member 2 (NSUN2), mRNA	0.0009117	-2.78
XR_027542.2	PREDICTED: Bos taurus misc_RNA (LOC538959), miscRNA	0.0128684	-3.74
NM_175814.2	Bos taurus succinate dehydrogenase complex, subunit C, integral membrane protein, 15kDa (SDHC), nuclear gene encoding mitochondrial protein, mRNA	0.0054062	-2.48
NM_001014860.2	Bos taurus heterogeneous nuclear ribonucleoprotein F (HNRNPF), mRNA	0.0051763	-5.45
NM_001045935.2	Bos taurus CTD (carboxy-terminal domain, RNA polymerase II, polypeptide A) small phosphatase 2 (CTDSP2), mRNA	0.0435216	-6.39
NM_001046520.1	Bos taurus YTH domain containing 1 (YTHDC1), mRNA	0.0437184	-5.99
NM_001034335.1	Bos taurus KIAA0174 (KIAA0174), mRNA	0.0484906	-3.71
XR_042975.1	PREDICTED: Bos taurus misc_RNA (LOC784058), miscRNA	0.0398500	-5.21
NM_001080301.1	Bos taurus LUC7-like (S. cerevisiae) (LUC7L), mRNA	0.0169183	-6.86
XM_583514.4	PREDICTED: Bos taurus phosphoglucomutase 2 (PGM2), mRNA	0.0324241	-5.44
NM_001083726.1	Bos taurus SET domain and mariner transposase fusion gene (SETMAR), mRNA	0.0178443	-3.77
NM_001031760.1	Bos taurus solute carrier family 38, member 11 (SLC38A11), mRNA	0.0141571	-3.98
NM_001083466.1	Bos taurus heterogeneous nuclear ribonucleoprotein U-like 1 (HNRNPUL1), mRNA	0.0406447	-6.60
XM_001788653.1	PREDICTED: Bos taurus similar to endonuclease reverse transcriptase (LOC100138878), mRNA	0.0146295	-4.67
XM_001787703.1	PREDICTED: Bos taurus similar to endonuclease reverse transcriptase (LOC100137861), mRNA	0.0155975	-5.87
NM_001046044.1	Bos taurus cytidine monophosphate (UMP-CMP) kinase 1, cytosolic (CMPK1), mRNA	0.0002082	-2.16
XM_001249987.2	PREDICTED: Bos taurus similar to eukaryotic translation elongation factor 1 alpha 1, transcript variant 1 (EEF1A1),	0.0298200	-3.47

	mRNA		
XM_864796.3	PREDICTED: Bos taurus adenylosuccinate synthase, transcript variant 3 (ADSS), mRNA	0.0152255	-2.39
XR_042755.1	PREDICTED: Bos taurus misc_RNA (FBL), miscRNA	0.0489360	-6.01
NM_001098013.1	Bos taurus COX10 homolog, cytochrome c oxidase assembly protein, heme A: farnesyltransferase (yeast) (COX10), nuclear gene encoding mitochondrial protein, mRNA	0.0302652	-3.84
NM_001076209.1	Bos taurus SMAD family member 4 (SMAD4), mRNA	0.0179492	-6.40
NM_001046142.1	Bos taurus general transcription factor IIB (GTF2B), mRNA	0.0260409	-3.12
NM_001076155.1	Bos taurus interleukin 1 receptor accessory protein (IL1RAP), mRNA	0.0056952	-2.21
NM_001035272.1	Bos taurus splicing factor, arginine/serine-rich 6 (SFRS6), mRNA	0.0403233	-4.00
NM_001040479.1	Bos taurus periostin, osteoblast specific factor (POSTN), mRNA	0.0040323	-4.93
NM_001075788.1	Bos taurus damage-specific DNA binding protein 2, 48kDa (DDB2), mRNA	0.0243865	-7.41
NM_001038153.1	Bos taurus eukaryotic translation initiation factor 5B (EIF5B), mRNA	0.0245873	-3.06
XM_589161.4	PREDICTED: Bos taurus synaptotagmin binding, cytoplasmic RNA interacting protein (SYNCRIP), mRNA	0.0297002	-7.71
XR_028112.2	PREDICTED: Bos taurus misc_RNA (LOC784517), miscRNA	0.0442164	-2.21
NM_001076070.1	Bos taurus 3-oxoacid CoA transferase 1 (OXCT1), nuclear gene encoding mitochondrial protein, mRNA	0.0280594	-2.52
XM_001790233.1	PREDICTED: Bos taurus similar to endonuclease reverse transcriptase (LOC100139370), mRNA	0.0155737	-3.28
XM_582135.4	PREDICTED: Bos taurus neurofilament, medium polypeptide (NEF3), mRNA	0.0034747	-19.72
XR_027849.2	PREDICTED: Bos taurus misc_RNA (LOC538561), miscRNA	0.0046641	-4.40
NM_001015533.1	Bos taurus signal sequence receptor, beta (translocon-associated protein beta) (SSR2), mRNA	0.0434364	-3.15
XM_001249745.2	PREDICTED: Bos taurus similar to bromodomain PHD finger transcription	0.0325768	-2.92

	factor, transcript variant 1 (BPTF), mRNA		
NM_001075947.1	Bos taurus F-box and leucine-rich repeat protein 14 (FBXL14), mRNA	0.0274017	-7.08
NM_001098006.1	Bos taurus BUD13 homolog (S. cerevisiae) (BUD13), mRNA	0.0099689	-7.60
XM_594391.4	PREDICTED: Bos taurus similar to G-protein signaling modulator 3 (AGS3-like, C. elegans) (GPSM3), mRNA	0.0334115	-4.70
NM_001099022.1	Bos taurus Era G-protein-like 1 (E. coli) (ERAL1), mRNA	0.0341951	-3.27
XM_001250989.2	PREDICTED: Bos taurus similar to heterogeneous nuclear ribonucleoprotein A3 (HNRPA3), mRNA	0.0346428	-3.21
NM_001082422.1	Bos taurus ribosomal protein S4, Y-linked 1 (RPS4Y1), mRNA	0.0202760	-5.89
XM_001249365.2	PREDICTED: Bos taurus similar to C6orf49-like protein (LOC781350), mRNA	0.0146829	-3.88
NM_001035068.1	Bos taurus acyl-CoA synthetase family member 3 (ACSF3), mRNA	0.0375326	-3.03
NM_001102264.1	Bos taurus cystinosis, nephropathic (CTNS), mRNA	0.0404995	-3.45
NM_001083725.1	Bos taurus heterogeneous nuclear ribonucleoprotein D-like (HNRPDL), mRNA	0.0004144	-4.72
NM_001034279.2	Bos taurus chromosome 1 open reading frame 50 ortholog (C3H1ORF50), mRNA	0.0056109	-3.99
XM_001787372.1	PREDICTED: Bos taurus PTK2 protein tyrosine kinase 2 (PTK2), mRNA	0.0288371	-2.29
XM_001253928.2	PREDICTED: Bos taurus similar to major histocompatibility complex, class II, DR beta 3 (LOC786695), mRNA	0.0106522	-2.58
XM_001254849.2	PREDICTED: Bos taurus similar to fibrillin3 (FBN3), mRNA	0.0354642	-2.33
NM_001076941.1	Bos taurus ring finger protein 220 (RNF220), mRNA	0.0478160	-2.25
XM_001252331.1	PREDICTED: Bos taurus similar to serine/arginine repetitive matrix 1, transcript variant 1 (SRRM1), mRNA	0.0374443	-2.56
NM_001075585.1	Bos taurus RIB43A domain with coiled-coils 1 (RIBC1), mRNA	0.0345273	-4.80
NM_001103287.1	Bos taurus zinc finger protein 64 homolog (mouse) (ZFP64), mRNA	0.0160239	-2.57
XM_001255563.2	PREDICTED: Bos taurus similar to pericentrin (kendrin) (PCNT), mRNA	0.0402414	-2.67
NM_001105358.1	Bos taurus C2CD2-like (C2CD2L), mRNA	0.0031397	-3.84

NM_001075649.1	Bos taurus N-acetyltransferase 15 (GCN5-related, putative) (NAT15), mRNA	0.0343933	-3.63
NM_001034399.1	Bos taurus FXYD domain containing ion transport regulator 6 (FXYD6), mRNA	0.0416590	-4.19
XM_592234.3	PREDICTED: Bos taurus similar to nuclear receptor binding SET domain protein 1 (NSD1), partial mRNA	0.0030047	-3.54
XM_001790611.1	PREDICTED: Bos taurus similar to ferritin L subunit, transcript variant 2 (LOC785987), mRNA	0.0395119	-2.47
NM_001024532.2	Bos taurus proteasome (prosome, macropain) 26S subunit, non-ATPase, 13 (PSMD13), mRNA	0.0202117	-3.58
NM_001075748.1	Bos taurus CCCTC-binding factor (zinc finger protein) (CTCF), mRNA	0.0443230	-2.11
XM_588351.4	PREDICTED: Bos taurus similar to ring finger protein 26 (RNF26), mRNA	0.0438387	-2.99
NM_001083745.1	Bos taurus GTF2I repeat domain containing 2 (GTF2IRD2), mRNA	0.0165003	-5.51
NM_174099.2	Bos taurus lactate dehydrogenase A (LDHA), mRNA	0.0396655	-2.31
NM_001034694.1	Bos taurus COP9 constitutive photomorphogenic homolog subunit 4 (Arabidopsis) (COPS4), mRNA	0.0288877	-3.29
NM_001034342.1	Bos taurus activating transcription factor 4 (tax-responsive enhancer element B67) (ATF4), mRNA	0.0344535	-4.48
NM_001038092.1	Bos taurus chromosome 17 open reading frame 49 ortholog (C19H17orf49), mRNA	0.0455655	-2.94
XR_042834.1	PREDICTED: Bos taurus misc_RNA (LOC786009), partial miscRNA	0.0392252	-6.14
XM_616885.4	PREDICTED: Bos taurus similar to membrane metallo endopeptidase (MME), mRNA	0.0383563	-3.12
NM_001083439.1	Bos taurus suppressor of Ty 5 homolog (S. cerevisiae) (SUPT5H), mRNA	0.0223104	-3.44
NM_001081717.1	Bos taurus EGF-containing fibulin-like extracellular matrix protein 1 (EFEMP1), mRNA	0.0186095	-2.43
XM_583103.4	PREDICTED: Bos taurus similar to Rho GTPase activating protein 30, transcript variant 1 (ARHGAP30), mRNA	0.0499581	-2.97
XM_580963.3	PREDICTED: Bos taurus similar to TBP-associated factor 1 (TAF1), mRNA	0.0078859	-3.79
XM_001251118.1	PREDICTED: Bos taurus similar to dynamin binding protein (DNMBP), mRNA	0.0489987	-2.03

NM_001040645.1	Bos taurus paired box 6 (PAX6), mRNA	0.0025796	-2.77
NM_001077113.1	Bos taurus chromosome 6 open reading frame 130 ortholog (C23H6orf130), mRNA	0.0005039	-4.02
NM_174778.1	Bos taurus ribosomal protein S27a (RPS27A), mRNA	0.0078379	-2.18
XM_001254701.2	PREDICTED: Bos taurus similar to Calponin 3, acidic, transcript variant 1 (CNN3), mRNA	0.0001859	-4.57
XM_587683.3	PREDICTED: Bos taurus similar to Six2 (SIX2), mRNA	0.0121558	-3.20
XM_581880.4	PREDICTED: Bos taurus similar to cartilage intermediate layer protein (CILP), mRNA	0.0173826	-4.49
NM_001100344.1	Bos taurus zinc finger protein 192 (ZNF192), mRNA	0.0223472	-2.66
NM_001077830.1	Bos taurus ribosomal protein S14 (RPS14), mRNA	0.0083007	-2.77
XM_583748.3	PREDICTED: Bos taurus similar to T-box transcription factor TBX21 (T-box protein 21) (Transcription factor TBLYM) (T-cell-specific T-box transcription factor T-bet) (TBX21), mRNA	0.0385482	-2.40
NM_001098929.1	Bos taurus splicing factor, arginine/serine-rich 5 (SFRS5), mRNA	0.0498861	-3.64
XM_590872.4	PREDICTED: Bos taurus similar to antigen identified by monoclonal antibody Ki-67 (MKI67), mRNA	0.0245835	-2.59
XM_001790641.1	PREDICTED: Bos taurus dishevelled, dsh homolog 2 (Drosophila) (DVL2), mRNA	0.0300229	-4.35
NM_001035280.1	Bos taurus chromosome 14 open reading frame 166 ortholog (C10H14ORF166), mRNA	0.0148839	-5.67
NM_001144095.1	Bos taurus EPH receptor A1 (EPHA1), mRNA	0.0437188	-4.21
NM_205799.1	Bos taurus lysosomal protein transmembrane 4 alpha (LAPTM4A), mRNA	0.0012534	-6.77
NM_001015628.1	Bos taurus eukaryotic translation initiation factor 3, subunit I (EIF3I), mRNA	0.0372000	-4.12
XM_001788161.1	PREDICTED: Bos taurus similar to putative utrophin (LOC534358), mRNA	0.0065054	-2.62
NM_001075992.1	Bos taurus tuberous sclerosis 1 (TSC1), mRNA	0.0476045	-3.51
XM_590380.4	PREDICTED: Bos taurus similar to ephrin receptor EphA2 (EPHA2), mRNA	0.0311043	-2.50
NM_001076076.1	Bos taurus sulfatase modifying factor 1	0.0410049	-2.09

	(SUMF1), mRNA		
NM_001105465.1	Bos taurus hypothetical protein LOC785988 (LOC785988), mRNA	0.0206683	-2.15
NM_001046133.1	Bos taurus poly-U binding splicing factor 60KDa (PUF60), mRNA	0.0199270	-3.21
NM_001045971.1	Bos taurus serine peptidase inhibitor, Kunitz type, 2 (SPINT2), mRNA	0.0024973	-3.45
NM_001080294.1	Bos taurus solute carrier family 6 (proline IMINO transporter), member 20 (SLC6A20), mRNA	0.0061160	-2.50
XR_027681.2	PREDICTED: Bos taurus misc_RNA (LOC783022), miscRNA	0.0347433	-5.16
NM_001105333.1	Bos taurus ubiquitin specific peptidase 20 (USP20), mRNA	0.0404030	-5.73
XM_589248.3	PREDICTED: Bos taurus similar to renin (REN), mRNA	0.0432776	-3.40
NM_001078161.2	Bos taurus hypothetical protein LOC777786 (LOC777786), mRNA	0.0288931	-3.84
NM_001076394.1	Bos taurus splicing factor, arginine/serine-rich 1 (SFRS1), mRNA	0.0167958	-6.22
XM_614225.4	PREDICTED: Bos taurus similar to zinc finger protein of the cerebellum 3, transcript variant 1 (ZIC3), mRNA	0.0476748	-2.43
NM_001017947.1	Bos taurus PDZ and LIM domain 7 (enigma) (PDLIM7), transcript variant 1, mRNA	0.0311574	-2.30
NM_001105378.1	Bos taurus synaptosomal-associated protein, 91kDa homolog (mouse) (SNAP91), mRNA	0.0174253	-2.82
NM_001035286.2	Bos taurus polymerase (DNA directed), mu (POLM), mRNA	0.0161732	-2.47
XM_001250804.2	PREDICTED: Bos taurus similar to fibroblast growth factor-binding protein (LOC783341), mRNA	0.0296001	-2.61
XM_001250304.2	PREDICTED: Bos taurus similar to cyclin T2 (CCNT2), mRNA	0.0041832	-2.70
XM_587361.4	PREDICTED: Bos taurus similar to rCG26042, transcript variant 1 (PPM1M), mRNA	0.0316281	-2.36
NM_001075283.1	Bos taurus poly(rC) binding protein 4 (PCBP4), mRNA	0.0143704	-2.76
XR_027358.1	PREDICTED: Bos taurus misc_RNA (LOC781886), miscRNA	0.0104707	-2.14
XR_028398.2	PREDICTED: Bos taurus misc_RNA (LOC504694), miscRNA	0.0123232	-2.02
XM_001255132.1	PREDICTED: Bos taurus similar to ribosomal protein S6-like (LOC787914),	0.0132118	-12.46

	mRNA		
XM_615600.4	PREDICTED: Bos taurus similar to patatin-like phospholipase domain containing 8 (PNPLA8), mRNA	0.0380442	-2.24
NM_001014901.1	Bos taurus RNA binding motif protein 14 (RBM14), mRNA	0.0306348	-2.34
XM_864691.3	PREDICTED: Bos taurus similar to cytoplasmic polyadenylation element binding protein 1, transcript variant 2 (CPEB1), mRNA	0.0220921	-2.34
NM_001077094.1	Bos taurus cytohesin 2 (CYTH2), mRNA	0.0017351	-3.54
NM_001034498.1	Bos taurus translocase of inner mitochondrial membrane 22 homolog (yeast) (TIMM22), nuclear gene encoding mitochondrial protein, mRNA	0.0423327	-3.18
XM_864142.3	PREDICTED: Bos taurus similar to Eukaryotic translation initiation factor 1A, X-chromosomal (eIF-1A X isoform) (eIF-4C), transcript variant 1 (LOC613487), mRNA	0.0339264	-5.24
NM_001015533.1	Bos taurus signal sequence receptor, beta (translocon-associated protein beta) (SSR2), mRNA	0.0162902	-3.12
NM_001034360.1	Bos taurus dolichyl-phosphate mannosyltransferase polypeptide 3 (DPM3), mRNA	0.0259220	-2.07
NM_174715.1	Bos taurus ribosomal protein L3 (Rpl3), mRNA	0.0331080	-12.45
NM_001035302.1	Bos taurus ARV1 homolog (S. cerevisiae) (ARV1), mRNA	0.0225546	-4.83
NM_001046128.1	Bos taurus phosphorylase kinase, gamma 2 (testis) (PHKG2), mRNA	0.0203012	-11.50
NM_001075154.1	Bos taurus ral guanine nucleotide dissociation stimulator-like 2 (RGL2), mRNA	0.0397883	-3.74
XM_866334.3	PREDICTED: Bos taurus similar to cell division cycle 25B, transcript variant 2 (CDC25B), mRNA	0.0291195	-2.43
XM_001787408.1	PREDICTED: Bos taurus similar to astrotactin 2 (LOC781555), partial mRNA	0.0206163	-3.10
NM_001101127.1	Bos taurus UDP-N-acetyl-alpha-D-galactosamine:polypeptide N-acetylgalactosaminyltransferase-like 1 (GALNTL1), mRNA	0.0289177	-2.29
XM_586902.3	PREDICTED: Bos taurus DEAD (Asp-Glu-Ala-Asp) box polypeptide 46 (DDX46),	0.0437300	-3.30

	mRNA		
NM_001034285.1	Bos taurus transmembrane protein 208 (TMEM208), mRNA	0.0191771	-2.24
NM_001098910.1	Bos taurus embryonal Fyn-associated substrate (EFS), mRNA	0.0043734	-2.45
XM_001250964.1	PREDICTED: Bos taurus similar to mCG114897 (LOC782315), mRNA	0.0067955	-2.50
NM_001034654.1	Bos taurus LSM14A, SCD6 homolog A (S. cerevisiae) (LSM14A), mRNA	0.0419574	-10.93

Appendix Table 2: Transcripts that were differentially expressed in LRECe vs. ECe
(*positive values for fold-change indicate that expression is greater in LRECe)

Bovine RefSeq_ID	**Bovine RefSeq_Description**	**P value**	**Fold change***
NR_001464.2	XIST X (inactive)-specific transcript	0.00028	10.00
XM_582069.4	Amyloid protein-binding protein 2 (Amyloid beta precursor protein-binding protein 2)	0.03882	5.88
NM_001046333.1	calcium/calmodulin-dependent protein kinase II delta (CAMK2D)	0.00005	5.88
NM_001046340.1	H2A histone family, member Y (H2AFY)	0.01908	5.26
NM_001046498.1	HBS1-like (S. cerevisiae) (HBS1L)	0.04813	4.54
NM_176659.2	NADH dehydrogenase (ubiquinone) 1 alpha subcomplex, 3, 9kDa (NDUFA3)	0.04817	4.00
XM_865587.3	ankyrin repeat domain 12 (ANKARD12)	0.02241	3.84
NM_001075649.1	N-acetyltransferase 15 (GCN5-related, putative) (NAT15)	0.00795	3.70
NM_001105433.1	Collagen type XIII alpha-1 chain, partial (31%)	0.02004	3.22
XM_001788478.1	dishevelled 3	0.03591	3.22
NM_001103236.1	Acyl-coenzyme A oxidase 3, peroxisomal (Pristanoyl-CoA oxidase)	0.00473	3.12
NM_001076543.1	Protein regulating cytokinesis 1 (Protein regulator of cytokinesis 1)	0.04865	3.12
XM_868289.2	Rnpc2 protein	0.02595	3.00
NM_001076945.1	Torsin B precursor (Torsin family 1 member B) (FKSG18 protein)	0.03605	3.00
NM_001098069.1	Probable transcriptional regulator, LysR family,	0.01694	3.00
NM_001078004.1	PELI1 pellino homolog 1 (Drosophila) [Bos taurus] (PELI1)	0.04298	2.94
XM_001250858.2	MON2 MON2 homolog (S. cerevisiae) [Bos taurus] (MON2)	0.03747	2.63
XR_027593.2	similar to Selenoprotein T (SELT)	0.03908	2.56
NM_001014862.2	Ribosomal protein L29/heparin/heparan sulfate interacting protein (Ribosomal protein L29/cell surface heparin binding protein HIP)	0.00830	2.56
NM_001024473.2	gypsy retrotransposon integrase 1 (GINI)	0.03900	2.50
XM_582124.3	GC-rich promoter binding protein 1-like 1 (GPBP1L1)	0.04107	2.43

NM_001083468.1	Serine/threonine protein phosphatase 2A, 56 kDa regulatory subunit, epsilon isoform (PP2A, B subunit, B' epsilon isoform) (PP2A, B subunit, B56 epsilon isoform) (PP2A, B subunit, PR61 epsilon isoform) (PP2A, B subunit, R5 epsilon isoform	0.00608	2.43
NM_001076900.1	Bos taurus heterogeneous nuclear ribonucleoprotein L-like (HNRPLL)	0.00849	2.43
XR_028008.2	SNF related kinase (SNRK)	0.04944	2.43
NM_001077051.1	Ataxin-10 (Spinocerebellar ataxia type 10 protein) (Brain protein E46 homolog)	0.04175	2.43
NM_001035056.1	transmembrane protein 111 (TMEM11)	0.03288	2.38
NM_001076835.1	Bos taurus kelch-like 20 (Drosophila) (KLHL20)	0.03386	2.38
XM_615597.4	Orphan nuclear receptor NR5A2 (Alpha-1-fetoprotein transcription factor) (Hepatocytic transcription factor) (B1-binding factor) (hB1F) (CYP7A promoter binding factor)	0.04533	2.32
XM_580860.4	PREDICTED: Bos taurus similar to transferrin receptor (TFRC)	0.01978	2.27
XM_593410.4	PREDICTED: Bos taurus similar to LKB1 interacting protein (STK11IP)	0.00803	2.27
XM_587229.4	PREDICTED: Bos taurus similar to serum-inducible kinase, transcript variant 1 (PLK2)	0.03486	2.22
NM_001078099.2	DPH2 homolog (S. cerevisiae) (DPH2)	0.04872	2.22
NM_001078161.2	Bos taurus ataxin 7-like 3B (ATXN7L3B)	0.03461	2.22
XM_001249400.2	PREDICTED: Bos taurus similar to fibronectin type III domain containing 3B, transcript variant 1 (FNDC3B)	0.03703	2.04
NM_174130.2	Ornithine decarboxylase (ODC)	0.03797	2.04
NM_001034373.1	Bos taurus cytochrome P450, family 4, subfamily V, polypeptide 2 (CYP4V2)	0.03165	2.04
XM_001254432.2	PREDICTED: Bos taurus zinc finger protein 347 (ZNF568)	0.04852	2.04
NM_001078021.1	HEAT repeat containing 3 (HEATR3)	0.03191	2.04

NM_001192779.1	Bos taurus protein tyrosine phosphatase, non-receptor type 11 (PTPN11)	0.00364	2.00
NM_001075334.1	Bos taurus microtubule-associated protein, RP/EB family, member 1 (MAPRE1)	0.00348	2.00
NM_001040471.1	Glucose-6-phosphate isomerase (GPI)	0.03622	2.00
NM_001102183.1	ERG v-ets erythroblastosis virus E26 oncogene homolog (avian) [Bos taurus] (ERG)	0.02054	-9.07
NM_001076842.1	signal transducing adaptor molecule (SH3 domain and ITAM motif) 1 (STAM)	0.03909	-7.66
XM_001790635.1	HLA-B associated transcript 2-like 2 (BAT2L2)	0.03624	-6.14
NM_001034697.1	Bos taurus tubulin, beta 4A class IVa (TUBB4A)	0.01665	-6.11
NM_001114520.1	Bos taurus calcium/calmodulin-dependent protein kinase II inhibitor 1 (CAMK2N1)	0.01249	-5.66
XR_028749.2	ciliary rootlet coiled-coil, rootletin (CROCC)	0.03916	-5.54
XM_001251162.2	IQ motif containing GTPase activating protein 1 (IQGAP1)	0.04492	-5.47
NM_001102106.1	coiled-coil domain containing 77 (CCDC77)	0.01134	-5.39
XM_581758.4	forkhead box N3 (FOXN3)	0.01970	-4.85
NM_001075317.1	RAB21, member RAS oncogene family (RAB21)	0.04531	-4.55
XM_001250666.2	FUS interacting protein (serine/arginine-rich) 1 (FUSIPI)	0.03230	-4.42
XM_591540.4	eukaryotic translation initiation factor 3, subunit F (EIF3F)	0.00763	-4.30
NM_001099155.1	Bos taurus CD177 molecule (CD177)	0.03054	-3.73
XM_593636.4	Microtubule-associated protein 1A (MAP 1A)	0.04977	-3.59
NM_001110004.1	Bos taurus HECT, UBA and WWE domain containing 1 (HUWE1)	0.01659	-3.57
XM_587001.3	PREDICTED: Bos taurus adenylate cyclase 6, transcript variant 1 (ADCY6)	0.03768	-3.50
XM_001253009.2	PREDICTED: Bos taurus hypothetical LOC785211 (LOC785211)	0.04511	-3.49
XM_001789611.1	PREDICTED: Bos taurus similar to WD repeat-containing protein C2orf44 homolog (LOC785211)	0.01830	-3.34
XR_028120.2	PREDICTED: Bos taurus misc_RNA (LOC518495)	0.02856	-3.19

XM_001787963.1	t-complex 11 (mouse)-like 1 (TCP11L1)	0.04744	-3.12
NM_001078081.1	chromosome 6 open reading frame 25 (C6orf25)	0.04016	-3.00
XM_001789698.1	PREDICTED: Bos taurus myeloid/lymphoid or mixed-lineage leukemia 5 (trithorax homolog, Drosophila), transcript variant 2 (MLL5)	0.02234	-2.93
XM_613386.4	PREDICTED: Bos taurus similar to KIAA1629 protein (ZNF532)	0.00618	-2.89
NM_001101171.1	Bos taurus abl-interactor 2 (ABI2)	0.02709	-2.88
XM_001790373.1	similar to Zinc finger protein 583 (Zinc finger protein L3-5) (ZFP583)	0.00629	-2.87
XM_872705.3	PREDICTED: Bos taurus zinc finger protein 142, transcript variant 2 (ZNF142)	0.01362	-2.84
NM_001102240.1	Bos taurus cysteinyl leukotriene receptor 2 (CYSLTR2)	0.00143	-2.80
XM_001256033.2	SWI/SNF related, matrix associated, actin dependent regulator of chromatin, subfamily d, member 2 (SMARCD2)	0.00668	-2.78
XM_615671.3	anaphase promoting complex subunit 1 (ANAPC1)	0.01744	-2.78
NM_001037591.1	chromosome 2 open reading frame 39 ortholog (C11H2ORF39)	0.02215	-2.73
XM_611789.4	ataxin 2 (ATXN2)	0.02135	-2.69
NM_001098042.1	Bos taurus striatin, calmodulin binding protein 3 (STRN3)	0.04872	-2.69
NM_001008666.1	Bos taurus solute carrier family 14 (urea transporter), member 1 (Kidd blood group) (SLC14A1)	0.01839	-2.61
NM_001102151.1	Bos taurus enhancer of zeste homolog 1 (Drosophila) (EZH1)	0.03810	-2.57
XM_598421.4	PREDICTED: Bos taurus centrosomal protein 110kDa (CEP110)	0.01443	-2.55
NM_001046442.1	Bos taurus KH domain containing, RNA binding, signal transduction associated 1 (KHDRBS1)	0.04034	-2.55
XM_882161.2	PREDICTED: Bos taurus procollagen-lysine, 2-oxoglutarate 5-dioxygenase 3, transcript variant 6 (PLOD3)	0.02340	-2.53

NM_001101060.1	v-yes-1 Yamaguchi sarcoma viral oncogene homolog 1 (YES1)	0.04456	-2.51
XM_001790627.1	HIV-1 Tat specific factor 1 (HTATSF1)	0.04214	-2.46
XM_872313.3	PREDICTED: Bos taurus similar to Nucleosome assembly protein 1-like 1 (NAP-1-related protein) (hNRP), transcript variant 4 (LOC540136)	0.00906	-2.43
NM_001034521.1	SAR1a gene homolog (SAR1A)	0.03600	-2.42
NM_001101898.1	Bos taurus inter-alpha (globulin) inhibitor H3 (ITIH3)	0.03701	-2.41
XM_866155.3	PREDICTED: Bos taurus similar to proline-serine-threonine phosphatase interacting protein 1, transcript variant 2 (PSTPIP1)	0.00129	-2.40
NM_001046329.1	Bos taurus thyroid hormone receptor, alpha (THRA)	0.02331	-2.40
NM_001105620.1	ankyrin 3, node of Ranvier (ankyrin G) (ANK3)	0.04038	-2.40
XM_870871.3	PREDICTED: Bos taurus similar to SAPS domain family, member 1 (SAPS1)	0.01407	-2.37
XM_001251703.2	PREDICTED: Bos taurus ribosomal protein S29-like	0.03232	-2.36
NM_001102098.1	Zinc finger protein 304 (ZNF304)	0.04097	-2.33
NM_001034765.1	Bos taurus Thy-1 cell surface antigen (THY1)	0.03373	-2.33
NM_001040520.1	Ribosomal protein L7A (RPL7A)	0.04975	-2.31
NM_001024527.1	Bos taurus FYVE, RhoGEF and PH domain containing 3 (FGD3)	0.05003	-2.26
XR_027956.2	PREDICTED: Bos taurus hypothetical protein LOC540222 (LOC540222)	0.04955	-2.26
NM_001109808.1	Bos taurus adaptor-related protein complex 1, gamma 2 subunit (AP1G2)	0.02072	-2.26
NM_001105437.1	Potassium channel tetramerisation domain containing 17 (KCTD17)	0.02854	-2.25
XM_591190.4	Uncharacterized protein C17orf68 homolog	0.02661	-2.24
NM_001080322.1	Terminal uridylyl transferase 1, U6 snRNA-specific (TUT1)	0.00801	-2.21

XM_601083.4	PREDICTED: Bos taurus Kruppel-like factor 10 (KLF10)	0.04792	-2.20
NM_001083456.1	Bos taurus KIAA0907 ortholog (KIAA0907)	0.03512	-2.18
NM_001014901.1	Bos taurus RNA binding motif protein 14 (RBM14)	0.02644	-2.16
XR_028120.2	PREDICTED: Bos taurus misc_RNA (LOC518495)	0.03913	-2.16
NM_001114517.1	Cytochrome c oxidase subunit VIII-H (heart/muscle) (COX8B)	0.00111	-2.15
NM_001192981	Bos taurus low density lipoprotein receptor-related protein 12 (LRP12)	0.01258	-2.13
NM_001034406.1	Bos taurus zinc finger CCCH-type containing 14 (ZC3H14)	0.04964	-2.10
NM_174656.2	Bos taurus solute carrier family 25 (mitochondrial carrier; citrate transporter), member 1(SLC25A1), nuclear gene encoding mitochondrial protein	0.01608	-2.08
XM_606901.4	Protein kinase C, iota (PRKCI)	0.00988	-2.05
NM_001035428.1	Bos taurus coiled-coil domain containing 47 (CCDC47)	0.00534	-2.03
NM_001046027.1	Bos taurus thromboxane A synthase 1 (platelet) (TBXAS1)	0.03955	-2.02
XM_601785.4	PREDICTED: Bos taurus similar to myosin IE (MYO1E)	0.00529	-2.01

Appendix Table 3: Transcripts that were differentially expressed in LRECb vs. LRECe
(*positive values for fold-change indicate that expression is greater in LRECb)

Bovine RefSeq_ID	Bovine RefSeq_Description	P value	Fold change*
NM_001046430.1	Bos taurus ubiquitin specific peptidase 15 (USP15), mRNA	0.00052	16.67
NM_001081611.1	Bos taurus F-box protein 34 (FBXO34), mRNA	0.00392	16.67
XM_001254067.2	PREDICTED: Bos taurus similar to trichohyalin, putative (LOC786372), mRNA	0.02744	14.28
NM_001098874.1	Bos taurus ribosomal protein S7 (RPS7), mRNA	0.04479	12.50
NM_001015655.1	Bos taurus cofilin 1 (non-muscle) (CFL1), mRNA	0.04363	8.33
XM_594080.4	PREDICTED: Bos taurus similar to RNA polymerase I-specific transcription initiation factor RRN3 (Transcription initiation factor IA) (TIF-IA) (RRN3), mRNA	0.03211	7.14
NM_174520.2	Bos taurus collagen, type I, alpha 2 (COL1A2), mRNA	0.02700	7.14
NM_178317.3	Bos taurus tribbles homolog 2 (Drosophila) (TRIB2), mRNA	0.00146	6.67
NM_001076027.1	Bos taurus heat shock protein, alpha-crystallin-related, B6 (HSPB6), mRNA	0.01972	6.67
XM_590933.4	PREDICTED: Bos taurus similar to nucleoporin 153kDa (NUP153), mRNA	0.02673	6.25
XM_001251703.2	PREDICTED: Bos taurus similar to mCG7602 (LOC784384), mRNA	0.01326	6.25
XM_001253131.2	PREDICTED: Bos taurus similar to solute carrier family 10 (sodium/bile acid cotransporter family), member 5 (SLC10A5), mRNA	0.04262	5.88
NM_001015543.1	Bos taurus ribosomal protein L13 (RPL13), mRNA	0.00814	5.88
XM_611689.4	PREDICTED: Bos taurus similar to Laminin subunit gamma-1 precursor (Laminin B2 chain) (LAMC1), mRNA	0.02142	5.88
NM_001040479.1	Bos taurus periostin, osteoblast specific factor (POSTN), mRNA	0.03043	5.55
NM_001034765.1	Bos taurus Thy-1 cell surface antigen (THY1), mRNA	0.00330	5.55
NM_001038582.1	Bos taurus electron-transfer-flavoprotein, beta polypeptide (ETFB), mRNA	0.01836	5.00
NM_001076331.1	Bos taurus MAX interactor 1 (MXI1), mRNA	0.02888	5.00
NM_001098071.1	Bos taurus G1 to S phase transition 1 (GSPT1), mRNA	0.03986	5.00

XM_615405.4	PREDICTED: Bos taurus WD-repeat protein 33 (WDR33), mRNA	0.01603	5.00
XR_043027.1	PREDICTED: Bos taurus misc_RNA (LOC789346), miscRNA	0.00720	4.76
XM_872002.3	PREDICTED: Bos taurus similar to APG16 autophagy 16-like, transcript variant 5 (ATG16L1), mRNA	0.00737	4.76
NR_024614.1	Bos taurus ribosomal protein S27 (RPS27), transcript variant 3, transcribed RNA	0.01351	4.76
NM_001040487.1	Bos taurus eukaryotic translation elongation factor 1 gamma (EEF1G), mRNA	0.00711	4.76
NM_001075946.1	Bos taurus cell adhesion molecule 3 (CADM3), mRNA	0.01029	4.34
NM_001078157.1	Bos taurus ADP-ribosylation factor-like 6 interacting protein 1 (ARL6IP1), mRNA	0.02483	4.34
XM_001790104.1	PREDICTED: Bos taurus NFKB activating protein, transcript variant 1 (NKAP), mRNA	0.01801	4.34
NM_001081616.1	Bos taurus VMA21 vacuolar H+-ATPase homolog (S. cerevisiae) (VMA21), mRNA	0.00728	4.34
XM_615786.4	PREDICTED: Bos taurus peptidylprolyl isomerase (cyclophilin)-like 4, transcript variant 1 (PPIL4), mRNA	0.00801	4.16
NM_001101894.1	Bos taurus F-box protein 11 (FBXO11), mRNA	0.04165	4.00
NM_175801.2	Bos taurus follistatin (FST), mRNA	0.01199	4.00
XM_603300.3	PREDICTED: Bos taurus similar to nuclear receptor interacting protein 1 (NRIP1), mRNA	0.01573	4.00
NM_001080314.1	Bos taurus GTP-binding protein 10 (putative) (GTPBP10), mRNA	0.04093	4.00
XM_588451.4	PREDICTED: Bos taurus similar to NFBD1 (MDC1), mRNA	0.03057	4.00
XM_612368.4	PREDICTED: Bos taurus similar to RAN binding protein 17 (LOC533085), mRNA	0.03247	3.84
NM_001076468.1	Bos taurus HLA-B associated transcript 4 (BAT4), mRNA	0.03791	3.84
NM_001035272.1	Bos taurus splicing factor, arginine/serine-rich 6 (SFRS6), mRNA	0.00604	3.84
XM_614458.4	PREDICTED: Bos taurus CAP-GLY domain containing linker protein 1, transcript variant 1 (CLIP1), mRNA	0.01541	3.84
NM_001034684.1	Bos taurus cisplatin resistance-associated overexpressed protein (CROP), mRNA	0.04997	3.84
NM_001015551.1	Bos taurus aminoadipate aminotransferase (AADAT), mRNA	0.02881	3.70
XM_614308.4	PREDICTED: Bos taurus coiled-coil domain containing 66 (CCDC66), mRNA	0.01006	3.70

NM_001075601.1	Bos taurus monocyte to macrophage differentiation-associated (MMD), mRNA	0.01548	3.70
XM_866635.2	PREDICTED: Bos taurus similar to Echinoderm microtubule-associated protein-like 4 (EMAP-4) (Restrictedly overexpressed proliferation-associated protein) (Ropp 120), transcript variant 3 (EML4), mRNA	0.01380	3.70
XM_867978.3	PREDICTED: Bos taurus chromosome 9 open reading frame 16 ortholog (C11H9orf16), mRNA	0.00067	3.70
XM_868974.2	PREDICTED: Bos taurus THAP domain containing 9 (THAP9), mRNA	0.02239	3.57
XM_611908.4	PREDICTED: Bos taurus similar to mutS homolog 6, transcript variant 1 (MSH6), mRNA	0.04898	3.57
NM_001035432.1	Bos taurus CCR4-NOT transcription complex, subunit 4 (CNOT4), mRNA	0.01503	3.57
NM_001083643.1	Bos taurus NIMA (never in mitosis gene a)-related kinase 3 (NEK3), mRNA	0.00078	3.44
NM_174564.2	Bos taurus NADH dehydrogenase (ubiquinone) 1, subcomplex unknown, 1, 6kDa (NDUFC1), mRNA	0.00282	3.44
NM_001034555.2	Bos taurus S100 calcium binding protein B (S100B), mRNA	0.01983	3.44
NM_174033.3	Bos taurus CYB5 protein (CYB5), mRNA	0.00081	3.44
NM_001046143.1	Bos taurus CDKN2A interacting protein (CDKN2AIP), mRNA	0.01020	3.44
NM_174301.3	Bos taurus chemokine (C-X-C motif) receptor 4 (CXCR4), mRNA	0.03667	3.44
NM_001075297.1	Bos taurus interleukin 33 (IL33), mRNA	0.00711	3.33
NM_001076023.1	Bos taurus chromosome 12 open reading frame 49 ortholog (C9H12orf49), mRNA	0.03312	3.33
XM_600235.4	PREDICTED: Bos taurus myeloid/lymphoid or mixed-lineage leukemia (trithorax homolog, Drosophila); translocated to, 3 (MLLT3), mRNA	0.03043	3.33
NM_174387.2	Bos taurus mannosidase, beta A, lysosomal (MANBA), mRNA	0.01136	3.33
NM_001114082.1	Bos taurus angiotensinogen (serpin peptidase inhibitor, clade A, member 8) (AGT), mRNA	0.00681	3.33
XM_597427.4	PREDICTED: Bos taurus similar to phosphatidylinositol glycan class V (PIGV), mRNA	0.02774	3.33
NM_001102259.1	Bos taurus chromosome 10 open reading frame 6 ortholog (C26H10ORF6), mRNA	0.03744	3.33
NM_174043.2	Bos taurus dopamine receptor D2 (DRD2), mRNA	0.04227	3.33
NM_001046507.1	Bos taurus ELL associated factor 2 (EAF2),	0.04827	3.33

	mRNA		
NM_174087.3	Bos taurus insulin-like growth factor 2 (somatomedin A) (IGF2), mRNA	0.00711	3.22
NM_001002887.1	Bos taurus paternally expressed 3 (PEG3), mRNA	0.01719	3.22
XM_001787646.1	PREDICTED: Bos taurus similar to phospholipase C-like 1 (LOC537873), partial mRNA	0.00028	3.22
NM_001046461.1	Bos taurus TRIM6-TRIM34 readthrough transcript (TRIM6-TRIM34), mRNA	0.00422	3.22
XR_042825.1	PREDICTED: Bos taurus misc_RNA (MAML3), partial miscRNA	0.02367	3.22
XM_001249464.2	PREDICTED: Bos taurus similar to intersectin 1 long form (ITSN1), mRNA	0.03861	3.22
NM_001077991.1	Bos taurus RecQ protein-like (DNA helicase Q1-like) (RECQL), mRNA	0.01667	3.22
XM_606010.4	PREDICTED: Bos taurus similar to solute carrier family 35, member B3 (SLC35B3), mRNA	0.03799	3.22
NM_001034591.1	Bos taurus zinc finger, C3HC-type containing 1 (ZC3HC1), mRNA	0.00205	3.22
XM_588427.3	PREDICTED: Bos taurus similar to cell division cycle 2-like 5, transcript variant 3 (CDC2L5), mRNA	0.00594	3.12
XM_582124.3	PREDICTED: Bos taurus similar to GC-rich promoter binding protein 1-like 1, transcript variant 1 (GPBP1L1), mRNA	0.01704	3.12
NM_001080289.1	Bos taurus hypothetical LOC526913 (MGC148942), mRNA	0.00460	3.12
XM_001790627.1	PREDICTED: Bos taurus HIV-1 Tat specific factor 1 (HTATSF1), mRNA	0.03675	3.12
XM_614320.4	PREDICTED: Bos taurus similar to Dmx-like 1 (DMXL1), mRNA	0.02635	3.12
NM_001015565.1	Bos taurus poly(rC) binding protein 1 (PCBP1), mRNA	0.04980	3.12
NM_001076320.1	Bos taurus ADP-ribosylation factor-like 10 (ARL10), mRNA	0.01185	3.12
XM_582283.3	PREDICTED: Bos taurus similar to huntingtin interacting protein 1 (HIP1), mRNA	0.01904	3.12
NM_203323.2	Bos taurus spermidine/spermine N1-acetyltransferase family member 2 (SAT2), mRNA	0.01429	3.00
NM_001099033.1	Bos taurus guanine nucleotide binding protein (G protein), beta polypeptide 4 (GNB4), mRNA	0.00063	3.00

XM_001787807.1	PREDICTED: Bos taurus similar to Leucine-rich PPR motif-containing protein, mitochondrial precursor (130 kDa leucine-rich protein) (LRP 130) (GP130) (LOC509995), mRNA	0.00516	3.00
XM_001251924.2	PREDICTED: Bos taurus similar to enhancer of rudimentary homolog (LOC783761), mRNA	0.03672	3.00
XM_864250.3	PREDICTED: Bos taurus similar to DNA repair and recombination protein RAD54B (RAD54 homolog B), transcript variant 2 (RAD54B), mRNA	0.04770	3.00
NM_001078069.1	Bos taurus protein tyrosine phosphatase, non-receptor type 18 (brain-derived) (PTPN18), mRNA	0.04115	3.00
NM_001035428.1	Bos taurus coiled-coil domain containing 47 (CCDC47), mRNA	0.01911	3.00
XM_593991.4	PREDICTED: Bos taurus similar to transmembrane 6 superfamily member 2 (TM6SF2), mRNA	0.02394	2.94
XR_027597.2	PREDICTED: Bos taurus misc_RNA (LOC532189), miscRNA	0.00015	2.94
XR_028749.2	PREDICTED: Bos taurus misc_RNA (LOC530641), miscRNA	0.00281	2.94
NM_001046517.1	Bos taurus lymphocyte antigen 96 (LY96), mRNA	0.03013	2.94
XM_591415.4	PREDICTED: Bos taurus similar to Uncharacterized protein C1orf160 (LOC513687), mRNA	0.01677	2.94
NM_001034673.1	Bos taurus chromosome 12 open reading frame 23 ortholog (C5H12orf23), mRNA	0.03579	2.94
NM_001103319.1	Bos taurus phospholamban (PLN), mRNA	0.00565	2.85
XM_584232.4	PREDICTED: Bos taurus hypothetical LOC539014, transcript variant 1 (LOC539014), mRNA	0.02942	2.85
XR_043032.1	PREDICTED: Bos taurus misc_RNA (AOC3), miscRNA	0.01480	2.85
XM_584266.4	PREDICTED: Bos taurus similar to partner and localizer of BRCA2 (PALB2), mRNA	0.01058	2.85
NM_001099710.1	Bos taurus muscleblind-like 2 (Drosophila) (MBNL2), mRNA	0.01823	2.85
NM_001109795.1	Bos taurus alpha-2-macroglobulin (A2M), mRNA	0.01895	2.85
NM_001105341.1	Bos taurus TRAF and TNF receptor associated protein (TTRAP), mRNA	0.00817	2.85
NM_001034583.1	Bos taurus component of oligomeric golgi complex 4 (COG4), mRNA	0.03471	2.85

XM_601617.4	PREDICTED: Bos taurus topoisomerase I binding, arginine/serine-rich (TOPORS), mRNA	0.01047	2.77
XM_598625.4	PREDICTED: Bos taurus similar to calmodulin regulated spectrin-associated protein 1-like 1 (LOC520385), mRNA	0.02197	2.77
XR_028796.2	PREDICTED: Bos taurus misc_RNA (LOC615883), miscRNA	0.03802	2.77
NM_001098038.1	Bos taurus kinesin family member 23 (KIF23), mRNA	0.01480	2.77
NM_001083469.1	Bos taurus transmembrane protein 156 (TMEM156), mRNA	0.04739	2.77
NM_001078131.1	Bos taurus nuclear receptor binding factor 2 (NRBF2), mRNA	0.04746	2.77
NM_001101843.1	Bos taurus collectin sub-family member 12 (COLEC12), mRNA	0.04699	2.77
NM_001076414.1	Bos taurus transmembrane BAX inhibitor motif containing 6 (TMBIM6), mRNA	0.01504	2.77
XM_869402.2	PREDICTED: Bos taurus similar to MYST histone acetyltransferase (monocytic leukemia) 3 (LOC529373), mRNA	0.04771	2.77
XM_585792.4	PREDICTED: Bos taurus similar to Oxysterol-binding protein-related protein 7 (OSBP-related protein 7) (ORP-7), transcript variant 1 (OSBPL7), mRNA	0.03672	2.70
NM_001035361.1	Bos taurus RNA binding motif, single stranded interacting protein 1 (RBMS1), mRNA	0.02621	2.70
XM_879087.2	PREDICTED: Bos taurus similar to transcriptional repressor BSR/RACK7/PRKCBP1, transcript variant 7 (ZMYND8), mRNA	0.04257	2.70
NM_001037463.1	Bos taurus WW domain containing E3 ubiquitin protein ligase 1 (WWP1), mRNA	0.00585	2.70
XM_611206.4	PREDICTED: Bos taurus similar to adducin 1 (alpha) (ADD1), mRNA	0.03464	2.70
NM_001101925.1	Bos taurus transmembrane and coiled-coil domain family 1 (TMCC1), mRNA	0.04075	2.70
NM_001083468.1	Bos taurus protein phosphatase 2, regulatory subunit B', epsilon isoform (PPP2R5E), mRNA	0.00087	2.70
NM_001098122.1	Bos taurus synovial sarcoma translocation, chromosome 18 (SS18), mRNA	0.02415	2.70
NM_001099209.1	Bos taurus hypothetical protein LOC788754 (MGC152484), mRNA	0.03043	2.70
XM_863836.2	PREDICTED: Bos taurus microtubule-associated protein 1B, transcript variant 2 (MAP1B), mRNA	0.03384	2.63

XR_042701.1	PREDICTED: Bos taurus misc_RNA (LOC786759), miscRNA	0.01586	2.63
NM_001143867.1	Bos taurus DEAD (Asp-Glu-Ala-Asp) box polypeptide 6 (DDX6), mRNA	0.04126	2.63
XM_600663.4	PREDICTED: Bos taurus nestin (NES), mRNA	0.00303	2.63
NM_001034629.1	Bos taurus epoxide hydrolase 1, microsomal (xenobiotic) (EPHX1), mRNA	0.00935	2.63
XM_584315.4	PREDICTED: Bos taurus similar to chromosome 14 open reading frame 106 (LOC507661), mRNA	0.02230	2.63
XM_585218.4	PREDICTED: Bos taurus similar to bromodomain adjacent to zinc finger domain, 1B (BAZ1B), mRNA	0.04863	2.63
XM_604909.4	PREDICTED: Bos taurus similar to crooked neck-like 1 protein (CRNKL1), partial mRNA	0.01894	2.63
NM_001035362.1	Bos taurus tetraspanin 13 (TSPAN13), mRNA	0.00244	2.63
XM_584555.4	PREDICTED: Bos taurus similar to nuclear pore complex-associated protein TPR, transcript variant 1 (TPR), mRNA	0.00608	2.63
NM_001101898.1	Bos taurus inter-alpha (globulin) inhibitor H3 (ITIH3), mRNA	0.03844	2.63
NM_194465.2	Bos taurus murine retrovirus integration site 1 homolog (MRVI1), transcript variant 2, mRNA	0.03526	2.63
NM_001102502.1	Bos taurus CDC42 binding protein kinase gamma (CDC42BPG), mRNA	0.00869	2.63
XM_592333.4	PREDICTED: Bos taurus similar to transcriptional regulator ATRX (ATRX), mRNA	0.04112	2.63
NM_001076846.1	Bos taurus far upstream element (FUSE) binding protein 1 (FUBP1), mRNA	0.02223	2.63
NM_174028.1	Bos taurus colony stimulating factor 3 (granulocyte) (CSF3), mRNA	0.04807	2.56
XM_864645.3	PREDICTED: Bos taurus similar to alkylglycerone phosphate synthase, transcript variant 2 (AGPS), mRNA	0.00919	2.56
NM_001100313.1	Bos taurus dehydrogenase/reductase (SDR family) member 12 (DHRS12), mRNA	0.02334	2.56
XR_028142.1	PREDICTED: Bos taurus misc_RNA (LOC535967), miscRNA	0.04114	2.56
NM_001011681.3	Bos taurus growth factor receptor-bound protein 14 (GRB14), mRNA	0.02877	2.56
NM_001014883.1	Bos taurus nuclear receptor subfamily 1, group H, member 2 (NR1H2), mRNA	0.03541	2.56
NM_001034515.1	Bos taurus G protein-coupled receptor, family C, group 5, member A (GPRC5A), mRNA	0.03894	2.56

XM_001256832.2	PREDICTED: Bos taurus similar to Pre-mRNA-splicing factor SYF2 (CCNDBP1-interactor) (p29) (LOC790322), partial mRNA	0.00113	2.56
NM_001075641.1	Bos taurus myotubularin related protein 7 (MTMR7), mRNA	0.01876	2.56
NM_001102325.1	Bos taurus activating transcription factor 7 interacting protein (ATF7IP), mRNA	0.00789	2.56
NM_001075366.2	Bos taurus HLA-B associated transcript 3 (BAT3), mRNA	0.03587	2.56
NM_001076334.1	Bos taurus small nuclear ribonucleoprotein polypeptide C (SNRPC), mRNA	0.01243	2.56
NM_001078001.1	Bos taurus hypothetical LOC534560 (MGC152232), mRNA	0.04503	2.50
XM_864293.3	PREDICTED: Bos taurus similar to Transcription cofactor vestigial-like protein 1 (Vgl-1) (Protein TONDU), transcript variant 4 (VGLL1), mRNA	0.03602	2.50
NM_001077980.1	Bos taurus polycomb group ring finger 5 (PCGF5), mRNA	0.03170	2.50
XM_865593.3	PREDICTED: Bos taurus similar to Midasin (MIDAS-containing protein), transcript variant 2 (MDN1), mRNA	0.03172	2.44
NM_001101096.1	Bos taurus nudix (nucleoside diphosphate linked moiety X)-type motif 9 (NUDT9), mRNA	0.04002	2.44
NM_001046314.1	Bos taurus ubiquitin-fold modifier 1 (UFM1), mRNA	0.04398	2.44
XM_871152.2	PREDICTED: Bos taurus similar to TRD@ protein (LOC618831), mRNA	0.04936	2.44
NM_001034524.1	Bos taurus heat shock 70kDa protein 9 (mortalin) (HSPA9), nuclear gene encoding mitochondrial protein, mRNA	0.04059	2.44
XM_594786.4	PREDICTED: Bos taurus similar to RIKEN cDNA 1110067D22 (LOC516629), mRNA	0.03133	2.44
XM_001251030.1	PREDICTED: Bos taurus cutC copper transporter homolog (E. coli), transcript variant 1 (CUTC), partial mRNA	0.03286	2.44
NM_001037629.1	Bos taurus translocase of inner mitochondrial membrane 8 homolog B (yeast) (TIMM8B), nuclear gene encoding mitochondrial protein, mRNA	0.00489	2.44
XM_001787477.1	PREDICTED: Bos taurus similar to dedicator of cytokinesis 10 (LOC539421), mRNA	0.02126	2.38
NM_001103096.1	Bos taurus nucleoporin 43kDa (NUP43), mRNA	0.02101	2.38
NM_174087.3	Bos taurus insulin-like growth factor 2 (somatomedin A) (IGF2), mRNA	0.03194	2.38
NM_001075285.1	Bos taurus nucleoporin 54kDa (NUP54), mRNA	0.01310	2.38

NM_001101170.2	Bos taurus sine oculis binding protein homolog (Drosophila) (SOBP), mRNA	0.00167	2.38
XM_868213.3	PREDICTED: Bos taurus similar to Transcobalamin-1 precursor (Transcobalamin I) (TCI) (TC I) (TCN1), mRNA	0.04905	2.38
NM_174712.2	Bos taurus rhesus-like protein (LOC282685), mRNA	0.04955	2.38
NM_001100293.1	Bos taurus chemokine (C-C motif) receptor 4 (CCR4), mRNA	0.03768	2.38
NM_001102082.1	Bos taurus zinc finger CCCH-type containing 18 (ZC3H18), mRNA	0.01653	2.38
NM_001034714.1	Bos taurus chromosome 2 open reading frame 42 ortholog (C11H2orf42), mRNA	0.01792	2.38
NM_177945.3	Bos taurus peroxisome proliferator-activated receptor gamma, coactivator 1 alpha (PPARGC1A), mRNA	0.03376	2.38
XM_614758.4	PREDICTED: Bos taurus similar to Thrombospondin type-1 domain-containing protein 4 (LOC534844), mRNA	0.03417	2.32
NM_174587.1	Bos taurus protein kinase C, beta (PRKCB), mRNA	0.01678	2.32
XM_615405.4	PREDICTED: Bos taurus WD-repeat protein 33 (WDR33), mRNA	0.04315	2.32
XM_001256289.2	PREDICTED: Bos taurus similar to mucin 2 (LOC789571), partial mRNA	0.00945	2.32
XM_591968.4	PREDICTED: Bos taurus similar to aurora borealis, transcript variant 1 (LOC514162), mRNA	0.03991	2.32
XM_582828.3	PREDICTED: Bos taurus similar to exonuclease 1 (EXO1), mRNA	0.01591	2.32
NM_174715.1	Bos taurus ribosomal protein L3 (Rpl3), mRNA	0.04690	2.32
NM_001105258.1	Bos taurus kinesin family member 20B (KIF20B), mRNA	0.01761	2.32
NM_001075823.1	Bos taurus sulfotransferase family, cytosolic, 1B, member 1 (SULT1B1), mRNA	0.01267	2.32
XM_867682.3	PREDICTED: Bos taurus hypothetical LOC615784 (LOC615784), mRNA	0.03488	2.32
XM_592611.4	PREDICTED: Bos taurus fibroblast growth factor 10, transcript variant 2 (FGF10), mRNA	0.04468	2.32
NM_001038543.1	Bos taurus sperm associated antigen 7 (SPAG7), mRNA	0.03018	2.27
XM_591440.3	PREDICTED: Bos taurus similar to Importin-7 (Imp7) (Ran-binding protein 7) (RanBP7) (IPO7), mRNA	0.04102	2.27
NM_001078013.1	Bos taurus RAB7B, member RAS oncogene family (RAB7B), mRNA	0.02049	2.27

XM_865774.3	PREDICTED: Bos taurus similar to Heat shock 70 kDa protein 4L (Osmotic stress protein 94) (Heat shock 70-related protein APG-1), transcript variant 3 (HSPA4L), mRNA	0.03347	2.27
NM_001098885.1	Bos taurus golgi SNAP receptor complex member 2 (GOSR2), mRNA	0.03655	2.27
XM_617171.4	PREDICTED: Bos taurus similar to cytidine monophosphate-N-acetylneuraminic acid hydroxylase, transcript variant 1 (LOC537017), mRNA	0.01249	2.27
XM_001252878.1	PREDICTED: Bos taurus similar to LOC522191 protein (MTERF), mRNA	0.02951	2.27
XR_043028.1	PREDICTED: Bos taurus misc_RNA (LOC100138100), miscRNA	0.00517	2.27
XM_001790491.1	PREDICTED: Bos taurus IQ motif containing with AAA domain (IQCA), mRNA	0.03127	2.27
NM_001045999.1	Bos taurus hypothetical LOC508280 (MGC127461), mRNA	0.01102	2.22
XM_001790095.1	PREDICTED: Bos taurus coiled-coil domain containing 76 (CCDC76), mRNA	0.00272	2.22
XM_001256605.1	PREDICTED: Bos taurus similar to pregnancy-associated glycoprotein 8 (LOC790008), partial mRNA	0.01145	2.22
XM_582594.4	PREDICTED: Bos taurus similar to zinc finger protein 77 (pT1) (LOC506181), partial mRNA	0.03953	2.22
NM_001080357.1	Bos taurus anaphase promoting complex subunit 10 (ANAPC10), mRNA	0.01297	2.22
XR_042974.1	PREDICTED: Bos taurus misc_RNA (METTL10), miscRNA	0.02732	2.22
XM_001253151.2	PREDICTED: Bos taurus similar to von Willebrand factor C and EGF domains (VWCE), mRNA	0.02884	2.22
XM_581757.3	PREDICTED: Bos taurus similar to cytochrome P450 2C92 (LOC505468), mRNA	0.01054	2.22
NM_174056.3	Bos taurus fibroblast growth factor 2 (basic) (FGF2), mRNA	0.04033	2.22
NM_001077928.1	Bos taurus plexin domain containing 2 (PLXDC2), mRNA	0.02503	2.22
NM_001015642.2	Bos taurus carboxypeptidase X (M14 family), member 1 (CPXM1), mRNA	0.04359	2.17
NM_001083500.1	Bos taurus hypothetical LOC541171 (MGC143035), mRNA	0.03365	2.17
NM_001103224.1	Bos taurus annexin A6 (ANXA6), mRNA	0.04137	2.17
XM_610845.4	PREDICTED: Bos taurus serum deprivation response (phosphatidylserine binding protein) (SDPR), partial mRNA	0.02345	2.17

XM_870123.2	PREDICTED: Bos taurus similar to Amiloride-sensitive sodium channel subunit gamma (Epithelial Na(+) channel subunit gamma) (Gamma-ENaC) (Nonvoltage-gated sodium channel 1 subunit gamma) (SCNEG) (Gamma-NaCH) (SCNN1G), mRNA	0.00310	2.17
XM_882441.2	PREDICTED: Bos taurus hypothetical LOC617028 (LOC617028), mRNA	0.04925	2.17
NM_001083503.1	Bos taurus ubiquitin-conjugating enzyme E2M (UBC12 homolog, yeast) (UBE2M), mRNA	0.02430	2.17
NM_001103224.1	Bos taurus annexin A6 (ANXA6), mRNA	0.04495	2.17
XM_587287.4	PREDICTED: Bos taurus proline-rich cyclin A1-interacting protein (PROCA1), mRNA	0.03110	2.17
XM_615597.4	PREDICTED: Bos taurus similar to nuclear receptor subfamily 5, group A, member 2, transcript variant 1 (NR5A2), mRNA	0.04968	2.17
XM_616144.4	PREDICTED: Bos taurus desmocollin 3 (DSC3), mRNA	0.04708	2.17
XM_592197.3	PREDICTED: Bos taurus similar to Desmoplakin (DP) (250/210 kDa paraneoplastic pemphigus antigen), transcript variant 1 (DSP), mRNA	0.01086	2.17
XR_042741.1	PREDICTED: Bos taurus misc_RNA (LOC785805), miscRNA	0.04058	2.12
XM_001788305.1	PREDICTED: Bos taurus similar to calcium activated chloride channel 2 (LOC534256), mRNA	0.01044	2.12
NM_001076427.1	Bos taurus cytochrome P450, family 2, subfamily C, polypeptide 87 (CYP2C87), mRNA	0.02339	2.12
NM_001034447.1	Bos taurus fructose-1,6-bisphosphatase 1 (FBP1), mRNA	0.04555	2.12
XM_592304.4	PREDICTED: Bos taurus similar to Protein flightless-1 homolog, transcript variant 1 (FLII), mRNA	0.00334	2.12
NM_001101213.1	Bos taurus isochorismatase domain containing 1 (ISOC1), mRNA	0.04217	2.12
NM_001046332.1	Bos taurus cell division cycle 42 (GTP binding protein, 25kDa) (CDC42), mRNA	0.04187	2.12
XM_588697.4	PREDICTED: Bos taurus similar to tumor necrosis factor, alpha-induced protein 1, transcript variant 1 (TNFAIP1), mRNA	0.01922	2.12
XR_027344.2	PREDICTED: Bos taurus misc_RNA (LOC781850), miscRNA	0.03912	2.12
NM_001076136.1	Bos taurus GINS complex subunit 3 (Psf3 homolog) (GINS3), mRNA	0.00375	2.12

NM_001102004.1	Bos taurus URB2 ribosome biogenesis 2 homolog (S. cerevisiae) (URB2), mRNA	0.02762	2.12
XM_865933.2	PREDICTED: Bos taurus similar to KIAA1946 (LOC614438), mRNA	0.04601	2.12
XM_001253129.2	PREDICTED: Bos taurus similar to programmed cell death protein 7 (PDCD7), mRNA	0.00648	2.08
XM_582278.4	PREDICTED: Bos taurus chromosome 6 open reading frame 115 ortholog (H9C6ORF115), mRNA	0.03368	2.08
XM_001788143.1	PREDICTED: Bos taurus similar to transmembrane protein with EGF-like and two follistatin-like domains 1 (LOC100139803), mRNA	0.03039	2.08
XM_001787893.1	PREDICTED: Bos taurus similar to echinoderm microtubule associated protein like 5 (LOC537305), partial mRNA	0.02931	2.08
NM_174386.2	Bos taurus microfibrillar associated protein 5 (MFAP5), mRNA	0.01789	2.08
XM_614691.3	PREDICTED: Bos taurus topoisomerase (DNA) I (TOP1), mRNA	0.02338	2.08
XM_001250628.2	PREDICTED: Bos taurus similar to ATP synthase subunit epsilon, mitochondrial (LOC782270), mRNA	0.04762	2.08
NM_173942.2	Bos taurus cleavage and polyadenylation specific factor 4, 30kDa (CPSF4), mRNA	0.01118	2.08
XM_583652.3	PREDICTED: Bos taurus similar to pleckstrin homology domain containing, family A (phosphoinositide binding specific) member 8 (PLEKHA8), mRNA	0.04434	2.04
XM_580330.4	PREDICTED: Bos taurus similar to nadrin (ARHGAP17), mRNA	0.01185	2.04
NM_174399.1	Bos taurus neural cell adhesion molecule 1 (NCAM1), mRNA	0.03915	2.04
XM_597858.4	PREDICTED: Bos taurus similar to myosin 18A, transcript variant 2 (MYO18A), mRNA	0.01654	2.04
XM_614586.4	PREDICTED: Bos taurus similar to histone cluster 2, H2aa4 (LOC541108), mRNA	0.02442	2.04
NM_001035074.1	Bos taurus acidic (leucine-rich) nuclear phosphoprotein 32 family, member B (ANP32B), mRNA	0.01055	2.04
NM_001034469.1	Bos taurus mesoderm development candidate 2 (MESDC2), mRNA	0.01206	2.04
NM_001077839.1	Bos taurus chemokine (C-C motif) receptor 1 (CCR1), mRNA	0.04002	2.04

XM_001249810.2	PREDICTED: Bos taurus similar to LON peptidase N-terminal domain and RING finger protein 3, transcript variant 1 (LONRF3), mRNA	0.01397	2.04
NM_001076926.1	Bos taurus neuronal guanine nucleotide exchange factor (NGEF), mRNA	0.04147	2.00
XR_042959.1	PREDICTED: Bos taurus misc_RNA (TAF5), miscRNA	0.01026	2.00
XM_592026.4	PREDICTED: Bos taurus caspase 1, apoptosis-related cysteine peptidase (interleukin 1, beta, convertase), transcript variant 1 (CASP1), mRNA	0.04651	2.00
NM_001081526.1	Bos taurus protein-L-isoaspartate (D-aspartate) O-methyltransferase domain containing 1 (PCMTD1), mRNA	0.02648	2.00
NM_001035490.1	Bos taurus chromosome 8 open reading frame 4 ortholog (C27H8orf4), mRNA	0.01950	2.00
NM_001038117.1	Bos taurus coiled-coil domain containing 52 (CCDC52), mRNA	0.00121	2.00
NM_001098929.1	Bos taurus splicing factor, arginine/serine-rich 5 (SFRS5), mRNA	0.03955	-3.68
NR_001464.2	Bos taurus X (inactive)-specific transcript (XIST), non-coding RNA	0.01175	-5.59
NM_001078161.2	Bos taurus hypothetical protein LOC777786 (LOC777786), mRNA	0.00770	-2.98
NM_001038092.1	Bos taurus chromosome 17 open reading frame 49 ortholog (C19H17orf49), mRNA	0.01536	-3.93
XM_587229.4	PREDICTED: Bos taurus similar to serum-inducible kinase, transcript variant 1 (PLK2), mRNA	0.02743	-2.52
NM_001075347.1	Bos taurus THAP domain containing, apoptosis associated protein 3 (THAP3), mRNA	0.01731	-3.66
NM_174212.2	Bos taurus UDP-glucose pyrophosphorylase 2 (UGP2), mRNA	0.01212	-3.35
XM_865719.3	PREDICTED: Bos taurus chromosome X open reading frame 15 ortholog, transcript variant 3 (HXCXORF15), mRNA	0.02060	-2.58
NM_001040471.1	Bos taurus glucose phosphate isomerase (GPI), mRNA	0.00658	-2.51
XM_864691.3	PREDICTED: Bos taurus similar to cytoplasmic polyadenylation element binding protein 1, transcript variant 2 (CPEB1), mRNA	0.01679	-2.97
NM_001024488.2	Bos taurus solute carrier family 3 (activators of dibasic and neutral amino acid transport), member 2 (SLC3A2), mRNA	0.04640	-3.27
NM_001075681.1	Bos taurus coiled-coil domain containing 107 (CCDC107), mRNA	0.04065	-2.68

NM_001102306.1	Bos taurus eukaryotic translation initiation factor 4E family member 3 (EIF4E3), mRNA	0.01196	-3.27
NM_001046333.1	Bos taurus calcium/calmodulin-dependent protein kinase II delta (CAMK2D), mRNA	0.01793	-3.27
NM_001035302.1	Bos taurus ARV1 homolog (S. cerevisiae) (ARV1), mRNA	0.04777	-2.55
XM_867976.2	PREDICTED: Bos taurus similar to ankyrin repeat and sterile alpha motif domain containing 3, transcript variant 2 (ANKS3), mRNA	0.03831	-2.55
XM_864973.3	PREDICTED: Bos taurus SLAM family member 9 (SLAMF9), mRNA	0.00261	-2.04
NM_001034606.1	Bos taurus syntaxin 17 (STX17), mRNA	0.04349	-2.40
XM_593410.4	PREDICTED: Bos taurus similar to LKB1 interacting protein (STK11IP), mRNA	0.01437	-3.66
NM_001034784.1	Bos taurus fission 1 (mitochondrial outer membrane) homolog (S. cerevisiae) (FIS1), nuclear gene encoding mitochondrial protein, mRNA	0.03793	-2.09
XM_001790641.1	PREDICTED: Bos taurus dishevelled, dsh homolog 2 (Drosophila) (DVL2), mRNA	0.03482	-2.86
XM_586727.4	PREDICTED: Bos taurus similar to zinc finger protein 74 (ZNF74), mRNA	0.02021	-2.25
NM_001045945.1	Bos taurus RCAN family member 3 (RCAN3), mRNA	0.01413	-2.57
NM_001102266.1	Bos taurus A kinase (PRKA) anchor protein 7 (AKAP7), mRNA	0.03703	-2.36
NM_001034670.1	Bos taurus anterior pharynx defective 1 homolog A (C. elegans) (APH1A), mRNA	0.03605	-2.22
XM_001251118.1	PREDICTED: Bos taurus similar to dynamin binding protein (DNMBP), mRNA	0.04047	-2.13
NM_001046376.1	Bos taurus ubiquitin specific peptidase 21 (USP21), mRNA	0.02988	-2.15
XM_614921.4	PREDICTED: Bos taurus similar to 60S ribosomal protein L26-like 1, transcript variant 1 (RPL26L1), mRNA	0.01993	-2.05
XM_600364.4	PREDICTED: Bos taurus similar to additional sex combs like 1 (ASXL1), mRNA	0.03269	-2.19
NM_001083407.1	Bos taurus spermatogenesis associated 20 (SPATA20), mRNA	0.03165	-2.28

Appendix Table 4: Transcripts that were differentially expressed in ECb vs. ECe

(*positive values for fold-change indicate that expression is greater in ECb)

Bovine RefSeq_ID	Bovine RefSeq_Description	P value	Fold change*
XM_612798.4	PREDICTED: Bos taurus similar to protein inhibitor of activated STAT X, transcript variant 1 (PIAS2), mRNA	0.00247	25.00
XM_588088.4	PREDICTED: Bos taurus similar to delangin (NIPBL), mRNA	0.03253	20.00
XM_001250465.1	PREDICTED: Bos taurus similar to ubiquitin specific peptidase 54 (LOC784739), mRNA	0.01715	16.67
NM_174345.3	Bos taurus heat shock 70kDa protein 8 (HSPA8), mRNA	0.00069	16.67
NM_001034039.1	Bos taurus collagen, type I, alpha 1 (COL1A1), mRNA	0.00135	16.67
XM_001788124.1	PREDICTED: Bos taurus similar to cleavage stimulation factor subunit 3 (LOC613678), mRNA	0.00230	16.67
XR_028410.2	PREDICTED: Bos taurus misc_RNA (LOC614926), miscRNA	0.00291	16.67
XM_582135.4	PREDICTED: Bos taurus neurofilament, medium polypeptide (NEF3), mRNA	0.01724	14.28
NM_174715.1	Bos taurus ribosomal protein L3 (Rpl3), mRNA	0.00002	14.28
XR_028569.2	PREDICTED: Bos taurus misc_RNA (LOC535649), miscRNA	0.00318	14.28
NM_001035014.1	Bos taurus ribosomal protein L23 (RPL23), mRNA	0.02095	12.50
NM_176645.3	Bos taurus ras homolog gene family, member A (RHOA), mRNA	0.00002	12.50
NR_001464.2	Bos taurus X (inactive)-specific transcript (XIST), non-coding RNA	0.02390	12.50
NM_174464.2	Bos taurus secreted protein, acidic, cysteine-rich (osteonectin) (SPARC), mRNA	0.02412	12.50
NM_001105045.1	Bos taurus neuronal protein 3.1 (LOC100125763), mRNA	0.01061	12.50
XM_001255132.1	PREDICTED: Bos taurus similar to ribosomal protein S6-like (LOC787914), mRNA	0.00373	11.11
NM_174568.2	Bos taurus poly(A) binding protein, cytoplasmic 1 (PABPC1), mRNA	0.02252	11.11
NM_001034039.1	Bos taurus collagen, type I, alpha 1 (COL1A1), mRNA	0.00790	11.11

NM_174780.3	Bos taurus brain abundant, membrane attached signal protein 1 (BASP1), mRNA	0.03227	11.11
XM_589161.4	PREDICTED: Bos taurus synaptotagmin binding, cytoplasmic RNA interacting protein (SYNCRIP), mRNA	0.01538	11.11
XM_001250700.1	PREDICTED: Bos taurus similar to Serine/threonine-protein phosphatase 2A 55 kDa regulatory subunit B gamma isoform (PP2A, subunit B, B-gamma isoform) (PP2A, subunit B, B55-gamma isoform) (PP2A, subunit B, PR55-gamma isoform) (PP2A, subunit B, R2-gamma isoform) (IMYPNO1) (PPP2R2C), mRNA	0.02041	10.00
XM_001255541.2	PREDICTED: Bos taurus similar to metastasis suppressor 1 (LOC788499), mRNA	0.04351	10.00
XR_028031.2	PREDICTED: Bos taurus misc_RNA (LOC536267), miscRNA	0.01138	10.00
NM_001012670.1	Bos taurus heat shock 90kD protein 1, alpha (HSPCA), mRNA	0.00861	9.00
NM_001046347.1	Bos taurus RAB3A interacting protein (rabin3) (RAB3IP), mRNA	0.04279	9.00
NM_174464.2	Bos taurus secreted protein, acidic, cysteine-rich (osteonectin) (SPARC), mRNA	0.03973	9.00
NM_174062.3	Bos taurus ferritin, heavy polypeptide 1 (FTH1), mRNA	0.04736	9.00
NM_001101886.1	Bos taurus DEAD (Asp-Glu-Ala-Asp) box polypeptide 31 (DDX31), mRNA	0.00165	8.33
XM_582135.4	PREDICTED: Bos taurus neurofilament, medium polypeptide (NEF3), mRNA	0.04293	8.33
NM_001111103.1	Bos taurus polymerase I and transcript release factor (PTRF), transcript variant 2, mRNA	0.02888	8.33
NM_001034500.1	Bos taurus emopamil binding protein (sterol isomerase) (EBP), mRNA	0.00682	8.33
NM_174386.2	Bos taurus microfibrillar associated protein 5 (MFAP5), mRNA	0.00176	8.33
NM_174053.1	Bos taurus fibrillin 1 (FBN1), mRNA	0.00607	7.69
NM_001080347.1	Bos taurus hypothetical protein LOC783068 (MGC151567), mRNA	0.01231	7.69
NM_174815.2	Bos taurus Y box binding protein 1 (YBX1), mRNA	0.02221	7.69
NM_174333.3	Bos taurus protein disulfide isomerase family A, member 3 (PDIA3), mRNA	0.01194	7.69

XM_598984.4	PREDICTED: Bos taurus similar to Mediator of RNA polymerase II transcription subunit 1 (Mediator complex subunit 1) (Peroxisome proliferator-activated receptor-binding protein) (PBP) (PPAR-binding protein) (Thyroid hormone receptor-associated protein complex 220 kDa com, transcript variant 1 (MED1), mRNA	0.00075	7.14
NM_001034039.1	Bos taurus collagen, type I, alpha 1 (COL1A1), mRNA	0.01894	7.14
NM_001035497.1	Bos taurus ubiquitin-conjugating enzyme E2 variant 1 (UBE2V1), mRNA	0.00758	7.14
NM_001035306.1	Bos taurus ribosomal protein L5 (RPL5), mRNA	0.00458	7.14
NM_001025339.1	Bos taurus ribosomal protein S24 (RPS24), mRNA	0.01487	7.14
XM_001252331.1	PREDICTED: Bos taurus similar to serine/arginine repetitive matrix 1, transcript variant 1 (SRRM1), mRNA	0.02549	7.14
NM_001076067.1	Bos taurus proteasome (prosome, macropain) 26S subunit, non-ATPase, 14 (PSMD14), mRNA	0.04760	6.66
NM_001101162.1	Bos taurus hypothetical LOC535277 (LOC535277), mRNA	0.00887	6.66
NM_001098006.1	Bos taurus BUD13 homolog (S. cerevisiae) (BUD13), mRNA	0.00653	6.66
NM_001083466.1	Bos taurus heterogeneous nuclear ribonucleoprotein U-like 1 (HNRNPUL1), mRNA	0.00492	6.66
XR_027885.2	PREDICTED: Bos taurus misc_RNA (LOC613460), miscRNA	0.01760	6.66
NM_001079637.1	Bos taurus heat shock 90kDa protein 1, beta (HSP90AB1), mRNA	0.00413	6.25
NM_001075515.1	Bos taurus 5'-nucleotidase, cytosolic III-like (NT5C3L), mRNA	0.00166	6.25
NM_174464.2	Bos taurus secreted protein, acidic, cysteine-rich (osteonectin) (SPARC), mRNA	0.01074	6.25
NM_001114192.1	Bos taurus heat shock 70kDa protein 4 (HSPA4), mRNA	0.00451	5.88
NM_174663.2	Bos taurus platelet-activating factor acetylhydrolase, isoform Ib, alpha subunit 45kDa (PAFAH1B1), mRNA	0.00093	5.88
NM_001014388.1	Bos taurus tumor protein, translationally-controlled 1 (TPT1), mRNA	0.00153	5.88
NM_001037468.1	Bos taurus cell division cycle 7 homolog (S. cerevisiae) (CDC7), mRNA	0.03038	5.88
XM_883110.3	PREDICTED: Bos taurus similar to Histone H3.3B CG8989-PA, transcript variant 4	0.01938	5.88

	(H3F3B), mRNA		
NM_001038558.1	Bos taurus cell adhesion molecule 1 (CADM1), mRNA	0.00104	5.88
NM_001015533.1	Bos taurus signal sequence receptor, beta (translocon-associated protein beta) (SSR2), mRNA	0.01524	5.88
NM_001034614.1	Bos taurus BCL2/adenovirus E1B 19kDa interacting protein 3-like (BNIP3L), mRNA	0.00843	5.55
NM_001007806.2	Bos taurus prostaglandin E synthase 3 (cytosolic) (PTGES3), mRNA	0.02171	5.55
NM_001014388.1	Bos taurus tumor protein, translationally-controlled 1 (TPT1), mRNA	0.01722	5.55
NM_174087.3	Bos taurus insulin-like growth factor 2 (somatomedin A) (IGF2), mRNA	0.00028	5.55
XR_027849.2	PREDICTED: Bos taurus misc_RNA (LOC538561), miscRNA	0.03222	5.55
NM_001015522.1	Bos taurus vacuolar protein sorting 16 homolog (S. cerevisiae) (VPS16), mRNA	0.01103	5.55
NM_001076831.1	Bos taurus collagen, type III, alpha 1 (COL3A1), mRNA	0.04352	5.26
XM_602857.3	PREDICTED: Bos taurus similar to ubiquitin specific protease 25 (USP25), mRNA	0.02442	5.26
XM_867454.3	PREDICTED: Bos taurus similar to transmembrane anterior posterior transformation 1 (TAPT1), mRNA	0.00546	5.26
NM_001080301.1	Bos taurus LUC7-like (S. cerevisiae) (LUC7L), mRNA	0.01602	5.26
XM_614281.4	PREDICTED: Bos taurus similar to Probable E3 ubiquitin-protein ligase MYCBP2 (Myc-binding protein 2) (Protein associated with Myc) (Pam/highwire/rpm-1 protein) (MYCBP2), mRNA	0.04158	5.26
NM_001101931.1	Bos taurus hypothetical protein LOC510660 (LOC510660), mRNA	0.01724	5.00
XM_879644.2	PREDICTED: Bos taurus RNA binding motif protein 25, transcript variant 5 (RBM25), mRNA	0.03258	5.00
NM_174062.3	Bos taurus ferritin, heavy polypeptide 1 (FTH1), mRNA	0.03393	5.00
NM_001077928.1	Bos taurus plexin domain containing 2 (PLXDC2), mRNA	0.03094	4.76
XM_589795.4	PREDICTED: Bos taurus similar to coiled-coil domain containing 15 (CCDC15), mRNA	0.04905	4.76
NM_001075436.1	Bos taurus heterochromatin protein 1, binding protein 3 (HP1BP3), mRNA	0.03309	4.76

XM_867461.3	PREDICTED: Bos taurus similar to ubiquitin-conjugating enzyme E2E 1, transcript variant 2 (UBE2E1), mRNA	0.00409	4.76
XM_590860.4	PREDICTED: Bos taurus similar to zinc finger, CCHC domain containing 6, transcript variant 1 (ZCCHC6), mRNA	0.00807	4.76
NM_174763.2	Bos taurus peroxiredoxin 2 (PRDX2), nuclear gene encoding mitochondrial protein, mRNA	0.01602	4.54
XM_609842.3	PREDICTED: Bos taurus similar to BTB and CNC homology 1 (BACH1), mRNA	0.00056	4.54
NM_001075788.1	Bos taurus damage-specific DNA binding protein 2, 48kDa (DDB2), mRNA	0.00302	4.54
NM_001081510.1	Bos taurus splicing factor 3a, subunit 1, 120kDa (SF3A1), mRNA	0.03436	4.54
NM_001075649.1	Bos taurus N-acetyltransferase 15 (GCN5-related, putative) (NAT15), mRNA	0.00341	4.54
XR_028633.2	PREDICTED: Bos taurus misc_RNA (LOC788293), miscRNA	0.04815	4.54
XM_001254709.2	PREDICTED: Bos taurus similar to topoisomerase (DNA) II beta 180kDa (TOP2B), mRNA	0.01366	4.34
NM_001075402.1	Bos taurus TatD DNase domain containing 1 (TATDN1), mRNA	0.02649	4.34
XM_001249987.2	PREDICTED: Bos taurus similar to eukaryotic translation elongation factor 1 alpha 1, transcript variant 1 (EEF1A1), mRNA	0.00999	4.34
NM_001040487.1	Bos taurus eukaryotic translation elongation factor 1 gamma (EEF1G), mRNA	0.04782	4.34
XM_867149.3	PREDICTED: Bos taurus similar to Poly [ADP-ribose] polymerase 4 (PARP-4) (Vault poly(ADP-ribose) polymerase) (VPARP) (193 kDa vault protein) (PARP-related/IalphaI-related H5/proline-rich) (PH5P) (PARP4), mRNA	0.01237	4.34
XM_597007.4	PREDICTED: Bos taurus similar to F-box/LRR-repeat protein 7 (F-box and leucine-rich repeat protein 7) (F-box protein FBL6/FBL7) (FBXL7), mRNA	0.02811	4.34
NM_001037468.1	Bos taurus cell division cycle 7 homolog (S. cerevisiae) (CDC7), mRNA	0.03266	4.16
XM_592234.3	PREDICTED: Bos taurus similar to nuclear receptor binding SET domain protein 1 (NSD1), partial mRNA	0.00032	4.16
NM_001045883.1	Bos taurus 3-hydroxy-3-methylglutaryl-Coenzyme A synthase 2 (mitochondrial) (HMGCS2), nuclear gene encoding mitochondrial protein, mRNA	0.03160	4.16

XM_001250706.2	PREDICTED: Bos taurus similar to 60S ribosomal protein L9, transcript variant 1 (LOC782631), mRNA	0.01374	4.16
XM_001249528.2	PREDICTED: Bos taurus similar to Histone H3.3B CG8989-PA (LOC781224), mRNA	0.04295	4.16
NM_001033762.1	Bos taurus GDP dissociation inhibitor 2 (GDI2), mRNA	0.01586	4.16
NM_001035008.1	Bos taurus ribosomal protein L37a (RPL37A), mRNA	0.02059	4.16
NM_001101933.1	Bos taurus TSR1, 20S rRNA accumulation, homolog (S. cerevisiae) (TSR1), mRNA	0.01696	4.16
NM_001034484.1	Bos taurus eukaryotic translation initiation factor 3, subunit D (EIF3D), mRNA	0.00217	4.16
XR_027807.2	PREDICTED: Bos taurus misc_RNA (LOC614207), miscRNA	0.00606	4.16
NM_174004.3	Bos taurus caveolin 1, caveolae protein, 22kDa (CAV1), mRNA	0.00648	4.16
XM_865029.3	PREDICTED: Bos taurus similar to splicing factor 3b, subunit 1, transcript variant 2 (SF3B1), mRNA	0.00144	4.00
NM_001024535.1	Bos taurus KIAA0141 protein (KIAA0141), mRNA	0.04788	4.00
XM_001250706.2	PREDICTED: Bos taurus similar to 60S ribosomal protein L9, transcript variant 1 (LOC782631), mRNA	0.01001	4.00
NM_001015533.1	Bos taurus signal sequence receptor, beta (translocon-associated protein beta) (SSR2), mRNA	0.04078	4.00
NM_205799.1	Bos taurus lysosomal protein transmembrane 4 alpha (LAPTM4A), mRNA	0.01650	4.00
XM_602832.4	PREDICTED: Bos taurus similar to ribosomal protein S19 (LOC524507), mRNA	0.02472	4.00
NM_001098874.1	Bos taurus ribosomal protein S7 (RPS7), mRNA	0.03551	4.00
XM_864796.3	PREDICTED: Bos taurus adenylosuccinate synthase, transcript variant 3 (ADSS), mRNA	0.00346	3.84
NM_001105374.1	Bos taurus protein arginine methyltransferase 5 (PRMT5), mRNA	0.02074	3.84
NM_001046454.1	Bos taurus casein kinase 2, beta polypeptide (CSNK2B), mRNA	0.04487	3.84
NM_001083725.1	Bos taurus heterogeneous nuclear ribonucleoprotein D-like (HNRPDL), mRNA	0.02938	3.84
XM_001249610.1	PREDICTED: Bos taurus similar to mitogen-activated protein kinase kinase kinase kinase 5, transcript variant 1 (MAP4K5), mRNA	0.00753	3.84
XM_867454.3	PREDICTED: Bos taurus similar to transmembrane anterior posterior transformation	0.03659	3.84

	1 (TAPT1), mRNA		
XM_606667.4	PREDICTED: Bos taurus similar to jumonji, AT rich interactive domain 2 protein, transcript variant 6 (JARID2), mRNA	0.04826	3.84
NM_001083515.1	Bos taurus transmembrane protein 87A (TMEM87A), mRNA	0.00219	3.84
NM_001075294.1	Bos taurus chromosome 20 open reading frame 149 ortholog (C13H20orf149), mRNA	0.03967	3.84
NM_001035008.1	Bos taurus ribosomal protein L37a (RPL37A), mRNA	0.01029	3.70
NM_001076070.1	Bos taurus 3-oxoacid CoA transferase 1 (OXCT1), nuclear gene encoding mitochondrial protein, mRNA	0.01278	3.70
NM_001035445.1	Bos taurus ribosomal protein S4, Y-linked 2 (RPS4Y2), mRNA	0.01743	3.70
XM_589329.4	PREDICTED: Bos taurus similar to Chromosome 7 open reading frame 43 (LOC511902), mRNA	0.03715	3.57
NM_001101231.1	Bos taurus splicing factor, arginine/serine-rich 4 (SFRS4), mRNA	0.01625	3.57
NM_001081587.1	Bos taurus ring finger protein 20 (RNF20), mRNA	0.01993	3.57
NM_174788.3	Bos taurus ribosomal protein, large, P2 (RPLP2), mRNA	0.01368	3.57
XM_616885.4	PREDICTED: Bos taurus similar to membrane metallo endopeptidase (MME), mRNA	0.02783	3.44
XM_869402.2	PREDICTED: Bos taurus similar to MYST histone acetyltransferase (monocytic leukemia) 3 (LOC529373), mRNA	0.02918	3.44
NM_001079777.1	Bos taurus hypothetical protein LOC526597 (LOC526597), mRNA	0.02754	3.44
NM_001017950.2	Bos taurus follistatin-like 1 (FSTL1), mRNA	0.01569	3.44
NM_001046526.1	Bos taurus methionine adenosyltransferase II, beta (MAT2B), mRNA	0.02552	3.44
NM_001078043.1	Bos taurus zinc finger protein 75 (D8C6) (ZNF75), mRNA	0.04206	3.44
NM_001076448.1	Bos taurus similar to HEAT repeat containing protein 1 (Protein BAP28) (LOC617204), mRNA	0.02203	3.33
NM_001012673.1	Bos taurus signal transducer and activator of transcription 5A (STAT5A), mRNA	0.00350	3.33
NM_001037595.1	Bos taurus tetraspanin 31 (TSPAN31), mRNA	0.02073	3.33
XR_042784.1	PREDICTED: Bos taurus misc_RNA (LOC100141269), miscRNA	0.01680	3.33
NM_001034294.1	Bos taurus valosin-containing protein (VCP),	0.00064	3.33

	mRNA		
NM_001014928.1	Bos taurus ribosomal protein L7 (RPL7), mRNA	0.04903	3.33
NM_001034502.1	Bos taurus actin, alpha 2, smooth muscle, aorta (ACTA2), mRNA	0.00339	3.33
XM_594391.4	PREDICTED: Bos taurus similar to G-protein signaling modulator 3 (AGS3-like, C. elegans) (GPSM3), mRNA	0.04637	3.22
NM_001015533.1	Bos taurus signal sequence receptor, beta (translocon-associated protein beta) (SSR2), mRNA	0.01268	3.22
NM_001015608.1	Bos taurus chloride intracellular channel 1 (CLIC1), mRNA	0.02809	3.22
NM_001105629.1	Bos taurus transmembrane and tetratricopeptide repeat containing 4 (TMTC4), mRNA	0.00638	3.22
NM_001025339.1	Bos taurus ribosomal protein S24 (RPS24), mRNA	0.04503	3.22
NM_001076831.1	Bos taurus collagen, type III, alpha 1 (COL3A1), mRNA	0.02176	3.22
XM_870555.3	PREDICTED: Bos taurus similar to Splicing factor, proline- and glutamine-rich (Polypyrimidine tract-binding protein-associated-splicing factor) (PTB-associated-splicing factor) (PSF) (DNA-binding p52/p100 complex, 100 kDa subunit) (100 kDa DNA-pairing protein) (hPOMp100 (SFPQ), mRNA	0.02566	3.22
NM_001035280.1	Bos taurus chromosome 14 open reading frame 166 ortholog (C10H14ORF166), mRNA	0.01719	3.12
XM_874550.3	PREDICTED: Bos taurus ubiquitin C, transcript variant 12 (UBC), mRNA	0.03275	3.12
NM_001076000.1	Bos taurus dihydropyrimidinase-like 2 (DPYSL2), mRNA	0.00757	3.12
NM_001034666.1	Bos taurus AHA1, activator of heat shock 90kDa protein ATPase homolog 1 (yeast) (AHSA1), mRNA	0.04169	3.12
NM_001077114.1	Bos taurus HIG1 domain family, member 1D (HIGD1D), mRNA	0.00319	3.12
NM_001034335.1	Bos taurus KIAA0174 (KIAA0174), mRNA	0.01399	3.12
XM_588094.4	PREDICTED: Bos taurus spectrin, beta, non-erythrocytic 1, transcript variant 1 (SPTBN1), mRNA	0.03598	3.12
XM_001251796.1	PREDICTED: Bos taurus similar to Zinc finger X-linked protein ZXDB (LOC783265), mRNA	0.00169	3.12
XM_882704.3	PREDICTED: Bos taurus hypothetical LOC617275 (CCDC72), mRNA	0.00325	3.00
NM_001034502.1	Bos taurus actin, alpha 2, smooth muscle, aorta (ACTA2), mRNA	0.01898	3.00

NM_001034746.1	Bos taurus coiled-coil-helix-coiled-coil-helix domain containing 9 (CHCHD9), mRNA	0.03301	3.00
NM_001046593.1	Bos taurus coactosin-like 1 (Dictyostelium) (COTL1), mRNA	0.03799	3.00
NM_001034222.1	Bos taurus nucleoporin 88kDa (NUP88), mRNA	0.02062	3.00
XM_600663.4	PREDICTED: Bos taurus nestin (NES), mRNA	0.01881	3.00
XM_001788124.1	PREDICTED: Bos taurus similar to cleavage stimulation factor subunit 3 (LOC613678), mRNA	0.00864	3.00
NM_174368.2	Bos taurus integrin, beta 1 (fibronectin receptor, beta polypeptide, antigen CD29 includes MDF2, MSK12) (ITGB1), mRNA	0.02471	3.00
XM_605970.4	PREDICTED: Bos taurus similar to tripartite motif protein TRIM4, transcript variant 1 (TRIM4), partial mRNA	0.00422	2.94
NM_174591.1	Bos taurus RAB guanine nucleotide exchange factor (GEF) 1 (RABGEF1), mRNA	0.00449	2.94
NM_001034373.1	Bos taurus cytochrome P450, family 4, subfamily V, polypeptide 2 (CYP4V2), mRNA	0.00741	2.94
NM_001099206.1	Bos taurus myeloid cell leukemia sequence 1 (BCL2-related) (MCL1), mRNA	0.04033	2.94
NM_001098070.1	Bos taurus O-linked N-acetylglucosamine (GlcNAc) transferase (UDP-N-acetylglucosamine:polypeptide-N-acetylglucosaminyl transferase) (OGT), mRNA	0.03993	2.94
XM_001788858.1	PREDICTED: Bos taurus centrosomal protein 170kDa (CEP170), mRNA	0.03040	2.94
XM_615128.3	PREDICTED: Bos taurus similar to Myosin-VI (Unconventional myosin VI) (MYO6), mRNA	0.00205	2.94
NM_174310.3	Bos taurus eukaryotic translation initiation factor 4E (EIF4E), mRNA	0.00111	2.85
NM_001105474.1	Bos taurus prenylcysteine oxidase 1 (PCYOX1), mRNA	0.02639	2.85
NM_174133.2	Bos taurus polyubiquitin (LOC281370), mRNA	0.00251	2.85
NM_001080738.1	Bos taurus leucine-rich repeats and calponin homology (CH) domain containing 4 (LRCH4), mRNA	0.02023	2.85
XM_864796.3	PREDICTED: Bos taurus adenylosuccinate synthase, transcript variant 3 (ADSS), mRNA	0.03269	2.85
XM_585215.4	PREDICTED: Bos taurus similar to CG2943 CG2943-PA (LOC508439), mRNA	0.04330	2.85
NM_001075135.1	Bos taurus similar to Putative ubiquitin-conjugating enzyme E2 D3-like protein (UBE2D3P), mRNA	0.00318	2.85
NM_001077113.1	Bos taurus chromosome 6 open reading frame 130 ortholog (C23H6orf130), mRNA	0.00627	2.77

XR_042605.1	PREDICTED: Bos taurus misc_RNA (CSF2RA), miscRNA	0.02525	2.77
NM_001034277.1	Bos taurus splicing factor, arginine/serine-rich 7, 35kDa (SFRS7), mRNA	0.02041	2.77
XM_584927.4	PREDICTED: Bos taurus SLAM family member 6 (SLAMF6), mRNA	0.03793	2.77
XM_879302.3	PREDICTED: Bos taurus eukaryotic translation initiation factor 3, subunit A, transcript variant 4 (EIF3A), mRNA	0.04119	2.77
NM_174019.2	Bos taurus chondroadherin (CHAD), mRNA	0.03660	2.77
NM_001102122.1	Bos taurus signal sequence receptor, alpha (SSR1), mRNA	0.03922	2.70
NM_001098982.1	Bos taurus coiled-coil domain containing 80 (CCDC80), mRNA	0.03248	2.70
XR_027685.2	PREDICTED: Bos taurus misc_RNA (LOC540561), miscRNA	0.04354	2.70
NM_001099133.1	Bos taurus lactamase, beta (LACTB), nuclear gene encoding mitochondrial protein, mRNA	0.01701	2.70
NM_001083792.1	Bos taurus tetratricopeptide repeat domain 9C (TTC9C), mRNA	0.00364	2.63
NM_001015567.2	Bos taurus serine/threonine kinase receptor associated protein (STRAP), mRNA	0.00971	2.63
NM_001033624.1	Bos taurus ribosomal protein S16 (RPS16), mRNA	0.02779	2.63
NM_001076970.1	Bos taurus G protein-coupled receptor 89 (GPR89), mRNA	0.04322	2.63
XM_582017.4	PREDICTED: Bos taurus similar to la related protein (LARP1), mRNA	0.03818	2.63
NM_001035428.1	Bos taurus coiled-coil domain containing 47 (CCDC47), mRNA	0.00910	2.63
NM_001098956.1	Bos taurus sorting nexin family member 27 (SNX27), mRNA	0.03458	2.56
NM_001113727.1	Bos taurus cationic trypsin (LOC780933), mRNA	0.04485	2.56
XM_615298.4	PREDICTED: Bos taurus similar to Exportin-T (tRNA exportin) (Exportin(tRNA)) (XPOT), mRNA	0.01987	2.56
XM_866612.3	PREDICTED: Bos taurus similar to Rab5B, transcript variant 3 (RAB5B), mRNA	0.01137	2.56
NM_001045878.1	Bos taurus glycine amidinotransferase (L-arginine:glycine amidinotransferase) (GATM), nuclear gene encoding mitochondrial protein, mRNA	0.02772	2.56
NM_174244.1	Bos taurus ATP synthase, H+ transporting, mitochondrial F1 complex, O subunit (ATP5O), nuclear gene encoding mitochondrial protein,	0.02371	2.56

	mRNA		
XM_866403.3	PREDICTED: Bos taurus homeobox and leucine zipper encoding, transcript variant 1 (HOMEZ), mRNA	0.01811	2.56
NM_001014389.2	Bos taurus H3 histone, family 3A (H3F3A), mRNA	0.01167	2.50
XM_869563.3	PREDICTED: Bos taurus similar to karyopherin beta 1, transcript variant 2 (KPNB1), mRNA	0.01118	2.50
NM_174663.2	Bos taurus platelet-activating factor acetylhydrolase, isoform Ib, alpha subunit 45kDa (PAFAH1B1), mRNA	0.01787	2.50
XR_042975.1	PREDICTED: Bos taurus misc_RNA (LOC784058), miscRNA	0.04409	2.50
XM_597797.4	PREDICTED: Bos taurus similar to PDZ domain containing 8 (PDZD8), mRNA	0.02648	2.50
NM_001103278.1	Bos taurus splicing factor 4 (SF4), mRNA	0.02864	2.50
XM_001251494.2	PREDICTED: Bos taurus similar to Protein jagged-1 precursor (Jagged1) (hJ1) (CD339 antigen) (JAG1), mRNA	0.00193	2.50
NM_001081727.1	Bos taurus chloride intracellular channel 2 (CLIC2), mRNA	0.02756	2.50
NM_001076867.1	Bos taurus ubiquitin specific peptidase 16 (USP16), mRNA	0.02283	2.41
XM_001254235.2	PREDICTED: Bos taurus similar to Tubulin, alpha 1, transcript variant 1 (LOC787568), mRNA	0.02604	2.41
NM_001098131.1	Bos taurus ribosomal protein L22-like 1 (RPL22L1), mRNA	0.04917	2.41
NM_001102531.1	Bos taurus RAP2B, member of RAS oncogene family (RAP2B), mRNA	0.01492	2.41
XM_584555.4	PREDICTED: Bos taurus similar to nuclear pore complex-associated protein TPR, transcript variant 1 (TPR), mRNA	0.04555	2.41
XM_580963.3	PREDICTED: Bos taurus similar to TBP-associated factor 1 (TAF1), mRNA	0.01076	2.41
NM_001034398.1	Bos taurus solute carrier family 29 (nucleoside transporters), member 1 (SLC29A1), nuclear gene encoding mitochondrial protein, mRNA	0.04353	2.41
NM_001075121.1	Bos taurus eukaryotic translation elongation factor 2 (EEF2), mRNA	0.01478	2.41
NM_001046594.1	Bos taurus pituitary tumor-transforming 1 interacting protein (PTTG1IP), mRNA	0.01913	2.41

XM_864599.3	PREDICTED: Bos taurus similar to splicing factor, arginine/serine-rich 12, transcript variant 2 (SFRS12), mRNA	0.00418	2.41
NM_001034528.1	Bos taurus transmembrane protein 86B (TMEM86B), mRNA	0.04554	2.38
XM_001249420.1	PREDICTED: Bos taurus similar to jumonji domain containing 1C, transcript variant 2 (JMJD1C), mRNA	0.02585	2.38
XM_001250793.2	PREDICTED: Bos taurus similar to small nuclear ribonucleoprotein polypeptide G (SNRPG), mRNA	0.04243	2.38
NM_001100319.1	Bos taurus ubiquitin specific peptidase 4 (proto-oncogene) (USP4), mRNA	0.03189	2.38
NM_001034504.1	Bos taurus high mobility group nucleosomal binding domain 3 (HMGN3), mRNA	0.01764	2.38
NM_001076219.1	Bos taurus Yip1 domain family, member 3 (YIPF3), mRNA	0.03889	2.32
NM_001076104.1	Bos taurus nuclear factor I/B (NFIB), mRNA	0.00833	2.32
NM_001101198.1	Bos taurus chromobox homolog 3 (HP1 gamma homolog, Drosophila) (CBX3), mRNA	0.02541	2.32
NM_174778.1	Bos taurus ribosomal protein S27a (RPS27A), mRNA	0.02806	2.32
XM_617685.4	PREDICTED: Bos taurus similar to tousled-like kinase 1 (TLK1), mRNA	0.02889	2.32
NM_001038647.1	Bos taurus transmembrane protein 57 (TMEM57), mRNA	0.00809	2.27
NM_001037142.1	Bos taurus catenin, beta interacting protein 1 (CTNNBIP1), mRNA	0.04481	2.27
NM_001034674.1	Bos taurus ribosomal protein L14 (RPL14), mRNA	0.01643	2.27
NM_205799.1	Bos taurus lysosomal protein transmembrane 4 alpha (LAPTM4A), mRNA	0.03764	2.27
NM_001002883.2	Bos taurus ST3 beta-galactoside alpha-2,3-sialyltransferase 6 (ST3GAL6), mRNA	0.03361	2.27
XM_001788161.1	PREDICTED: Bos taurus similar to putative utrophin (LOC534358), mRNA	0.00966	2.22
XM_865008.3	PREDICTED: Bos taurus similar to Protein LAP2 (Erbb2-interacting protein) (Erbin) (Densin-180-like protein), transcript variant 3 (ERBB2IP), mRNA	0.00857	2.17
XM_594174.3	PREDICTED: Bos taurus NOL1/NOP2/Sun domain family, member 2 (NSUN2), mRNA	0.01622	2.12
XM_590469.4	PREDICTED: Bos taurus similar to RAS protein activator like 1 (GAP1 like) (RASAL1), mRNA	0.01531	2.12

XM_591153.4	PREDICTED: Bos taurus similar to pleckstrin homology domain containing, family B (evectins) member 2 (LOC513469), mRNA	0.02690	2.12
NM_001046142.1	Bos taurus general transcription factor IIB (GTF2B), mRNA	0.01959	2.12
NM_001076113.1	Bos taurus ribosomal modification protein rimK-like family member B (RIMKLB), mRNA	0.01976	2.08
NM_001034360.1	Bos taurus dolichyl-phosphate mannosyltransferase polypeptide 3 (DPM3), mRNA	0.04680	2.08
NM_001099859.1	Bos taurus eukaryotic translation initiation factor 4 gamma, 2 (EIF4G2), mRNA	0.03340	2.04
NM_001034421.1	Bos taurus RAB5-interacting protein (RIP5), mRNA	0.03586	2.04
NM_001075982.1	Bos taurus MAPK scaffold protein 1 (MAPKSP1), mRNA	0.02002	2.04
XR_027860.2	PREDICTED: Bos taurus misc_RNA (LOC510487), miscRNA	0.02833	2.00
NM_001040516.1	Bos taurus ribosomal protein L19 (RPL19), mRNA	0.03902	2.00
NM_001015640.2	Bos taurus myosin regulatory light chain MRCL3 (MRCL3), mRNA	0.01077	2.00
NM_001075983.1	Bos taurus matrix metallopeptidase 19 (MMP19), mRNA	0.00020	-2.12
XR_028120.2	PREDICTED: Bos taurus misc_RNA (LOC518495), miscRNA	0.00054	-2.08
XM_866155.3	PREDICTED: Bos taurus similar to proline-serine-threonine phosphatase interacting protein 1, transcript variant 2 (PSTPIP1), mRNA	0.00105	-2.26
NM_001075540.1	Bos taurus hydroxyacylglutathione hydrolase-like (HAGHL), mRNA	0.00182	-2.24
NM_001035088.1	Bos taurus dehydrogenase/reductase (SDR family) member 11 (DHRS11), mRNA	0.00284	-2.02
NM_001045884.2	Bos taurus adaptor-related protein complex 1, mu 1 subunit (AP1M1), mRNA	0.00341	-2.27
XR_027682.2	PREDICTED: Bos taurus misc_RNA (LOC509550), miscRNA	0.00343	-2.06
NM_001024514.1	Bos taurus zinc finger, CCCH-type with G patch domain (ZGPAT), mRNA	0.00368	-2.18
XM_001250409.1	PREDICTED: Bos taurus similar to Eukaryotic translation initiation factor 4E type 2 (eIF4E type 2) (eIF-4E type 2) (mRNA cap-binding protein type 3) (Eukaryotic translation initiation factor 4E-like 3) (Eukaryotic translation initiation factor 4E homologous protein) (mR (EIF4E2), mRNA	0.00413	-2.70

NM_001101280.1	Bos taurus TNF receptor-associated factor 4 (TRAF4), mRNA	0.00430	-2.12
XM_864253.3	PREDICTED: Bos taurus similar to erythroid differentiation-related factor 1, transcript variant 2 (LOC534065), mRNA	0.00525	-2.61
XM_618409.4	PREDICTED: Bos taurus similar to glycine N-methyltransferase, transcript variant 1 (GNMT), mRNA	0.00530	-2.29
XM_001254499.2	PREDICTED: Bos taurus similar to NCK interacting protein with SH3 domain, transcript variant 1 (NCKIPSD), mRNA	0.00785	-2.24
XM_001253142.1	PREDICTED: Bos taurus similar to Kinase suppressor of Ras 2 (hKSR2) (LOC784995), mRNA	0.00861	-2.05
NM_001075134.1	Bos taurus glycine C-acetyltransferase (2-amino-3-ketobutyrate coenzyme A ligase) (GCAT), nuclear gene encoding mitochondrial protein, mRNA	0.00875	-2.07
NM_001080288.1	Bos taurus solute carrier family 13 (sodium-dependent dicarboxylate transporter), member 3 (SLC13A3), mRNA	0.00929	-2.00
XM_001788131.1	PREDICTED: Bos taurus similar to cytochrome P450, family 2, subfamily J (LOC100140018), mRNA	0.01023	-2.21
XM_580939.4	PREDICTED: Bos taurus similar to solute carrier family 25, member 28 (LOC538529), mRNA	0.01047	-2.42
NM_001103286.1	Bos taurus glyceronephosphate O-acyltransferase (GNPAT), mRNA	0.01157	-2.13
XM_001790246.1	PREDICTED: Bos taurus obscurin-like 1 (OBSL1), mRNA	0.01448	-2.09
NM_001075629.1	Bos taurus procollagen C-endopeptidase enhancer 2 (PCOLCE2), mRNA	0.01504	-2.46
NM_001083394.1	Bos taurus lipolysis stimulated lipoprotein receptor (LSR), mRNA	0.01515	-2.04
NM_001024487.1	Bos taurus peptidase inhibitor 16 (PI16), mRNA	0.01537	-2.11
XM_864270.2	PREDICTED: Bos taurus similar to Interferon-inducible protein (LOC613464), mRNA	0.01577	-2.20
XM_587039.3	PREDICTED: Bos taurus complement component 1, q subcomponent, C chain, transcript variant 1 (C1QC), mRNA	0.01715	-2.32
XM_001789528.1	PREDICTED: Bos taurus similar to Serine/threonine-protein kinase LMTK3 precursor (Lemur tyrosine kinase 3) (LOC100140306), partial mRNA	0.01734	-2.04
NM_001076378.1	Bos taurus aquaporin 7 (AQP7), mRNA	0.01795	-2.15

XM_618475.4	PREDICTED: Bos taurus similar to Src homology 2 domain containing adaptor protein B (SHB), mRNA	0.01810	-2.53
XM_591615.4	PREDICTED: Bos taurus similar to TBC1 domain family, member 10B, transcript variant 1 (TBC1D10B), mRNA	0.01869	-2.25
NM_001076830.1	Bos taurus Rho GTPase activating protein 10 (ARHGAP10), mRNA	0.01914	-2.18
XM_867736.3	PREDICTED: Bos taurus similar to EPB41L1 protein, transcript variant 2 (EPB41L1), mRNA	0.02015	-2.32
NM_001114976.1	Bos taurus selenoprotein N, 1 (SEPN1), mRNA	0.02158	-2.01
XM_864753.3	PREDICTED: Bos taurus similar to Potassium-transporting ATPase subunit beta (Proton pump beta chain) (Gastric H(+)/K(+) ATPase subunit beta) (gp60-90), transcript variant 1 (ATP4B), mRNA	0.02162	-2.32
NM_001102351.1	Bos taurus butyrophilin-like 2 (MHC class II associated) (BTNL2), mRNA	0.02321	-2.48
NM_001110445.1	Bos taurus Purkinje cell protein 4 like 1 (PCP4L1), mRNA	0.02385	-2.15
NM_001040486.1	Bos taurus solute carrier family 38, member 3 (SLC38A3), mRNA	0.02393	-2.03
NM_181028.2	Bos taurus cellular retinoic acid binding protein 1 (CRABP1), mRNA	0.02453	-2.66
NM_001075598.2	Bos taurus DDHD domain containing 2 (DDHD2), mRNA	0.02515	-2.58
NM_001034697.1	Bos taurus tubulin, beta 4 (TUBB4), mRNA	0.02585	-2.97
XM_617909.4	PREDICTED: Bos taurus similar to PHD finger protein 2 (PHF2), mRNA	0.02640	-2.82
XR_028567.2	PREDICTED: Bos taurus misc_RNA (LOC615842), miscRNA	0.02667	-2.17
XR_028705.2	PREDICTED: Bos taurus misc_RNA (LOC507766), miscRNA	0.02709	-2.00
NM_001143862.1	Bos taurus LSM7 homolog, U6 small nuclear RNA associated (S. cerevisiae) (LSM7), mRNA	0.02782	-2.23
NM_174251.1	Bos taurus biliverdin reductase B (flavin reductase (NADPH)) (BLVRB), mRNA	0.02817	-3.11
NM_001046021.1	Bos taurus CD1b molecule (CD1B), mRNA	0.02830	-3.04
NM_001102295.1	Bos taurus transmembrane 6 superfamily member 1 (TM6SF1), mRNA	0.02853	-2.37
NM_175808.2	Bos taurus cleavage and polyadenylation specific factor 2, 100kDa (CPSF2), mRNA	0.02982	-2.54
NM_001102212.1	Bos taurus triple functional domain (PTPRF interacting) (TRIO), mRNA	0.02988	-2.01
NM_001103183.1	Bos taurus polymerase (DNA-directed), delta interacting protein 3 (POLDIP3), mRNA	0.02993	-2.01

NM_001098972.1	Bos taurus G patch domain containing 3 (GPATCH3), mRNA	0.03019	-2.53
NM_001100337.1	Bos taurus exostoses (multiple)-like 1 (EXTL1), mRNA	0.03020	-2.19
NM_174277.2	Bos taurus clathrin, light polypeptide B (light chain B) (CLTLB), mRNA	0.03088	-2.18
NM_001114513.1	Bos taurus chromosome 10 open reading frame 116 ortholog (C28H10ORF116), mRNA	0.03138	-2.04
NM_001024549.2	Bos taurus Ras association (RalGDS/AF-6) domain family (N-terminal) member 8 (RASSF8), mRNA	0.03163	-2.46
NM_001098037.1	Bos taurus RecQ protein-like 4 (RECQL4), mRNA	0.03181	-2.05
XM_873628.2	PREDICTED: Bos taurus similar to UDP glucuronosyltransferase 2 family, polypeptide B4, transcript variant 2 (UGT2B4), mRNA	0.03263	-2.02
XM_870302.2	PREDICTED: Bos taurus similar to interleukin 21 receptor (IL21R), mRNA	0.03277	-2.36
NM_001110004.1	Bos taurus HECT, UBA and WWE domain containing 1 (HUWE1), mRNA	0.03281	-2.57
NM_001079649.1	Bos taurus cysteine-rich protein 2 (CRIP2), mRNA	0.03336	-2.08
NM_001081609.1	Bos taurus transmembrane emp24 protein transport domain containing 3 (TMED3), mRNA	0.03466	-2.56
NM_001144082.1	Bos taurus DAB2 interacting protein (DAB2IP), mRNA	0.03508	-2.38
NM_173991.2	Bos taurus apolipoprotein E (APOE), mRNA	0.03818	-2.03
NM_001102068.1	Bos taurus phosphodiesterase 7B (PDE7B), mRNA	0.03837	-2.52
XM_875593.2	PREDICTED: Bos taurus similar to chloride channel 3, transcript variant 4 (CLCN3), mRNA	0.04025	-2.01
XM_865879.2	PREDICTED: Bos taurus myosin, heavy chain 8, skeletal muscle, perinatal, transcript variant 2 (MYH8), mRNA	0.04045	-3.12
XR_027344.2	PREDICTED: Bos taurus misc_RNA (LOC781850), miscRNA	0.04137	-2.16
NM_001034792.1	Bos taurus suppressor of Ty 4 homolog 1 (S. cerevisiae) (SUPT4H1), mRNA	0.04173	-2.05
NM_001075302.1	Bos taurus heat shock 105kDa/110kDa protein 1 (HSPH1), mRNA	0.04238	-3.11
NM_001045877.1	Bos taurus bone morphogenetic protein 4 (BMP4), mRNA	0.04262	-2.26
NM_001075834.1	Bos taurus nicotinamide nucleotide adenylyltransferase 1 (NMNAT1), mRNA	0.04279	-2.20
NM_001046552.1	Bos taurus chromosome 20 open reading frame 196 ortholog (C13H20orf196), mRNA	0.04398	-2.19

NM_001083525.1	Bos taurus GTPase activating Rap/RanGAP domain-like 1 (GARNL1), mRNA	0.04535	-2.01
XM_604345.4	PREDICTED: Bos taurus matrix metallopeptidase 16 (membrane-inserted) (MMP16), mRNA	0.04552	-2.02
NM_174627.1	Bos taurus TYRO protein tyrosine kinase binding protein (TYROBP), mRNA	0.04845	-3.13
XM_588427.3	PREDICTED: Bos taurus similar to cell division cycle 2-like 5, transcript variant 3 (CDC2L5), mRNA	0.04958	-3.13
XM_871071.2	PREDICTED: Bos taurus similar to deleted in lung and esophageal cancer 1 (DLEC1), mRNA	0.04960	-2.23

Appendix Table 5. The 387 genes (partial list) enriched in LRECb vs. ECb and their general functional category.

Functional category	Genes
Cancer (75)	ABP1, ADH1C, ATP8B1, BAMBI, BRAF, CASP1, CCR4, CD33, CD3E, CD8A, CDK6, CPA4, CXCR4, DNM1L, DPYD, DRD2, EXO1, FAM134B, FAM149B1, FGF1, FGF2, FGF10, FLII, FST, FXYD3, GCH1, GRINL1A, HAVCR1, HDAC7, HIF1A, HNF4A, HPGD, HRH1, HSD17B6, IGFBP1, ISOC1, KIF20B, KLHL20, KNG1, LAMC2, LMBRD1, MAPK8, MAPT, MORC2, MRVI1, MSH6, MSMB, MYD88, NLGN1, NRIP1, NUP107, OSMR, PLAT, PLG, PPP1R3C, PPPDE1, PRKCB, PSAT1, RBM15, REV3L, RGS1, RGS4, RPS11, RTN1, SAT2, SDPR, SERPINA3, SOSTDC1, TCN1, TERF1, TNNT3, TUBE1, UBE2D1, WEE1, ZC3H13
Inflammatory disease (82)	ACTA1, AGPS, AK5, ASB7, ATP8B1, AUH, C12ORF35, C13ORF34, C1QTNF6, C1QTNF7, C9ORF150, CASP1, CCDC11, CCL8, CCR4, CD33, CD3E, CD8A, CDK6, CELA2A, COL4A3, CTNS, CXCR4, CYFIP1, DPYD, DRD2, EAF1, ESD, F5, FAM69A, FETUB, FGF2, FGF10, GBA3, GCA, GLIPR2, GLRB, HAVCR1, HDAC7, HLA-DQA2, HPGD, HRH1, JARID2, KIAA0247, KLHL20, KLRB1, KNG1, KYNU, LAMC2, LUZP2, MAGI1, MAN2A1, MAPT, MBOAT1, MYD88, NLGN1, NMT2, NR5A2, NT5C3, NUP153, OSMR, PAM, PLAT, PLEKHA2, PLG, PLXDC2, PPA1, PRKCB, PWP1, RAMP1, RSBN1, S100A12, SERPINA3, SLC25A24, SPAG1, TAOK3, TCF12, TMEM156, TUBE1, USP15, ZNF605, ZNF639
Cellular growth and proliferation (49)	AGPS, ATP5A1, BRAF, CASP1, CASR, CD33, CD3E, CD8A, CDK6, COL4A3, CRTAM, CXCR4, CYP2C9, DRD2, FGF1, FGF2, FGF10, FST, GCNT1, GNE, GRB14, HAVCR1, HDAC7, HIF1A, HNF4A, HPGD, HRH1, IGFBP1, IL22RA1, KNG1, LATS1, MAPK8, MAPT, MSMB, MYD88, MYH14, NFE2, NRIP1, NT5C3, PLAT, PLG, PRKCB, RGS4, RGS16, SIRT1, SIRT2, SYNM, TCF12, TERF1
Organism Survival (30)	ADH1C, BRAF, BRD4, CASP1, CASR, CCR4, CD3E, CD8A, CDK6, COL4A3, CXCR4, DRD2, FGF2, FLII, GCH1, HIF1A, HRH1, LTBP2, MAN2A1, MAPK8, MEF2C, MSH6, MYD88, NCAPG2, NFE2, NR5A2, PLAT, PLG, REV3L, TCF12
Cell Cycle (29)	ASPM, BRAF, BRD4, CD320, CD3E, CDK6, CKAP2, CLIP1, CSE1L, DNM1L, FGF1, FGF2, FGF10, HAVCR1, HIF1A, HPGD, JARID2, KIF20B, KNG1, LATS1, MAPK8, MYH14, PLG, PPP2R3A, PRKCB, RECQL, SIRT1, TERF1, WEE1
Post-Translational Modification (25)	CASP1, CD33, CD3E, CD8A, CDK6, CLPX, CSRP2BP, DUSP11, DUSP12, ERCC8, FGF1, FGF2, KNG1, MAPT, MTMR7, NMT2, PAM, PLAT, PPEF1, SIRT1, SIRT2, ST3GAL6, SULT1B1, UBE2D1, WWP1
Cell signaling	CASR, CCL8, CCR4, CD3E, CD8A, CXCR4, DRD2, FGF1, FGF2,

(16)	HNF4A, KNG1, MAPT, MRVI1, PLG, PRKCB, RGS1
Angiogenesis (14)	COL4A3, CXCR4, DRD2, FGF1, FGF2, FGF10, GCH1, HIF1A, KLHL20, KNG1, MEF2C, PLAT, PLG, RBM15
Cell death (9)	ALDH3B1, CASP1, CASR, MAPK8, MAPT, PKN2, RGS4, SIRT2, TCF12
Cell-to-cell signaling & adhesion (11)	COL4A3, FGF1, FGF2, KNG1, PLG, CASR, CD8A, MAN2A1, PKN2, CD3E, HAVCR1

Appendix Figure 2. IPA figure legend

Symbols and relationships depicted in IPA networks.

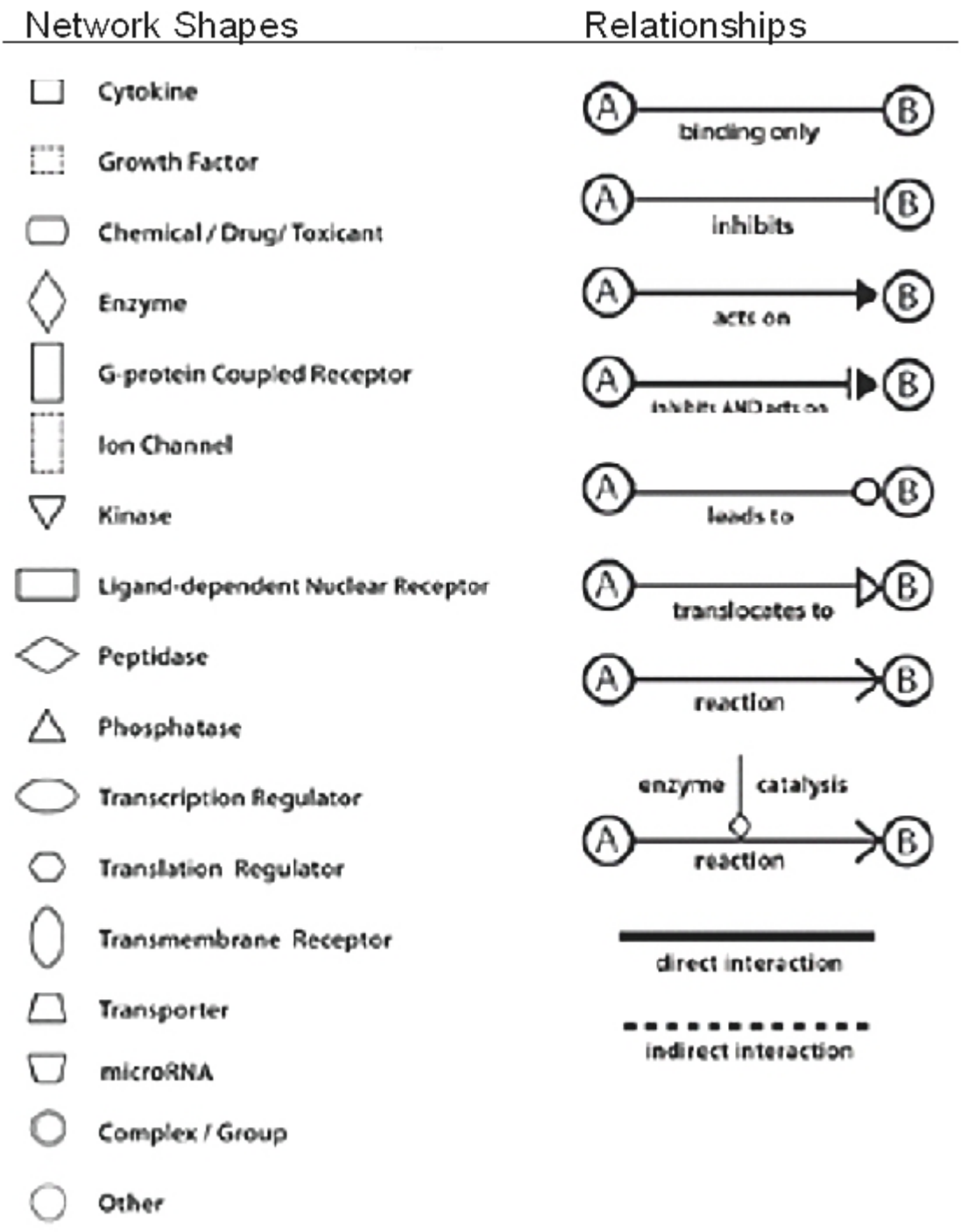

Appendix Table 6. Transcripts of cell surface protein that were upregulated in LRECb vs. ECb

(*All genes listed are expressed at higher level in LRECb)

Symbol	Gene name	Fold change*
SAT2	Spermidine/spermine N1-acetyltransferase family member 2	4.34
IL22RA1	Interleukin 22 receptor, alpha 1	4.34
CXCR4	Chemokine (C-X-C motif) receptor 4	4
SDPR	Serum deprivation response	3.57
RTP3	Receptor (chemosensory) transporter protein 3	3.44
RGS1	Regulator of G-protein signaling 1	3.33
CRB1	Crumbs homolog 1 (Drosophila)	3.22
CASR	Calcium-sensing receptor	3.12
DRD2	Dopamine receptor D2	3.12
HAVCR1	Hepatitis A virus cellular receptor 1	3.12
GNGT1	Guanine nucleotide binding protein (G protein), gamma transducing activity polypeptide 1	2.94
RARRES1	Retinoic acid receptor responder (tazarotene induced) 1	2.94
CCR4	Chemokine (C-C motif) receptor 4	2.77
FXYD3	FXYD domain containing ion transport regulator 3	2.7
GRB14	Growth factor receptor-bound protein 14	2.63
GLRB	Glycine receptor, beta	2.56
F5	Coagulation factor V (proaccelerin, labile factor)	2.56
ATP8B1	ATPase, class I, type 8B, member 1	2.56
CD8A	CD8A molecule	2.5
MAGI1	Membrane associated guanylate kinase, WW and PDZ domain containing 1	2.43
NLGN1	Neuroligin 1	2.38
P2RY14	Purinergic receptor P2Y, G-protein coupled, 14	2.38
LAPTM5	Lysosomal protein transmembrane 5	2.38

Bibliography

Agur, Z., Kogan, Y., Levi, L., Harrison, H., Lamb, R., Kirnasovsky, O. U., and Clarke, R. B. (2010). Disruption of a Quorum Sensing mechanism triggers tumorigenesis: a simple discrete model corroborated by experiments in mammary cancer stem cells. *Biol Direct*. **5**, 20.

Akers, R. M., McFadden, T. B., Purup, S., Vestergaard, M., Sejrsen, K., and Capuco, A. V. (2000). Local IGF-I axis in peripubertal ruminant mammary development. *J Mammary Gland Biol Neoplasia*. **5**, 43-51.

Alvi, A. J., Clayton, H., Joshi, C., Enver, T., Ashworth, A., Vivanco, M. M., Dale, T. C, and Smalley, M. J. (2003). Functional and molecular characterisation of mammary side population cells. *Breast Cancer Res.* **5**, 1-8.

Anderson, E. and Clarke, R. B. (2004). Steroid receptors and cell cycle in normal mammary epithelium. *J Mammary Gland Biol Neoplasia*. **9**, 3-13.

Annicotte, J., Chavey, C., Servant, N., Teyssier, J., Bardin, A., Licznar, A., Badia, E., Pujol, P., Vignon, F., Lazennec, G., et al. (2005). The nuclear receptor liver receptor homolog-1 is an estrogen receptor target gene. *Oncogene*. **24**, 8167-8175.

Armstrong, L., Stojkovic, M., Dimmick, I., Ahmad, S., Stojkovic, P., Hole, N., and Lako, M. (2004). Phenotypic characterization of murine primitive hematopoietic progenitor cells isolated on basis of aldehyde dehydrogenase activity. *Stem Cells.* **22**, 1142-51.

Asselin-Labat, M.-L., Shackleton, M., Stingl, J., Vaillant, F., Forrest, N. C., Eaves, C. J., Visvader, J. E., and Lindeman, G. J. (2006). Steroid hormone receptor status of mouse mammary stem cells. *J Natl Cancer Inst.* **98**, 1011-4.

Asselin-Labat, M.-L., Vaillant, F., Sheridan, J. M., Pal, B., Wu, D., Simpson, E. R., Yasuda, H., Smyth, G. K., Martin, T. J., Lindeman, G. J., et al. (2010). Control of mammary stem cell function by steroid hormone signalling. *Nature*. **465**, 798-802.

Ballagh, K., Korn, N., Riggs, L., Pratt, S. L., Dessauge, F., Akers, R. M., and Ellis, S. (2008). Hot topic: Prepubertal ovariectomy alters the development of myoepithelial cells in the bovine mammary gland. *J Dairy Sci*. **91**, 2992-5.

Battle, M. A., Konopka, G., Parviz, F., Gaggl, A. L., Yang, C., Sladek, F. M., and Duncan, S. A. (2006). Hepatocyte nuclear factor 4alpha orchestrates expression of cell adhesion proteins during the epithelial transformation of the developing liver. *Proc Natl Acad Sci U S A.* **103**, 8419-24.

Bickenbach, J. R. (1981). Identification and behavior of label-retaining cells in oral mucosa and skin. *J Dental Res.* **60,** 1611-20.

Blake, R. D. and Delcourt, S. G. (1996). Thermodynamic effects of formamide on DNA stability. *Nucleic Acids Res.* **24**, 2095-103.

Bolstad, B. M., Irizarry, R. A., Astrand, M., and Speed, T. P. (2003). A comparison of normalization methods for high density oligonucleotide array data based on variance and bias. *Bioinformatics.* **19**, 185-93.

Booth, B. W., Boulanger, C. A., Anderson, L. H., Jimenez-Rojo, L., Brisken, C., and Smith, G. H. (2010). Amphiregulin mediates self-renewal in an immortal mammary epithelial cell line with stem cell characteristics. *Exp Cell Res.*, **316**, 422-32.

Bouras, T., Pal, B., Vaillant, F., Harburg, G., Asselin-Labat, M.-L., Oakes, S. R., Lindeman, G. J., and Visvader, J. E. (2008). Notch signaling regulates mammary stem cell function and luminal cell-fate commitment. *Cell Stem Cell*. **3**, 429-41.

Bowditch, R. D., Hariharan, M., Tominna, E. F., Smith, J. W., Yamada, K. M., Getzoff, E. D., and Ginsberg, M. H. (1994). Identification of a novel integrin binding site in fibronectin. Differential utilization by beta 3 integrins. *J Biol Chem.* **269**, 10856-63.

Bray, S. J. (2006). Notch signalling: a simple pathway becomes complex. *Nature Rev Mol Cell Biol.* **7**, 678-89.

Brisken, C. and Duss, S. (2007). Stem cells and the stem cell niche in the breast: an integrated hormonal and developmental perspective. *Stem Cell Rev.* **3**, 147-56.

Brisken, C. and O'Malley, B. (2010). Hormone action in the mammary gland. *Cold Spring Harb Perspectives Biol.* **2**, a003178.

Brisken, C., Heineman, A., Chavarria, T., Elenbaas, B., Tan, J., Dey, S. K., McMahon, J. A., McMahon, A. P., and Weinberg, R. A. (2000). Essential function of Wnt-4 in mammary gland development downstream of progesterone signaling. *Genes Dev.* **14**, 650-654.

Capelson, M., Liang, Y., Schulte, R., Mair, W., Wagner, U., and Martin, W. (2011). Chromatin-bound nuclear pore components regulate gene expression in higher eukaryotes. *Mol Cell Biol.* **140**, 1-22.

Capuco, A. V. (2007). Identification of putative bovine mammary epithelial stem cells by their retention of labeled DNA strands. *Exp Biol Med.* **232**, 1381-90.

Capuco, A. V. and Akers, R. M. (1999). Mammary involution in dairy animals. *J Mammary Gland Biol Neoplasia*. **4**, 137-44.

Capuco, A. V., Akers, R. M., and Smith, J. J. (1997). Mammary growth in Holstein cows during the dry period: quantification of nucleic acids and histology. *J Dairy Sci*. **80**, 477-87.

Capuco, A. V., Ellis, S., Wood, D. L., Akers, R. M., and Garrett, W. (2002). Postnatal mammary ductal growth: three-dimensional imaging of cell proliferation, effects of estrogen treatment, and expression of steroid receptors in prepubertal calves. *Tissue Cell*. **34**, 143-54.

Capuco, A. V., Evock-Clover, C. M., Minuti, A., and Wood, D. L. (2009). In vivo expansion of the mammary stem/ progenitor cell population by xanthosine infusion. *Exp Biol Med.* **234**, 475-82.

Capuco, A. V., Wood, D. L., Baldwin, R., Mcleod, K., and Paape, M. J. (2001). Mammary cell number, proliferation, and apoptosis during a bovine lactation: relation to milk production and effect of bST. *J Dairy Sci*. **84**, 2177-87.

Chepko, G. and Smith, G. H. (1997). Three division-competent, structurally-distinct cell populations contribute to murine mammary epithelial renewal. *Tissue Cell*. **29**, 239-53.

Choudhary, R. K., Daniels, K. M., Evock-Clover, C. M., Garrett, W., and Capuco, A. V. (2010a). Technical note: A rapid method for 5-bromo-2'-deoxyuridine (BrdU) immunostaining in bovine mammary cryosections that retains RNA quality. *J Dairy Sci.* **93**, 2574-9.

Choudhary, R. K., Li, R. W., Evock-Clover, C. M., and Capuco, A. V. (2010b). Bovine mammary stem cells: Transcriptome profiling and the stem cell niche. *J Dairy Sci.* **93**, ii-iii.

Colitti, M. and Farinacci, M. (2009). Expression of a putative stem cell marker, Musashi 1, in mammary glands of ewes. *J Mol Histol.* **40**, 139-49.

Conboy, M. J., Karasov, A. O., and Rando, T. A. (2007). High incidence of non-random template strand segregation and asymmetric fate determination in dividing stem cells and their progeny. *PLoS Biol.* **5**, e102.

Covello, K. L., Kehler, J., Yu, H., Gordan, J. D., Arsham, A. M., Hu, C.J., Labosky, P. A., Simon, M. C., and Keith, B. (2006). HIF-2alpha regulates regulates Oct-4: effects of hypoxia on stem cell function, embryonic development, and tumor growth. *Genes Dev.* **20**, 557-70.

Daniel, C. W., Silberstein, G. B., Van Horn, K., Strickland, P., and Robinson, S. (1989). TGF-beta1-induced inhibition of mouse mammary ductal growth: developmental specificity and characterization. *Dev Biol.* **135**, 20-30.

DeOme, K. B., Faulkin, L. J., Bern, H. A., and Blair, P. B. (1959). Development of mammary tumors from hyperplastic alveolar nodules transplanted into gland-free mammary fat pads of female C3H mice. *Cancer Res.* **19**, 515-20.

Delaforest, A., Nagaoka, M., Si-Tayeb, K., Noto, F. K., Konopka, G., Battle, M. A., and Duncan, S. A. (2011). HNF4A is essential for specification of hepatic progenitors from human pluripotent stem cells. *Development.* **138**, 4143-53.

Dey, D., Saxena, M., Paranjape, A. N., Krishnan, V., Giraddi, R., Kumar, M. V., Mukherjee, G., and Rangarajan, A. (2009). Phenotypic and functional characterization of human mammary stem/progenitor cells in long term culture. *PloS One*. **4**, e5329.

Dontu, G., Abdallah, W. M., Foley, J. M., Jackson, K. W., Clarke, M. F., Kawamura, M. J., and Wicha, M. S. (2003). In vitro propagation and transcriptional profiling of human mammary stem / progenitor cells. *Genes Dev.* **17**, 1253-1270.

Dontu, G., Jackson, K. W., McNicholas, E., Kawamura, M. J., Abdallah, W. M., and Wicha, M. S. (2004). Role of Notch signaling in cell-fate determination of human mammary stem/progenitor cells. *Breast Cancer Res.* **6**, R605-15.

Douville, J., Beaulieu, R., and Balicki, D. (2009). ALDH1 as a functional marker of cancer stem and progenitor cells. *Stem Cells Dev.* **18**, 17-25.

Edgar, R., Domrachev, M., and Lash, A. E. (2002). Gene Expression Omnibus: NCBI gene expression and hybridization array data repository. *Nucleic Acids Res.* **30**, 207-10.

Ellis, S. and Capuco, A. V. (2002). Cell proliferation in bovine mammary epithelium: identification of the primary proliferative cell population. *Tissue Cell*. **34**, 155-63.

Esmailpour, T. and Huang, T. (2008). Advancement in mammary stem cell research. *Pathol.* **4**, 131-138.

Fend, F., Emmert-Buck, M. R., Chuaqui, R., Cole, K., Lee, J., Liotta, L. A., and Raffeld, M. (1999). Immuno-LCM: laser capture microdissection of immunostained frozen sections for mRNA analysis. *Am J Pathol.* **154**, 61-6.

Feng, Y., Manka, D., Wagner, K.-U., and Khan, S. A. (2007). Estrogen receptor-alpha expression in the mammary epithelium is required for ductal and alveolar morphogenesis in mice. *Proc Natl Acad Sci U S A.* **104**, 14718-23.

Ferguson, D. J. (1985). Ultrastructural characterisation of the proliferative (stem?) cells within the parenchyma of the normal “resting” breast. *Virchows Archiv. A, Pathol Anatomy Histopathol*. **407**, 379-85.

Fleige, S. and Pfaffl, M. W. (2006). RNA integrity and the effect on the real-time qRT-PCR performance. *Mol Aspects Med.* **27**, 126-39.

Fuxe, J., Vincent, T., and Garcia de Herreros, A. (2010). Transcriptional crosstalk between TGF-β and stem cell pathways in tumor cell invasion: role of EMT promoting Smad complexes. *Cell Cycle.* **9**, 2363-74.

Geiger, B., Bershadsky, A., Pankov, R., and Yamada, K. M. (2001). Transmembrane crosstalk between the extracellular matrix--cytoskeleton crosstalk. *Mol Cell Biol.* **2**, 793-805.

Ginestier, C., Hur, M. H., Charafe-Jauffret, E., Monville, F., Dutcher, J., Brown, M., Jacquemier, J., Viens, P., Kleer, C. G., Liu, S., et al. (2007). ALDH1 is a marker of normal and malignant human mammary stem cells and a predictor of poor clinical outcome. *Cell Stem Cell*, **1**, 555-67.

Gotte, M., Wolf, M., Staebler, A., Buchweitz, O., Kelsch, R., Schüring, A. N., and Kiesel, L. (2008). Increased expression of the adult stem cell marker Musashi-1 in endometriosis and endometrial carcinoma. *J Pathol.* **215**, 317-29.

Gotte, M, Greve, B., Kelsch, R., Müller-Uthoff, H., Weiss, K., Kharabi M. B., Sibrowski, W., Kiesel, L., and Buchweitz, O. (2011). The adult stem cell marker musashi-1 modulates endometrial carcinoma cell cycle progression and apoptosis via Notch-1 and p21WAF1/CIP1. *Int J Cancer.* **129**, 2042-49.

Gratzner, H. G. (1982). Monoclonal antibody to 5-bromo- and 5-iododeoxyuridine: A new reagent for detection of DNA replication. *Science*. **218**, 474-5.

Guo, L., Lobenhofer, E. K., Wang, C., Shippy, R., Harris, S. C., Zhang, L., Mei, N., Chen, T., Herman, D., Goodsaid, F. M., et al. (2006). Rat toxicogenomic study reveals analytical consistency across microarray platforms. *Nature Biotech*. **24**, 1162-9.

Gyorki, D. E., Asselin-Labat, M.-L., van Rooijen, N., Lindeman, G. J., and Visvader, J. E. (2009). Resident macrophages influence stem cell activity in the mammary gland. *Breast Cancer Res.* **11**, R62.

Heng, J.-C. D., Feng, B., Han, J., Jiang, J., Kraus, P., Ng, J.-H., Orlov, Y. L., Huss, M., Yang, L., Lufkin, T., et al. (2010). The nuclear receptor NR5A2 can replace OCT4 in the reprogramming of murine somatic cells to pluripotent cells. *Cell Stem Cell*. **6**, 167-74.

Hess, D. A., Meyerrose, T. E., Wirthlin, L., Craft, T. P., Herrbrich, P. E., Creer, M. H., and Nolta, J. A. (2004). Functional characterization of highly purified human hematopoietic repopulating cells isolated according to aldehyde dehydrogenase activity. *Blood*. **104**, 1648-55.

Hovey, R. C. and Aimo, L. (2010). Diverse and active roles for adipocytes during mammary gland growth and function. *J Mammary Gland Biol Neoplasia*. **15**, 279-90.

Huang, D. W., Sherman, B. T., and Lempicki, R. A. (2009). Systematic and integrative analysis of large gene lists using DAVID bioinformatics resources. *Nature Protoc.* **4**, 44-57.

Humphreys, R. C., Lydon, J., O'Malley, B. W., and Rosen, J. M. (1997). Mammary gland development is mediated by both stromal and epithelial progesterone receptors. *Mol Endocrinol.* 801-11.

Hynes, N. E. and Watson, C. J. (2010). Mammary gland growth factors: roles in normal development and in cancer. *Cold Spring Harb Perspectives Biol.* **2**, a003186.

Irizarry, R. A, Hobbs, B., Collin, F., Beazer-Barclay, Y. D., Antonellis, K. J., Scherf, U., and Speed, T. P. (2003). Exploration, normalization, and summaries of high density oligonucleotide array probe level data. *Biostatistics.* **4**, 249-64.

Jackson, K., Yu, M. C., Arakawa, K., Fiala, E., Youn, B., Fiegl, H., Müller-Holzner, E., Widschwendter, M., and Ehrlich, M. (2004). DNA hypomethylation is prevalent even in low-grade breast cancers. *Therapy*. 1225-31.

Jones, P. H., Harper, S., and Watt, F. M. (1995). Stem cell patterning and fate in human epidermis. *Cell*. **80**, 83-93.

Joshi, P. A., Jackson, H. W., Beristain, A. G., Di Grappa, M. A., Mote, P. A., Clarke, C. L., Stingl, J., Waterhouse, P. D., and Khokha, R. (2010). Progesterone induces adult mammary stem cell expansion. *Nature*. **465**, 803-7.

Kakarala, M., Brenner, D. E., Korkaya, H., Cheng, C., Tazi, K., Ginestier, C., Liu, S., Dontu, G., and Wicha, M. S. (2010). Targeting breast stem cells with the cancer preventive compounds curcumin and piperine. *Breast Cancer Res. Treat.* **122**, 777-85.

Kang, H., Watkins, G., Douglas-Jones, A., Mansel, R. E., and Jiang, W. G. (2005). The elevated level of CXCR4 is correlated with nodal metastasis of human breast cancer. *Breast.* **14**, 360-7.

Katoh, M. (2006). Cross-talk of Wnt and FGF signaling pathways at GSK3beta to regulate beta-catenin and SNAIL signaling cascades. *Cancer Biol Ther.* **5**, 1059-64.

Kaufman, D. S. (2010). HIF hits Wnt in the stem cell niche. *Nature Cell Biol.* **12**, 926-7.

Keeshan, K., He, Y., Wouters, B. J., Shestova, O., Xu, L., Sai, H., Rodriguez, C. G., Maillard, I., Tobias, J. W., Valk, P., et al. (2010). Tribbles homolog 2 (Trib2)

inactivates C/EBPalpha and causes acute myelogenous leukemia. *Cancer cell*. **10**, 401-11.

Kendrick, H., Regan, J. L., Magnay, F.-A., Grigoriadis, A., Mitsopoulos, C., Zvelebil, M., and Smalley, M. J. (2008). Transcriptome analysis of mammary epithelial subpopulations identifies novel determinants of lineage commitment and cell fate. *BMC Genomics.* **9**, 591.

Kiel, M. J., He, S., Ashkenazi, R., Gentry, S. N., Teta, M., Kushner, J. A., Jackson, T. L., and Morrison, S. J. (2007). Haematopoietic stem cells do not asymmetrically segregate chromosomes or retain BrdU. *Nature*. **449**, 238-42.

Koh, W., Sheng, C. T., Tan, B., Lee, Q. Y., Kuznetsov, V., Kiang, L. S., and Tanavde, V. (2010). Analysis of deep sequencing microRNA expression profile from human embryonic stem cells derived mesenchymal stem cells reveals possible role of let-7 microRNA family in downstream targeting of hepatic nuclear factor 4 alpha. *BMC Genomics.* **11** (Suppl 1), S6.

Kordon, E. C. and Smith, G. H. (1998). An entire functional mammary gland may comprise the progeny from a single cell. *Development.* **125**, 1921-30.

Kordon, E. C., McKnight, R. A., Jhappan, C., Hennighausen, L., Merlino, G., and Smith, G. H. (1995). Ectopic TGF beta 1 expression in the secretory mammary epithelium induces early senescence of the epithelial stem cell population. *Dev Biol.* **168**, 47-61.

Korkaya, H., Paulson, A., Charafe-Jauffret, E., Ginestier, C., Brown, M., Dutcher, J., Clouthier, S. G., and Wicha, M. S. (2009). Regulation of mammary stem/progenitor cells by PTEN/Akt/beta-catenin signaling. *PLoS Biol.* **7**, e1000121.

Kristiansen, G., Winzer, K.-J., Mayordomo, E., Bellach, J., Schluns, K., Denkert, C., Dahl, E., Pilarsky, C., Altevogt, P., Guski, H., et al. (2003). CD24 expression is a new prognostic marker in breast cancer. *Clin Cancer Res.* **9**, 4906-13.

Kucia, M., Jankowski, K., Reca, R., Wysoczynski, M., Bandura, L., Allendorf, D. J., Zhang, J., Ratajczak, J., and Ratajczak, M. Z. (2004). CXCR4-SDF-1 signalling, locomotion, chemotaxis and adhesion. *J Mol Histol.* **35**, 233-45.

Landskroner-Eiger, S., Park, J., Israel, D., Pollard, J. W., and Philipp, S. E. (2010). Morphogenesis of the developing mammary gland: stage-dependent impact of adipocytes. *Dev Biol.* **344**, 968-78.

Lee, H.-S., Crane, G. G., Merok, J. R., Tunstead, J. R., Hatch, N. L., Panchalingam, K., Powers, M. J., Griffith, L. G., and Sherley, J. L .(2003). Clonal expansion of adult rat hepatic stem cell lines by suppression of asymmetric cell kinetics (SACK). *Biotech Bioeng.* **83**, 760-71.

Lepic, E., Burger, D., Lu, X., Song, W., and Feng, Q. (2006). Lack of endothelial nitric oxide synthase decreases cardiomyocyte proliferation and delays cardiac maturation. *Am J Physiol Cell Physiol.* **291**, C1240-6.

Levi, B. P., Yilmaz, O. H., Duester, G., and Morrison, S. J. (2009). Aldehyde dehydrogenase 1a1 is dispensable for stem cell function in the mouse hematopoietic and nervous systems. *Blood*. **113**, 1670-80.

Lewis, F., Maughan, N. J., Smith, V., Hillan, K., and Quirke, P. (2001). Unlocking the archive gene expression in paraffin-embedded tissue. *J Pathol.* **195**, 66-71.

Lewis, M. T. and Veltmaat, J. M. (2004). Next stop, the twilight zone: hedgehog network regulation of mammary gland development. *J Mammary Gland Biol Neoplasia*. **9**, 165-81.

Li, L. and Xie, T. (2005). Stem cell niche: structure and function. *Annu Rev Cell Dev Biol.* **21**, 605-31.

Li, N., Singh, S., Cherukuri, P., Li, H., Yuan, Z., Ellisen, L. W., Wang, B., Robbins, D., and Direnzo, J. (2008). Reciprocal intraepithelial interactions between TP63 and hedgehog signaling regulate quiescence and activation of progenitor elaboration by mammary stem cells. *Stem Cells.* **26**, 1253-64.

Li, R. W. and Capuco, A. V. (2008). Canonical pathways and networks regulated by estrogen in the bovine mammary gland. *Funct Integr Genomics*. **8**, 55-68.

Li, R. W., Meyer, M. J., Van Tassell, C. P., Sonstegard, T. S., Connor, E. E., Van Amburgh, M. E., Boisclair, Y. R., and Capuco, A. V. (2006). Identification of estrogen-responsive genes in the parenchyma and fat pad of the bovine mammary gland by microarray analysis. *Physiol Genomics.* **27**, 42-53.

Luetteke, N. C., Qiu, T. H., Fenton, S. E., Troyer, K. L., Riedel, R. F., Chang, A., and Lee, D. C. (1999). Targeted inactivation of the EGF and amphiregulin genes reveals distinct roles for EGF receptor ligands in mouse mammary gland development. *Development.* **126**, 2739-50.

Lupu, F., Alves, A., Anderson, K., Doye, V., and Lacy, E. (2009). Nuclear pore composition regulates neural stem/progenitor cell differentiation in the mouse embryo. *Dev Cell.* **14**, 831-42.

Mailleux, A. A., Spencer-Dene, B., Dillon, C., Ndiaye, D., Savona-Baron, C., Itoh, N., Kato, S., Dickson, C., Thiery, J. P., and Bellusci, S. (2002). Role of FGF10/FGFR2b signaling during mammary gland development in the mouse embryo. *Development.* **129**, 53-60.

Mallepell, S., Krust, A., Chambon, P., and Brisken, C. (2006). Paracrine signaling through the epithelial estrogen receptor alpha is required for proliferation and morphogenesis in the mammary gland. *Proc Natl Acad Sci U S A.* **103**, 2196-201.

Mazumdar, J., O'Brien, W. T., Johnson, R. S., LaManna, J. C., Chavez, J. C., Klein, P. S., and Simon, M. C. (2010). O2 regulates stem cells through Wnt/β-catenin signalling. *Nature Cell Biol.* **12**, 1007-13.

Meeker, A. K. and Coffey, D. S. (1997). Telomerase: a promising marker of biological immortality of germ, stem, and cancer cells. A review. *Biochemistry (Mosc).* **62**, 1323-31.

Mendjan, S., Taipale, M., Kind, J., Holz, H., Gebhardt, P., Schelder, M., Vermeulen, M., Buscaino, A., Duncan, K., Mueller, J., et al. (2006). Nuclear pore components are involved in the transcriptional regulation of dosage compensation in Drosophila. *Mol Cell.* **21**, 811-23.

Morrison, B. and Cutler, M. L. (2009). Mouse mammary epithelial cells form mammospheres during lactogenic differentiation. *J Visualized Exp.* **32**, 1265.

Motyl, T., Bierła, J. B., Kozłowski, M., Gajewska, M., Gajkowska, B., and Koronkiewicz, M. (2011). Identification, quantification and transcriptional profile of potential stem cells in bovine mammary gland. *Livestock Sci.* **136**, 136-149.

Murakami, H., Liotta, L., and Star, R. A. (2000). IF-LCM: Laser capture microdissection of immunofluorescently defined cells for mRNA analysis rapid communication. *Kidney Int.* **58**, 1346-53.

Muschler, J. and Streuli, C. H. (2010). Cell-matrix interactions in mammary gland development and breast cancer. *Cold Spring Harb Perspectives Biol.* **2**, a003202.

Navarro, P., Chambers, I., Karwacki-Neisius, V., Chureau, C., Morey, C., Rougeulle, C., and Avner, P. (2008). Molecular coupling of Xist regulation and pluripotency. *Science*. **321**, 1693-5.

Neumeister, V. and Rimm, D. (2010). Is ALDH1 a good method for definition of breast cancer stem cells? *Breast Cancer Res Treat.* **123**, 109-11.

Nguyen, A. V. and Pollard, J. W. (2000). Transforming growth factor beta3 induces cell death during the first stage of mammary gland involution. *Development.* **127**, 3107-18.

Nishizuka, M., Kishimoto, K., Kato, A., Ikawa, M., Okabe, M., Sato, R., Niida, H., Nakanishi, M., Osada, S., and Imagawa, M. (2009). Disruption of the novel gene fad104 causes rapid postnatal death and attenuation of cell proliferation, adhesion, spreading and migration. *Exp Cell Res.* **315**, 809-19.

Okano, H., Kawahara, H., Toriya, M., Nakao, K., Shibata, S., and Imai, T. (2005). Function of RNA-binding protein Musashi-1 in stem cells. *Exp Cell Res.* **306**, 349-56.

Plickert, G. and Kroiher, M. (1988). Proliferation kinetics and cell lineages can be studied in whole mounts and macerates by means of BrdU/anti-BrdU technique. *Development.* **103**, 791-4.

Pollard, J. W. and Hennighausen, L. (1994). Colony stimulating factor 1 is required for mammary gland development during pregnancy. *Proc Natl Acad Sci U S A.* **91**, 9312-6.

Polyak, K. and Hu, M. (2005). Do myoepithelial cells hold the key for breast tumor progression? *J Mammary Gland Biol Neoplasia*. **10**, 231-47.

Potten, C S, Hume, W. J., Reid, P., and Cairns, J. (1978). The segregation of DNA in epithelial stem cells. *Cell*, **15**, 899-906.

Potten, C. S, Booth, C., Tudor, G. L., Booth, D., Brady, G., Hurley, P., Ashton, G., Clarke, R., Sakakibara, S., and Okano, H. (2003). Identification of a putative intestinal stem cell and early lineage marker; Musashi-1. *Differentiation.* **71**, 28-41.

Potten, C. S, Owen, G., and Booth, D. (2002). Intestinal stem cells protect their genome by selective segregation of template DNA strands. *J Cell Sci.* **115**, 2381-8.

Rahal, O. M. and Simmen, R. C. M. (2011). Paracrine-acting adiponectin promotes mammary epithelial differentiation and synergizes with genistein to enhance transcriptional response to estrogen receptor β signaling. *Endocrinology*. **152**, 3409-21.

Rambhatla, L., Ram-Mohan, S., Cheng, J. J., and Sherley, J. L. (2005). Immortal DNA strand cosegregation requires p53/IMPDH-dependent asymmetric self-renewal associated with adult stem cells. *Cancer Res.* **65**, 3155-61.

Raouf, A., Zhao, Y., To, K., Stingl, J., Delaney, A., Barbara, M., Iscove, N., Jones, S., McKinney, S., Emerman, J., et al. (2008). Transcriptome analysis of the normal human mammary cell commitment and differentiation process. *Cell Stem Cell*. **3**, 109-18.

Ratajczak, M. Z., Zuba-Surma, E., Kucia, M., Reca, R., Wojakowski, W., and Ratajczak, J. (2006). The pleiotropic effects of the SDF-1-CXCR4 axis in organogenesis, regeneration and tumorigenesis. *Leukemia*. **20**, 1915-24.

Reynolds, B. A., Tetzlaff, W., and Weiss, S. (1992). A multipotent EGF-responsive striatal embryonic progenitor cell produces neurons and astrocytes. *J Neurosci.* **12**, 4565-74.

Rezza, A., Skah, S., Roche, C., Nadjar, J., Samarut, J., and Plateroti, M. (2010). The overexpression of the putative gut stem cell marker Musashi-1 induces tumorigenesis through Wnt and Notch activation. *J Cell Sci.* **123**, 3256-65.

Rietze, R. L., Valcanis, H., Brooker, G. F., Thomas, T., Voss, A. K., and Bartlett, P. F. (2001). Purification of a pluripotent neural stem cell from the adult mouse brain. *Nature*. **412**, 736-9.

Riley, L. G., Gardiner-Garden, M., Thomson, P. C., Wynn, P. C., Williamson, P., Raadsma, H. W., and Sheehy, P. A. (2010). The influence of extracellular matrix and prolactin on global gene expression profiles of primary bovine mammary epithelial cells in vitro. *Anim Genet.* **41**, 55-63.

Rizzino, A. (2009). Sox2 and Oct-3 / 4: a versatile pair of master regulators that orchestrate the self-renewal and pluripotency of embryonic stem cells. *WIREs System Biol Med.* **1**, 228-36.

Robinson, G. W., Hennighausen, L., and Johnson, P. F. (2000). Side-branching in the mammary gland: the progesterone-Wnt connection. *Genes Dev.* **14**, 889-94.

Roth, V. (2006) calculating cell population doubling time. In: http://www.doubling-time.

com/compute.php.

Ruan, W. and Kleinberg, D. L. (1999). Insulin-like growth factor I is essential for terminal end bud formation and ductal morphogenesis during mammary development. *Endocrinology*. **140**, 5075-81.

Ruan, W., Newman, C. B., and Kleinberg, D. L. (1992). Intact and amino-terminally shortened forms of insulin-like growth factor I induce mammary gland differentiation and development. *Proc Natl Acad Sci U S A.* **89**, 10872-6.

Rusan, N. M. and Peifer, M. (2007). A role for a novel centrosome cycle in asymmetric cell division. *J Cell Biol.*, **177**, 13-20.

Savarese, F., Flahndorfer, K., Jaenisch, R., Busslinger, M., and Wutz, A. (2006). Hematopoietic precursor cells transiently reestablish permissiveness for X inactivation. *Mol Cell Biol.* **26**, 7167-77.

Scheel, C., Eaton, E. N., Li, S. H.-J., Chaffer, C. L., Reinhardt, F., Kah, K.-J., Bell, G., Guo, W., Rubin, J., Richardson, A. L., et al. (2011). Paracrine and autocrine signals induce and maintain mesenchymal and stem cell states in the breast. *Cell*. **145**, 926-40.

Schroeder, A., Mueller, O., Stocker, S., Salowsky, R., Leiber, M., Gassmann, M., Lightfoot, S., Menzel, W., Granzow, M., and Ragg, T. (2006). The RIN: an RNA

integrity number for assigning integrity values to RNA measurements. *BMC Mol Biol.* **7**, 3.

Shackleton, M., Vaillant, F., Simpson, K. J., Stingl, J., Smyth, G. K., Asselin-Labat, M.-L., Wu, L., Lindeman, G. J., and Visvader, J. E. (2006). Generation of a functional mammary gland from a single stem cell. *Nature*. **439**, 84-8.

Sherley, J. L. (1991). Guanine nucleotide biosynthesis is regulated by the cellular p53 concentration. *J Biol Chem.* **266**, 24815-28.

Sherley, J. L., Stadler, P. B., and Johnson, D. R. (1995). Expression of the wild-type p53 antioncogene induces guanine nucleotide-dependent stem cell division kinetics. *Proc Natl Acad Sci U S A.* **92**, 136-40.

Shi, W. and Harris, A. L. (2006). Notch signaling in breast cancer and tumor angiogenesis: cross-talk and therapeutic potentials. *J Mammary Gland Biol Neoplasia*. **11**, 41-52.

Shinin, V., Gayraud-Morel, B., Gomès, D., and Tajbakhsh, S. (2006). Asymmetric division and cosegregation of template DNA strands in adult muscle satellite cells. *Nature Cell Biol.* **8**, 677-87.

Silberstein, G. B. (2001). Tumour-stromal interactions. Role of the stroma in mammary development. *Breast Cancer Res.***3**, 218-23.

Silberstein, G. B. and Daniel, C. W. (1987). Reversible inhibition of mammary gland growth by transforming growth factor-beta. *Science*. **237**, 291-3.

Sinha, Y. N. and Tucker, H. A. (1969). Mammary development and pituitary prolactin level of heifers from birth through puberty and during the estrous cycle. *J Dairy Sci.* **52**, 507-12.

Sinowatz, F., Schams, D., Habermann, F., Berisha, B., and Vermehren, M. (2006). Localization of fibroblast growth factor I (acid fibroblast growth factor) and its mRNA in the bovine mammary gland during mammogenesis, lactation and involution. *Anat Histol Embryol* **35**, 202-7.

Sladek, N. E. (2003). Human aldehyde dehydrogenases: potential pathological, pharmacological, and toxicological impact. *J Biochem Mol Toxicol.* **17**, 7-23.

Sleeman, K. E., Kendrick, H., Robertson, D., Isacke, C. M., Ashworth, A., and Smalley, M. J. (2007). Dissociation of estrogen receptor expression and in vivo stem cell activity in the mammary gland. *J Cell Biol.* **176**, 19-26.

Smith, G. H. (2005). Label-retaining epithelial cells in mouse mammary gland divide asymmetrically and retain their template DNA strands. *Development.* **132**, 681-7.

Smith, G. H. and Chepko, G. (2001). Mammary epithelial stem cells. *Microsc Res Tech.* **52**, 190-203.

Smith, G. H. and Medina, D. (1988). A morphologically distinct candidate for an epithelial stem cell in mouse mammary gland. *J Cell Sci.* **90**, 173-83.

Smith, G. H. and Medina, D. (2008). Re-evaluation of mammary stem cell biology based on *in vivo* transplantation *Breast Cancer Res.* **10**, 203.

Stingl, J., Eirew, P., Ricketson, I., Shackleton, M., Vaillant, F., Choi, D., Li, H. I., and Eaves, C. J. (2006). Purification and unique properties of mammary epithelial stem cells. *Nature*. **439**, 993-7.

Streuli, C. H. (2009). Integrins and cell-fate determination. *J Cell Sci.* **122**, 171-7.

Tang, X., Falls, D. L., Li, X., Lane, T., and Luskin, M. B. (2007). Antigen-retrieval procedure for bromodeoxyuridine immunolabeling with concurrent labeling of nuclear DNA and antigens damaged by HCl pretreatment. *The J Neurosci.* **27**, 5837-44.

Tsai, Y. C., Lu, Y., Nichols, P. W., Zlotnikov, G., Jones, P. A., and Smith, H. S. (1996). Contiguous patches of normal human mammary epithelium derived from a single stem cell: implications for breast carcinogenesis. *Cancer Res.* **56**, 402-4.

Vaquerizas, J. M., Suyama, R., Kind, J., Miura, K., Luscombe, N. M., and Akhtar, A. (2010). Nuclear pore proteins NUP153 and megator define transcriptionally active regions in the Drosophila genome. *PLoS Genet.* **6**, e1000846.

Vincek, V., Nassiri, M., Nadji, M., and Morales, A. R. (2003). A tissue fixative that protects macromolecules (DNA, RNA, and protein) and histomorphology in clinical samples. *Lab Invest.* **83**, 1427-35.

Wang, X.-Y., Yin, Y., Yuan, H., Sakamaki, T., Okano, H., and Glazer, R. I. (2008). Musashi-1 modulates mammary progenitor cell expansion through proliferin-mediated activation of the Wnt and Notch pathways. *Mol Cell Biol.* **28**, 3589-99.

Weber-Hall, S. J., Phippard, D. J., Niemeyer, C. C., and Dale, T. C. (1994). Developmental and hormonal regulation of Wnt gene expression in the mouse mammary gland. *Differentiation*. **57**, 205-14.

Wellnitz, O. and Kerr, D. E. (2004). Cryopreserved bovine mammary cells to model epithelial response to infection. *Vet Immunol Immunopathol*. **101**, 191-202.

Welm, B. E., Tepera, S. B., Venezia, T., Graubert, T. A., Rosen, J. M., and Goodell, M. A. (2002). Sca-1(pos) cells in the mouse mammary gland represent an enriched progenitor cell population. *Dev Biol.* **245**, 42-56.

Williams, J. M. and Daniel, C. W. (1983). Mammary ductal elongation: differentiation of myoepithelium and basal lamina during branching morphogenesis. *Dev Biol.* **97**, 274-90.

Wiseman, B. S. and Werb, Z. (2002). Stromal effects on mammary gland development and breast cancer. *Science*. **296**, 1046-9.

Zeng, Y. A. and Nusse, R. (2010). Wnt proteins are self-renewal factors for mammary stem cells and promote their long-term expansion in culture. *Cell Stem Cell*. **6**, 568-77.

Zhao, K., Liu, H.-Y., Zhou, M.-M., and Liu, J.-X. (2010). Establishment and characterization of a lactating bovine mammary epithelial cell model for the study of milk synthesis. *Cell Biol Int.* **4**, 717-21.

Zhou, L. and Panté, N. (2010). The nucleoporin NUP153 maintains nuclear envelope architecture and is required for cell migration in tumor cells. *FEBS Letters*. **584**, 3013-20.

Zhou, S., Schuetz, J. D., Bunting, K. D., Colapietro, A. M., Sampath, J., Morris, J. J., Lagutina, I., Grosveld, G. C., Osawa, M., Nakauchi, H., et al. (2001). The ABC transporter Bcrp1/ABCG2 is expressed in a wide variety of stem cells and is a molecular determinant of the side-population phenotype. *Nature Med.* **7**, 1028-34.